University of Alberta

Electrophoretic Separations of Biopolymers

by

Dawn P. Richards

A thesis submitted to the Faculty of Graduate Studies and Research in partial fulfillment of the requirements for the degree of Doctor of Philosophy

Department of Chemistry

Edmonton, Alberta

Fall 2000

National Library of Canada
Acquisitions and Bibliographic Services
395 Wellington Street
Ottawa ON K1A 0N4
Canada

Bibliothèque nationale du Canada
Acquisitions et services bibliographiques
395, rue Wellington
Ottawa ON K1A 0N4
Canada

Your file Votre référence

Our file Notre référence

The author has granted a non-exclusive licence allowing the National Library of Canada to reproduce, loan, distribute or sell copies of this thesis in microform, paper or electronic formats.

L'auteur a accordé une licence non exclusive permettant à la Bibliothèque nationale du Canada de reproduire, prêter, distribuer ou vendre des copies de cette thèse sous la forme de microfiche/film, de reproduction sur papier ou sur format électronique.

The author retains ownership of the copyright in this thesis. Neither the thesis nor substantial extracts from it may be printed or otherwise reproduced without the author's permission.

L'auteur conserve la propriété du droit d'auteur qui protège cette thèse. Ni la thèse ni des extraits substantiels de celle-ci ne doivent être imprimés ou autrement reproduits sans son autorisation.

0-612-59661-3

Canada

University of Alberta

Library Release Form

Name of Author: Dawn Patricia Richards

Title of Thesis: Electrophoretic Separations of Biopolymers

Degree: Doctor of Philosophy

Year this Degree Granted: 2000

Permission is hereby granted to the University of Alberta Library to reproduce single copies of this thesis and to lend or sell such copies for private, scholarly or scientific research purposes only.

The author reserves all other publication and other rights in association with the copyright in the thesis, and except as herein before provided, neither the thesis nor any substantial portion thereof may be printed or otherwise reproduced in any material form whatever without the author's prior written permission.

Dawn Richards

#12, 8525-107 St.
Edmonton, Alberta
T6E 4L1

Sept. 19, 2000

Abstract

In the past decade separations science has shifted focus from genomic to proteomic research. With the recent completion of the human genome, exciting new protein research awaits scientists. This thesis demonstrates the change in emphasis from genomic to proteomic separations.

A polymer has been developed for capillary electrophoresis (CE) DNA sequencing which is compatible with uncoated capillaries for high temperature DNA sequencing. Utilization of this polymer eliminates coating chemistry, increases capillary lifetime, and decreases compression likelihood because of its high temperature compatibility. Column efficiency was not affected by capillary reuse.

CE with laser-induced fluorescence (LIF) detection has many advantages over slab gel electrophoresis, and may one day replace traditional two-dimensional analysis systems. This thesis shows the development of a capillary isoelectric focusing (CIEF) method with LIF detection. It demonstrates that fluorescent labeling of proteins can change their isoelectric points due to changes in their charges and their denaturation. For CIEF with LIF detection to be utilized routinely, solutions must be found to this labeling problem.

CE SDS separation with LIF detection is a relatively young separation technique. The size-based separations of proteins utilizing hydroxyethylcellulose, linear polyacrylamide, and dextran are presented. Separations of real, complex cell extracts have been achieved. The best separations were achieved when the cell extracts were further fractionated into specific cellular compartments. The marriage

of CIEF and CE SDS separations will one day yield an incredibly powerful separation technique.

Until a two-dimensional CE system is constructed, conventional methods must be utilized. Traditional slab gel techniques were employed in the attempts to identify two proteins from human lung cancer cells. One protein was induced and the other protein was repressed by different doses of γ-irradiation. In-gel digestion followed by matrix assisted laser desorption and ionization time of flight mass spectrometry or tandem mass spectrometry were utilized to identify the proteins. The irradiation-induced protein has been identified as the 40S ribosomal protein S3a.

University of Alberta

Faculty of Graduate Studies and Research

The undersigned certify that they have read, and recommend to the Faculty of Graduate Studies and Research for acceptance, a thesis entitled Electrophoretic Separations of Biopolymers submitted by Dawn P. Richards in partial fulfillment of the requirements for the degree of Doctor of Philosophy.

Dr. N.J. Dovichi

Dr. L. Li

Dr. F.F. Cantwell

Dr. M. Klobukowski

Dr. P. Choi

Dr. D. Bornhop

Sept. 18, 2000

Acknowledgements

I would like to thank Norm Dovichi for giving me the opportunity to work in his research group.

There are many group members and former group members who supported my work and myself over my years as a graduate student. Darren Lewis is not only a great friend but was able to fix any computer/instrument/electronic glitch immediately following a smoke break. Thanks to Rob Polakowski who helped me out with IEF, SDS-PAGE, any protein troubles, and who also provided much comic relief. I would like to thank Lillian Cook for her tissue culture expertise and for learning and performing new techniques with me in my last year of studies. Thank you to Alison (Cyto)Skelley for all of her help with my last project. I would like to thank Kim Roy for her help over the summer months of 1999. Thanks to XingFang Li for all of her advice and her friendship during her time here. Diana Shaw became a very good friend and shared many whiny sessions with me over coffee and hot chocolate. I also need to thank Bernd Keller for performing the MALDI-TOF-MS analyses for me and for all of his critical thinking and advice. I thank Eric Carpenter for squashing any WORD bugs I found during my writing and for all of his advice and help during his time with the group. Thanks goes to Pieter Roos for his guidance and stimulating discussions regarding my DNA sequencing work. I would like to thank Comet Stathakis for his help with my CIEF work- for much excellent advice and many helpful suggestions. I very much appreciated the friendship and advice of both Chris and Amy DAMBRO during my time with the group. Thank you to Heather Cain and King Tan for editing my thesis.

I would also like to thank Dr. Cantwell for his advice, friendship, and our mutual teasing. Thank you to Dr. Palcic for generously allowing me to work in her lab space and to utilize her equipment from time to time. Dr. Li also allowed me to work in his lab on occasion for which I express gratitude. Thank you to Dr. Weinfeld for his advice and input on cellular irradiation and to Jane Lee for helping us with the irradiation experiments. Thanks are extended to Daniel Figeys and Brett Larsen at MDS Ocata for running the tandem MS of my samples on such short notice.

I would like to thank my family who has put up with my long work hours during my graduate studies and for all of their support of my educational endeavors over the years. My husband Bryce completely unconditionally and tirelessly supported me throughout my studies. He has provided much inspiration, motivation, and also frustration. For all of those things and for above all believing in me and my abilities, I thank him.

Table of Contents

Chapter 1: Introduction.....1

1.1 Capillary zone electrophoresis (CZE).....2

1.1.1 Basic principles of CZE.....2

1.2 Capillary gel electrophoresis (CGE).....2

1.2.1 Basic principles of CGE.....2

1.2.2 The Ogston model.....3

1.2.3 The biased reptation model.....4

1.2.4 Resolution in CGE DNA sequencing.....5

1.2.5 High throughput CGE DNA sequencing.....7

1.3 Capillary isoelectric focusing (CIEF).....7

1.3.1 Basic principles of CIEF.....7

1.3.2 Focusing.....8

1.3.3 Mobilization.....9

1.3.4 Resolution in CIEF.....10

1.3.5 The potential of CIEF.....11

1.4 Sodium dodecyl sulfate capillary gel electrophoresis (SDS CGE) of proteins.....11

1.4.1 Basic principles of protein size-based separations.....11

1.4.2 Ferguson plot analysis.....12

1.4.3 A comparison of SDS-PAGE and SDS CGE.....13

1.4.4 A brief history of SDS CGE separations.....13

1.5 The proteomics approach to protein identification.....14

1.5.1 An introduction to proteomics.....14

1.5.2 Two dimensional (2-D) gel electrophoresis.....15

1.5.3 Mass spectrometry for protein identification.....16

1.6 Thesis summary.....18

1.7 References.....18

Chapter 2: Replaceable Sieving Matrices for Capillary Gel Electrophoresis DNA Sequencing.....25

2.1 Introduction.....26

2.2 Experimental.....28

2.2.1 Materials and reagents.....28

2.2.2 Preparation of polydimethylacrylamide (PDMA).....28

2.2.3 Preparation of T-terminated sequencing samples.....29
2.2.4 Preparation of capillaries.....30
2.2.5 Capillary electrophoresis.....30
2.2.6 Viscosity measurement.....30
2.3 Results and Discussion.....31
2.3.1 Reusing and refilling capillaries with a PDMA sieving matrix..31
2.3.2 Variation of migration time.....31
2.3.3 Capillary reuse.....36
2.3.4 Effects of electric field strength on separation.....43
2.4 Conclusion.....51
2.5 References.....51

Chapter 3: Capillary Isoelectric Focusing using Laser-Induced Fluorescence Detection: Green Fluorescent Protein as a Model Protein.....54
3.1 Introduction.....55
3.2 Experimental.....57
3.2.1 Materials and reagents.....57
3.2.2 FQ-labeled ampholyte preparation.....58
3.2.3 FQ-labeled Pharmacia IEF standard preparation.....58
3.2.4 FQ-labeled GFP sample preparation.....58
3.2.5 Sample preparation for fluorometer readings.....59
3.2.6 CZE-LIF.....59
3.2.7 Slab gel IEF.....59
3.2.8 Capillary preparation.....60
3.2.9 CIEF-LIF with anodic mobilization.....63
3.2.10 Fluorometer measurements.....63
3.3 Results and Discussion.....63
3.3.1 Labeling possibilities.....63
3.3.2 Slab gel IEF of FQ-labeled IEF standards.....64
3.3.3 CZE of FQ-labeled GFP.....68
3.3.4 Changes in GFP's pI upon FQ-labeling.....68
3.3.5 CIEF-LIF detection of changes in GFP's pI.....68
3.3.6 Denaturation of GFP upon conjugation with FQ.....73
3.4 Conclusion.....73
3.5 References.....76

Chapter 4: Hydroxyethylcellulose as a Sieving Matrix for Sodium Dodecyl Sulfate Capillary Gel Electrophoresis of Proteins with Laser-Induced Fluorescence Detection.....78
4.1 Introduction.....79
4.2 Experimental.....81
4.2.1 Materials and reagents.....81
4.2.2 FQ labeling of individual protein standards.....82
4.2.3 Capillary preparation.....82
4.2.4 Sieving matrix preparation.....82
4.2.5 Capillary electrophoresis instrument.....82
4.2.6 CE using a LPA Grignard coated capillary.....83
4.2.7 CE using a polyAAP Grignard coated capillary.....83
4.3 Results and Discussion.....83
4.3.1 CZE of a mixture of standard proteins.....83
4.3.2 CGE using different percentages of HEC sieving matrices.....85
4.3.3 Standardization curve construction.....85
4.3.4 Effect of electric field on separation using a LPA Grignard coated capillary with a HEC sieving matrix.....85
4.3.5 Effect of electric field on separation using a polyAAP Grignard coated capillary with a HEC sieving matrix.....88
4.3.6 Effect of electric field on separation using a polyAAP Grignard coated capillary with HEC as a sieving matrix and running buffer.....92
4.3.7 Plots of time versus inverse electric field strength for different capillary coatings.....95
4.3.8 Same-day migration time variability.....99
4.3.9 Day-to-day migration time variability.....108
4.3.10 Capillary failure.....108
4.3.11 Protein concentration limits.....111
4.4 Conclusion.....111
4.5 References.....112

Chapter 5: Linear Polyacrylamide as a Sieving Matrix for Sodium Dodecyl Sulfate Capillary Gel Electrophoresis with Laser-Induced Fluorescence Detection of Human Colorectal Cancer Proteins.....115
5.1 Introduction.....116

5.2 Experimental....117
5.2.1 Materials and reagents....117
5.2.2 Cell culture....118
5.2.3 Cell extract preparation and fractionation....118
5.2.4 SDS-PAGE sample preparation....121
5.2.5 FQ labeling of standard proteins....121
5.2.6 FQ labeling of HT29 samples....121
5.2.7 SDS-PAGE....121
5.2.8 Capillary preparation....122
5.2.9 Capillary electrophoresis instrument....122
5.2.10 SDS CGE protein separations....122
5.3 Results and Discussion....122
5.3.1 SDS CGE of standard proteins using different percentages of LPA sieving matrices....122
5.3.2 Ferguson plot analysis of LPA sieving matrices....124
5.3.3 Standardization curve construction....125
5.3.4 Application of LPA sieving matrices to the separation of water-soluble HT29 cell extract proteins....131
5.3.5 Application of LPA sieving matrices to the separation of fractionated HT29 cell extract proteins....131
5.4 Conclusion....137
5.5 References....139

Chapter 6: Dextran as a Sieving Matrix for Sodium Dodecyl Sulfate Capillary Gel Electrophoresis of Proteins with Laser-Induced Fluorescence Detection....141
6.1 Introduction....142
6.2 Experimental....143
6.2.1 Materials and reagents....143
6.2.2 Cell culture....144
6.2.3 Cell extract preparation and fractionation....144
6.2.4 A549 nuclear protein concentration....145
6.2.5 FQ labeling of standard proteins....145
6.2.6 FQ labeling of A549 protein samples....145
6.2.7 Capillary preparation....146
6.2.8 Dextran sieving matrix preparation....146

6.2.9 CE instrument.....146
6.2.10 SDS CGE separations.....146
6.3 Results and Discussion.....147
6.3.1 SDS CGE of standard proteins utilizing different percentages of dextran sieving matrices.....147
6.3.2 Ferguson plot analysis of dextran sieving matrices with high and low ionic strength buffers.....150
6.3.3 Standardization curve construction.....158
6.3.4 Qualitative effects of different buffer systems on the SDS CGE separations.....158
6.3.5 Migration time for replicate runs.....167
6.3.6 Day-to-day migration time variability.....176
6.3.7 Application of a dextran sieving matrix to the SDS CGE separation of water-soluble A549 cell extract proteins.....176
6.3.8 Application of a dextran sieving matrix to the SDS CGE separation of A549 nuclear proteins.....176
6.4 Conclusion.....181
6.5 References.....183

Chapter 7: Observation and Identification of Irradiation-Induced Nuclear Protein Changes From Human Lung Cancer Cells.....185
7.1 Introduction.....186
7.2 Experimental.....187
7.2.1 Materials and reagents.....187
7.2.2 Cell culture.....188
7.2.3 γ-Irradiation of cells.....189
7.2.4 Cell fractionation.....189
7.2.5 Protein quantitation.....189
7.2.6 SDS-PAGE sample preparation.....190
7.2.7 Two-dimensional (2-D) electrophoresis sample preparation.....190
7.2.8 SDS-PAGE.....190
7.2.9 2-D electrophoresis.....191
7.2.10 Protein digestion.....193
7.2.11 MALDI-TOF MS and database search.....194
7.3 Results and Discussion.....194

7.3.1 Irradiation-induced changes in A549 nuclear protein expression detected by SDS-PAGE.....194
7.3.2 Irradiation-induced changes in A549 nuclear protein expression detected by 2-D electrophoresis.....196
7.3.3 Problems and solutions encountered while attempting to identify proteins utilizing MALDI-TOF MS.....200
7.3.4 Failure to identify the high molecular weight protein of interest.....202
7.3.5 Identification of the low molecular weight protein of interest. 203
7.4 Conclusion.....203
7.5 References.....205

Chapter 8: Conclusions and Future Work.....208
8.1 Thesis summary and future directions.....209

List of Tables

Chapter 2

Table 2.1 A comparison of average migration times of selected fragment lengths of DNA between different PDMA sieving matrices.....38

Table 2.2 Comparison of average normalized resolution for different fragment lengths between PDMA sieving matrices made two different ways...42

Table 2.3 Comparison of capillary efficiency at different fragment lengths for two types of PDMA sieving matrices.....46

Table 2.4 Comparison of resolution between selected fragment lengths for sequencing runs at -150V/cm and -300V/cm using a methanol-hexanes PDMA sieving matrix.....49

Table 2.5 Comparison of theoretical plate numbers at selected fragment lengths for sequencing runs at -150V/cm and -300V/cm using a methanol-hexanes PDMA sieving matrix.....50

Chapter 3

Table 3.1 Pharmacia LKB Phastsystem program used for slab gel IEF.....61

Table 3.2 Pharmacia LKB Phastsystem development program utilized to silver stain IEF gels.....62

Chapter 4

Table 4.1 Correlation coefficients obtained from plots of migration time versus the inverse of the electric field strength for standard proteins separated under different conditions.....101

Table 4.2 Line equations obtained from plots of migration time versus the inverse of the electric field strength for standard proteins separated under different conditions.....102

Table 4.3 Average migration times of 3 protein standards run on the same day using a 1% HEC sieving matrix with a LPA Grignard coated capillary and an electric field of -400 V/cm.....104

Table 4.4 Average migration times of 3 protein standards run on the same day using a 1% HEC sieving matrix with polyAAP Grignard coated capillary and an electric field of -400 V/cm.....107

Table 4.5 Average migration times of 3 protein standards run on the different days using a 1% HEC sieving matrix in the same LPA Grignard coated capillary using an electric field of -400 V/cm.....110

Chapter 5

Table 5.1 Differential detergent fractionation extraction buffers and their compositions.....120

Table 5.2 Retardation coefficients of the 5 protein standards derived from a Ferguson plot.....127

Table 5.3 Ferguson plot y-intercept values for the 5 protein standards utilizing LPA concentrations of 6-9%.....128

Table 5.4 Comparison of standardization curve linearity for different percentages of LPA sieving matrices.....130

Chapter 6

Table 6.1 Retardation coefficients of 6 protein standards obtained using a high ionic strength buffer.....154

Table 6.2 Retardation coefficients of 6 protein standards obtained using a low ionic strength buffer. 155

Table 6.3 Ferguson plot y-intercept values for 6 protein standards employing a high ionic strength buffer.....156

Table 6.4 Ferguson plot y-intercept values for 6 protein standards employing a low ionic strength buffer.....157

Table 6.5 Comparison of standardization curve linearity for different percentages of dextran sieving matrices in high ionic strength buffer.....160

Table 6.6 Comparison of standardization curve linearity for different percentages of dextran sieving matrices in low ionic strength buffer.....161

Table 6.7 Average migration times for the 6 protein standards run on the same day utilizing a 10% dextran sieving matrix with a 5 mM TrisHCl, 0.1% SDS, pH 8.8, buffer and an electric field of -400 V/cm.....171

Table 6.8 Average migration times for the 6 protein standards run on the same day utilizing a 12% dextran sieving matrix with a 5 mM TrisHCl, 0.1% SDS, pH 8.8, buffer and an electric field of -400 V/cm.....173

Table 6.9 Average migration times for the 5 protein standards run on the same day utilizing a 14% dextran sieving matrix with a 5 mM TrisHCl, 0.1% SDS, pH 8.8, buffer and an electric field of -400 V/cm.....175

Table 6.10 Average migration times for the 6 protein standards run on different days utilizing a 10% dextran sieving matrix with a 5 mM TrisHCl, 0.1% SDS, pH 8.8, buffer and an electric field of -400 V/cm.....178

Chapter 7

Table 7.1 IEF program utilized for 2-D electrophoresis of A549 nuclear extracts.....192

List of Figures

Chapter 2

Figure 2.1 Electropherogram of a T-termination DNA sequencing run using a methanol-hexanes PDMA sieving matrix for the first time in an uncoated capillary.....32

Figure 2.2 Electropherogram of a T-termination DNA sequencing run using a methanol-hexanes PDMA sieving matrix for the twenty-seventh time in the same uncoated capillary.....33

Figure 2.3 Electropherogram of a T-termination DNA sequencing run using a PDMA sieving matrix of PDMA which was polymerized and not further dissolved in methanol or washed with hexanes.....34

Figure 2.4 Migration time versus the number of times the capillary has been used for a methanol-hexanes sieving matrix.....35

Figure 2.5 Migration time versus the number of times the capillary has been used for a methanol PDMA sieving matrix.....37

Figure 2.6 The dependence of normalized resolution on the number of times a capillary is reused with a methanol-hexanes PDMA sieving matrix...40

Figure 2.7 The dependence of normalized resolution on the number of times a capillary is reused with a methanol PDMA sieving matrix.....41

Figure 2.8 Capillary efficiency changes as the capillary is refilled and reused with a methanol-hexanes PDMA sieving matrix.....44

Figure 2.9 Capillary efficiency as the capillary is refilled and reused with a methanol PDMA sieving matrix.....45

Figure 2.10 Electropherogram of a T-termination sequencing run with a methanol-hexanes PDMA sieving matrix at high electric field strength.....47

Figure 2.11 Comparison of migration times for a methanol-hexanes PDMA sieving matrix at field strengths of -150 V/cm and -300 V/cm.....48

Chapter 3

Figure 3.1 A schematic diagram of the focusing and mobilization steps in CIEF.....56

Figure 3.2 CZE of FQ-labeled pH 3/10 ampholytes.....65

Figure 3.3 CZE of FQ-labeled IEF standards.....66

Figure 3.4 Slab gel IEF of FQ-labeled IEF standards.....67

Figure 3.5 CZE of unlabeled and FQ-labeled GFP with GFP native fluorescence detection.....69

Figure 3.6 IEF slab gel determination of how FQ-labeling effects the pI of GFP.....70
Figure 3.7 Calibration curve (n=5) used to determine pIs of GFP and FQ-labeled GFP.....71
Figure 3.8 CIEF-LIF of the GFP's pI changes upon FQ-labeling.....72
Figure 3.9 Change in GFP's native fluorescence upon FQ-labeling.....74
Figure 3.10 CZE observation of denaturation of GFP upon FQ labeling.....75

Chapter 4
Figure 4.1 CZE of a mixture of molecular weight standards.....84
Figure 4.2 How percentage of HEC in the sieving matrix effects separation.....86
Figure 4.3 Standardization curve of migration time versus molecular weight....87
Figure 4.4 Comparison of separations at different electric field strengths using 1% HEC and a LPA Grignard coated capillary.....89
Figure 4.5 Standardization curves at various electric field strengths using 1% HEC in a LPA Grignard coated capillary.....90
Figure 4.6 Comparison of separations at different electric field strengths using 1% HEC and a polyAAP Grignard coated capillary.....91
Figure 4.7 Standardization curves at various electric field strengths using a 1% HEC sieving matrix in a polyAAP Grignard coated capillary.....93
Figure 4.8 Comparison of separations at different electric field strengths using 1% HEC as a sieving matrix and running buffer with a polyAAP Grignard coated capillary.....94
Figure 4.9 Calibration curves at various electric field strengths using a 1% HEC sieving matrix and 1% HEC in the running buffer with a polyAAP Grignard coated capillary.....96
Figure 4.10 Migration time versus inverse of electric field strength using a 1% HEC sieving matrix and a LPA Grignard coated capillary.....97
Figure 4.11 Migration time versus inverse of electric field strength using a 1% HEC sieving matrix in a polyAAP Grignard coated capillary.....98
Figure 4.12 Migration time versus inverse of electric field strength using a 1% HEC sieving matrix and 1% HEC in the running buffer with a polyAAP Grignard coated capillary.....100
Figure 4.13 Same-day variation in migration times using a 1% HEC sieving matrix with a LPA Grignard coated capillary.....103

Figure 4.14 Same-day variation in migration times using a 1% HEC sieving matrix with a polyAAP Grignard coated capillary.....106
Figure 4.15 Day-to-day variation in migration times using a 1% HEC sieving matrix with a LPA Grignard coated capillary.....109

Chapter 5
Figure 5.1 Differential detergent fractionation method utilized to fractionate HT29 cells.....119
Figure 5.2 The molecular weight-based separation of standard proteins utilizing different percentages of a LPA sieving matrix.....123
Figure 5.3 Ferguson plot for 6-9% LPA sieving matrices.....126
Figure 5.4 Standardization curve of migration time versus molecular weight utilizing a 9% LPA sieving matrix.....129
Figure 5.5 SDS CGE separation of HT29 water-soluble proteins employing a 9% LPA sieving matrix.....132
Figure 5.6 Comparison of SDS-PAGE gel and SDS CGE separations of the HT29 membrane/organelle fraction.....134
Figure 5.7 Comparison of SDS-PAGE gel and SDS CGE separations of the HT29 cytosolic fraction.....135
Figure 5.8 Comparison of SDS-PAGE gel and SDS CGE separations of the HT29 cytoskeletal fraction.....136
Figure 5.9 Comparison of SDS-PAGE gel and SDS CGE separations of the HT29 nuclear fraction.....138

Chapter 6
Figure 6.1 Separation of standard proteins utilizing different percentages of dextran with a high ionic strength buffer.....148
Figure 6.2 Separation of standard proteins utilizing different percentages of dextran with a low ionic strength buffer.....149
Figure 6.3 Ferguson plot for 8-12% dextran sieving matrices with a high ionic strength buffer.....151
Figure 6.4 Ferguson plot for 10-14% dextran sieving matrices with a low ionic strength buffer.....152
Figure 6.5 Standardization curve of log of migration time versus log of molecular weight constructed from a separation utilizing a 6% dextran sieving matrix.....159

Figure 6.6 Separation of standard proteins utilizing a 10% dextran sieving matrix and 50 mM TrisCHES, 0.1% SDS buffer system.....163
Figure 6.7 Separation of standard proteins utilizing a 10% dextran sieving matrix and 50 mM TrisHCl, 0.1% SDS buffer system.....164
Figure 6.8 Separation of standard proteins utilizing a 10% dextran sieving matrix and 10 mM TrisHCl, 0.1% SDS buffer system.....165
Figure 6.9 Separation of standard proteins utilizing a 10% dextran sieving matrix and 7.5 mM TrisHCl, 0.1% SDS buffer system.....166
Figure 6.10 Separation of standard proteins utilizing a 10% dextran sieving matrix and 5 mM TrisHCl, 0.1% SDS buffer system.....168
Figure 6.11 Migration time of replicate runs utilizing a 10% dextran sieving matrix with a 5 mM TrisHCl, 0.1% SDS, pH 8.8, buffer.....169
Figure 6.12 Migration time of replicate runs utilizing a 12% dextran sieving matrix with a 5 mM TrisHCl, 0.1% SDS, pH 8.8, buffer.....172
Figure 6.13 Migration time of replicate runs utilizing a 14% dextran sieving matrix with a 5 mM TrisHCl, 0.1% SDS, pH 8.8, buffer.....174
Figure 6.14 Day-to-day variation in migration times employing a 10% dextran sieving matrix with a 5 mM TrisHCl, 0.1% SDS, pH 8.8, buffer.....177
Figure 6.15 SDS CGE separation of A549 water-soluble proteins employing a 12% dextran sieving matrix.....179
Figure 6.16 SDS CGE separation of A549 nuclear proteins employing a 10% dextran sieving matrix.....180
Figure 6.17 SDS CGE separation of A549 nuclear proteins employing a 10% dextran sieving matrix.....182

Chapter 7
Figure 7.1 SDS-PAGE of A549 nuclear fractions irradiated with 5 Gy.....195
Figure 7.2 SDS-PAGE of A549 nuclear fractions irradiated with 10 Gy.....197
Figure 7.3 SDS-PAGE of A549 nuclear fractions irradiated with 2 Gy.....198
Figure 7.4 2-D electrophoresis gel of A549 nuclear fraction control sample irradiated with 5 Gy.....199
Figure 7.5 2-D electrophoresis of A549 nuclear fraction 24 hour recovery sample irradiated with 5 Gy.....201
Figure 7.6 Unique portion of the mass spectrum of the low molecular weight protein.....204

List of Abbreviations and Symbols

A549	human lung cancer cell line
AAP	acryloylaminopropanol
AIBN	2,2-azobisisobutyronitrile
APS	ammonium persulfate
Asn	asparagine
Asp	aspartate
BSA	bovine serum albumin
C	concentration
CE	capillary electrophoresis
CGE	capillary gel electrophoresis
CHAPS	(3-[3-cholamidopropyl)dimethylammonio]-1-propanesulfonate
CHES	2-[*N*-cyclohexylamino]ethane-sulfonic acid
CIEF	capillary isoelectric focusing
CZE	capillary zone electrophoresis
ΔpI	resolving power of isoelectric focusing
$d\mu/dpH$	protein mobility curve
dpH/dx	pH gradient slope along separation axis
D	diffusion coefficient
D	length of the flight tube
Da	Dalton
DOC	deoxycholic acid
DMA	*N,N*-dimethylacrylamide
DNA	deoxyribonucleic acid
DTT	dithiothreitol
e	charge of an electron
E	electric field
EDTA	ethylenediaminetetra-acetic acid
EOF	electro-osmotic flow
ESI	electrospray ionization
EtOH	ethanol
FQ	3-(2-furoyl)quinoline-2-carboxaldehyde
GC	gas chromatography
GFP	green fluorescent protein
Gly	glycine

Gy	Gray
HAc	hydrochloric acid
HEC	hydroxyethylcellulose
He-Ne	helium-neon
HPC	hydroxypropylcellulose
HPMC	hydroxypropylmethylcellulose
HT29	human colorectal cancer cell line
I	current
I.D.	inner diameter
IEF	isoelectric focusing
IPG	immobilized pH gradient
κ	conductivity
K_r	retardation coefficient
l	average length of polymer strands
L	capillary length
L	distance to detector
LIF	laser-induced fluorescence
LPA	linear polyacrylamide
μ_{ep}	electrophoretic mobility
μ_o	free solution mobility
m	analyte mass
mRNA	messenger ribonucleic acid
MALDI	matrix assisted laser desorption and ionization
MC	methylcellulose
M_D	molecular size of DNA molecule in bases
M_n	number average molecular weight
MS	mass spectrometry
m/z	mass to charge ratio
n	average number of polymer strands per unit volume
n_{H^+}	number of protons per unit volume
N	number of theoretical plates
N	DNA fragment length in bases
N^*	DNA fragment length at the onset of biased reptation
N_{H^+}	number of protons
O.D.	outer diameter
PA	polyacrylamide

PBS	phosphate-buffered saline
PCR	polymerase chain reaction
PDMA	polydimethylacrylamide
PEG	poly(ethylene glycol)
PEO	poly(ethylene oxide)
pI	isoelectric point
PIPES	piperazine-*N,N'*-bis(2-ethanesulfonic acid)
PMSF	phenylmethylsulfonyl fluoride
PPO	poly(propylene)oxide
Pro	proline
PSS	poly(styrenesulfonate)
PVA	polyvinylalcohol
PVP	poly(vinylpyrrolidone)
q	cross-sectional area of capillary
r	thickness of polymer strands
R	resolution
R	protein molecule's radius
R_g	radius of gyration
R^2	correlation coefficient
RNA	ribonucleic acid
σ	standard deviation/zone width in isoelectric focusing
σ^2_D	peak variance due to diffusion
ss	single stranded
SDS	sodium dodecyl sulfate
SDS-PAGE	sodium dodecyl sulfate-polyacrylamide gel electrophoresis
t	migration time
T	temperature
Taps	*N*-tris[hydroxymethyl]methyl-3-amino-propanesulfonic acid
TCA	trichloroacetic acid
TEMED	*N,N,N',N'*-tetramethylethylenediamine
TGS	Tris-glycine-SDS buffer
THF	tetrahydrofuran
TOF	time of flight
Tris	tris[hydroxymethyl]aminomethane
TrisCHES	Tris-CHES buffer
TrisHCl	Tris-hydrochloric acid buffer

Triton X-100	t-octylphenoxypolyethoxyethanol
Trizma base	tris[hydroxymethyl]aminomethane
TTE	Tris-Taps-EDTA buffer
Tween-40	polyoxyethylenesorbitan monopalmitate
UV	ultraviolet
v_{ep}	electrophoretic velocity
v	analyte velocity
V	voltage
W	peak width at baseline
ξ	average pore size
z	analyte charge
2-D	two dimensional
3-D	three dimensional
4-HCCA	α-cyano-4-hydroxycinnamic acid
%C	ratio of bisacrylamide to acrylamide plus bisacrylamide
%T	total acrylamide plus bisacrylamide concentration

Chapter 1
Introduction

1.1 Capillary zone electrophoresis (CZE)

1.1.1 Basic principles of CZE

Electrophoresis is a separation method in which charged particles are separated by the employment of an electric field. Commonly separations of biological molecules are carried out on a slab of gel or inside a capillary column.

Capillary zone electrophoresis was introduced by Jorgenson and Lukacs in 1981 (1-3). The velocity (v_{ep}) of a solute in m/s is given as:

$$v_{ep} = \mu_{ep} E \qquad (1.1)$$

where μ_{ep} is the electrophoretic mobility in m^2/Vs and E is the electric field in V/m. The electric field is a function of the voltage and the length of the capillary. The solute's mobility is determined both by its charge and the friction it encounters as it travels through the capillary. It can then be written that the time the solute takes to migrate through the capillary is:

$$t = \frac{L}{v_{ep}} \qquad (1.2)$$

where t is the migration time in seconds and L is the length of the capillary in metres. Substituting Equation 1.1 into Equation 1.2:

$$t = \frac{L}{\mu_{ep} E} \qquad (1.3)$$

where the variables are as defined above.

These equations are only applicable in the absence of electro-osmosis. Since the majority of the separations presented in this thesis are performed in the absence of electro-osmosis, only these equations are presented. The equations which pertain to the separation in the presence of electro-osmosis will not be discussed.

1.2 Capillary gel electrophoresis (CGE)

1.2.1 Basic principles of CGE

DNA molecules possess similar mass-to-charge ratios which means that their mobilities in free solution are identical because they are independent of molecular size (4-6). For separation to be achieved, DNA must be sieved according to size by a polymer matrix inside of a capillary (7-10). DNA has also been separated in free

solution utilizing a technique called end-labeled free-flow capillary electrophoresis (5, 6), which will not be discussed in this brief introduction.

During electrophoresis, DNA molecules collide with the sieving polymer which results in a reduction of mobility. The DNA molecules of different sizes interact differently with the sieving matrix and undergo different mobility changes based on size. It is these interactions with the sieving matrix which result in a size-based separation of DNA molecules. Two theories have been proposed to describe the movement of DNA through sieving matrices in the presence of an electric field- the Ogston model (11) and the biased reptation model (12-17). These two models will be discussed in the following two sections.

1.2.2 The Ogston model

Ogston developed a model to describe the pore size distribution that exists in a random network of linear fibres (agarose in this case) in 1958 (11). The polymer matrix in this model is treated as a molecular sieve and the DNA molecules are treated as nondeformable particles with a radius equal to their radius of gyration. The mobility of the DNA is a function of both its free solution mobility and the probability that the DNA will meet a pore large enough to allow the passage of DNA through it. This is shown as follows:

$$\mu = \mu_o P(\xi \geq R_g) \qquad (1.4)$$

where μ is the mobility of the DNA molecule, μ_o is the free solution mobility of the DNA fragment, $P(\xi \geq R_g)$ is the probability that a pore has a radius greater than or equal to the radius of the DNA molecule, ξ is the average pore size, and R_g is the radius of gyration of the DNA molecule. Ogston's model of pore size distribution for a network of linear polymers predicts that the volume fraction of pores that are large enough to allow a DNA molecule of radius, R_g, to enter is:

$$P(\xi \geq R_g) = e^{[-\pi n l (r+R_g)^2]} \qquad (1.5)$$

where n is the average number of polymer strands per unit volume, l is the average length of the polymer strands, and r is the thickness of the polymer strands. The model assumes that the concentration of the gel, C, is the product of n and l. Thus, Equation 1.5 can be written as:

$$P(\xi \geq R_g) = e^{[-KC(r+R_g)^2]} \qquad (1.6).$$

Upon combination of Equations 1.4 and 1.6, Equation 1.7 is obtained:

$$\mu = \mu_o e^{[-KC(r+R_g)^2]} \qquad (1.7)$$

where the term $K(r+R_g)^2$ is called the retardation coefficient, K_r (18). The retardation coefficient is a species' characteristic in a certain polymer system. Equation 1.7 can then be written as:

$$\log \mu = \log \mu_o - 2.303 K_r C \qquad (1.8).$$

A plot of logarithm of mobility versus gel concentration will yield a straight line and is termed a Ferguson plot (19).

There are many problems with the oversimplification that the Ogston model presents of DNA movement through a gel. The model does not address the connectedness of the pores available to the DNA fragments (20). Associated with this concern is the assumption that the agarose gel medium is a random network of agarose fibres (20). Secondly, the model assumes that the DNA are undeformable entities. This fails to presume that the DNA may deform as a result of the electric field (20) or may deform in order to pass through a pore not predicted large enough for this to occur (21). The theory predicts that a DNA molecule with a radius much greater than the average pore size will have an electrophoretic mobility which eventually reaches zero. However this phenomenon has been dispelled by experimental observations (16, 22, 23). It is clear that the Ogston model is applicable only to small fragments of DNA. To describe the mobility of larger fragments of DNA through a polymer matrix, the biased reptation model has been developed.

1.2.3 The biased reptation model

The reptation mechanism was first presented in 1971 (24-26) and then later adapted to describe gel electrophoresis of biopolymers (27). The biased reptation model describes the DNA's movement through the sieving matrix as being analogous to a reptile slithering head first through grass. The DNA fragment is not considered undeformable, but rather is considered to be constricted to moving through the tubes which are formed by the polymer matrix. The mobility of the DNA fragment is predicted to be inversely proportional to the fragment length:

$$\mu \approx \frac{1}{N} \qquad (1.9)$$

where N is the fragment length in bases.

The biased reptation model takes into account that when the electric field strength is increased, the DNA molecule may change from a random coil into an elongated strand. The mobility of the DNA is still inversely related to fragment length:

$$\mu = \chi\left[\frac{1}{N} + \frac{1}{N^*}\right] \qquad (1.10)$$

where χ is a constant and N^* is the fragment length at which the onset of biased reptation is apparent. Furthermore, Equation 1.10 can also be written as:

$$\mu = \chi\left[\frac{1}{N} + \left(\alpha\frac{E}{T}\right)^{\beta}\right] \qquad (1.11)$$

where α is a constant, E is the electric field strength, T is the temperature, and β is a constant. Biased reptation theory predicts β to be 2, however a newer model termed biased reptation with fluctuations (15, 16) predicts that β is 1. The limiting mobility of the DNA decreases proportionally with electric field (17, 28). The key prediction of the biased reptation model, which has been experimentally proven (29), is that as molecular size of the DNA increases, or as the electrical field increases, the mobility's dependence on molecular size decreases. In other words, when the DNA molecules maintain a random-coil conformation, their mobility decreases proportionally with the inverse of their number of bases (30, 31). Large molecules, however, orient in the electric field direction and their mobility essentially becomes size-independent after a certain threshold size of DNA fragments (12, 31, 32).

The biased reptation model also predicts a phenomenon called band inversion (33). When band inversion occurs, large DNA fragments move faster than small fragments. Band inversion is due to the so called self-trapping (i.e. in U-shaped conformations) of intermediate-sized DNA fragments into zero-velocity, compact molecular shapes (34, 35). Experimental observations have confirmed this prediction (34).

At low electric fields, both the Ogston model and the biased reptation with fluctuations model are valid. However, caution must be exercised when utilizing either of these models to predict the movement of DNA molecules separated at high electric field strengths such as those employed by capillary electrophoresis.

1.2.4 Resolution in CGE DNA sequencing

Much attention has been paid to the development of electrophoretic velocity in DNA sequencing theory, however band broadening has not been addressed adequately. As in chromatography, the resolution of a DNA sequencing run can be utilized to judge whether or not the separation is sufficient. In DNA sequencing, satisfactory resolution (R) is ≥ 0.5, and is calculated as follows:

$$R = \frac{2(t_2 - t_1)}{W_1 + W_2} \qquad (1.12)$$

where t_1 and t_2 are the migration times of the two peaks and W_1 and W_2 are the peak widths at baseline of the two peaks. Obviously, for DNA sequencing, it is required that the resolving power of the separation be able to differentiate single bases.

There are many sources of band broadening in DNA sequencing (36-38). Because of both a better understanding and more technical progress, many of these band broadening factors can be minimized. The band width can be affected by loading width, the temperature gradient, the electric field gradient, interactions between the DNA and the capillary walls, and also the detection system capabilities (37, 39). Since most of these aforementioned factors affecting bandwidth can be governed, their effects on band broadening are minimized, except for thermal diffusion, which is not controllable (31, 35, 39). The Einstein equation represents the peak variance due to diffusion:

$$\sigma_D^2 = 2Dt \qquad (1.13)$$

where D is the diffusion coefficient and t is the migration time of the DNA molecule. Based on the biased reptation with fluctuations model, Slater has shown that the Einstein equation does not apply to DNA molecules in an electric field (35). Slater's calculations show that the diffusion coefficient for DNA in an electric field should be much larger than the Einstein equation predicts (35).

Experiments have now been developed which allow the measure of the diffusion coefficient of DNA during electrophoresis (40, 41). The results of these experiments confirm the above findings of Slater regarding the actual diffusion coefficient of DNA (35). It is predicted that at extremely low electric fields, the diffusion coefficient is unaffected by the electric field's presence and should be identical to that in the absence of a field altogether (42). For fields utilized for slab gel sequencing, the diffusion coefficient scales as:

$$D \sim \frac{E}{\sqrt{M_D}} \qquad (1.14)$$

where M_D is the molecular size of the DNA molecule in bases. This equation has devastating effects on CGE sequencing as the diffusion coefficient increases proportionally with electric field strength and only decreases slowly with the molecular size. At the extreme of very high fields, diffusion coefficients are independent of molecular size and the fragments co-migrate.

1.2.5 High throughput CGE DNA sequencing

The past two years have been a very exciting time in the field of CGE DNA sequencing. The realization of high throughput sequencing has come about with the employment of multi-capillary CGE sequencing machines which run twenty-four hours a day, seven days a week. Utilizing this technology, Celera Genomics has been able to sequence the entire human genome as well as over one billion bases of the mouse genome (43-45). These accomplishments have been made with a number of improvements over conventional DNA CGE sequencing.

A number of advances have been made to allow for high throughput sequencing to be a reality. As mentioned, robust, reliable multi-capillary machines have been built. These sequencing machines contain 96 capillaries and are capable of running continuously around the clock. Secondly, a number of improvements have been made on a smaller scale which deal with the capillaries themselves. A replaceable sieving matrix has been designed which is fabricated of polydimethylacrylamide (PDMA) (10). These nonviscous sieving matrices can be pumped into and out of the capillaries between runs. The low viscosity of these PDMA sieving matrices is a major advantage which results in cost savings as well as the elimination of problems associated with polymerizing inside of capillaries. Furthermore, PDMA sieving matrices are compatible with bare silica capillaries, thus doing away with the need to derivatize capillaries in attempts to eliminate electro-osmotic flow.

Chapter 2 examines the DNA sequencing capabilities of a replaceable PDMA sieving matrix in uncoated capillaries at high temperatures.

1.3 Capillary isoelectric focusing (CIEF)

1.3.1 Basic principles of CIEF

CIEF is a separation technique which distinguishes proteins from one another by their isoelectric points (pIs), i.e. the point at which a protein is electrically neutral. CIEF was introduced by Hjertén *et. al.* in 1985 (46). Sample and ampholytes are introduced together into the capillary. In an applied electric field, the ampholytes create a pH gradient. Ampholytes are molecules which have both acidic and basic groups (i.e. zwitterionic compounds) with pI values which span the entire pH gradient. In CIEF, the acid is at the anode and the base is at the cathode. Generally, the catholyte (e.g. sodium hydroxide) molarity is two times that of the anolyte (e.g. phosphoric acid). During electrophoresis, the sample components focus to their pI values. If the sample

bands diffuse, they will acquire a charge and migrate back to their pI. Detection is achieved through either the mobilization of the capillary's contents past a detector or whole column scanning.

1.3.2 Focusing

The compounds responsible for setting up the pH gradient in CIEF are the ampholytes. Besides having many pIs, ampholytes must also be suitable buffers and suitable conductors at their pIs. These properties are important so that the ampholytes can carry the electric current as well as maintain a uniform pH gradient. Ampholytes will not exit the capillary during electrophoresis because the pH outside of the capillary is either higher or lower than the ampholytes' pIs. In order to achieve resolution between two compounds, at least one ampholyte must have a pI which is intermediary to the two components to be resolved (47).

Focusing begins with the immersion of the capillary's ends in anolyte and catholyte, and then the application of an electric field. At the same time that the ampholytes create a pH gradient, the sample components are migrating to their pIs to achieve a steady state. At this steady state, the proteins form narrow zones at their pI values. Focusing is accompanied by a drop in current. At the beginning of the separation, sample components and ampholytes are charged and thus carry current. However, as the capillary's contents become focused, they become electrically neutral and the current drops. Focusing is considered complete when the current is 10% of its original value- focusing beyond this indication point dramatically increases the likelihood of protein precipitation. The steady state condition is described as:

$$C_{H^+} + \Sigma C_{NH_3^+} = C_{OH^-} + \Sigma C_{COO^-} \qquad (1.15)$$

where C_{H^+}, C_{OH^-}, $C_{NH_3^+}$, and C_{COO^-} are the concentrations of protons, hydroxyl ions, positive, and negative groups in the ampholytes, respectively, in units of M or Coulomb/m^3 (48). The number of protons, N_{H^+}, electrophoretically passing from the anolyte across the boundary between anolyte and medium per unit time is:

$$N_{H^+} = v_{H^+} q n_{H^+} \qquad (1.16)$$

where v_{H^+} is the protons' migration velocity in the anolyte, q is the capillary's cross-sectional area, and n_{H^+} is the number of protons in the anolyte per unit volume. Since,

$$v_{H^+} = E\mu_{H^+} \qquad (1.17)$$

where E is the electric field strength, and μ_{H^+} is the mobility of the protons in the anolyte, and

$$E = \frac{I}{q\kappa} \qquad (1.18)$$

where I is the current, and κ is the anolyte's conductivity, the following expression is obtained:

$$N_{H^+} = \frac{I\mu_{H^+}\nu_{H^+}}{\kappa} \qquad (1.19).$$

1.3.3 Mobilization

There are different modes of mobilization in CIEF, including chemical mobilization, hydrodynamic mobilization, and electro-osmotic flow mobilization. The first two modes involve a capillary which has no electro-osmotic flow present. Chemical mobilization was introduced by Hjertén *et. al.* (46, 48) and involves changing the chemical composition at one end of the capillary, which induces a pH change and thus causes the capillary's contents to be expelled. Hydrodynamic mobilization is achieved by applying pressure (46, 49), a vacuum (50), or a siphon (51) to one end of the capillary to expel the focused protein zones. It should also be noted that occasionally no mobilization method is required as the capillary is scanned through a detector (48, 52) or alternatively the detector, such as a concentration gradient detector, is scanned along the capillary (53-62). In Chapter 3 of this thesis, chemical mobilization at the anodic end of the capillary is employed, hence this will be the only form of mobilization which is described in depth.

Anodic mobilization involves changing the composition of the anolyte and results in the ampholytes and sample components gaining a net negative charge. The equation which accompanies this increase in pH is the addition of a positive term to the left side of Equation 1.15:

$$C_{X^{n+}} + C_{H^+} + \Sigma C_{NH_3^+} = C_{OH^-} + \Sigma C_{COO^-} \qquad (1.20)$$

where X^{n+} (n is the valency of the ion) is the cation added to the anolyte to induce mobilization. Equation 1.20 demonstrates how mobilization is accomplished by replacing the anolyte with a cation which will enter the capillary via electrophoresis.

The course of events which occurs during mobilization can be revealed upon examination of how the anolyte's composition affects the flux of protons into the capillary. Similar to Equation 1.19 written for the steady state during focusing, an equation can be written for the mobilization step:

$$N'_{H^+} = \frac{I'\mu'_{H^+} n'_{H^+}}{\kappa'} \qquad (1.21)$$

where the primed parameters refer to the mobilization step conditions, i.e. I' is the current in the capillary, n'_{H+} is the number of protons in the mobilization anolyte, and κ' is the conductivity of the mobilization anolyte. In the initial stages of mobilization, the current, I', is about the same value as I in the focusing step and μ_{H+} is approximately equal to μ'_{H+}, the following equation is obtained:

$$\frac{N_{H^+}}{N'_{H^+}} = \frac{\kappa'}{\kappa} \cdot \frac{n_{H^+}}{n'_{H^+}} \qquad (1.22).$$

Thus, if the number of protons is not changed from focusing to mobilization, then

$$\frac{N_{H^+}}{N'_{H^+}} = \frac{\kappa'}{\kappa} \qquad (1.23).$$

If the conditions are such that $\kappa << \kappa'$, the ratio of N_{H+}/N'_{H+} will be $>>1$. Because of the increase in conductivity due to supplementing the anolyte with a cation, the number of protons entering the capillary from the anolyte decreases, and thus the resulting increase in pH in the capillary.

Chemical mobilization is accompanied by a change in current. Initially the change in current is negligible, however as cations from the mobilizing anolyte enter the capillary, the current gradually increases (63, 64).

1.3.4 Resolution in CIEF

The zone width (i.e. standard deviation), σ, is given by the following equation:

$$\sigma = \sqrt{\frac{D}{\left(d\mu/dpH\right)\left(dpH/dx\right)}} \qquad (1.24)$$

where $d\mu/dpH$ is the mobility curve of the protein and dpH/dx is the slope of the pH gradient along the separation axis.

The resolving power of this technique is expressed as ΔpI, i.e. the difference between pIs of a protein and its just resolved nearest contaminant is (65):

$$\Delta pI = 3\sqrt{\frac{D\left(dpH/dx\right)}{E\left(-d\mu/dpH\right)}} \qquad (1.25).$$

Equation 1.25 shows that satisfactory resolution is obtainable with components which have low diffusion coefficients and high mobility slopes at the isoelectric point. The aforementioned characteristics are true of all proteins (66). Experimental conditions

must be optimized to minimize ΔpI. High electric field strengths and shallow pH gradients are desired to achieve the best resolution (67, 68). For immobilized pH gradients, the ΔpI is as low as 0.0001 pH units because extremely narrow pH gradients can be generated (67, 68).

1.3.5 The potential of CIEF

IEF was originally developed as a preparative technique. Although CIEF is still in its early stages of development, CIEF applications involve both preparative and separative techniques. CIEF is an attractive technique because of its protein concentrating abilities, and it can also be coupled to another technique for two-dimensional analysis. For example, CIEF's concentrating powers are utilized as a preparative technique for mass spectrometry (69, 70). In recent years, extensive work has also been done to design two dimensional systems of CIEF and mass spectrometry (71-78). Since CIEF is still in its infancy, much more research has yet to be done with this powerful separation technique.

Chapter 3 will delve into the realm of CIEF with laser-induced fluorescence (LIF) detection employing a model protein.

1.4 Sodium dodecyl sulfate capillary gel electrophoresis (SDS CGE) of proteins

1.4.1 Basic principles of protein size-based separations

One of the most common separation methods of proteins is by sodium dodecyl sulfate polyacrylamide gel electrophoresis (SDS-PAGE). SDS binds to denatured proteins with a constant ratio of 1.4 g of SDS to 1 g of denatured protein (79), which is equivalent to about one SDS molecule per two amino acid residues (80). The consequences of this constant binding are proteins which are all highly negatively charged and have similar mass-to-charge ratios. Exceptions to this SDS binding ratio are glycoproteins, proteins which are very acidic, and special cases (81), which bind very little SDS, for e.g. pepsin binds under 0.2 g SDS per 1 g of protein (82). It is important that proteins are completely denatured when mixed with SDS because if the proteins contain any disulfide bonds they will only bind in a ratio of 0.9 g to 1 g of SDS to 1 g of protein (83). A polyacrylamide slab gel is utilized to separate the proteins based on molecular weight. The pore size of the gel will determine which proteins are

best separated- low or high molecular weight proteins. Polyacrylamide gels are referred to as x %T and x %C where %T is the total acrylamide plus bisacrylamide concentration and %C is the ratio of bisacrylamide to acrylamide plus bisacrylamide. The polyacrylamide gels utilized for SDS-PAGE are composed of a stacking gel and a separating gel. The proteins are loaded onto the stacking gel which has large pores and allows the proteins to migrate uniformly, thus "stacking" at the interface between the stacking and separating gels. The separating gel has smaller pores and is the gel which actually separates the proteins according to size.

1.4.2 Ferguson plot analysis

In 1964, following Smithies (84), Ferguson demonstrated through experiments that a linear plot of logarithm of protein mobility versus agarose gel concentration has a slope which is proportional to molecular size (19). The relationship between the protein mobility and the sieving matrix concentration is found in Equation 1.8 in Section 1.2.2, and is:

$$\log \mu = \log \mu_o - K_r C \qquad (1.26).$$

Ogston's model (11) is the basis for the derivation of the relationship between the retardation coefficient and the protein's radius:

$$K_r = \pi l'(r + R)^2 \qquad (1.27)$$

where R is the radius of the protein molecule.

Ferguson plots are employed to test whether or not a separation technique is based on size. Obviously, linear plots indicate that the separation is size-based. Deviations from linearity indicate that the separation is not necessarily size-based or that the concentration of sieving matrix is not optimal. For example, if the Ferguson plot slopes for two proteins intersect at a point on the Ferguson plot other than at the y-axis, this indicates that the protein migration order may be unknown for separations employing gel concentrations which are lower than the point of intersection. The utilization of Ferguson plots allows for the selection of the optimum sieving matrix concentration for separations of given proteins.

Information obtainable from a Ferguson plot indicates more than solely whether or not a separation is size-based. The y-intercept from the Ferguson plot is a measure of a protein's free solution mobility. Because of the constant binding ratio of SDS to proteins, the free solution mobilities of the given proteins should be identical. An unknown protein's retardation coefficient is extracted from the slope of the Ferguson plot. A standard curve of logarithm molecular weight versus square root of K_r is

constructed from the separation results of known proteins. The unknown protein's K_r is then utilized to determine its molecular weight from a standard curve.

1.4.3 A comparison of SDS-PAGE and SDS CGE

Even though SDS-PAGE is an incredibly popular method of protein separation, it has some inherent drawbacks. Compared to SDS CGE, SDS-PAGE utilizes larger quantities of chemicals, even when the mini-gel format is employed. SDS-PAGE is conducted on polyacylamide gels, of which the monomers of acrylamide and bisacrylamide are known neurotoxins (85). Since some SDS CGE separations are performed with polymers other than acrylamide, the utilization of acrylamide can be avoided altogether. SDS-PAGE gels required microlitre volumes of proteins, whereas SDS CGE separations only utilize nanolitre volumes of what are usually precious samples. SDS-PAGE gels require a staining procedure to visualize the bands on a gel, such as silver stain or Coomassie stain, and then are evaluated by a densitometer. SDS CGE separations do not require this labourious staining step and can be directly quantitated by the detector. In the case of UV detection, the natural fluorescence of amino acids is detected, however in the case of LIF detection, the proteins must be chemically derivatized with a fluorescent dye. However, this fluorescent derivatization step still requires less time overall than either silver or Coomassie staining require. Unless utilizing a multi-capillary instrument, SDS CGE separations only run one sample at a time. However, since many of the polymer solutions utilized for SDS CGE separations are replaceable, many samples can be run in the same amount of time it would take to perform an SDS-PAGE analysis. Moreover, whereas Ferguson plot analysis is tedious with SDS-PAGE, Ferguson plots are easily generated by CGE techniques by simply diluting the sieving buffer (86, 87).

1.4.4 A brief history of SDS CGE separations

The area of SDS CGE separations is still relatively young. The first reports of this type of separation method only date back to 1987 (88, 89). Initially cross-linked polyacrylamide (PA) was employed as a sieving matrix. However, the utilization of cross-linked PA is plagued by problems associated with polymerizing the sieving matrix *in situ* (90). Thus came a shift to linear PA (LPA) sieving matrices for SDS CGE separations by a number of research groups (90-94). A commercial replaceable LPA sieving matrix was also available for a time, but has since gone off the market.

Replaceable sieving matrices are preferred for separations for a number of reasons. As previously mentioned, working with a sieving matrix which is not polymerized *in situ* simplifies many aspects of preparation. When a replaceable sieving matrix is utilized obviously sieving matrix preparation is less tedious, the capillary preparation is generally simpler, problems associated with polymerization inside of the capillary are eliminated, and cross-contamination concerns between runs are abolished. The quest to find a suitable replaceable sieving matrix for SDS CGE size-based separations has increased the number of different polymers which are employed. Poly(ethylene oxide) (PEO) (95, 96) and poly(ethylene glycol) (PEG) (92, 96) have both been utilized as sieving matrices for SDS CGE separations. PEO and PEG are successful sieving matrix components as these two polymers have been the basis of a commercially available sieving matrix kit. Nakatani *et. al.* demonstrated that pullulan can also be employed as a sieving matrix for proteins (97). Dextran has also been reportedly used by a number of research groups to separate proteins based on size (92, 95, 98-101).

Chapters 4, 5, and 6 of this thesis examine the utilization of different sieving matrices to separate protein molecular weight markers and complex, real samples by SDS CGE with LIF detection.

1.5 The proteomics approach to protein identification

1.5.1 An introduction to proteomics

The term proteome was coined in 1996 by Wilkins to define an organism's total protein complement (102). This phrase is the sister of the catch phrase genome which describes the total genetic make up of an organism. The field of proteomics is a huge undertaking by scientists to decipher cellular information at the level of proteins. An organism's genetic sequence, for example, that of the human, represents an incredible amount of data. However, knowing the DNA sequence of an organism does not allow the prediction of which proteins are going to be expressed by that organism. Proteomics is an attempt to study which proteins are expressed, and in which form(s) they are expressed.

There are many possibilities regarding the fate of DNA of an organism. When a gene is expressed, it results in the transcription of its DNA sequence into mRNA which is then processed and translated into a protein. When the DNA is transcribed into mRNA, some of the primary mRNA sequence may be spliced out and does not

form part of the mature mRNA sequence. Genes may be present, mutated, and not necessarily transcribed or some genes may be transcribed into mRNA but not translated into proteins (103). Furthermore, levels of mRNA do not correlate well with levels of protein expression (104, 105). Post-translational modifications occur to proteins to control their functions, but this post-translational modification cannot be predicted. The processes of protein growth and degradation are incredibly dynamic and are capable, independently of mRNA levels, of altering the final amount of active protein. Predictions about protein expression and dynamics cannot be made solely on the basis of knowing a genetic code.

1.5.2 Two dimensional (2-D) gel electrophoresis

2-D gel electrophoresis technology was originally described in 1975 by O'Farrell (106). The first dimension of separation is by IEF and the second dimension is SDS-PAGE (106-108). Initially, the first dimension was run utilizing cast tube gels. However, tube gel preparation is somewhat of an art and employment of tube gels can lead to large reproducibility problems between laboratories. IEF technology has lead to the development of immobilized pH gradients (IPGs) (109-111) in which the pH gradient is covalently immobilized and the polyacrylamide gel is attached to a rigid plastic support. The advent of IPG technology has led to greater reproducibility of 2-D gels, enhanced resolution (as pH gradients as narrow as 0.05 pH/cm can be established (103)), and increased 2-D map information exchange between laboratories (112).

2-D electrophoresis is currently one of the most powerful separation techniques available to separate complex mixtures of proteins. The resulting protein map can represent up to 10 000 proteins (113). The 2-D gel separation allows the proteins to be characterized not only qualitatively, but also quantitatively. Qualitatively, the map reveals new protein expression, post-translational modifications, and relative abundance of proteins (103). Quantitatively the map reveals up and down regulation and co-regulation of proteins (103).

Inherently, there are some drawbacks to 2-D electrophoresis. First of all, only highly abundant proteins are seen on the gels. One solution to this problem is to carry out sample preparation which fractionates a complex sample into smaller parts (114). Another problem, which is related to the aforementioned problem, is that one spot on the gel may actually represent more than one protein. Estimates are that for prokaryotes, about 20% of all spots contain more than one protein (115), whereas with eukaryotes, approximately 40% of all spots on the gel represent more than one protein. A possible

solution to this problem is the utilization of either very large format gels (116) or by constructing a large map out of many overlapping narrow pH range gels (117). The latter solution, by analogy to genome mapping, is a technique called 'Proteome Contigs' (117). Lastly, although 2-D gels reveal much information about a protein such as pI, molecular weight, relative abundance, post-translational modifications, etc., they do not identify proteins. This is where the powerful technique of mass spectrometry (MS) enters the proteomics equation.

1.5.3 Mass spectrometry for protein identification

The soft ionization techniques in MS have greatly aided in the efforts of protein identification. These two techniques are electrospray ionization (ESI) developed by Fenn *et. al.* (118) and matrix assisted laser desorption and ionization (MALDI) developed by Hillenkamp *et. al.* (119). Peptide levels of detection utilizing MALDI with time of flight (TOF) is femtomoles (120). Only MALDI TOF will be discussed here because it is utilized in Chapter 7 of this thesis for protein identification.

In MALDI, the analyte is incorporated into the crystalline structure of a matrix. The matrix is composed of small UV-absorbing molecules which provide a vehicle for ions to be created from polar or charged biomolecules (121). For ionization to occur, the organic matrix crystals must absorb at the wavelength of the laser, which is usually the nitrogen laser (λ=337 nm) (122). The laser strikes the matrix molecules which absorb light and are heated. The sublimation and expansion of both matrix and analyte results from this rapid heating. Ion formation can occur through proton-transfer reactions in the gas phase mixture with matrix molecules. This ionization process also serves to remove contaminants such as buffer and salt from the analyte. Singly precharged ions are created by MALDI, resulting in a one-to-one ratio between ions in the mass spectrum and the analytes in the original mixture (123).

In TOF MS, mass-to-charge ratios are determined by measuring how long it takes for ions to move through a field-free region. The kinetic energy of the ions is expressed as:

$$\text{kinetic energy} = \frac{1}{2}mv^2 \tag{1.28}$$

and,

$$\frac{1}{2}mv^2 = Ve \tag{1.29}$$

where m is the apparent mass of the ion, v is the velocity, V is the voltage, and e is the charge of an electron. Since velocity is the length of the flight tube (D) divided by the time required to travel the distance (t), Equation 1.29 can be rearranged to obtain:

$$t = D\sqrt{\frac{m}{2Ve}} \qquad (1.30).$$

In the case of multiply charged ions, m is equivalent to the mass to charge (m/z) ratio, so that Equation 1.30 can be written as:

$$t = D\sqrt{\frac{m}{2zVe}} \qquad (1.31).$$

Once a 2-D gel is run and stained, the protein spot of interest is carefully excised from the gel and subjected to a digestion procedure resulting in signature peptide fragments. Digestion of a protein is performed either with enzymes or chemicals which cleave the protein into peptide fragments. Chemical cleavage may be accomplished with cyanogen bromide (methionine cleavage), 2-nitro-5-thiocyano-benzoic acid (cysteine cleavage), 2-(2-nitrophenylsulfenyl)-3-methyl-3-bromoindolenine (tryptophan cleavage), hydroxylamine (cleavage of Asn-Gly bonds), and acid (cleavage of Asp-Pro bonds) (124). However the most useful of these chemical cleavages is that of cyanogen bromide as the other methods cleave scarce amino acids and are more inclined to produce side reactions (124). Enzymatic digestions involve the utilization of trypsin (cleavage of lysine and arginine) or chymotrypsin (cleavage of uncharged residues of residues with aromatic or hydrophobic side chains). Specifically, in Chapter 7 of this thesis, trypsin digestion is employed utilizing the methods of Shevchenko *et. al.* (125) and Wilm *et. al.* (126). The protein digestion is performed in gel and the resulting peptides are extracted for MS analysis.

Peptide mass fingerprinting is the process by which proteins are identified from their peptides utilizing MS. The concept of peptide mass fingerprinting was introduced independently by five groups in 1993 (127-131). The fingerprint analogy is utilized because MS analysis of a protein's peptides is a unique characteristic of the protein. The identity of a protein is determined by comparing the peptide map of the unknown protein with the theoretical peptide maps produced by the digestion of proteins in the database. A single peptide mass is not unique to a specific protein and the rule of thumb is that at least three peptides derived from one protein must be utilized for a database search (132). An identity match is made when most of the m/z values in the mass spectrum match most of those of the theoretical digest. It is important to be able

to determine the *m/z* values with a high degree of accuracy, as when the accuracy increases, the number of peptides in the database that will match the weight decreases.

Chapter 7 of this thesis utilizes peptide mass fingerprinting to identify proteins from a human lung cancer (A549) cell line which are affected by γ-irradiation.

1.6 Thesis summary

The work in this thesis spans the shift in thinking between genome and proteome.

Chapter 2 presents the development and characterization of a CGE DNA sequencing polymer. This technology is key in high throughput DNA sequencing.

Chapter 3 presents the utilization of CIEF with LIF detection to study the effects fluorescent labeling has on the pI of a model protein. The work in this chapter also indicates that fluorescent labeling of a protein can lead to its denaturation.

Chapters 4, 5, and 6 present the employment of different sieving matrices for SDS CGE size-based separations of proteins. The chapters demonstrate differences in sieving capabilities of three matrices and the potential use of these methods to separate complex mixtures of proteins.

Chapter 7 illustrates the power of peptide mass fingerprinting as well as demonstrates some of the difficulties encountered with this new field of proteomics. Attempts to identify two proteins of interest were undertaken. Information regarding the identity of one of the proteins is presented.

1.7 References

(1) Jorgenson, J. W.; Lukacs, K. D. *Analytical Chemistry* **1981,** *53*, 1298-1302.

(2) Jorgenson, J. W.; Lukacs, K. D. *Journal of Chromatography* **1981,** *218*, 209-216.

(3) Jorgenson, J. W.; Lukacs, K. D. *Science* **1981,** *222*, 266-272.

(4) Olivera, B. M.; Baine, P.; Davidson, N. *Biopolymers* **1964,** *2*, 245-257.

(5) Heller, C.; Slater, G. W.; Mayer, P.; Dovichi, N. J.; Pinto, D.; Viovy, J.-L.; Drouin, G. *Journal of Chromatography A* **1998,** *806*, 113-121.

(6) Ren, H.; Karger, A. E.; Oaks, F.; Menchen, S.; Slater, G. W.; Drouin, G. *Electrophoresis* **1999,** *20*, 2501-2509.

(7) Sunada, W. M.; Blanch, H. W. *Electrophoresis* **1997,** *18*, 2243-2254.

(8) Dovichi, N. J. *Electrophoresis* **1997,** *18*, 2393-2399.

(9) Quesada, M. A. *Current Opinion in Biotechnology* **1997,** *8*, 82-93.

(10) Madabhushi, R. S. *Electrophoresis* **1998,** *19*, 224-230.

(11) Ogston, A. G. *Transactions of the Faraday Society* **1958,** *54*, 1754-1757.

(12) Lumpkin, O. J.; Dejardin, P.; Zimm, B. H. *Biopolymers* **1985,** *24*.

(13) Slater, G. W.; Mayer, P.; Hubert, S. J.; Drouin, G. *Applied and Theoretical Electrophoresis* **1994,** *4*, 71-79.

(14) Mayer, P.; Slater, G. W.; Drouin, G. *Applied and Theoretical Electrophoresis* **1993,** *3*, 147-155.

(15) Duke, T. A.; Viovy, J.-L.; Semenove, A. N. *Biopolymers* **1994,** *34*, 239-247.

(16) Heller, C.; Duke, T. A.; Viovy, J.-L. *Biopolymers* **1994,** *34*, 249-259.

(17) Viovy, J. L.; Duke, T. *Electrophoresis* **1993,** *14*, 322-329.

(18) Rodbard, D.; Chrambach, A. *Proceedings of the National Academy of Sciences, USA* **1970,** *65*, 970-977.

(19) Ferguson, K. A. *Metabolism* **1964,** *13*, 985-1002.

(20) Slater, G. W.; Rousseau, J.; Noolandi, J.; Turmel, C.; Lalande, M. *Biopolymers* **1988,** *27*, 509-524.

(21) Grossman, P. D.; Soane, D. S. *Biopolymers* **1991,** *31*, 1221-1228.

(22) Holmes, D. L.; Stellwagen, N. C. *Electrophoresis* **1990,** *11*, 5-15.

(23) Yan, J. Y.; Best, N.; Zhang, J. Z.; Ren, H. J.; Jiang, R.; Hou, J.; Dovichi, N. J. *Electrophoresis* **1996,** *17*, 1037-1045.

(24) de Gennes, P. G. *Journal of Chemical Physics* **1971,** *55*.

(25) de Gennes, P. G. *Scaling Concepts in Polymer Physcis*; Cornell University Press: Ithaca, 1979.

(26) Doi, M.; Edwards, S. F. *Journal of the Chemical Society Faraday Transactions II* **1978,** *79*, 1789-1818.

(27) Lerman, L. S.; Frisch, H. L. *Biopolymers* **1982,** *21*, 995-997.

(28) Duke, T.; Viovy, J.-L. *Physical Reviews* **1994,** *49*, 2408-2416.

(29) Hervet, H.; Bean, C. P. *Biopolymers* **1987,** *26*, 727-742.

(30) Lumpkin, O. J.; Zimm, B. H. *Biopolymers* **1982,** *21*, 2315-2316.

(31) Slater, G. W.; Drouin, G. *Electrophoresis* **1992,** *13*, 574-582.

(32) Slater, G. W.; Noolandi, J. *Biopolymers* **1986,** *25*, 431-454.

(33) Noolandi, J.; Rousseau, J.; Slater, G. W.; Turmel, C.; Lalande, M. *Physics Review Letters* **1987,** *58*, 2428-2431.

(34) Slater, G. W.; Turmel, C.; Lalande, M.; Noolandi, J. *Biopolymers* **1989,** *28*, 1793-1799.

(35) Slater, G. W. *Electrophoresis* **1993,** *14*, 1-7.

(36) Slater, G. W. In *Analysis of Nucleic Acids by Capillary Electrophoresis*; Heller, C., Ed.; Vieweg & Son: Wiesbaden, 1997, pp 24-66.

(37) Grossman, P. D. In *Capillary Electrophoresis Theory and Practice*; Grossman, P. D., Colburn, J. C., Eds.; Academic Press: San Diego, 1992, Chapter 1.

(38) Gas, B.; Stedry, M.; Kenndler, E. *Electrophoresis* **1997,** *18*, 2123-2133.

(39) Slater, G.; Kist, T. B. L.; Ren, H.; Drouin, G. *Electrophoresis* **1998,** *19*, 1525-1541.

(40) Tinland, B. *Electrophoresis* **1996,** *17*, 1519-1523.

(41) Tinland, B.; Pernodet, N.; Pluen, A. *Biopolymers* **1998,** *46*, 201-214.

(42) Doi, M.; Edwards, S. F. *The Theory of Polymer Dynamics*; Oxford University Press: New York, 1986.

(43) http://www.pe-corp.com/press/prccorp040600.html.

(44) http://www.pe-corp.com/press/prccorp062600.html.

(45) http://www.pe-corp.com/press/prccorp060100.html.

(46) Hjertén, S.; Zhu, M.-D. *Journal of Chromatography* **1985,** *346*, 265-270.

(47) Wehr, T.; Rodriguez-Diaz, R.; Zhu, M. *Capillary Electrophoresis of Proteins*; Marcel Dekker: New York, 1999.

(48) Hjertén, S.; Liao, J.-L.; Yao, K. *Journal of Chromatography* **1987,** *387*, 127-138.

(49) Huang, T. L.; Shieh, P. C. H.; Cooke, N. *Chromatographia* **1994,** *39*, 543-548.

(50) Chen, S.-M.; Wiktorowicz, J. E. *Analytical Biochemistry* **1992,** *206*, 84-90.

(51) Rodriguez, R.; Siebert, C. : 6th International Symposium of Capillary Electrophoresis, San Diego, CA, 1994.

(52) Wang, T. S.; Hartwick, R. A. *Analytical Chemistry* **1992,** *64*, 1745-1747.

(53) Wu, J.; Pawliszyn, J. *Analytical Chemistry* **1992,** *64*, 219-224.

(54) Wu, J.; Pawliszyn, J. *Journal of Chromatography* **1992,** *608*, 121-130.

(55) Wu, J.; Pawliszyn, J. *Electrophoresis* **1993,** *14*, 469-474.

(56) Wu, N.; Sun, P.; Aiken, J. H.; Wang, T.; Huie, C. W.; Hartwick, R. *Journal of Liquid Chromatography* **1993,** *16*, 2293-2298.

(57) Wu, J.; Pawliszyn, J. *Journal of Liquid Chromatography* **1993,** *16*, 3675-3687.

(58) Wu, J.; Pawliszyn, J. *Analytical Chemistry* **1994,** *66*, 867-873.

(59) Wu, J.; Pawliszyn, J. *Analytical Chemistry* **1992,** *64*, 224-227.

(60) Wu, J.; Pawliszyn, J. *Journal of Chromatography B* **1994,** *657*, 327-332.

(61) Vonguyen, L.; Wu, J.; Pawliszyn, J. *Journal of Chromatography B* **1994,** *657*, 333-338.

(62) Wu, J.; Pawliszyn, J. *Electrophoresis* **1995,** *16*, 670-673.

(63) Kilár, F. *Journal of Chromatography* **1991,** *545*, 403-406.

(64) Kilár, F. In *CRC Handbook of Capillary Electrophoresis: A Practical Approach*; Landers, J. P., Ed.; CRC Press: Boca Raton, 1994, pp 95-109.

(65) Righetti, P. G.; Drysdale, J. W. *Biochimica et Biophysica Acta* **1971,** *236*, 435-455.

(66) Righetti, P. G. *Isoelectric Focusing: Theory, Methodology, and Applications*; Elsevier Biomedical Press: Amsterdam, 1983.

(67) Liu, X.; Sosic, Z.; Krull, I. S. *J. Chromatogr.* **1996,** *735*, 165-190.

(68) Righetti, P. G.; Bossi, A. *Analytica Chimica Acta* **1998,** *372*, 1-19.

(69) Foret, F.; Muller, O.; Thorne, J.; Gotzinger, W.; Karger, B. L. *Journal of Chromatography A* **1995,** *716*, 157-166.

(70) Minarik, M.; Foret, F.; Karger, B. L. *Electrophoresis* **2000,** *21*, 247-254.

(71) Jensen, P. K.; Harrata, A. K.; Lee, C. S. *Analytical Chemistry* **1998,** *70*, 2044-2049.

(72) Jensen, P. K.; Pasa-Tolic, L.; Anderson, G. A.; Horner, J. A.; Lipton, M. S.; Bruce, J. E.; Smith, R. D. *Analytical Chemistry* **1999,** *71*, 2076-2084.

(73) Lyubarskaya, Y. V.; Carr, S. A.; Dunnington, D.; Prichett, W. P.; Fisher, S. M.; Appelbaum, E. R.; Jones, C. S.; Karger, B. L. *Analytical Chemistry* **1998,** *70*, 4761-4770.

(74) Severs, J. C.; Hofstadler, S. A.; Zhao, Z.; Senh, R. T.; Smith, R. D. *Electrophoresis* **1996,** *17*, 1808-1817.

(75) Tang, W.; Harrata, A. K.; Lee, C. S. *Analytical Chemistry* **1997,** *69*, 3177-3182.

(76) Veenstra, T. D.; Martinovic, S.; Anderson, G. A.; Pasa-Tolic, L.; Smith, R. D. *Journal of the American Society for Mass Spectrometry* **2000,** *11*, 78-82.

(77) Yang, L.; Tang, Q.; Harrata, A. K.; Lee, C. S. *Analytical Biochemistry* **1996,** *243*, 140-149.

(78) Yang, L.; Lee, C. S.; Hofstadler, S. A.; Smith, R. D. *Analytical Chemistry* **1998,** *70*, 4945-4950.

(79) Weber, K.; Osborn, M. *Journal of Biological Chemistry* **1969,** *244*, 4406-4412.

(80) Tanford, C. *The Hydrophobic Effect: Formation of Micelles and Biological Membranes*, 2nd ed.; Wiley: New York, 1980.

(81) Gordon, A. H. *Electrophoresis of Proteins in Polyacrylamide and Starch Gels*, 7th ed.; Elsevier/North-Holland Biomedical Press: Amsterdam, 1975.

(82) Nelson, C. A. *Journal of Biological Chemistry* **1971,** *246*, 3895-3901.

(83) Pitt-Rivers, R.; Impiombato, F. S. A. *Biochemical Journal* **1968,** *109*, 825-830.

(84) Smithies, O. *Archives of Biochemistry and Biophysics, Supplement* **1962,** *1*, 125-131.

(85) Fullerton, P. M.; Barnes, J. M. *British Journal of Industrial Medicine* **1966,** *23*, 210-221.

(86) Werner, W. E.; Demorest, D. M.; Wiktorowicz, J. E. *Electrophoresis* **1993,** *14*, 759-763.

(87) Guttman, A.; Shieh, P.; Lindahl, J.; Cooke, N. *Journal of Chromatography A* **1994,** *676*, 227-231.

(88) Cohen, A. S.; Karger, B. L. *Journal of Chromatography* **1987,** *397*, 409-417.

(89) Cohen, A. S.; Paulus, A.; Karger, B. L. *Chromatographia* **1987,** *24*, 15-24.

(90) Wu, D.; Regnier, F. E. *Journal of Chromatography* **1992,** *608*, 349-356.

(91) Widhalm, A.; Schwer, C.; Blaas, D.; Kenndler, E. *Journal of Chromatography* **1991,** *549*, 446-451.

(92) Ganzler, K.; Greve, K. S.; Cohen, A. S.; Karger, B. L.; Guttman, A.; Cooke, N. C. *Analytical Chemistry* **1992,** *64*, 2665-2671.

(93) Wise, E. T.; Singh, N.; Hogan, B. L. *Journal of Chromatography A* **1996,** *746*, 109-121.

(94) Harvey, M. D.; Bandilla, D.; Banks, P. R. *Electrophoresis* **1998,** *19*, 2169-2174.

(95) Guttman, A.; Horvath, J.; Cooke, N. *Analytical Chemistry* **1993,** *65*, 199-203.

(96) Benedek, K.; Thiede, S. *Journal of Chromatography A* **1994,** *676*, 209-217.

(97) Nakatani, M.; Shibukawa, A.; Nakagawa, T. *Electrophoresis* **1996,** *17*, 1584-1586.

(98) Karim, M. R.; Janson, J.-C.; Takagi, T. *Electrophoresis* **1994,** *15*, 1531-1534.

(99) Takagi, T.; Karim, M. R. *Electrophoresis* **1995,** *16*, 1463-1467.

(100) Zhang, Y.; Lee, H. K.; Li, S. F. Y. *Journal of Chromatography A* **1996,** *744*, 249-257.

(101) Craig, D. B.; Polakowski, R. M.; Arriaga, E.; Wong, J. C. Y.; Ahmadzadeh, H.; Stathakis, C.; Dovichi, N. J. *Electrophoresis* **1998,** *19*, 2175-2178.

(102) Wilkins, J. *Biotechnology and Genetic Engineering Reviews* **1996,** *13*, 19-50.

(103) Celis, J. E.; Østergaard, M.; Jensen, N. A.; Gromova, I.; Holm Rasmussen, H.; Gromov, P. *FEBS Letters* **1998,** *430*, 64-72.

(104) Anderson, L.; Seilhamer, J. *Electrophoresis* **1998,** *18*, 533-537.

(105) Haynes, P. A.; Gygi, S. P.; Figeys, D.; Aebersold, R. *Electrophoresis* **1998,** *19*, 1862-1871.

(106) O'Farrell, P. H. *Journal of Biological Chemistry* **1975,** *250*, 4007-4021.

(107) O'Farrell, P. Z.; Goodman, H. M.; O'Farrell, P. *Cell* **1977,** *12*, 1133-1141.

(108) Klose, J. *Humangenetik* **1975,** *26*, 231-243.

(109) Bjellqvist, B.; Ek, K.; Righetti, p. G.; Gianazza, G.; Görg, A.; Westermeier, R.; Postel, W. *Journal of Biochemical and Biophysical Methods* **1982,** *3*, 317-339.

(110) Görg, A.; Postel, W.; Günther, S. *Electrophoresis* **1988,** *9*, 531-546.

(111) Righetti, P. G. *Immobolized pH Gradients: Theory and Methodology*; Elsevier: Amsterdam, 1990.

(112) James, P. *Biochemical and Biophysical Research Communications* **1997,** *132*, 1-6.

(113) Klose, J.; Kobalz, U. *Electrophoresis* **1995,** *16*, 1034-1059.

(114) Williams, K. *Electrophoresis* **1999,** *20*, 678-688.

(115) Link, A. J.; Hays, L. G.; Carmack, E. B.; Yates III, J. R. *Electrophoresis* **1997,** *18*, 1314-1334.

(116) Voris, B. P.; Young, D. A. *Analytical Biochemistry* **1980,** *104*, 478-484.

(117) Wasinger, V. C.; Bjellqvist, B.; Humphery-Smith, I. *Electrophoresis* **1997,** *18*, 1373-1383.

(118) Whitehouse, C. D.; Dreyer, R. N.; Yamashita, M.; Fenn, J. B. *Analytical Chemistry* **1985,** *57*, 675-681.

(119) Karas, M.; Bachmann, D.; Hillenkamp, F. *Analytical Chemistry* **1985,** *57*, 2935-2939.

(120) Vorm, O.; Mann, M. *Journal of the American Society for Mass Spectrometry* **1994,** *5*, 955-958.

(121) Karas, M.; Hillenkamp, F. *Analytical Chemistry* **1988,** *60*, 2299-2301.

(122) Yates III, J. R. *Journal of Mass Spectrometry* **1998,** *33*, 1-19.

(123) Beavis, R. C.; Chait, B. T. *Proceedings of the National Academy of Sciences, USA* **1990,** *87*, 6873-6877.

(124) Quadroni, M.; James, P. *Electrophoresis* **1999,** *20*, 664-677.

(125) Shevchenko, A.; Wilm, M.; Vorm, O.; Mann, M. *Analytical Chemistry* **1996,** *68*, 850-858.

(126) Wilm, M.; Shevchenko, A.; Houthaeve, T.; Breit, S.; Schweigerer, L.; Fotsis, T.; Mann, M. *Nature* **1996,** *379*, 466-469.

(127) Henzel, W. J.; Billeci, T. M.; Stults, J. T.; Wondg, S. C.; Grimley, C.; Watanabe, C. *Proceedings of the National Academy of Sciences, USA* **1993,** *90*, 5011-5015.

(128) James, P.; Quadroni, M.; Carafoli, E.; Gonnet, G. *Biochemical and Biophysical Research Communications* **1993,** *195*, 58-64.

(129) Mann, M.; Hojrup, P.; Roepstorff, P. *Biological Mass Spectrometry* **1993,** *22*, 338-345.

(130) Pappin, D. J. C.; Hojrup, P.; Bleasby, A. J. *Current Biology* **1993,** *3*, 327-332.

(131) Yates III, J. R.; Speicher, S.; Griffin, P. R.; Hunkapiller, T. *Analytical Biochemistry* **1993,** *214*, 397-408.

(132) Yates III, J. R. *Trends in Genetics* **2000,** *16*, 1-6.

Chapter 2
Replaceable Sieving Matrices for Capillary Gel Electrophoresis DNA Sequencing

2.1 Introduction

Many different types of sieving matrices have been used for capillary electrophoresis (CE) DNA separations, including liquified agarose (1-3) and a number of celluose derivatives (2, 6, 4-16). The cellulose derivatives include methylcellulose (MC) (4-7), hydroxyethylcellulose (HEC) (8-13), hydroxypropylcellulose (HPC) (13, 14), and hydroxypropylmethylcellulose (HPMC) (2, 6, 14-16). Other groups have reported the use of poly(ethylene glycol) (PEG)(15, 17), PEG which has been end-capped with micelle-forming fluorocarbon tails (18), polyvinylalcohol (PVA) (2, 17), poly(ethylene oxide) (PEO) (19, 20), poly(vinylpyrrolidone) (PVP) (21), and a viscosity-adjustable block copolymer made of $PEO_{99}PPO_{69}PEO_{99}$ (where PPO denotes poly(propylene)oxide) (22). Linear polyacrylamide (LPA) (16, 23-35) has been widely utilized, and some of its derivatives, such as polydimethylacrylamide (PDMA) (36-39), polyacryloylaminoethoxyethanol (40), and poly(acryloylaminoethoxy)ethyl-β-D-glucopyranoside (37), are gaining popularity as new sieving matrices for CE.

Among all of the current sieving matrices for CE, few are replaceable. The recent accomplishment of sequencing the human genome has shown that replaceable sieving matrices are invaluable with the use of automated, multi-capillary instruments. Hjertén has reported the application of replaceable agarose gels for field inversion CE of DNA fragments (3). Yeung's group has reported two types of replaceable sieving matrices for CE DNA analysis: PEO (19, 20, 41) and PVP (21). PEO has been used to separate 1000 base pairs of a sequencing ladder in 7 hours with an electric field strength of 75 V/cm (20). The utilization of PEO requires tedious capillary regeneration steps (19, 20, 41), although when these cleaning steps are properly executed, single capillaries have been reported to last more than 30 (19) and 50 (41) runs. An obvious drawback of using PEO for CE DNA sequencing is the time required for such a separation (including capillary regeneration steps). CE DNA sequencing of ssM13mp18 using a very low viscosity PVP sieving matrix has shown good resolution up to 500 bases (21). This separation was performed at 150 V/cm and was accomplished in about 1.5 hours (21). Capillary regeneration is simple and capillary lifetime is at least 30 uses (21). Sudor *et. al.* reported the employment of a replaceable LPA sieving matrix for oligonucleotide separation in 1991 (42). Karger's group has reported a number of highly successful replaceable LPA sieving matrices since 1993 (32-35). Initially, a two-colour DNA sequencing run of ssM13mp18 using a replaceable LPA matrix yielded accurate sequencing information for 350 bases in about 30 minutes (35). Upon subsequent improvements to the matrix and sequencing

conditions, the authors were able to routinely sequence 1000 bases in 50-90 minutes, with a column lifetime of more than 300 experiments (32-34). More recently there have been reports of the use of PDMA as a replaceable sieving matrix (36-39). Chiari *et. al.* demonstrated the use of PDMA to separate DNA ladders and fragments (37). Madabhushi describes the utilization of a nonviscous PDMA sieving matrix to 4-colour sequence 600 bases of ssM13mp18 in about 2 hours, at elevated temperature, with a moderate electric field (160 V/cm) (39). Furthermore, Madabhushi illustrated that capillary regeneration is not necessary between successive runs and that the capillary lifetime is more than 100 uses (39). This nonviscous PDMA sieving matrix is marketed by PE Biosystems as the DNA sequencing polymer solution POP6® for use with the ABI Prism® 3700 DNA Analyzer. Xiong *et. al.* describe the employment of Madabushi's sieving matrix for base stacking in DNA sequencing (38). Ren *et. al.* used the POP6® polymer as a running buffer additive for the free solution separation of ssM13mp18 sequencing fragments (43).

Even more attractive than replaceable CE sieving matrices are sieving matrices which are both replaceable and can be used in uncoated columns. It is necessary to use a liquified agarose sieving matrix in conjunction with capillaries which are first treated with a Bind-Silane solution in acetone and then coated with a thin layer of agarose (3). Sudor *et. al.* report that using a LPA sieving matrix in uncoated capillaries results in the expulsion of sieving matrix from the capillary due to electro-osmotic flow, therefore capillaries coated using Hjertén's method are used (42, 44). Karger's group utilizes an LPA sieving matrix with capillaries coated using Hjertén's method (35, 44) or with PVA (33, 34, 45). These PVA coated capillaries are available from Beckman Instruments (34). Replaceable sieving matrices which necessitate the employment of coated capillaries increase both the cost and the time of a project.

The only repleaceable sieving matrices successfully utilized in bare columns have been PEO (19, 20, 41), PVP (21), and PDMA (38, 39). These PEO, PVP, and PDMA sieving matrices suppress electro-osmotic flow as well as eliminate DNA-capillary wall interactions by adsorbing to the capillary walls (46). Although PEO and PVP separation matrices are replaceable and can be used in bare silica capillaries, their use also requires capillary regeneration between successive runs (19-21, 41). PDMA is advantageous as a replaceable medium because it does not require capillary regeneration between applications (38, 39).

This chapter describes the reuse of uncoated capillaries for high temperature DNA sequencing. A procedure to make a replaceable PDMA sieving matrix for

employment in uncoated capillaries is presented. This method differs fundamentally from the method reported by Madabhushi (39). Madabhushi reports four methods of polymerizing DMA: two involving polymerization in organic solvents and two involving polymerization in water (39). Madabhushi's presented results are of a PDMA synthesized in *t*-butanol, initiated with 2,2-azobisisobutyronitrile (39). 2,2-azobisisobutyronitrile (AIBN) which is available from Aldrich cannot be purchased in Canada due to United States export laws. An alternate Canadian supplier has yet to be located. Thus DMA is polymerized as is traditionally done with polyacrylamide, in water using the initiators ammonium persulfate (APS), which is insoluble in organic solvents, and *N,N,N',N'*- tetramethylethylenediamine (TEMED). To control the polymerizing chain lengths, and thus the resulting viscosity, the PDMA is washed in methanol shortly after polymerization. It is demonstrated through data analysis that the capillaries can be reused and refilled with two types of PDMA sieving matrix to give suitable sequencing runs.

2.2 Experimental

2.2.1 Materials and reagents

The *N,N*-dimethylacrylamide (DMA) was purchased from Aldrich (Milwaukee, WI). Ammonium persulfate (APS) was supplied by Bio-Rad Labs (Hercules, CA). *N,N,N',N'*- tetramethylethylenediamine (TEMED) and formamide were obtained from GibcoBRL (Grand Island, NY). Urea was from ICN Biomedicals (Aurora, OH). Tris[hydroxymethyl]aminomethane (Tris) and *N*-tris[hydroxymethyl]methyl-3-amino-propanesulfonic acid (Taps) were purchased from Sigma (St. Louis, MO). Ethylenediaminetetra-acetic acid (disodium salt) (EDTA) was obtained from BDH Chemicals (Vancouver, Canada). Methanol was acquired from Fisher Scientific (Nepean, Canada). Hexanes (reagent grade) and sodium hydroxide were purchased from Caledon Labs (Georgetown, Canada). The M13(-21) Forward Dye Primer Kit was purchased from Applied Biosystems (Foster City, CA). The ROX labeled primer and Thermosequenase T reagent were obtained from Amersham (Toronto, Canada).

2.2.2 Preparation of polydimethylacrylamide (PDMA)

DMA was polymerized in solution and dried. Filtration of 10X TTE (1 M Tris, 1 M Taps, pH 8.5- adjusted with NaOH, 10 mM EDTA) was performed using a 0.22 µm sterile Millipore filter (Millipore, Bedford, MA). Polymerization was as follows:

1 g of DMA and 1 mL of 10X TTE were dissolved in 8 mL of Nanopure water, stirred, and degassed under vacuum for 10 minutes. While under argon, 20 µL of 10% (w/v) APS in water and 10 µL of TEMED were added and the solution was stirred vigorously for a few seconds. The sealed solution was left to polymerize for 30 minutes at room temperature. After 30 minutes, the polymer solution was split into 3 approximately equal aliquots. To each aliquot 40 mL of methanol was added and this polymer-methanol solution was washed 3 times with 160 mL of hexanes. The hexanes washes were discarded and the methanol layer was evaporated overnight in a fumehood. Two variations of this procedure were performed: one without the hexanes washes and the other without the addition of either methanol or hexanes washes. The white solid PDMA was collected and placed in a dessicator under vacuum. Once dry, the PDMA was stored in the dark at room temperature.

The dried PDMA was dissolved to produce a 6% (w/v) sieving matrix for CE DNA separations. Urea (7M) was added to 5X TTE buffer and water, the solid was dissolved, and then the solution was filtered (0.22 µm). Next solid PDMA was added to this solution and the solution was stirred for a few hours to dissolve the polymer. Finally the sieving matrix was degassed under vacuum to prevent its degassing during high temperature sequencing (29). The presence of such gas bubbles can have detrimental effects on sequencing results. A plastic syringe (Becton Dickinson and Co., Franklin Lakes, NJ) was filled with the polymer solution, capped airtight, and stored in the dark at room temperature.

2.2.3 Preparation of T-terminated sequencing samples

Sequencing samples were prepared using cycle sequencing. To a 200 µL PCR tube (Rose Scientific, Edmonton, Canada), 1.5 µL of ssM13mp18 DNA, 18.5 µL of distilled water, 4 µL of ROX-labeled -21M13 universal primer, and 8 µL of Thermosequenase T reagent were added. The mixture was thermal cycled in a PTC-100 Programmable Thermal Controller (MJ Research, Watertown, MA) under the following conditions: 30 cycles, 30 seconds, 95°C; 30 cycles, 30 seconds, 55°C; reactions were held at 4°C. After cycle sequencing, the sample was cleaned according to the following protocol: the sample was placed in the center of a Microcon 30 microconcentrator (Amicon, Beverly, MA) sample reservoir, the PCR reaction tube was rinsed with distilled water and added to the reservoir, the water was centrifuged out, the sample was rinsed with water again, and finally the sample DNA was eluted from the sample reservoir using 10 µL of formamide. Samples were stored at -20°C until used. The

samples were diluted 1:1 with water that was saturated with urea immediately prior to injection.

2.2.4 Preparation of capillaries

Uncoated fused silica capillaries (Polymicro Technologies, Phoenix, AZ) were 140 μm O.D. × 50 μm I.D. × 65 cm long. The PDMA matrix was introduced into the injection-end of the capillary using a laboratory-made syringe pump. The injection end of the capillary was trimmed by about 1 mm and attached to the gel-filled syringe with a laboratory-made connector. The sieving matrix was forced through the capillary for 45 to 60 minutes. Before each sequencing run, the sieving matrix was replaced with new material by pumping it through the capillary for 45 to 60 minutes.

2.2.5 Capillary electrophoresis

The laboratory-made single-capillary instrument with sheath flow cuvette used for all sequencing separations is described elsewhere (47). A green (2 mW, λ = 543.5 nm) Helium-Neon (He-Ne) laser (Melles Griot, Carlsbad, CA) was used for excitation. The fluorescence was passed through a 580DF40 bandpass filter (Omega Optical, Brattleboro, VT) and was detected using an R1477 photomultiplier tube (Hamamatsu, Middlesex, NJ).

All sequencing separations were performed at 43±1°C. After the matrix was replaced, the capillary was run at 150 V/cm with reversed electric field polarity (cathode at the injection end) for 1 minute. Then the capillary was prerun at 150 V/cm with 1X TTE buffer for 10 minutes to allow the current to stabilize. Prior to injection, the capillary was run with reverse polarity at 100 V/cm for 5 seconds in the sample tube. Electrokinetic injection was at 100 V/cm for 35 seconds. Separation was performed at 150 V/cm with 1X TTE (0.22 μm filtered) used as the running buffer. The sheath flow buffer was also 1X TTE (0.22 μm filtered). Data was collected on a Macintosh computer equipped with LabView software.

2.2.6 Viscosity measurement

Viscosity measurements were performed using a falling ball (tantalum ball) type viscometer (Gilmont Instruments, Barrington, IL). Measurements were performed at room temperature.

2.3 Results and Discussion

2.3.1 Reusing and refilling capillaries with a PDMA sieving matrix

Figure 2.1 shows the electropherogram of a sequencing run generated using a PDMA sieving matrix in a new uncoated capillary. The sieving matrix was prepared from PDMA which was dissolved in methanol and then washed with hexanes three times after polymerization (henceforth referred to as the methanol-hexanes PDMA) as described in Section 2.2.2. The peaks show some tailing which may be indicative of electro-osmotic flow still present in the capillary. It is possible that the sieving matrix did not evenly coat the capillary's surface on this initial fill and thus did not completely suppress electro-osmotic flow during the run.

Figure 2.2 shows the electropherogram of a sequencing run generated using the same PDMA sieving matrix as in Figure 2.1, however this is the twenty-seventh refill and use of the same uncoated capillary. Qualitatively this run is comparable to if not better than the first run generated with this capillary. The peaks display no tailing and resolution appears to be better. These results illustrate the reproducibility of the sieving matrix when utilized repeatedly in the same uncoated capillary.

Sequencing runs were also obtained using a PDMA sieving matrix made of DMA which was polymerized and then neither dissolved in methanol nor subjected to a series of hexanes washes as described in Section 2.2.2. However, this PDMA was of poor quality for a sieving matrix. Figure 2.3 shows a preliminary experiment which was carried out at room temperature (as compared to 43°C) to see how well the polymer would perform. The sequencing data shows very poor resolution. Since the sequencing data obtained with this PDMA was poor, no further experiments were conducted with it.

2.3.2 Variation of migration time

The plot of migration time versus the capillary fill number for a methanol-hexanes PDMA sieving matrix is shown in Figure 2.4. As can be seen, migration time of various fragments does not vary significantly with the number of times the capillary has been filled and reused. The relative standard deviation in migration time from run-to-run is about 10%. These data indicate the suitability of this sieving matrix for sequencing in an uncoated capillary.

Figure 2.1 Electropherogram of a T-termination DNA sequencing run using a methanol-hexanes PDMA sieving matrix for the first time in an uncoated capillary.

See Section 2.2.3 for sample preparation and Section 2.2.5 for CE conditions. The peaks represent bases 26 to 702.

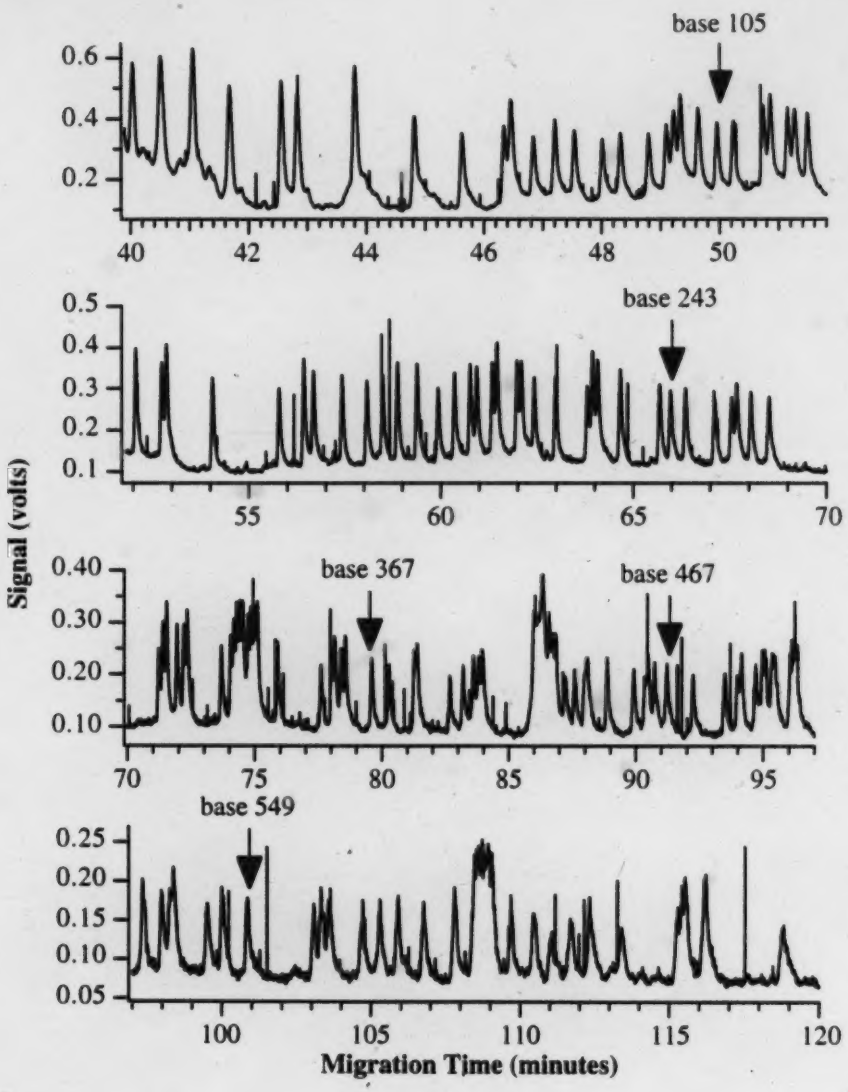

Figure 2.2 Electropherogram of a T-termination DNA sequencing run using a methanol-hexanes PDMA sieving matrix for the twenty-seventh time in the same uncoated capillary.

See Section 2.2.3 for sample preparation and Section 2.2.5 for CE conditions. The peaks represent bases 26 to 680.

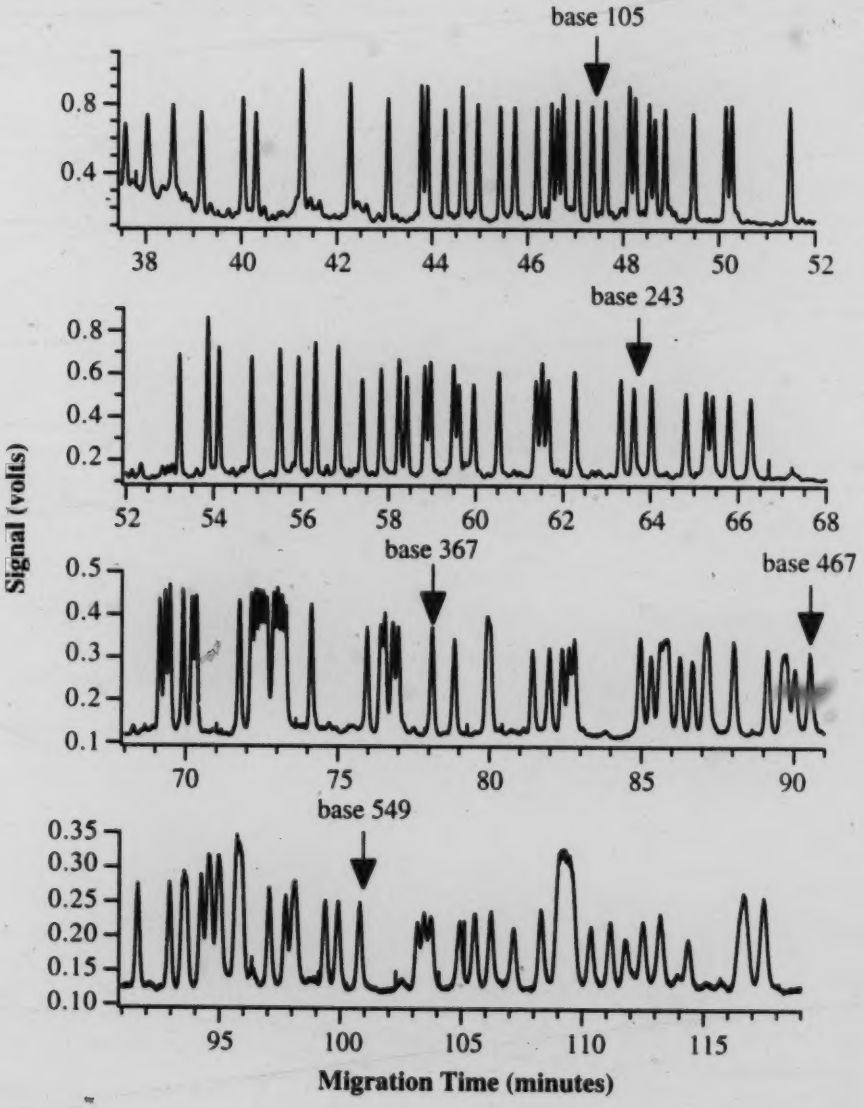

Figure 2.3 Electropherogram of a T-termination DNA sequencing run using a PDMA sieving matrix of PDMA which was polymerized and not further dissolved in methanol or washed with hexanes.

See Section 2.2.3 for sample preparation and Section 2.2.5 for CE conditions. The plateau artifact at 190 minutes is most likely the result of a bubble in the sheath flow line. The peaks represent bases 26 to 525.

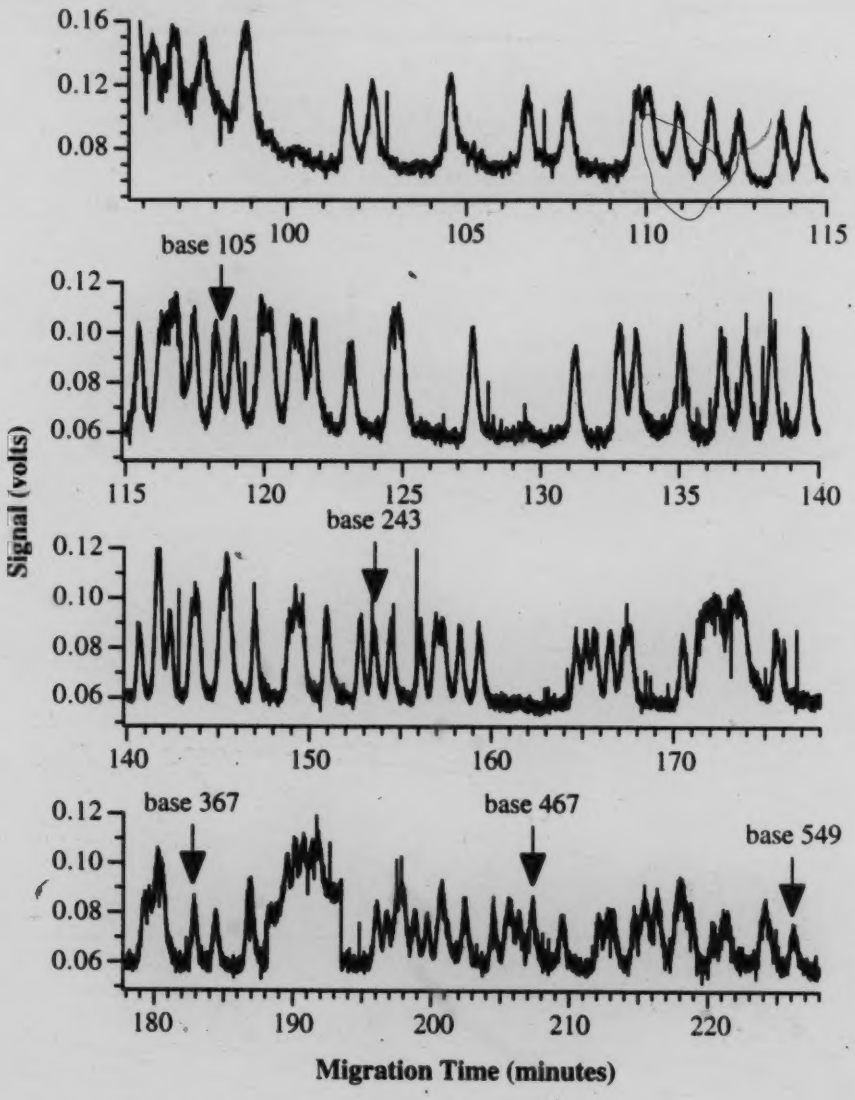

Figure 2.4 Migration time versus the number of times the capillary has been used for a methanol-hexanes sieving matrix.

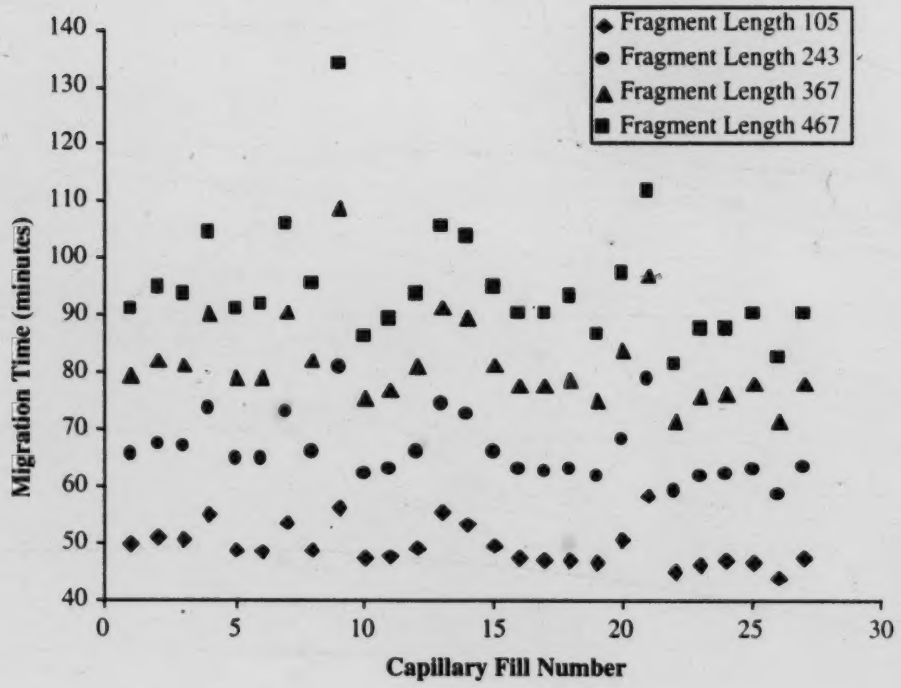

The plot of migration time versus the capillary fill number for a methanol PDMA sieving matrix is shown in Figure 2.5. As in Figure 2.4, migration times only vary slightly from run to run when the capillary is refilled and reused. The relative standard deviation in migration time from run-to-run is less than 6%. These data again demonstrate the suitability of this sieving matrix for DNA sequencing under the given conditions.

How the migration times differ between methanol-hexanes and methanol PDMA sieving matrices is shown in Table 2.1. A sieving matrix made from methanol-hexanes PDMA produces faster sequencing runs than the sieving matrix made from methanol PDMA. The same fragment lengths' average migration times differ anywhere from 8-9 minutes between the two sieving matrices. This difference in migration times must be the result of the washing of the PDMA in hexanes after polymerization. The hexanes wash removes nonpolar and hydrophobic components in the polymerization mixture which are still in excess after polymerization. The methanol PDMA prepared without the hexanes wash still contains these nonpolar and hydrophobic components remaining after polymerization. This wash may have a direct effect on the resulting polymer pore size. The results indicate that the since the migration times of the fragment lengths are shorter using a sieving matrix of methanol-hexanes PDMA, that this polymer is produced with a larger pore size than the methanol PDMA. Since pore size varies between the two types of matrices, viscosity must also be different. However, viscosity measurements were only performed for a methanol-hexanes PDMA sieving matrix, so this claim cannot be verified.

2.3.3 Capillary reuse

The ability of a capillary to be utilized repeatedly for sequencing runs can be determined by examining parameters such as resolution and theoretical plates. By determining how or if these factors change from run to run, a capillary's long-term performance can be evaluated. Resolution measures the separation of two peaks and is calculated as follows:

$$R = \frac{2(t_2 - t_1)}{W_1 + W_2} \qquad (2.1)$$

where t_2 and t_1 are the migration times of the two peaks and W_1 and W_2 are the peak widths at baseline. The normalized resolution is calculated using the following

Figure 2.5 Migration time versus the number of times the capillary has been used for a methanol PDMA sieving matrix.

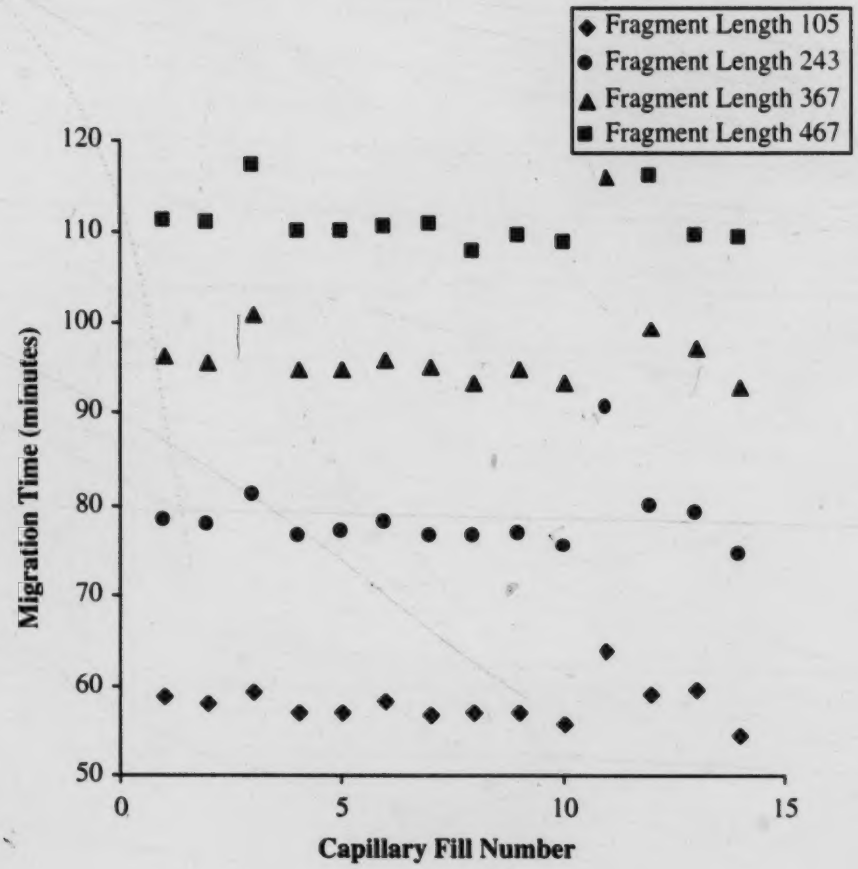

Table 2.1 A comparison of average migration times of selected fragment lengths of DNA between different PDMA sieving matrices.

	Type of PDMA Sieving Matrix	
	Methanol-hexanes	Methanol
DNA Fragment Length	Average Migration Time (minutes) (n=27)	Average Migration Time (minutes) (n=14)
105	49.6±3.6	58.2±2.2
243	66.4±5.7	78.5±3.9
367	81.9±8.2	97.2±5.9
467	95.1±10.7	103.0±2.8

equation:

$$\text{Normalized Resolution} = \frac{2(t_2 - t_1)}{W_1 + W_2} \bullet \frac{1}{M_2 - M_1} \qquad (2.2)$$

where M_2 and M_1 are the fragment lengths of the DNA.

The number of theoretical plates is an indicator of a column's efficiency. The number of theoretical plates, N, is calculated as follows:

$$N = \frac{16t^2}{W^2} \qquad (2.3)$$

where t is the peak migration time and W is the peak width at baseline.

Figure 2.6 displays the normalized resolution between selected fragment lengths versus number of times the capillary has been used for a methanol-hexanes PDMA sieving matrix. It can be seen that the normalized resolution trends for identified DNA fragments are uniformly independent of the number of times the capillary is reused. Figure 2.6 indicates that resolution is independent of the number of times the capillary is employed with this methanol-hexanes PDMA sieving matrix.

Figure 2.7 shows the normalized resolution between selected fragment lengths versus the number of times the capillary has been used with a methanol PDMA sieving matrix. This methanol PDMA sieving matrix exhibits the same resolution results as the methanol-hexanes sieving matrix. Figure 2.7 displays the independence of resolution on the number of times the capillary is utilized with a methanol PDMA sieving matrix.

Table 2.2 is a comparison of the average normalized resolution between different fragment lengths for the two different types of PDMA sieving matrices. As is seen in Table 2.2, the two types of sieving matrices have slightly different patterns of resolution. The methanol-hexanes PDMA does not sieve very small fragments as well as the larger ones. The methanol PDMA displays a trend in which the resolution essentially decreases with increasing fragment length. These observations may be an indication of the difference in pore size generated between the two types of polymers. As mentioned in Section 2.3.2, the methanol-hexanes sieving matrix most likely has larger pores and therefore is incapable of resolving well the smaller fragments.

A further indication of the possibility of capillary reuse is the theoretical plate numbers. Figure 2.8 is a graph of theoretical plates versus the number of times the capillary has been refilled and employed with a methanol-hexanes PDMA sieving

Figure 2.6 The dependence of normalized resolution on the number of times a capillary is reused with a methanol-hexanes PDMA sieving matrix.

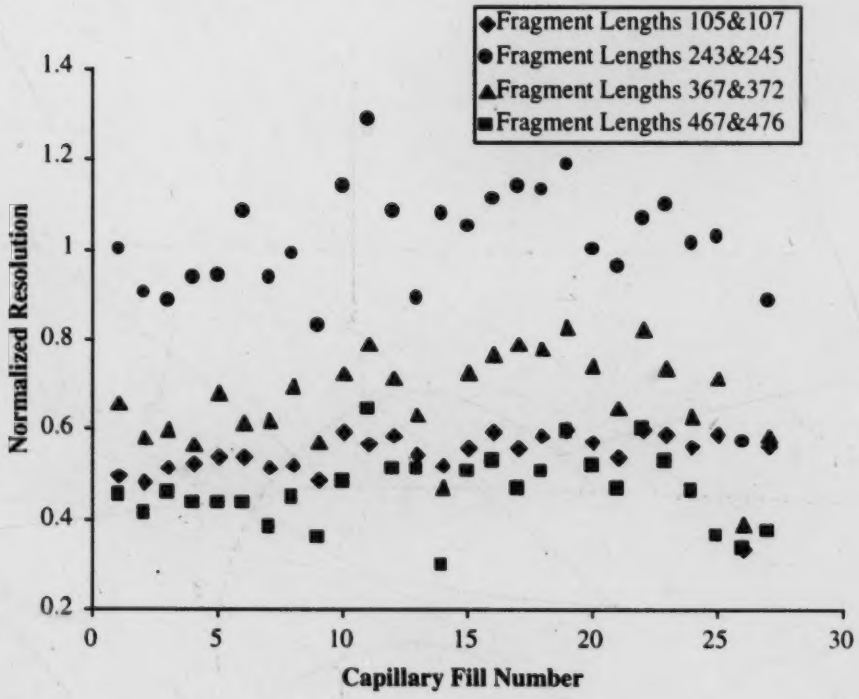

Figure 2.7 The dependence of normalized resolution on the number of times a capillary is reused with a methanol PDMA sieving matrix.

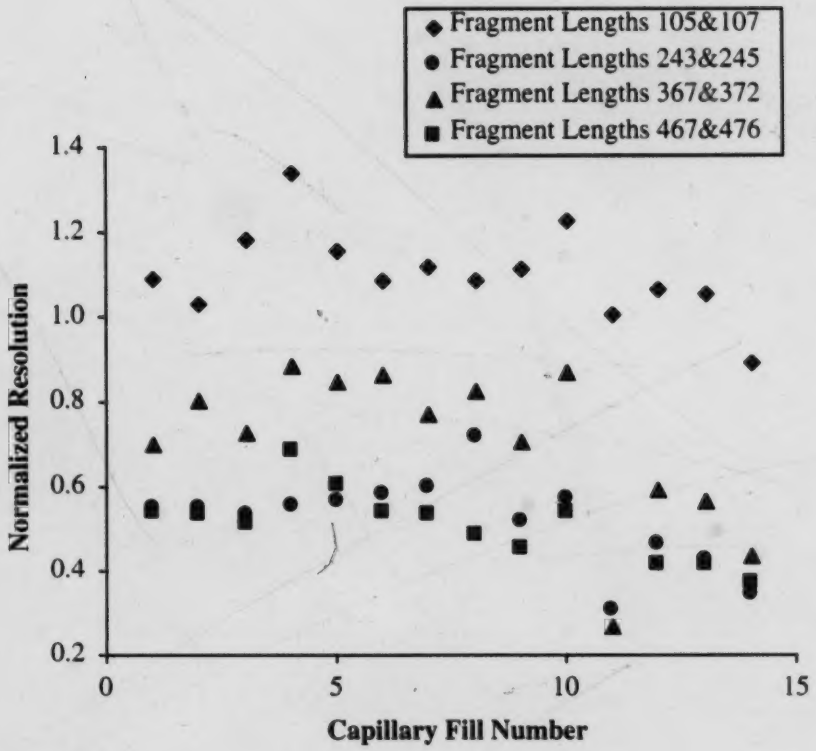

Table 2.2 Comparison of average normalized resolution for different fragment lengths between PDMA sieving matrices made two different ways.

	Type of Sieving Matrix	
	Methanol-hexanes	Methanol
DNA Fragment Length	Average Normalized Resolution (n=27)	Average Normalized Resolution (n=14)
105 & 107	0.5±0.1	1.1±0.1
243 & 245	1.0±0.1	0.5±0.1
367 & 372	0.7±0.1	0.7±0.2
467 & 476	0.5±0.1	0.5±0.1

matrix. As can be seen, a few of the sequencing runs have unusually low plate numbers, but this is true for all fragments analyzed for that run. This may be an indication that the capillary still has some residual electro-osmotic flow during these particular runs and thus is not functioning completely as a coated capillary. Besides these outliers, a trend is seen that the capillary performs consistently from run to run when employing this sieving matrix for repeated capillary use.

Figure 2.9 is a plot of theoretical plates versus the number of times the capillary has been refilled and reused for a methanol PDMA sieving matrix. For each fragment length, again, the plate number is independent of the number of times the capillary has been utilized. Again there are some outliers which indicate that the capillary is not functioning very well over the course of that specific run. However, it is deduced from Figure 2.9 that the methanol PDMA sieving matrix produces suitable results when pumped into the same capillary and sequencing runs are performed repeatedly.

Table 2.3 is a comparison of capillary efficiency at the different fragment lengths for the two types of sieving matrices employed. Table 2.3 indicates that sequencing with either sieving matrix produces the same orders of efficiency within error over many capillary uses.

2.3.4 Effects of electric field strength on separation

All sequencing runs were performed at a standard electric field strength of -150 V/cm. To investigate how the methanol-hexanes PDMA sieving matrix would perform at a higher field strength, the field strength was doubled to -300 V/cm. Figure 2.10 shows the electropherogram of this sequencing run. Apart from the obvious changes in migration time, qualitatively this electropherogram looks no different from those run at lower field strength (see Figures 2.1 and 2.2). To increase throughput, it would be advantageous to implement the use of a higher field strength with this methanol-hexanes sieving matrix. Figure 2.11 shows the differences in migration times with different field strength for select fragment lengths.

Further analyses were done to calculate both resolution and theoretical plates at this electric field strength and are shown in comparison to those values obtained at a regular separation field strength in Tables 2.4 and 2.5 respectively. Preliminary results (as this was only performed once to see how promising it was) indicate that the resolution at -300 V/cm is reasonable and decreases linearly with increased fragment size. Plate numbers at -300 V/cm are also comparable to those obtained at -150 V/cm. Plate numbers also decrease with increased fragment length.

Figure 2.8 Capillary efficiency changes as the capillary is refilled and reused with a methanol-hexanes PDMA sieving matrix.

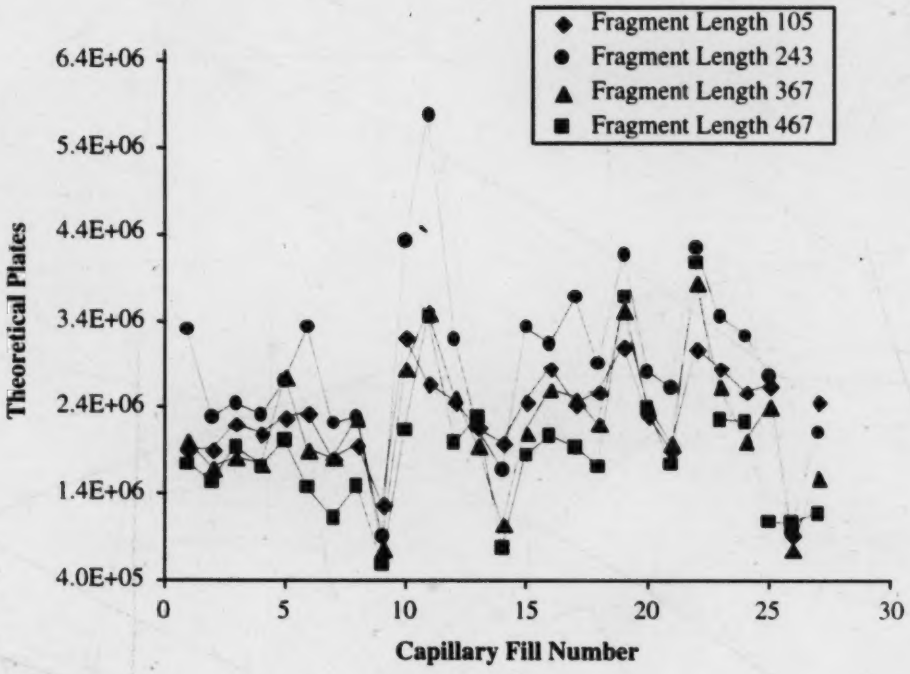

Figure 2.9 Capillary efficiency as the capillary is refilled and reused with a methanol PDMA sieving matrix.

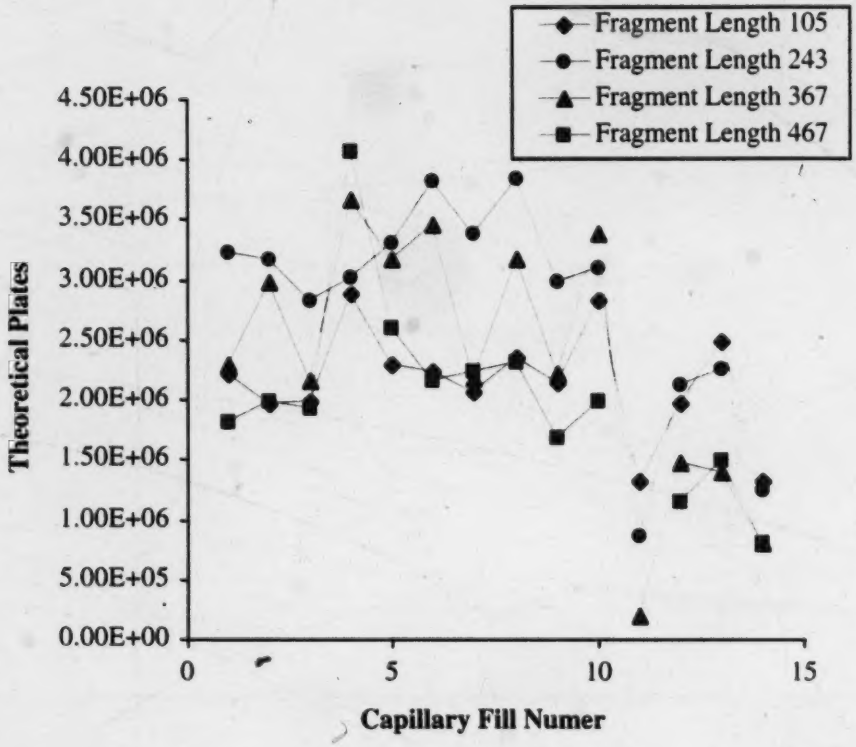

Table 2.3 Comparison of capillary efficiency at different fragment lengths for two types of PDMA sieving matrices.

	Type of Sieving Matrix	
	Methanol-hexanes	Methanol
DNA Fragment Length	Average Plates x 10^6 (n=27)	Average Plates x 10^6 (n=14)
105	2.3±0.5	2.1±0.5
243	2.9±1.0	2.8±0.9
367	2.2±0.7	2.3±1.1
467	1.9±0.8	1.8±0.8

Figure 2.10 Electropherogram of a T-termination sequencing run with a methanol-hexanes PDMA sieving matrix at high electric field strength.

The peaks represent bases 26 to 629.

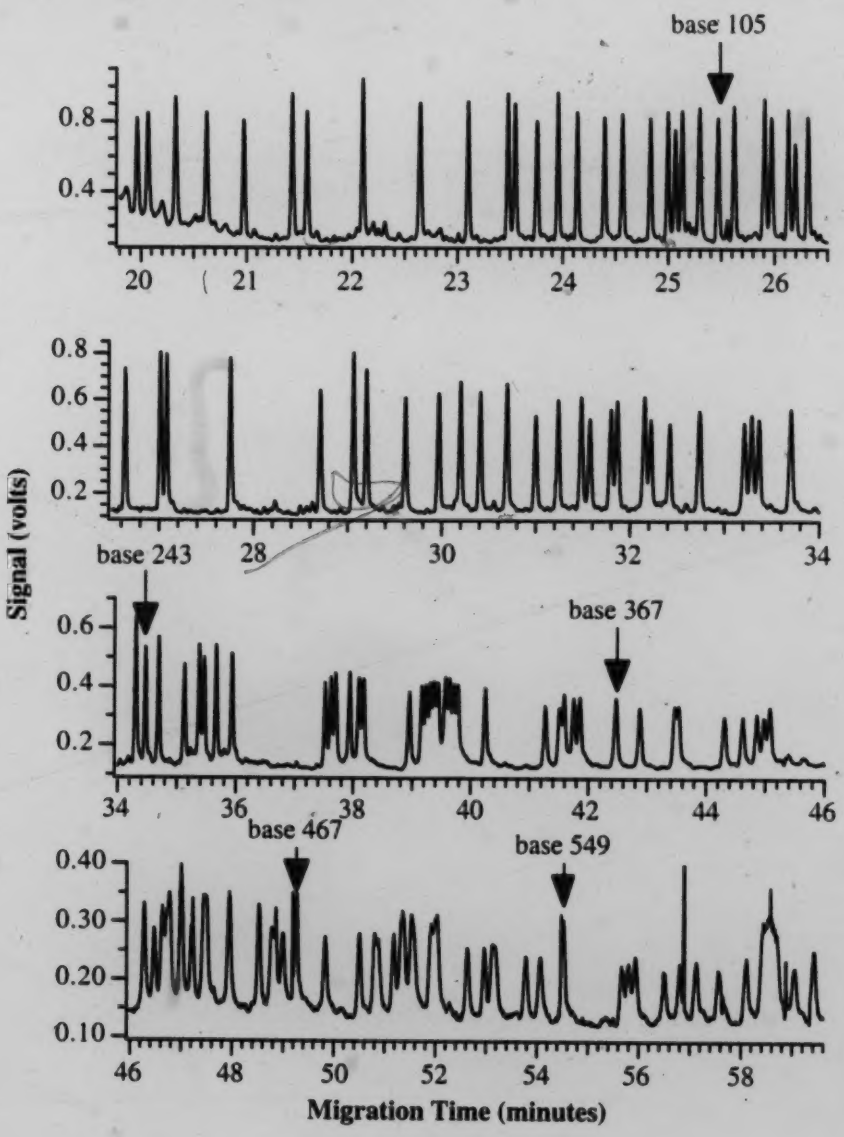

Figure 2.11 Comparison of migration times for a methanol-hexanes PDMA sieving matrix at field strengths of -150 V/cm and -300 V/cm.

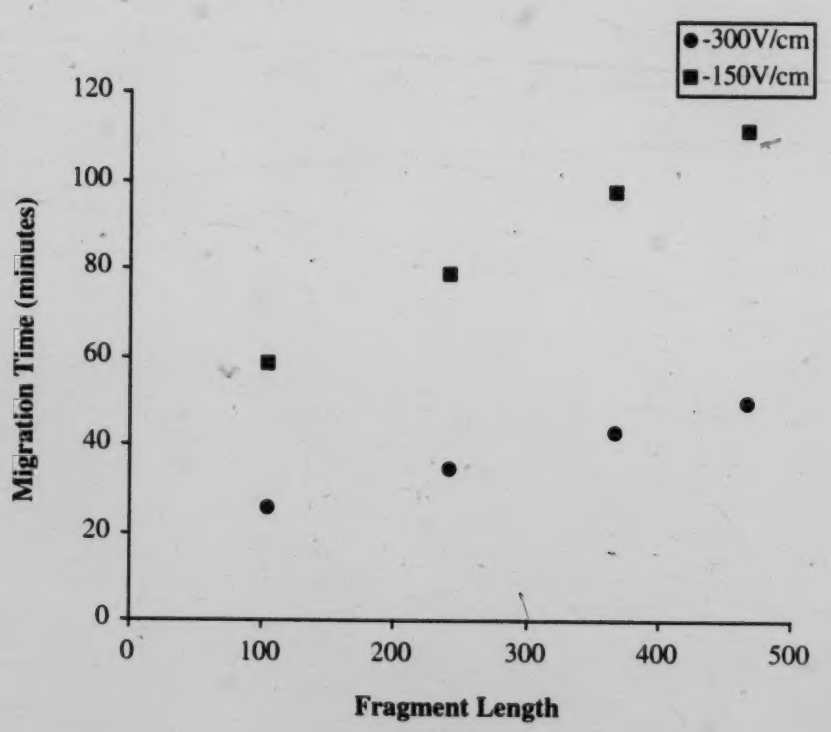

Table 2.4 Comparison of resolution between selected fragment lengths for sequencing runs at -150 V/cm and -300 V/cm using a methanol-hexanes PDMA sieving matrix.

	Electric Field Strength (V/cm)	
	-150	-300
DNA Fragment Length	Average Normalized Resolution (n=27)	Normalized Resolution (n=1)
105 & 107	0.5±0.1	1.3
243 & 245	1.0±0.1	0.9
367 & 372	0.7±0.1	0.6
467 & 472	0.5±0.1	0.4

Table 2.5 Comparison of theoretical plate numbers at selected fragment lengths for sequencing runs at -150 V/cm and -300 V/cm using a methanol-hexanes PDMA sieving matrix.

	Electric Field Strength (V/cm)	
	-150	-300
DNA Fragment Length	Average Plates x 10^6 (n=27)	Plates x 10^6 (n=1)
105	2.3±.05	3.0
243	2.9±1.0	2.0
367	2.2±0.7	1.7
467	1.9±0.8	1.4

2.4 Conclusion

In this chapter, the manufacture and use of a replaceable PDMA sieving matrix in uncoated capillaries for high temperature DNA sequencing is demonstrated. Three types of sieving matrices are prepared and their performance in DNA sequencing is evaluated. The two matrices which are dissolved in methanol after polymerization are the only suitable matrices out of the three tested. The PDMA is dissolved after polymerization in methanol to help control chain length and promote completion of the polymerization reaction (48). These sieving matrices can be utilized in uncoated capillaries as they suppress electro-osmotic flow by creating a viscous layer adsorbed to the capillary wall. Multiple uses of the same capillary with renewal of sieving matrix between runs is proven to be possible. Migration time, resolution, and theoretical plate analyses show that run-to-run variations are negligible.

2.5 References

(1) Bocek, P.; Chrambach, A. *Electrophoresis* **1992,** *13*, 31.

(2) Chrambach, A.; Aldroubi, A. *Electrophoresis* **1993,** *14*, 18-22.

(3) Chen, N.; Wu, L.; Palm, A.; Srichaiyo, T.; Hjertén, S. *Electrophoresis* **1996,** *17*, 1443-1450.

(4) Strege, M.; Lagu, A. *Analytical Chemistry* **1991,** *63*, 1233-1236.

(5) MacCrehan, W. A.; Rasmussen, H. T.; Northrup, D. M. *Journal of Chromatography* **1992,** *15*, 1063.

(6) Kim, Y.; Morris, M. D. *Analytical Chemistry* **1994,** *66*, 3081-3085.

(7) McGregor, D. A.; Yeung, E. S. *Journal of Chromatography* **1994,** *680*, 491-496.

(8) Grossman, P. D.; Soane, D. S. *Journal of Chromatography* **1991,** *559*, 257-266.

(9) McCord, B. R.; Jung, J. M.; Holleran, E. A. *Journal of Liquid Chromatography* **1993,** *16*, 1963-1981.

(10) Barron, A. E.; Soane, D. S.; Blanch, H. W. *Journal of Chromatography A* **1993,** *652*, 3-16.

(11) Zhu, H.; Clark, S. M.; Benson, S. C.; Rye, H. S.; Glazer, A. N.; Mathies, R. A. *Analytical Chemistry* **1994,** *66*, 1941-1948.

(12) Butler, J. M.; McCord, B. R.; Jung, J. M.; Allen, R. O. *Biotechniques* **1994,** *17*, 4-7.

(13) Barron, A. E.; Sunada, W. M.; Blanch, H. W. *Electrophoresis* **1996,** *17*, 744-757.

(14) Baba, Y.; Ishimaru, N.; Samata, K.; Tsuhako, M. *Journal of Chromatography* **1993,** *653*, 329-335.

(15) Schwartz, H. E.; Ulfelder, K.; Sunzeri, F. J.; Busch, M. P.; Brownlee, R. G. *Journal of Chromatography* **1991,** *559*, 267-283.

(16) Figeys, D.; Arriaga, E.; Renborg, A.; Dovichi, N. J. *Journal of Chromatography* **1994,** *669*, 205-216.

(17) Dolnik, V.; Novotny, M. *Journal of Microcolumn Separations* **1992,** *4*, 515-519.

(18) Menchen, S.; Johnson, B.; Winnik, M. A.; Xu, B. *Electrophoresis* **1996,** *17*, 1451-1459.

(19) Fung, E. N.; Yeung, E. S. *Analytical Chemistry* **1995,** *67*, 1913-1919.

(20) Kim, Y.; Yeung, E. S. *Journal of Chromatography A* **1997,** *781*, 315-325.

(21) Gao, Q.; Yeung, E. S. *Analytical Chemistry* **1998,** *70*, 1382-1388.

(22) Wu, C.; Liu, T.; Chu, B. *Electrophoresis* **1998,** *19*, 231-241.

(23) Tietz, D.; Gottlieb, M. H.; Fawcett, J. S.; Chrambach, A. *Electrophoresis* **1986,** *7*, 217-220.

(24) Heiger, D. N.; Cohen, A. S.; Karger, B. L. *Journal of Chromatography* **1990,** *516*, 33-48.

(25) Maschke, H. E.; Frenz, J.; Belenkii, A.; Karger, B. L.; Hancock, W. S. *Electrophoresis* **1993,** *14*, 509-514.

(26) Paulus, A.; Husken, D. *Electrophoresis* **1993,** *14*, 27-35.

(27) Gelfi, C.; Orsi, A.; Leoncini, F.; Righetti, P. G. *Journal of Chromatography* **1995,** *689*, 97-105.

(28) Manabe, T.; Chen, N.; Terabe, S.; Yohda, M.; Endo, I. *Analytical Chemistry* **1994,** *66*, 4243-4252.

(29) Zhang, J.; Fang, Y.; Hou, J. Y.; Ren, H. J.; Jiang, R.; Roos, P.; Dovichi, N. J. *Analytical Chemistry* **1995,** *67*, 4589-4593.

(30) Wu, C.; Quesada, M. A.; Schneider, D. K.; Farinato, R.; Studier, F. W.; Chu, B. *Electrophoresis* **1996,** *17*, 1103-1109.

(31) Swerdlow, H.; Jones, B. J.; Wittwer, C. T. *Analytical Chemistry* **1997,** *69*, 848-855.

(32) Goetzinger, W.; Kotler, L.; Carrilho, E.; Ruiz-Martinez, M. C.; Salas-Solano, O.; Karger, B. L. *Electrophoresis* **1998,** *19*, 242-248.

(33) Salas-Solano, O.; Carrilho, E.; Kotler, L.; Miller, A. W.; Goetzinger, W.; Sosic, Z.; Karger, B. L. *Analytical Chemistry* **1998,** *70*, 3996-4003.

(34) Carrilho, E.; Ruiz-Martinez, M. C.; Berka, J.; Smirnov, I.; Goetzinger, W.; Miller, A. W.; Brady, D.; Karger, B. L. *Analytical Chemistry* **1996,** *68*, 3305-3313.

(35) Ruiz-Martinez, M. C.; Berka, J.; Belenkii, A.; Foret, F.; Miller, A. W.; Karger, B. L. *Analytical Chemistry* **1993,** *65*, 2851-2858.

(36) Menchen, S.; Johnson, B.; Madabhushi, R.; Winnik, M. *Proc. SPIE*, San Jose, CA 1996; The International Society for Optical Engineering; 294-303.

(37) Chiari, M.; Riva, S.; Gelain, A.; Vitale, A.; Turati, E. *Journal of Chromatography A* **1997,** *781*, 347-355.

(38) Xiong, Y.; Park, S.-R.; Swerdlow, H. *Analytical Chemistry* **1998,** *70*, 3605-3611.

(39) Madabhushi, R. S. *Electrophoresis* **1998,** *19*, 224-230.

(40) Chiari, M.; Nesi, M.; Righetti, P. G. *Electrophoresis* **1994,** *15*, 616-622.

(41) Chang, H.-T.; Yeung, E. S. *Journal of Chromatography B* **1995,** *669*, 113-123.

(42) Sudor, J.; Foret, F.; Bocek, P. *Electrophoresis* **1991,** *12*, 1056-1058.

(43) Ren, H.; Karger, A. E.; Oaks, F.; Menchen, S.; Slater, G. W.; Drouin, G. *Electrophoresis* **1999,** *20*, 2501-2509.

(44) Hjertén, S. *Journal of Chromatography* **1985,** *347*, 191-198.

(45) Goetzinger, W.; Karger, B. L. In *International Patent Application WO 96/23220*, 1996.

(46) Slater, G.; Kist, T. B. L.; Ren, H.; Drouin, G. *Electrophoresis* **1998,** *19*, 1525-1541.

(47) Wu, S.; Dovichi, N. J. *Journal of Chromatography* **1989,** *480*, 141-155.

(48) Bergman, M.; Claessens, H.; Cramers, C. *Journal of Microcolumn Separations* **1998,** *10*, 19-26.

Chapter 3
Capillary Isoelectric Focusing using Laser-Induced Fluorescence Detection: Green Fluorescent Protein as a Model Protein

*Part of this chapter is published as: Richards, D.P.; Stathakis, C.; Polakowski, R.; Ahmadzadeh, H.; and Dovichi, N.J. *Journal of Chromatography A* **1999**, *853*, 21-25.

3.1 Introduction

Isoelectric focusing (IEF) is a tool used to characterize proteins on the basis of their isoelectric points (pIs). A protein's pI is the pH at which it has an overall charge of zero and is thus electrically neutral. In IEF, a pH gradient is created utilizing ampholytes which are mixtures of polyprotic compounds- i.e. complex alkanes with many carboxylic acid and amine substitutions. In the presence of an electric field ampholytes establish a pH gradient. When proteins are placed in the pH gradient, they migrate to their pIs. If a protein diffuses away from its pI, it will acquire a charge and be driven back to its pI.

Shortly after the introduction of capillary electrophoresis (CE) and its powerful separation capabilities came the adaptation of CE to perform IEF (CIEF) (1). CIEF seeks to improve upon the disadvantages of traditional slab gel IEF (which utilizes immobilized polyacrylamide pH gradients), such as laborious staining procedures which result in poor sensitivity (2) and small pore size of the gel matrix, which can prevent macromolecules from attaining their pI (3). At the same time, CE lends its advantages to CIEF such as the use of small sample volumes, effective Joule heat dissipation, and real-time data acquisition. CIEF requires an additional step of mobilizing the sample past the detector. This mobilization is accomplished one of three ways by utilizing electro-osmotic flow, pressure, or chemical means. Figure 3.1 shows a schematic cartoon of the focusing and mobilization steps of CIEF. This drawing is specific to the use of a coated capillary and chemical means of mobilization which are used in this chapter.

The traditional detector used for CIEF is UV-based (1, 4-6); however there are inherent sensitivity limits to this approach. Furthermore, the ampholytes used to create a pH gradient for CIEF are highly absorbing in the UV spectral region which causes great interference with sample signal (7, 8). Fluorescent labeling of proteins and laser-induced fluorescence (LIF) detection are used in CE to improve detection limits (9). In CIEF, LIF detection is used to solve the problems of UV-absorbant ampholytes (7, 8) and sample-limited volumes (10). CE-LIF detection limits of proteins have been achieved on the order of 10^{-12} M to 10^{-13} M (11). CIEF is an effective concentrating technique and because of this, CIEF-LIF detection limits should be superior to those of CE-LIF by at least an order of magnitude. On account of this effective concentration, CIEF-LIF has the potential to be used with biological samples to detect low copy number proteins. Most reports of CIEF-LIF rely on native fluorescence (10, 12),

Figure 3.1 A schematic diagram of the focusing and mobilization steps in CIEF.

This schematic represents CIEF in a coated capillary, thus the anode is at the injection end and the cathode is at the detector end. In step A, the proteins are focused into sharp, highly concentrated bands at their pIs. In step B, the bands are mobilized past a detector via anodic mobilization; base is placed at the detection end to disrupt the pH gradient and mobilize the capillary's contents past the detector.

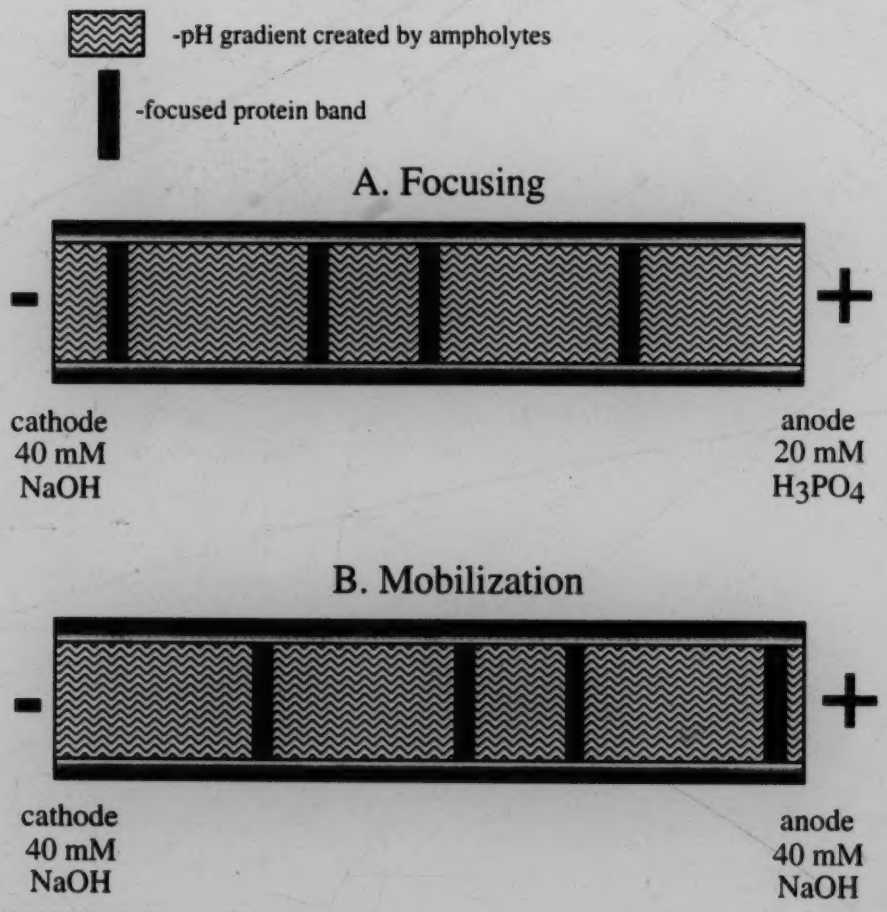

however in the recent past interest has peaked in the use of a fluorescent dye to tag the molecules of interest (7, 8, 13).

Concerns exist surrounding the use of a fluorescent dye to tag a protein and pI markers for CIEF-LIF. Labeling of peptides and proteins tagged with fluorescent dyes often results in heterogeneous products (7, 9, 14, 15). Furthermore, a protein's pI may change when it is fluorescently labeled. Due to the effect(s) labeling may have on the protein's three-dimensional structure, the protein's pI could also be effected (7, 16). It has been noted that upon conjugation with fluorescein isothiocyanate or tetramethyl rhodamine isothiocyanate, rabbit IgG experiences a pI decrease (17, 18). However, this decrease in pI may simply be due to the negative charge of fluorescein. It has also been deduced that labeling lysine groups on a protein will remove its positive charges and thus decrease the pI of the protein (7).

In this chapter, the effects of labeling proteins with the fluorogenic dye 3-(2-furoyl)quinoline-2-carboxaldehyde (FQ) on pI are presented. FQ reacts with the ε-amine groups of lysine residues to produce a fluorescent FQ-protein complex. Green fluorescent protein (GFP) was selected for this study. GFP from the jellyfish *Aequorea victoria* is a common gene marker capable of expression in both eukaryotic and prokaryotic systems (19). The use of GFP as a marker is attractive as it does not require any additional cofactors from the jellyfish to fluoresce (19). Thus, GFP's native fluorescence allows any changes in GFP's pI upon labeling with FQ to be monitored with CIEF-LIF. Capillary zone electrophoresis (CZE) is used to confirm that labeling with FQ is successful and slab gel IEF is utilized to confirm the CIEF-LIF results.

3.2 Experimental

3.2.1 Materials and reagents

Fused-silica capillary (50 μm ID, 140 μm OD) was purchased from PolyMicro Technologies (Phoenix, AZ). Recombinant GFP was obtained from Clontech Laboratories (Palo Alto, CA). Phastgel IEF 4-6.5 slab gels and Pharmacia Isoelectric Focusing Calibration Kit (Low pI Kit, pH 2.5-6.5) were from Pharmacia (Quebec, Canada). Bio-Lyte® 4/6 ampholytes, Bio-Lyte® 3/10 ampholytes, and ammonium persulfate (APS) were acquired from BioRad (Hercules, CA), and *N, N, N', N'*-tetramethylethylenediamine (TEMED) was purchased from GibcoBRL (Grand Island, NY). Sodium hydroxide (NaOH) and methanol were from Caledon (Georgetown, Canada). Phosphoric acid (H_3PO_4) was acquired from Fisher Scientific (Fair Lawn,

NJ). Di-sodium tetraborate (borate) and sodium carbonate (Na_2CO_3) were purchased from BDH Chemicals (Toronto, Canada). 3-(2-furoyl)quinoline-2-carboxaldehyde (FQ) was acquired from Molecular Probes (Eugene, OR). Vinylmagnesium bromide, tetrahydrofuran (THF), and potassium cyanide (KCN) were obtained from the Aldrich (Milwaukee, WI). Thionyl chloride was obtained from Acros Organics (Geel, Belgium). Trichloroacetic acid (TCA) and glacial acetic acid (HAc) were acquired from Anachemia (Montreal, Canada). Formaldehyde (37% photographic grade) and glutaraldehyde were from Sigma (St. Louis, MO). Silver nitrate ($AgNO_3$) was from ACP (Montreal, Canada). Ethanol (EtOH) was purchased from Commercial Alcohols (Winnipeg, Canada). Acryloylaminopropanol (AAP) was graciously provided by Prof. P. G. Righetti.

3.2.2 FQ-labeled ampholyte preparation

The FQ-labeled ampholyte reaction mixture contained 1 µL of a solution of 2% (v/v) Bio-Lyte® 3/10 ampholytes in 10 mM borate, 9 µL 25 mM KCN (in 10 mM borate), and 100 nmol FQ. The reaction was allowed to proceed for 1.5 minutes at room temperature whereupon it was diluted 10-fold with 10 mM borate to slow the reaction. The final concentration of ampholytes was 0.02% (v/v). A blank of this reaction mixture was prepared at the same time containing all of the identical components except the ampholytes.

3.2.3 FQ-labeled Pharmacia IEF standard preparation

One vial of the Pharmacia Low pI Isoelectric Focusing Calibration Kit (pH 2.5-6.5) was diluted in 1 mL of 10 mM borate. From this vial, a 9 µL aliquot was removed and added to 1 µL of 25 mM KCN (in 10 mM borate) and 100 nmol FQ. The reaction proceeded for 1.5 minutes at room temperature and was then slowed by dilution of the mixture 10-fold with 10 mM borate.

3.2.4 FQ-labeled GFP sample preparation

For CZE-LIF, unlabeled GFP was simply diluted to the appropriate concentration with 10 mM borate. For CZE-LIF of FQ-labeled GFP, reaction mixtures were as follows: 9 µL of 10^{-6} M GFP, 1 µL of 25 mM KCN (in 10 mM borate), and 100 nmol FQ. The reaction was carried out for one minute at room temperature and then diluted 100-fold with 10 mM borate to a final concentration of 9×10^{-8} M FQ-labeled GFP. For denaturation studies, labeling was done as follows: 9 µL of 10^{-6} M

GFP, 1 µL of 25 mM KCN (in 10 mM borate), and 100 nmol FQ were reacted for one minute at room temperature and then diluted 10-fold with 10 mM borate.

For slab gel IEF, the reaction mixture was as follows: 9 µL of 3.72×10^{-5} M GFP, 1 µL of 25 mM KCN (in 10 mM borate), and 100 nmol of dry FQ. These components were reacted for 1 minute at room temperature and diluted 100X with 10 mM borate to slow the reaction. The resulting 3.35×10^{-7} M FQ-labeled GFP mixture was loaded on to an application comb and then on to a gel.

For CIEF-LIF, the FQ labeling mixture was 1 µL of 3.72×10^{-5} M GFP, 9 µL of 25 mM KCN (in 10 mM borate), and 100 nmol of dry FQ. This mixture was reacted for 1 minute at room temperature and then diluted 100X with 10mM borate to slow the reaction. A solution of 3.72×10^{-9} M FQ-labeled GFP and 2% Bio-Lyte® 4/6 ampholytes in water was made which was put into a syringe and loaded into the capillary.

3.2.5 Sample preparation for fluorometer readings

A 3.72×10^{-7} M GFP solution was made of 1 µL of 3.72×10^{-5} M GFP in 99 µL of 10 mM borate. A 3.72×10^{-7} M FQ-labeled GFP solution was made of: 1 µL 3.72×10^{-5} M GFP, 9 µL of 25 mM KCN (in 10 mM borate), and 100 nmol FQ, which were reacted for 1 minute at room temperature and then diluted with 90 µL of 10 mM borate. The blank for these solutions was comprised only of 10 mM borate.

3.2.6 CZE-LIF

CZE was performed using the instrument described in Section 2.2.5. Uncoated capillaries were used which were 35 cm × 50 µm I.D. × 140 µm O.D.. Running and sheath flow buffers were 10 mM borate. FQ-labeled ampholytes were injected for 5s at 100 V/cm and run at 350 V/cm. IEF standards and FQ-labeled IEF standards were injected for 5 s at 100 V/cm and run at 350 V/cm. GFP was injected for 4 or 5 s at 250 V/cm and run at 350 V/cm while FQ-labeled GFP was injected for 5 s at 350 V/cm and run at 350 V/cm. For denaturation studies, samples were injected for 5 s at -350 V/cm and run at -350 V/cm in a 35 cm × 50 µm I.D. × 140 µm O.D. polyAAP Grignard coated capillary.

3.2.7 Slab gel IEF

A Pharmacia LKB Phastsystem was used for slab gel IEF. The slab gels had a pH 4-6.5 gradient. A Pharmacia Low pI Isoelectric Focusing Calibration Kit (pH 2.5-

6.5) was used for standard purposes. One vial of standards was dissolved in 1 mL of distilled deionized water (ddH_2O) before use. Table 3.1 displays the program used for IEF. The gel development was a variation of a silver stain protocol developed by Pharmacia. Table 3.2 shows the gel development program utilized to stain the gels. After development the gels were air-dried.

3.2.8 Capillary preparation

Capillaries were Grignard-coated according to the method of Cobb *et. al.* (20), and has been described elsewhere (21). Briefly, on the first day fused-silica capillary (5 m × 140 µm × 50 µm) was flushed with 1 M NaOH (3 hours), ddH_2O (1 hour), and methanol (1 hour) using nitrogen pressure (at 20 psi). The capillary was baked at 120°C overnight with nitrogen flowing through at 20 psi. The following day, the oven's temperature was reduced to 65°C with the capillary still inside. The capillary was removed and flushed with thionyl chloride at 20 psi for 30 minutes. The ends of the capillary were then capped with a GC septum and placed into the 65°C-oven. The thionyl chloride rinse was repeated 6-8 hours later. Then the capillary ends were capped and the capillary was placed into the oven (at 65°C) overnight. On the third day, the capillary was removed from the oven, about 1 cm from each end was trimmed, and the outlet end of the capillary was placed back inside the oven. The capillary was then flushed with a mixture of 0.20 M vinylmagnesium bromide in anhydrous THF, the outlet end of the capillary was removed from the oven and placed in anhydrous THF when the solution was observed exiting the capillary. The capillary was flushed for a total of 30 minutes at 20 psi with 0.20 M vinylmagnesium bromide. The capillary ends were then recapped with the GC septum and the capillary was placed in the oven overnight at 65°C. On the last day, the capillary was removed from the oven and the ends were trimmed about 1 cm. The capillary was rinsed with dry THF for 30 minutes at 20 psi. The capillary was then cut into desired lengths and flushed for 10 minutes at 25 psi with a polymerizing solution of AAP, polymerized with 1 µL of TEMED and 4 µL of fresh 10% (w/v) APS. The capillaries then sat for 30 minutes with the inlet end in ddH_2O, after which time they were rinsed for a few minutes with ddH_2O. The capillaries were then stored with their ends in ddH_2O.

Table 3.1 Pharmacia LKB Phastsystem program used for slab gel IEF.

Step	Voltage (V)	Current (mA)	Power (W)	Temperature (°C)	Volthours
1	2000	2.0	3.5	15	75
2	200	2.0	3.5	15	15
3	2000	5.0	3.5	15	410

Table 3.2 Pharmacia LKB Phastsystem development program utilized to silver stain IEF gels.

All solutions are volume/volume percentages except for silver nitrate, which was weight/volume percent. The developer is made of 0.03% (v/v) 37% formaldehyde in 2.5% (w/v) Na_2CO_3.

Step	Solution	Time (minutes)	Temperature (°C)
1	20% TCA	5	20
2	50% EtOH, 10% HAc	2	50
3	10% EtOH, 5% HAc	2	50
4	10% EtOH, 5% HAc	4	50
5	8.3% glutaraldehyde	6	50
6	10% EtOH, 5% HAc	3	50
7	10% EtOH, 5% HAc	5	50
8	ddH,O	2	50
9	ddH,O	2	50
10	0.5% $AgNO_3$	10	40
11	ddH,O	0.5	30
12	ddH,O	0.5	30
13	developer	0.5	27
14	developer	4.5	27
15	5% HAc	5	50

3.2.9 CIEF-LIF with anodic mobilization

The details of the capillary electrophoresis instrument are described in Section 2.2.5. In addition, a manual Hamilton T-valve (Chromatographic Specialties, Brockville, Canada) was added to the instrument's sheath flow line for mobilization purposes. Excitation was with a blue argon ion laser (3.5 mW, $\lambda = 488$ nm) (Uniphase, San Jose, CA,) and fluorescence was filtered through a 515DF20 bandpass filter (Omega Optical, Brattleboro, VT) to detect the native fluorescence of GFP or a 630DF30 bandpass filter to detect the fluorescence of FQ-protein conjugates.

IEF was performed in a 35 cm long × 50 µm I.D. × 140 µm O.D. fused silica capillary which was Grignard coated with polyAAP. Sample was focused for 30 minutes using a reversed electric field polarity of 350 V/cm. The running buffer (catholyte) was 40 mM NaOH and the sheath flow buffer (anolyte) was 20 mM H_3PO_4. To mobilize the sample past the detector, the sheath flow buffer was switched from 20 mM H_3PO_4 to 40 mM NaOH while the electric field was kept at -350V/cm.

3.2.10 Fluorometer measurements

All fluorometer measurements were performed using the TD-700 Fluorometer (Turner Designs, Sunnyvale, CA). Quartz cuvettes were 100 µL in volume and were obtained from National Scientific Co. (Quakertown, PA). Excitation was at 488 nm and emission was collected at 515 nm.

3.3 Results and Discussion

3.3.1 Labeling possibilities

On-column labeling is used in CE-LIF to decrease detection limits (22). The labeling technique used by Lee *et. al.* cannot be used in conjunction with CIEF-LIF, though, because the capillary must be completely filled with ampholytes and sample before focusing begins. Sample is not injected into the capillary as is done conventionally with CE. However, because CIEF is a sample-concentrating technique, very minute amounts of proteins can be detected. CIEF-LIF is ideally suited for the detection of very low abundance proteins, for example those in a cell extract or a single cell. Since samples must be mixed with ampholytes and then loaded on to the capillary, it is necessary to know if the sample labeling should be performed before or after mixing the sample with ampholytes. Thus, experiments were carried out to see whether

or not FQ reacts with and labels the ampholytes. Figure 3.2 shows the CZE-LIF results of ampholytes being subjected to FQ labeling. The CZE-LIF electropherograms clearly demonstrate that ampholytes are labeled by FQ. Furthermore, the sample CZE-LIF electropherogram shows a surprising signal considering the ampholyte concentration is 100-fold less than that used with samples in CIEF. The fact that FQ labels ampholytes is not surprising though, since ampholytes are made of compounds which contain amine groups (with which FQ reacts). However, it is remarkable that such a large signal is given by such a small concentration of ampholytes. These results indicate that the sample must be labeled with FQ prior to mixing it with ampholytes. If the sample and ampholytes were mixed together before labeling, the labeled ampholytes' signal would swamp that of the sample.

3.3.2 Slab gel IEF of FQ-labeled IEF standards

Confirmation of FQ-labeling of IEF standards was obtained by CZE. Figure 3.3 shows the CZE results of FQ-labeled IEF standards which illustrates that the derivatization reaction involving FQ was successful.

The IEF results of FQ-labeled standards are seen in Figure 3.4. There are changes in pI to three of the IEF standards upon conjugation with FQ. For each of the standards, only one band, indicating one pI, is seen in the unlabeled standards lanes. However, upon derivatization with FQ, each protein is effected by either a shifting of pI or by producing multiple pIs. FQ-labeled glucose oxidase appears as two bands which have more acidic pIs in comparison to unlabeled glucose oxidase (pI 4.15). Soybean trypsin inhibitor's pI is also affected by FQ labeling. In the labeled standards lanes, its band becomes two bands, which straddle the pI of unlabeled soybean trypsin inhibitor (pI 4.55). FQ-labeled β-lactoglobulin A appears as a large smear in a lower pI range than unlabeled β-lactoglobulin A. The higher pH region of the gel is difficult to see due to the staining method utilized. However, three bands are seen in the region of the pI of bovine carbonic anhydrase B. It is difficult to tell whether or not these bands are due to FQ-labeled bovine carbonic anhydrase B or human carbonic anhydrase B. Since this higher pH region is not visualized very well, there may be other changes to the pIs of the proteins that are not evident. However, these results indeed show that proteins' pIs can be changed upon conjugation with FQ. Usually an acidic shift in pI is seen upon labeling with FQ. This acidic shift in pI is due to the loss of positive charges as lysine groups are complexed by FQ. The more lysine groups that are labeled, the further acidic the pI will shift.

Figure 3.2 CZE of FQ-labeled pH 3/10 ampholytes.

See Section 3.2.2 for sample preparation: (A) blank, (B) FQ-labeled ampholytes. Data are median filtered every 3 points. CZE conditions: capillary: 40 cm × 140 µm O.D. × 50 µm I.D., running and sheath flow buffers: 10 mM borate, sample injection: 5 s, 150 V/cm, running voltage: 350 V/cm, excitation: 488 nm, emission filter : 630DF30.

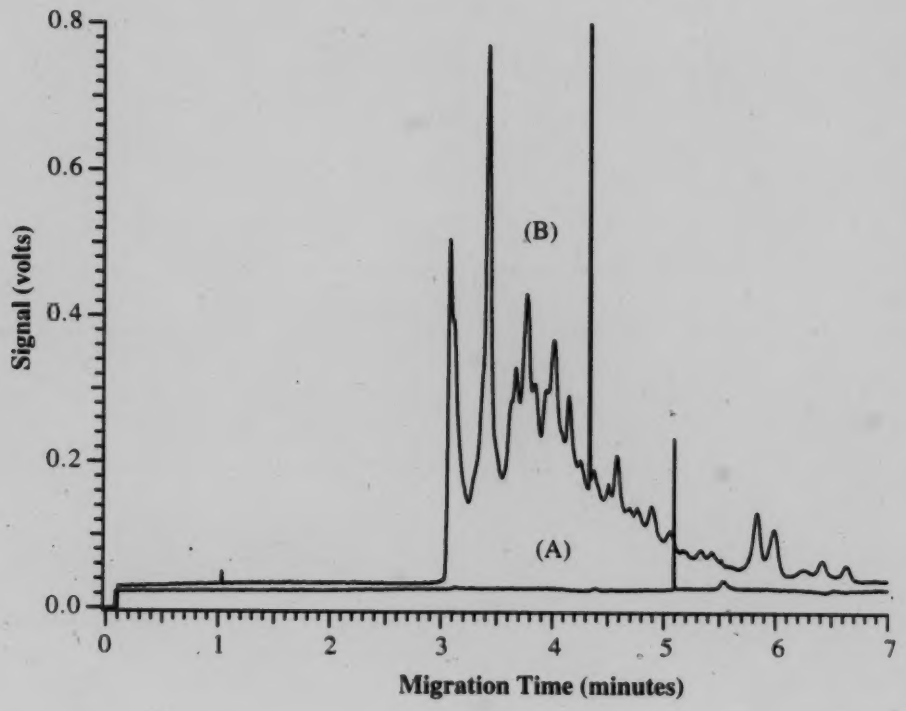

Figure 3.3 CZE of FQ-labeled IEF standards.

See Section 3.2.3 for sample preparation: (A) blank, (B) FQ-labeled IEF standards. Data are median filtered every third point. CZE conditions: capillary: 40 cm × 140 µm O.D. × 50 µm I.D., running and sheath flow buffers: 10 mM borate, sample injection: 5 s, 100 V/cm, running voltage: 350 V/cm, excitation: 488 nm, emission filter: 630DF30.

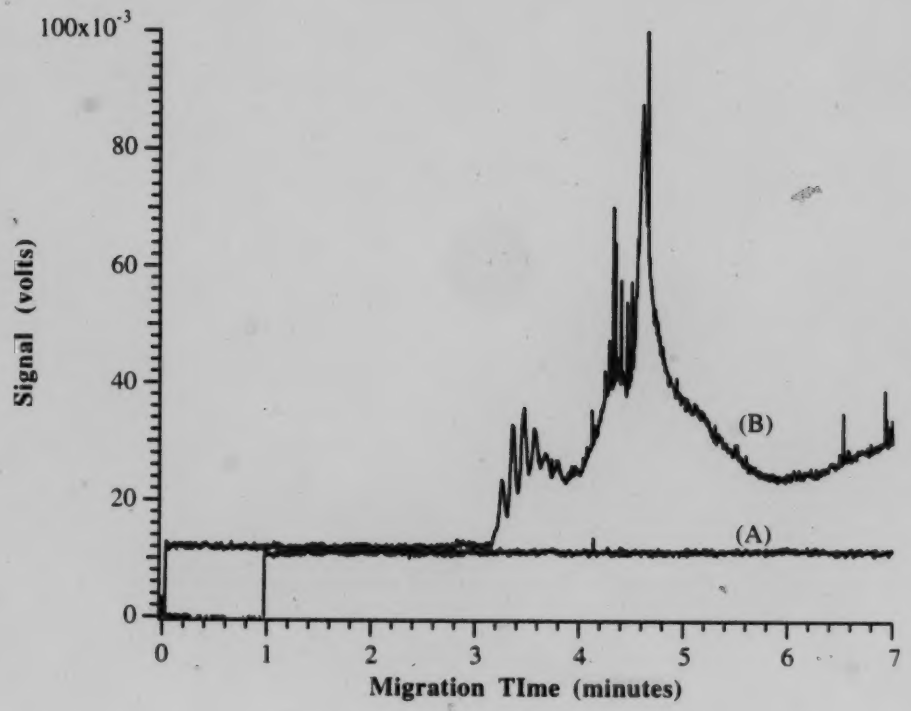

Figure 3.4 Slab gel IEF of FQ-labeled IEF standards.

This gel is pH 4-6.5 (pH 6.5 is at the top), run and stained as in Tables 3.1 and 3.2. See Section 3.2.3 for sample preparation. Lanes 1-4 are FQ-labeled IEF standards, lanes 5 and 6 are unlabeled IEF standards. The artifact in the middle of the gel is due to sample application. The standards and their pIs are as follows: glucose oxidase 4.15, soybean trypsin inhibitor 4.55, β-lactoglobulin A 5.20, bovine carbonic anhydrase B 5.85, human carbonic anhydrase B 6.55.

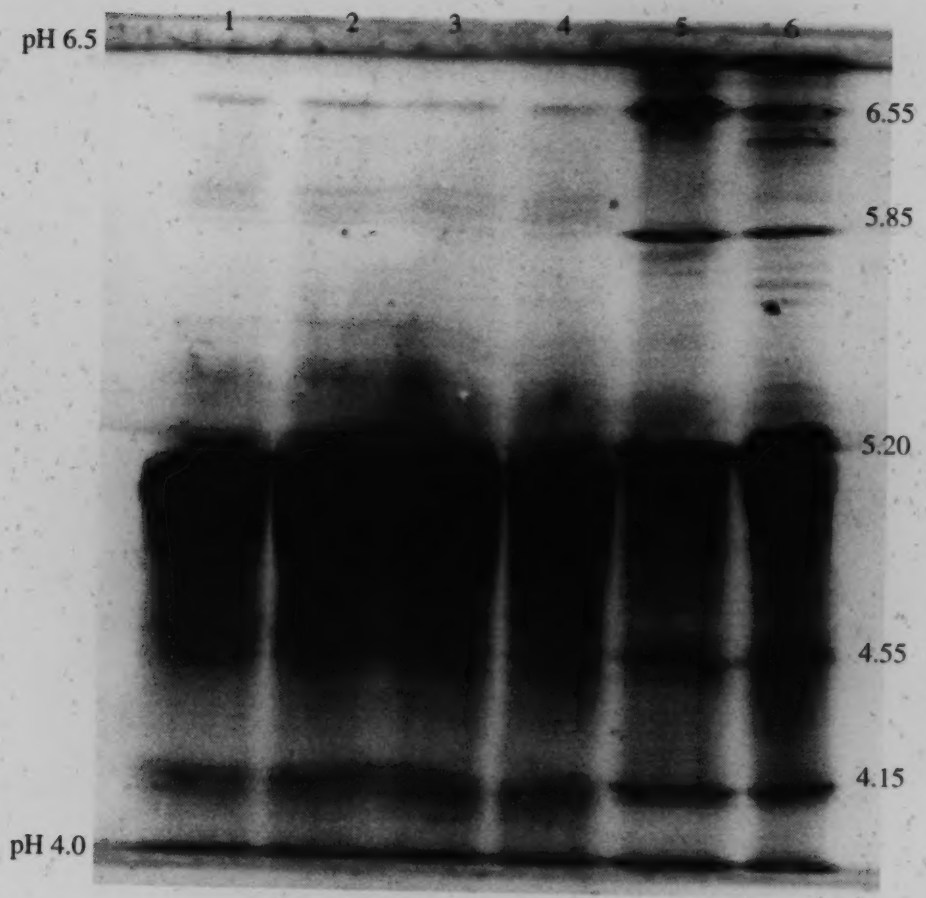

3.3.3 CZE of FQ-labeled GFP

CZE of FQ-labeled and unlabeled GFP was done to ensure that the GFP was in fact successfully derivatized. Figure 3.5 shows the detection of GFP's native fluorescence of labeled and unlabeled GFP. The unlabeled GFP shows two peaks- the peak just before 5 minutes is the monomer form of the protein and the smaller peak near 9 minutes is the dimer form of the protein. The labeled GFP shows many peaks which is an indication of labeling heterogeneity, and the dimer peak is still present. This heterogeneity in the FQ-derivatization of GFP was first reported by Craig *et. al.* (9). This labeling heterogeneity is due to the fact that GFP has many lysine groups which may react with FQ. These results show that FQ does not always react with the same lysine residue, and hence the multiple labeling pattern is seen. The next experiment investigated whether or not the FQ-derivatization of GFP has any effect on its pI.

3.3.4 Changes in GFP's pI upon FQ-labeling

Figure 3.6 is a picture of the IEF slab gel used to determine how the pI of GFP is effected upon conjugation with FQ. As can be seen, unlabeled GFP is actually a series of 3 bands- one major band and two very minor bands which flank the major band. The labeled GFP, however, appears at more acidic pIs than the unlabeled GFP. This result is due to the labeling with FQ which titrates successive lysine groups and shifts the pI of GFP to a more acidic region. Specifically, Figure 3.7 shows the calibration curve (R^2=0.9929) used to generate pI data for the labeled and unlabeled GFP. The pI of the main component of unlabeled GFP was found to be 5.00±0.04 (n=5 gels), with smaller bands flanking the main component with pIs of 4.88±0.05 and 5.19±0.04. The labeled GFP's pIs cannot be calculated because the multiple-labeled components here appear as a smear on the gel in the pH region of 4.6-4.9.

3.3.5 CIEF-LIF detection of changes in GFP's pI

Figure 3.8 shows the CIEF-LIF electropherograms of both unlabeled and FQ-labeled GFP. As can be seen, the unlabeled GFP exhibits one sharply focused peak which indicates only one pI. However, the FQ-labeled GFP shows many peaks, indicating that the pI of GFP has changed upon labeling. Furthermore, since the migration times of the FQ-labeled GFP peaks are shorter than that of the unlabeled GFP peak, it is deduced that the pIs of the FQ-labeled GFP variants are more acidic. This indicates that the FQ-labeled GFP has many pIs which are more acidic than that of the

Figure 3.5 CZE of unlabeled and FQ-labeled GFP with GFP native fluorescence detection.

See Section 3.2.4 for sample preparation: (A) unlabeled 10^{-8}M GFP, (B) 9×10^{-8} M FQ-labeled GFP. CZE conditions: capillary: 35 cm × 140 µm O.D. × 50 µm I.D., running and sheath flow buffers: 10 mM borate, sample injection: unlabeled GFP: 5 s, 250 V/cm, FQ-labeled GFP: 5 s, 350 V/cm, running voltage: 350 V/cm, excitation: 488 nm, emission filter: 515DF20.

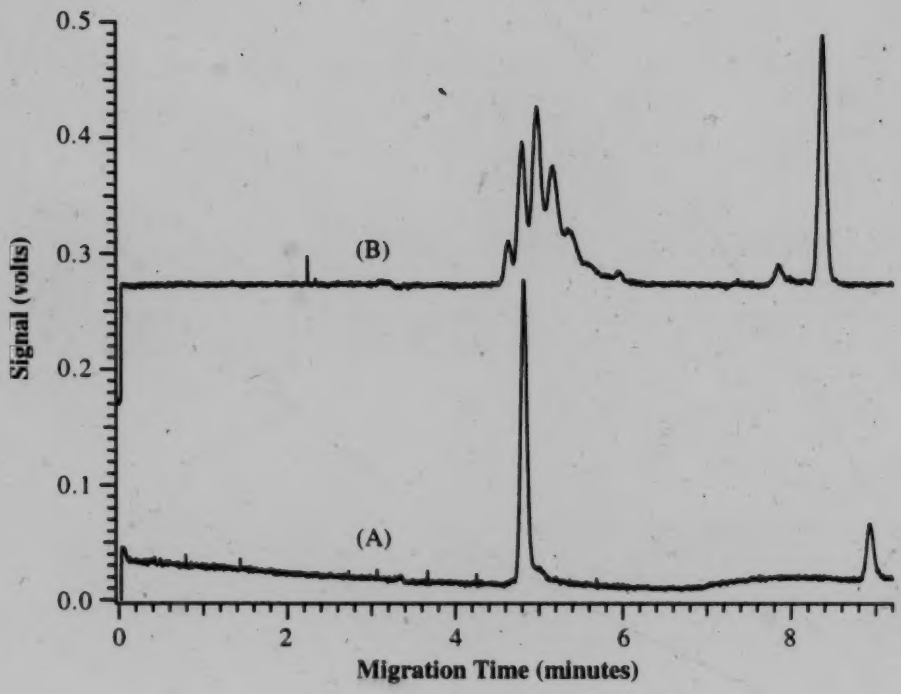

Figure 3.6 IEF slab gel determination of how FQ-labeling effects the pI of GFP.

This gel is pH 4-6.5 (pH 6.5 is at the top), run and stained as in Tables 3.1 and 3.2. See Section 3.2.4 for sample preparation. Lane 1 is 3.35×10^{-7} M FQ-labeled GFP, lane 2 is 3.72×10^{-7} M unlabeled GFP, and lane 3 is IEF standards with their pI values.

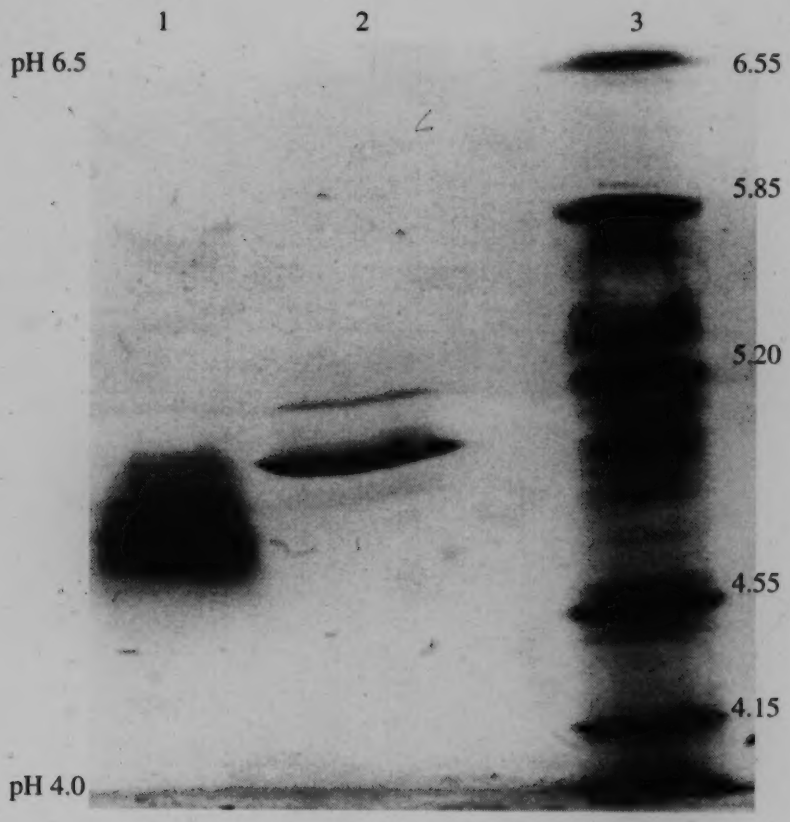

Figure 3.7 Calibration curve (n=5) used to determine pIs of GFP and FQ-labeled GFP.

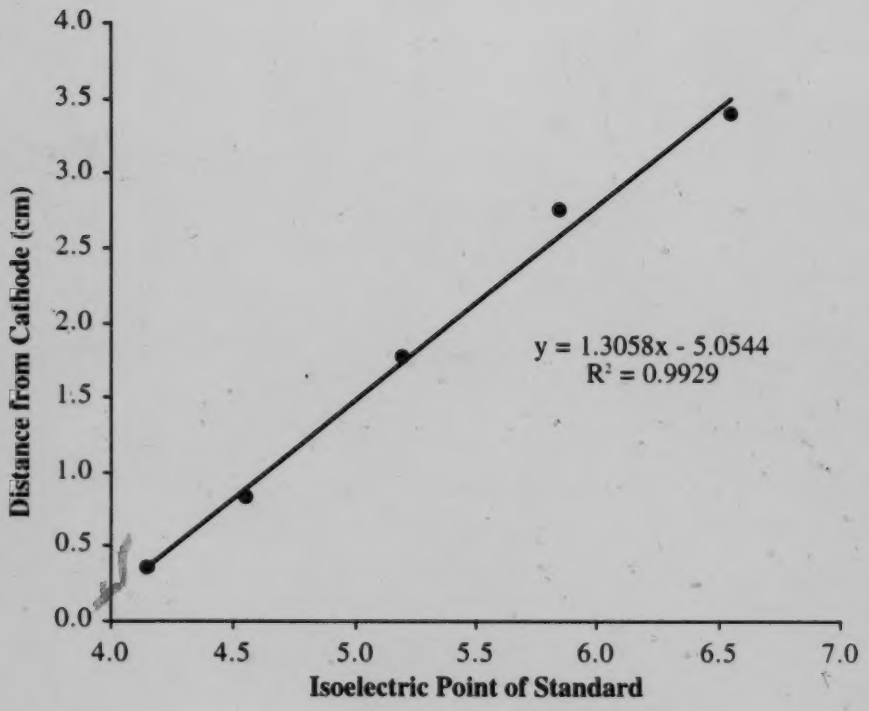

Figure 3.8 CIEF-LIF of the GFP's pI changes upon FQ-labeling.

See Section 3.2.4 for details of GFP labeling procedure. All samples are in 2% Bio-Lyte® 4/6 ampholytes in water: (A) 10^{-12} M GFP and (B) 3.72×10^{-9} M FQ-labeled GFP. CIEF conditions: polyAAP Grignard coated capillary 35 cm × 140 µm × 50 µm, catholyte: 40 mM NaOH, anolyte: 20 mM H_3PO_4, mobilization was at 30 minutes by changing the anolyte to 40 mM NaOH, excitation: 488 nm, and emission filter: 515DF20.

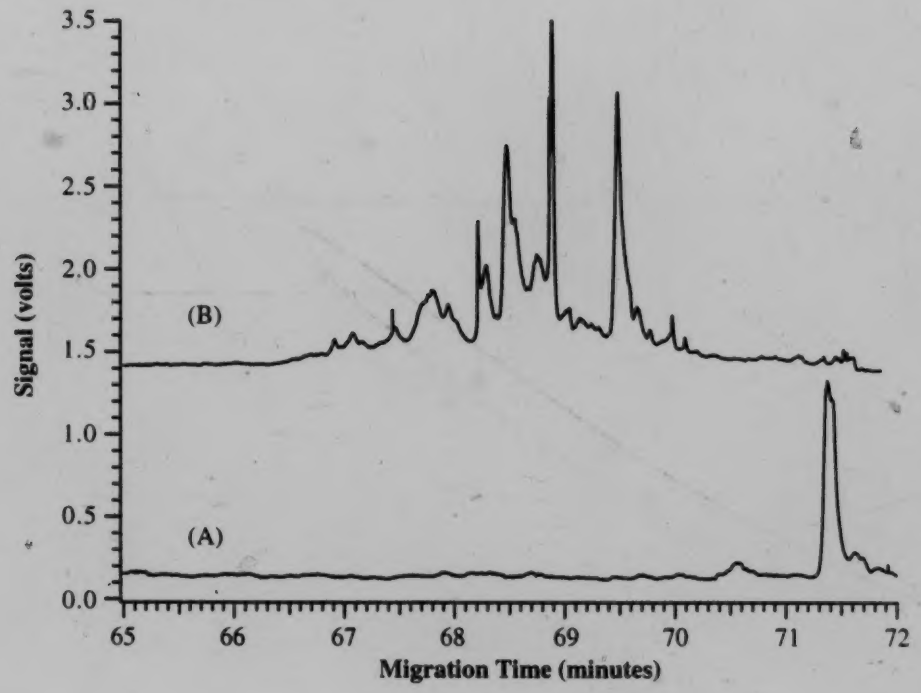

unlabeled GFP (recall that the acid is placed at the detector end during focusing). Also, many more peaks are seen with LIF detection rather than silver stain because LIF detection is more sensitive.

3.3.6 Denaturation of GFP upon conjugation with FQ

As was previously mentioned, there are possibilities of the 3-D structure of a protein changing upon conjugation with a dye molecule (7, 16). Studies were done to see the effects on the native fluorescence of GFP when it was conjugated to FQ. GFP is an uncharacteristically stable molecule in response to many pH and temperature ranges (23, 24), and resists denaturation by urea and proteolytic digestion using subtilisin (24, 25). However, GFP can be irreversibly denatured to give a nonfluorescent protein (24). It is believed that the production of different pIs upon FQ-labeling is not only a result of the titration of the positive charges of GFP, but also a result of the change in 3-D structure of the protein, or the denaturation of GFP.

Figure 3.9 displays the measurement of native fluorescence of GFP of both underivatized and FQ-derivatized GFP. As can be seen, shortly after FQ-labeling has occurred, the fluorescence of GFP has dropped by as much as 80%. This indicates that the 3-D structure of the protein has irreversibly changed upon derivatization and the abilities of its chromophore have been impaired. Denaturation of GFP and thus the destruction of its abilities to fluoresce are catalyzed by FQ-labeling.

Figure 3.10 shows CZE used to monitor the disappearance of GFP's native fluorescence and the appearance of fluorescence due to FQ-labeled GFP at periods of time over a total of five hours. The fluorescence monitored is that of the FQ-labeled product. At the beginning, the native fluorescence of GFP is strong enough that it overlaps into the spectral region of the FQ-fluorescence emission filter. Over time, the native fluorescence of GFP is observed decreasing while the fluorescence of the FQ-labeled product is increasing. Five hours after the reaction, the native fluorescence of GFP is barely detectable using the filter to measure FQ fluorescence. As with the fluorometer study, this decrease in native fluorescence indicates that changes have indeed taken place in the 3-D structure of GFP during FQ-labeling, resulting in partial or complete denaturation of GFP.

3.4 Conclusion

This chapter has shown the effects on pI of fluorescently labeling proteins with the fluorogenic substrate FQ. Both IEF standard proteins and the model protein, GFP,

Figure 3.9 Change in GFP's native fluorescence upon FQ-labeling.

See Section 3.2.5 for sample preparation details. See Section 3.2.10 for details of the fluorometer. Both the GFP and FQ-labeled GFP concentrations are 3.72×10^{-7} M (n=10 measurements/sample).

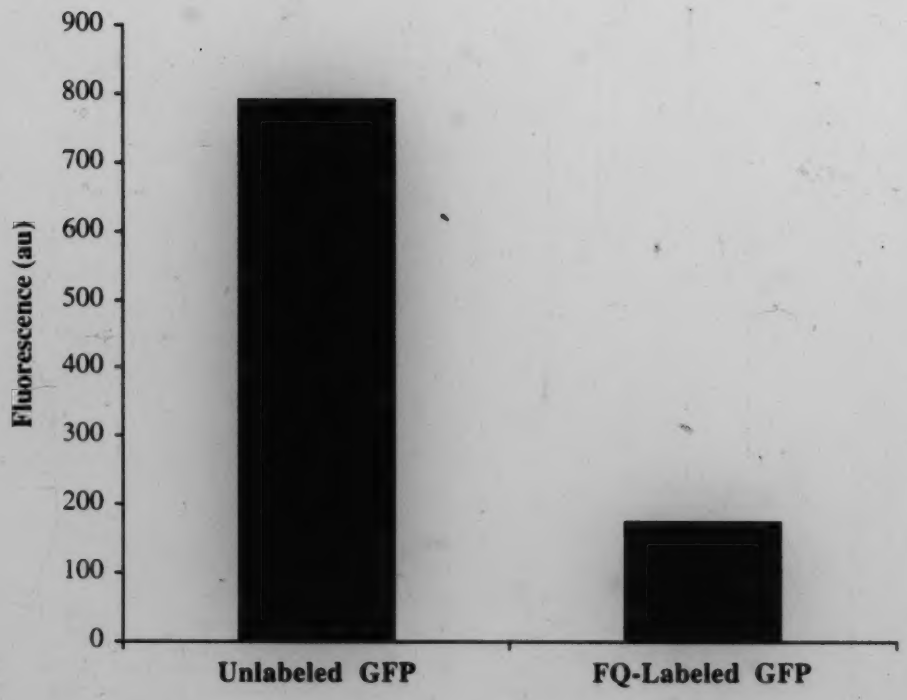

Figure 3.10 CZE observation of denaturation of GFP upon FQ labeling.

See Section 3.2.4 for details on sample preparation: (A) 10^{-8} M unlabeled GFP, (B)-(E) are 9×10^{-7}M FQ-labeled GFP; (B) immediately after reaction, (C) 15 minutes after reaction, (D) one hour after reaction, and (E) 5 hours after reaction. Data are median filtered every fifth point. CZE conditions: capillary: polyAAP Grignard coated, 35 cm × 140 µm O.D. × 50 µm I.D., running and sheath flow buffers: 10 mM borate, sample injection: 5 s, -350 V/cm, running voltage: -350 V/cm, excitation: 488 nm, emission filter: 630DF30.

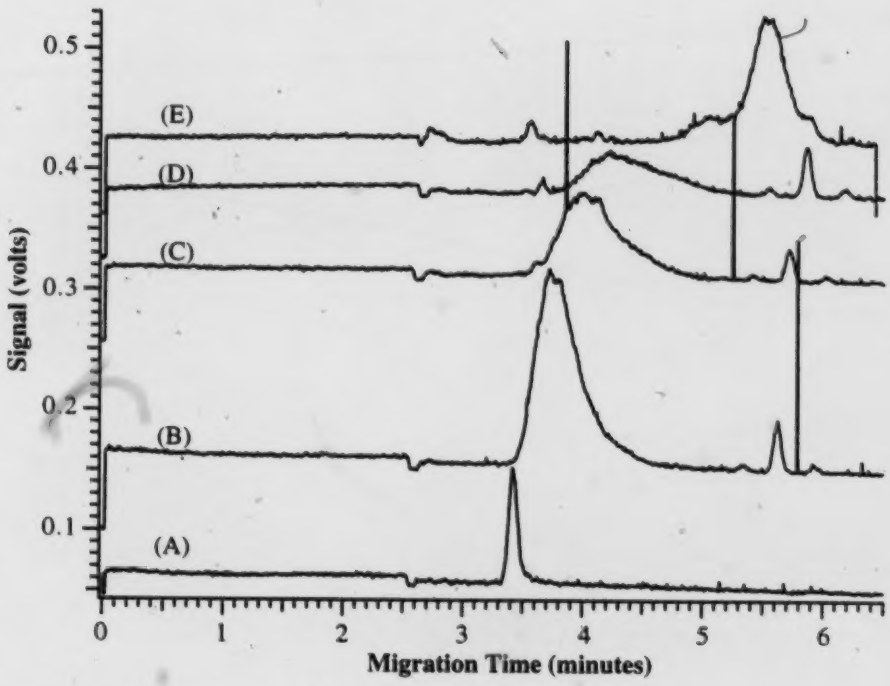

show changes in pI upon conjugation with FQ. In both cases, CZE was used to confirm the success of the FQ labeling reaction. CZE results of FQ-labeled ampholytes show that the amine groups of ampholytes can be derivatized by FQ and that samples must be conjugated with FQ prior to mixing with ampholytes and purging the capillary for CIEF-LIF. In the case of GFP, both slab gel IEF and CIEF-LIF results confirm that the protein's pI changes dramatically upon conjugation with FQ. GFP shows many heterogeneous labeling products as a result of FQ labeling. Each of these successive FQ labels titrates positive charge from the protein, moving its pI to a more acidic region. Furthermore, evidence has been given for the fact that the 3-D structure of GFP changes when it is reacted with FQ. A fluorometer study and a CZE study involving the monitor of GFP's fluorescence after FQ-labeling show that the protein's denaturation is catalyzed upon reaction with the dye.

3.5 References

(1) Hjertén, S.; Zhu, M.-D. *Journal of Chromatography* **1985,** *346*, 265-270.

(2) Schwer, C. *Electrophoresis* **1995,** *16*, 2121-2126.

(3) Schnabel, U.; Groiss, F.; Blaas, D.; Kenndler, E. *Analytical Chemistry* **1996,** *68*, 4300-4303.

(4) Hjertén, S.; Elenbring, K.; Kilar, F.; Liao, J.-L. *Journal of Chromatography* **1987,** *403*, 47-61.

(5) Kilár, F. In *CRC Handbook of Capillary Electrophoresis: A Practical Approach*; Landers, J. P., Ed.; CRC Press: Boca Raton, 1994, pp 95-109.

(6) Zhu, M.-D.; Hansen, D. L.; Burd, S.; Gannon, F. *Journal of Chromatography* **1989,** *480*, 311-319.

(7) Shimura, K.; Kasai, K.-i. *Electrophoresis* **1995,** *16*, 1479-1484.

(8) Verbeck IV, G. F.; Beale, S. C. *Journal of Microcolumn Separations* **1999,** *11*, 708-715.

(9) Craig, D. B.; Dovichi, N. J. *Analytical Chemistry* **1998,** *70*, 2493-2494.

(10) Lillard, S. J.; Yeung, E. S. *Journal of Chromatography B* **1996,** *687*, 363-369.

(11) Pinto, D. M.; Arriaga, E. A.; Craig, D.; Jordanka, A.; Sharma, N.; Ahmadzadeh, H.; Dovichi, N. J.; Boulet, C. A. *Analytical Chemistry* **1997,** *69*, 3015-3021.

(12) Korf, G. M.; Landers, J. P.; O'Kane, D. J. *Analytical Biochemistry* **1997,** *251*, 210-218.

(13) Wu, X.-Z.; Wu, J.; Pawliszyn, J. *Electrophoresis* **1995,** *16*, 1474-1478.

(14) Liu, J.; Hsieh, Y.-Z.; Wiesler, D.; Novotny, M. *Analytical Chemistry* **1991,** *63*, 408-412.

(15) Zhao, J. Y.; Waldron, K. C.; Miller, J.; Zhang, J.; Harke, H.; Dovichi, N. J. *Journal of Chromatography* **1992,** *608*, 239-242.

(16) Williamson, A. R.; Salamam, M. R.; Kreth, H. W. *Annals of the New York Academy of Sciences* **1973,** *209*, 210-224.

(17) Goding, J. W. *Journal of Immunological Methods* **1976,** *13*, 215-226.

(18) The, T. H.; Feltkamp, T. E. W. *Immunology* **1970,** *18*, 875-881.

(19) Chalfie, M.; Tu, Y.; Euskirchen, G.; Ward, W. W.; Prasher, D. C. *Science* **1994,** *263*, 802-805.

(20) Cobb, K. A.; Dolnik, V.; Novotny, M. *Analytical Chemistry* **1990,** *62*, 2478-2483.

(21) Gelfi, C.; Curcio, M.; Righetti, P. G.; Sebastiano, R.; Citterio, A.; Ahmadzadeh, H.; Dovichi, N. J. *Electrophoresis* **1998,** *19*, 1677-1682.

(22) Lee, I. H.; Pinto, D.; Arriaga, E. A.; Zhang, Z.; Dovichi, N. J. *Analytical Chemistry* **1998,** *70*, 4546-4548.

(23) Bokman, S. H.; Ward, W. W. *Biochemical and Biophysical Research Communications* **1981,** *101*, 1372-1380.

(24) Chalfie, M. *Photochemistry and Photobiology* **1995,** *62*, 651-656.

(25) Wampler, J. E.; Hori, K.; Lee, J. W.; Cormier, M. J. *Biochemistry* **1971,** *10*, 2903-2909.

Chapter 4
Hydroxyethylcellulose as a Sieving Matrix for Sodium Dodecyl Sulfate Capillary Gel Electrophoresis of Proteins with Laser-Induced Fluorescence Detection

4.1 Introduction

Sodium dodecyl sulfate polyacrylamide gel electrophoresis (SDS-PAGE) is an extremely common protein separation method. SDS-PAGE exploits the binding of SDS with denatured proteins in a constant ratio of 1.4 g SDS to 1 g of protein (1). This constant binding ratio produces proteins with overall negative charges and nearly constant charge-to-mass ratios. Due to this constant charge-to-mass ratio, a sieving matrix must be used in electrophoresis in order to separate proteins on the basis of their molecular weight. This electrophoretic method has traditionally employed cross-linked polyacrylamide slab gels. However in the past decade or so, SDS-PAGE has been successfully adapted for use with capillaries. The first SDS capillary gel electrophoresis (CGE) protein separation was performed in 1983 by Hjertén who employed a glass capillary column filled with polyacrylamide to separate membrane proteins (2). In 1987 Cohen *et. al.* used an SDS cross-linked polyacrylamide gel-filled capillary to separate peptides and proteins on a molecular weight basis (3). Other research groups have also reported the use of cross-linked polyacrylamide in the SDS CGE separation of proteins (4, 5). However due to various problems inherently associated with polymerizing cross-linked polyacrylamide inside capillaries (e.g. void formation due to gel shrinkage inside the column (6)), a natural progression towards the utilization of linear polyacrylamide (LPA) for protein SDS CGE has occurred (6-9). Since these initial SDS CGE experiments, which provided the basis for a new separation technique, the SDS CGE of proteins has since grown to include the employment of a host of sieving matrices other than the traditional polyacrylamide.

Progression towards using replaceable sieving matrices for the SDS CGE separation of proteins has furthered the search for sieving matrices beyond polyacrylamide. The employment of a replaceable sieving matrix in the SDS CGE of proteins is advantageous in that it decreases sample cross contamination which inevitably occurs when a sieving matrix is re-used inside a capillary. Dextran is one such replaceable sieving matrix as it is nonrigid. The use of dextran for the SDS CGE separation of proteins was first described by Ganzler *et. al.* (8). Following its introduction, various properties of dextran have been studied such as how temperature affects separations involving branched dextran (10) and how dextran molecular weight affects separation (11, 12). Furthermore, dextran has been successfully employed by a number of research groups utilizing SDS CGE to separate proteins of plasma samples (8), to separate myoglobin molecular mass markers (13), and to separate and detect

proteins using LIF (14). Use of poly(ethylene oxide) (PEO) for SDS CGE of proteins was first reported by Guttman *et. al.* (10). Studies have also been completed on how the molecular mass and concentration of PEO affects protein SDS CGE separations (15). Poly(ethylene glycol) (PEG) as a sieving matrix for SDS CGE protein separations was first reported by Ganzler *et. al.* (8), who demonstrated separations of crude *E. coli* extract and a monoclonal antibody. PEG concentration and molecular weight effects on hemoglobin polymer separations have also been studied (15). Nakatani *et. al.* demonstrated the employment of pullulan as a sieving matrix in SDS CGE separations by showing the achievement of baseline separations using pullulan concentrations of 3-10 % (w/v) (16). Commercial SDS CGE separation kits have since become available and many research groups have employed these for convenient protein molecular weight based separations (17-22). One such SDS CGE separation kit supplies a sieving matrix made of a mixture of PEO and PEG (18), while another kit exploits the dynamic sieving capabilities of LPA (23).

Hydroxyethylcellulose (HEC) is employed in capillary electrophoresis (CE) to aid with both DNA and protein separations. HEC is commonly used in DNA separations as a size-based sieving matrix (24-32). The migration regime models for these DNA separations in linear polycharged polymers such as HEC have been evaluated by Minarik *et. al.* (33). The authors employed a size-based separation of linear poly(styrenesulfonates) (PSS) in capillaries containing 0.03 M formate/Tris with differing concentrations and molecular weights of HEC (33). Oda *et. al.* separated transferrin sialoforms in a DB-17-coated capillary with a buffer system of 100 mM borate, pH 8.5 containing 0.5% HEC (no average molecular weight was given)(34). However, the authors concluded that the separations were charge-based rather than size-based (34). HEC is also used as a dynamic coating to suppress electro-osmotic flow (EOF) during capillary zone electrophoresis (CZE) protein separations. Righetti has published numerous articles on the utilization of HEC as an electro-osmotic flow-suppressor for the generation of protein maps in isoelectric buffers (35-38). For example, peptide maps of β-casein were generated using uncoated capillaries filled with 50 mM iminodiacetic acid in 0.5% HEC (average number weight molecular weight, M_n, of 27 000), and 6-8 M urea (35). Tryptic maps of α- and β-globin chains from human hemoglobin were generated in bare capillaries using a buffer system of 50 mM aspartic acid, 0.5% HEC (M_n 27 000), 5% trifluoroethanol, and 1% CHAPS (36). An identification method for maize lines involved separating zeins in an uncoated capillary with a buffer of 40 mM aspartic acid, 0.5% HEC (M_n 27 000), and 8 M urea (37).

Lastly, a similar buffer (40 mM aspartic acid, 0.5% HEC (M_n 27 000), and 7 M urea) was used to separate, in naked capillaries, gliadins to discriminate wheat culvar (38).

This chapter describes the use of HEC as a sieving matrix for SDS CGE protein separations. HEC is commonly used as a buffer additive for the CZE separation of proteins, however HEC's role has been to aid in charge-based, rather than size-based protein separations. This chapter presents the employment of HEC in size-based protein separations using coated capillaries and an SDS buffer system. Two different types of Grignard coated capillaries are utilized to generate data for the size-based protein separations. Different percentages of HEC are used to optimize separation conditions. Data are analyzed to see how same-day and day-to-day migration times differ and how electric field strength affects migration times. Standardization curves show the linear dependence of migration time on the molecular weight of proteins.

4.2 Experimental

4.2.1 Materials and reagents

Fused-silica capillary (50 µm I.D., 140 µm O.D.) was purchased from PolyMicro Technologies (Phoenix, AZ). 3-(2-furoyl)quinoline-2-carboxyaldehyde (FQ) was acquired from Molecular Probes (Eugene, OR). Sodium hydroxide was from Caledon Laboratories (Georgetown, Canada). Fisher (Fairlawn, NJ) supplied the methanol. Concentrated hydrochloric acid was obtained from Anachemia (Vancouver, Canada). *N,N,N',N'*- tetramethylethylenediamine (TEMED) and ammonium persulfate (APS) were purchased from Bio-Rad Laboratories (Hercules, CA, USA). Sodium cyanide (NaCN), sodium dodecyl sulfate (SDS), and di-sodium tetraborate (borate) were all from BDH (Toronto, Canada). Thionyl chloride was purchased from Acros Organics (Geel, Belgium). Hydroxyethyl cellulose (HEC) (average molecular weight 250 000, lot number 11116AN), β-mercaptoethanol, vinylmagnesium bromide, and tetrahydrofuran (THF) were supplied by Aldrich (Milwaukee, WI). Tris[hydroxymethyl]aminomethane (Trizma) base, lysozyme from chicken egg white (14.3 kDa), carbonic anhydrase from bovine erythrocyte (29 kDa), glyceraldehyde-3-phosphate dehydrogenase from rabbit muscle (36 kDa), chicken egg albumin, Grade VII (ovalbumin, 45 kDa), bovine serum albumin, Fraction V (BSA) (66 kDa), and phosphorylase b from rabbit muscle (97 kDa) were all acquired from Sigma (St. Louis, MO). Acrylamide was from GibcoBRL (Grand Island, NY). Acryloylaminopropanol (AAP) was graciously provided by Professor P. G. Righetti.

4.2.2 FQ labeling of individual protein standards

Individual protein stock solutions (lysozyme, carbonic anhydrase, glyceraldehyde-3-phosphate dehydrogenase, ovalbumin, bovine serum albumin, and phosphorylase b) were made up at 10^{-4}M in a solution of 10 mM borate, 5 mM SDS, 1.5 mM NaCN, and 1% (w/v) β-mercaptoethanol, pH 9.3. Prior to labeling, each protein stock (10 µL) was denatured at 95°C for 5 minutes. The 10 µL of denatured stock solution was then transferred to a vial which contained 100 nmol dry FQ. The subsequent mixture was reacted for 15 minutes at 65°C. After 15 minutes, each vial was diluted 10X with 10 mM TrisHCl, 5 mM SDS (pH 8.0) to slow the labeling reaction. Appropriate volumes of each stock solution were used to make the required sample solutions.

4.2.3 Capillary preparation

See Section 3.2.8 for complete capillary preparation details of polyacryloylaminopropyl (polyAAP) Grignard coated capillaries. LPA Grignard coated capillaries were prepared in the same manner as polyAAP coated capillaries. However a polymerizing 3% (w/v) acrylamide mixture was flushed through the capillary on the last day instead of a polymerizing AAP mixture.

4.2.4 Sieving matrix preparation

The appropriate weight of HEC was measured into a 15 mL Fisher tube and about 5 mL of 10 mM TrisHCl 5mM SDS, pH 8.0 were added. The tube was tumbled in an incubator at 37°C overnight to dissolve the HEC. The following day the tube was removed from the incubator and topped up with buffer to a total volume of 10 mL. Then the solution was mixed again to heterogeneity.

4.2.5 Capillary electrophoresis instrument

See Section 2.2.5 for details of the single-capillary instrument with sheath-flow cuvette and LIF detector used. A blue argon ion laser (3.5 mW, λ = 488 nm) (Uniphase, San Jose, CA) was used for sample excitation. Fluorescence was filtered through a 630DF30 bandpass filter (Omega Optical, Brattleboro, VT) and was then detected with an R1477 photomultiplier tube (Hamamatsu, Middlesex, NJ).

4.2.6 CE using a LPA Grignard coated capillary

The protein separations were performed in a LPA Grignard coated capillary which was either 37 or 40 cm long (140 µm O.D., 50 µm I.D.). Before each separation, the capillary was manually flushed with buffer (10 mM TrisHCl, 5 mM SDS, pH 8.0) for a few seconds, and then briefly with the HEC sieving matrix. Prior to injection, the capillary was equilibrated for 5 to 10 minutes by running it at 350 V/cm reversed polarity in 10 mM TrisHCl, 5 mM SDS, pH 8.0. Sample composition and injection varied and are described in detail in the figure captions which follow. Separations were studied at various electric fields using running and sheath flow buffers of 10 mM TrisHCl, 5 mM SDS, pH 8.0.

4.2.7 CE using a polyAAP Grignard coated capillary

The separations were performed in a polyAAP Grignard coated capillary which was either 32.5, 35, or 35.5 cm long (140 µm O.D., 50 µm I.D.). Before each separation, the capillary was manually flushed with buffer (10 mM TrisHCl, 5 mM SDS, pH 8.0) for a few seconds, and then briefly with the HEC sieving matrix. Prior to injection, the capillary was equilibrated for 6 minutes by running it at 400 V/cm reversed polarity in either 10 mM TrisHCl, 5 mM SDS, pH 8.0 or 1% HEC (dissolved in 10 mM TrisHCl, 5 mM SDS, pH 8.0). The sample composition and electrokinetic injections varied and are described in detail in the figure captions. Electrophoretic separations were studied at various electric fields using a running buffer of either 10 mM TrisHCl, 5 mM SDS, pH 8.0 or 1% HEC (dissolved in 10 mM TrisHCl, 5 mM SDS, pH 8.0), corresponding to whichever running buffer was used for preconditioning. The sheath flow buffer was always 10 mM TrisHCl, 5 mM SDS, pH 8.0.

4.3 Results and Discussion

4.3.1 CZE of a mixture of standard proteins

Figure 4.1 shows the CZE results of a mixture of the standard proteins of lysozyme (MW 14.3 kDa), carbonic anhydrase (MW 29 kDa), ovalbumin (MW 45 kDa), and BSA (MW 66 kDa). The standards co-migrate from the capillary which indicates that even though the proteins have different molecular weights, they have similar electrophoretic mobilities. Since the proteins have similar electrophoretic

Figure 4.1 CZE of a mixture of molecular weight standards.

CZE conditions: sample: mixture of 10^{-6} M of each of the following: lysozyme, carbonic anhydrase, ovalbumin, and BSA, capillary: LPA Grignard coated, 40 cm × 140 µm O.D. × 50 µm I.D., running and sheath flow buffers: 10 mM TrisHCl, 5 mM SDS, pH 8.0, sample injection: 5 s, -450 V/cm, running voltage: -350 V/cm, excitation: 488 nm, emission filter : 630DF30.

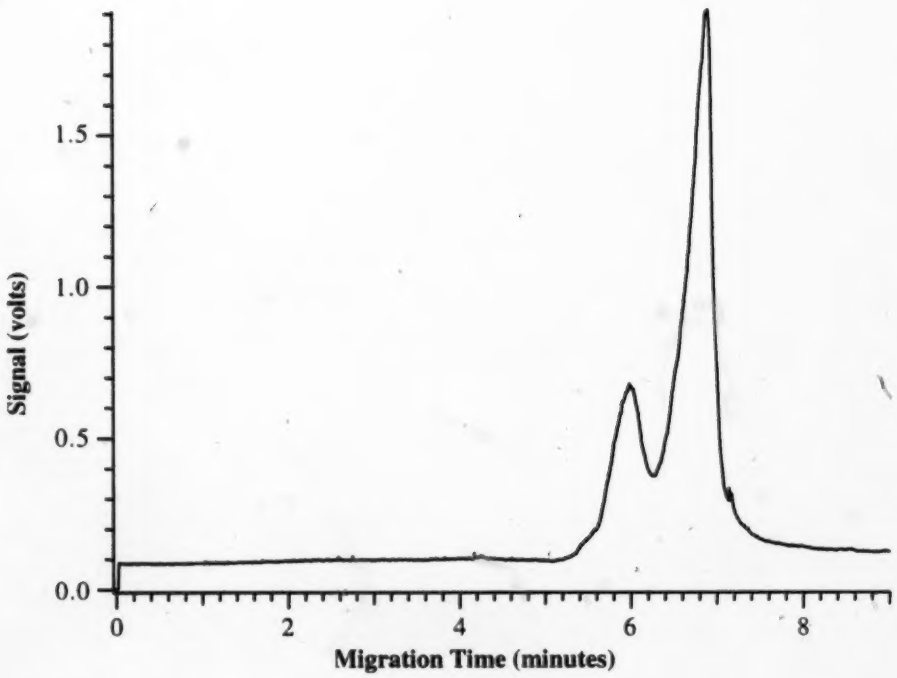

mobilities, they cannot be separated by CZE methods. This CZE electropherogram demonstrates the attempt to separate these standards in the absence of a sieving matrix. In the following sections, results will be shown of the standards separated using a HEC sieving matrix and SDS buffers to achieve size-based separations.

4.3.2 CGE using different percentages of HEC sieving matrices

Figure 4.2 shows the molecular weight-based separations of standard proteins using different percentages of HEC in the sieving matrix. It must be noted that same-day and day-to-day migration time reproducibility is a factor which will be addressed in Sections 4.3.8 and 4.3.9, so the migration times for select runs have been scaled to allow qualitative comparison of the separations. It has been determined that the proteins migrate in the order of lysozyme (MW 14.3 kDa), carbonic anhydrase (MW 29 kDa), and BSA (MW 66 kDa). Qualitatively, it is apparent that the higher percentages of HEC (i.e. 1.75% and 2%) in the sieving matrix produce ineffective separations of the mixture of three proteins. However, the 1.5%, 1.25%, 1%, and 0.5% HEC-containing sieving matrices separate successfully all three protein standards to differing extents. Since the peak shapes using 1% HEC consistently appear satisfactory and the fact that this sieving matrix consistently produced the most effective separations, it was this percentage of HEC chosen as the sieving matrix to be employed for the remainder of the experiments.

4.3.3 Standardization curve construction

In order for this separation method to be used to measure molecular weights of proteins, suitable standardization curves must be constructed from standard proteins. The 1% HEC sieving matrix, irregardless of the type of coated capillary utilized for separation, produces a linear standardization curve of migration time versus molecular weight. Figure 4.3 is the standardization curve produced by the separation of protein standards in a polyAAP Grignard coated capillary run at an electric field of -400 V/cm. The high R^2 value of 0.9995 indicates the plot's excellent linearity. To see how or if separation electric field strength had any effect(s) on the linearity of the standardization curves, further studies were carried out.

4.3.4 Effect of electric field on separation using a LPA Grignard coated capillary with a HEC sieving matrix

Figure 4.4 shows the electropherograms of separations performed at electric

Figure 4.2 How percentage of HEC in the sieving matrix effects separation.

See Section 4.2.2 for sample preparation details. Data are median filtered every 3 points. HEC sieving matrices are: (A) 2%, (B) 1.75%, (C) 1.5%, (D)1.25%, (E) 1%, (F) 0.5%. Samples are labeled as: (1) 10^{-6} M lysozyme, (2) 10^{-6} M carbonic anhydrase, (3) 10^{-6} M BSA. CE conditions: capillary: LPA Grignard coated, 37 or 40 cm × 140 µm O.D. × 50 µm I.D., running and sheath flow buffers: 10 mM TrisHCl, 5 mM SDS, pH 8.0, sample injection: 5 or 10 s, -450 V/cm, running voltage: -350 V/cm, excitation: 488 nm, emission filter: 630DF30.

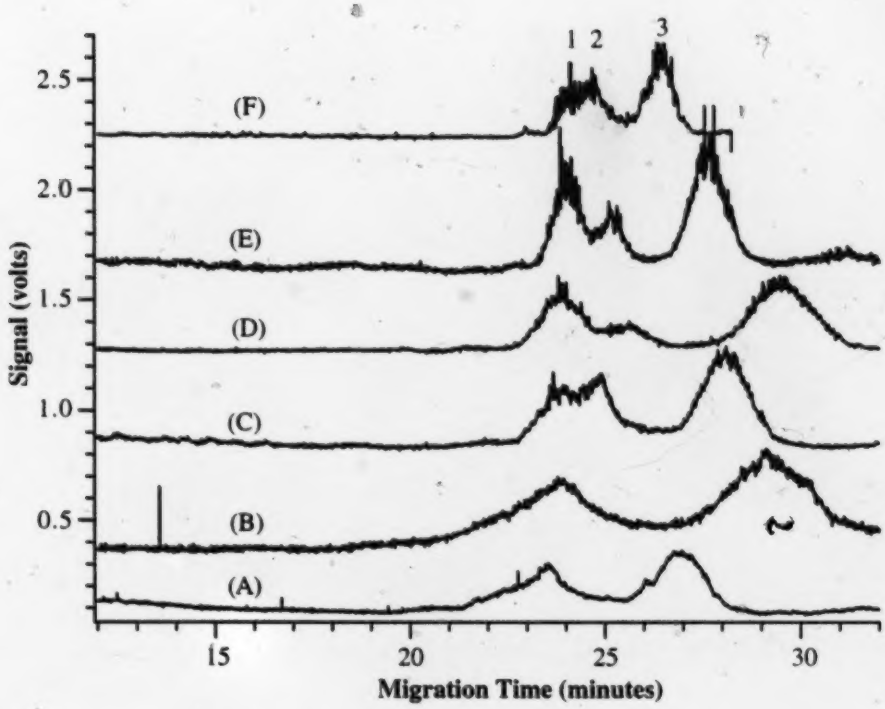

Figure 4.3 Standardization curve of migration time versus molecular weight.

See Section 4.2.2 for sample preparation details. CE conditions: sample: mixture of 5 $\times 10^{-6}$ M of each of the following: lysozyme, glyceraldehyde-3-phosphate dehydrogenase, and phosphorylase b, and 10^{-5} M BSA, capillary: polyAAP Grignard coated, 35.5 cm $\times$ 140 µm O.D. $\times$ 50 µm I.D., sieving matrix: 1% HEC, running and sheath flow buffers: 10 mM TrisHCl, 5 mM SDS, pH 8.0, sample injection: 5 s, -425 V/cm, running voltage: -400 V/cm, excitation: 488 nm, emission filter : 630DF30.

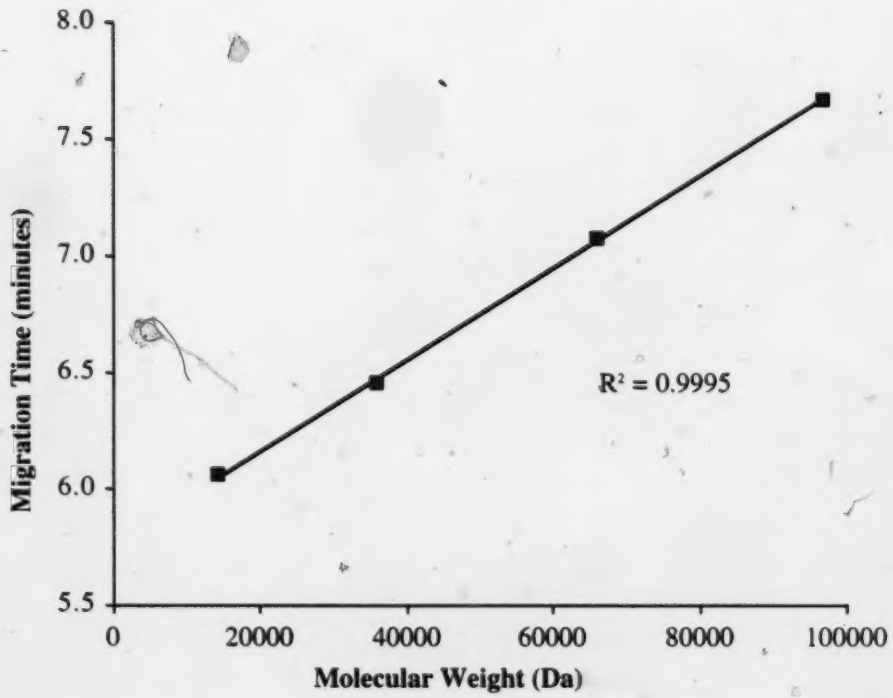

field strengths of -250 V/cm, -300 V/cm, and -350 V/cm employing a LPA Grignard coated capillary without HEC in the running buffer. Utilizing an electric field of -250 V/cm, the separation requires at least 42 minutes, an electric field of -300 V/cm requires a separation time of at least 30 minutes, and with an electric field of -350 V/cm the separation is accomplished in under 23 minutes. The migration times of the proteins essentially is halved by an increase in separation field of -250 V/cm to -350 V/cm. The separation window decreases quite dramatically in size with the change of electric field strength. A separation at -250 V/cm results in a separation window about 10 minutes wide, -300 V/cm produces a separation window about 8 minutes wide, and -350 V/cm produces a separation window only about 4 minutes wide.

Figure 4.5 displays the standardization curves for these standard proteins separated at different electric field strengths. Figure 4.5 displays how changing electric field changes migration time and effects the standardization curve linearity. The linearity of the standardization curve, as indicated by R^2, also increases with increasing separation field strength. The R^2 values range from 0.9979 using a field strength of -250 V/cm to 1.0000 using a field strength of -350 V/cm.

Overall this separation is not very satisfactory. Lysozyme (MW 14.3 kDa) and carbonic anhydrase (MW 29 kDa) differ in molecular weight by almost 15 kDa, but their respective peaks overlap to such a great extent that they are barely resolved. The peak widths of all of the proteins are minutes-wide. The separation of a complex mixture of proteins would be a very difficult feat using this 1% HEC sieving matrix. Overall poor separation may be the result of the inherent capabilities of HEC to function as a sieving matrix for these proteins.

4.3.5 Effect of electric field on separation using a polyAAP Grignard coated capillary with a HEC sieving matrix

Figure 4.6 demonstrates the separation of four protein standards using a 1% HEC sieving matrix inside a polyAAP Grignard coated capillary. HEC was not present in the running buffer for this separation. The range in separation electric fields here is from -300 V/cm to -400 V/cm. The changes in separation as a result of changes in electric field strength are not as visible as those encountered using a LPA Grignard coated capillary. The total time for separations to occur changes from 27 minutes at an electric field of -300 V/cm to 24 minutes using an electric field of -350 V/cm to 22 minutes with an electric field of -400 V/cm. The change in field from -300 V/cm to -400 V/cm decreases the migration time of each protein standard by only about 6 minutes.

Figure 4.4 Comparison of separations at different electric field strengths using 1% HEC and a LPA Grignard coated capillary.

For sample preparation see Section 4.2.2. Field strengths (V/cm) are: (A) -250, (B) -300, and (C) -350. Samples are labeled as: (1) 10^{-6} M lysozyme, (2) 10^{-6} M carbonic anhydrase, and (3) 10^{-6} M BSA. CE conditions: capillary: LPA Grignard coated, 37 cm × 140 µm O.D. × 50 µm I.D., running and sheath flow buffers: 10 mM TrisHCl, 5 mM SDS, pH 8.0, sample injection: 5 s, -450 V/cm, excitation: 488 nm, emission filter: 630DF30.

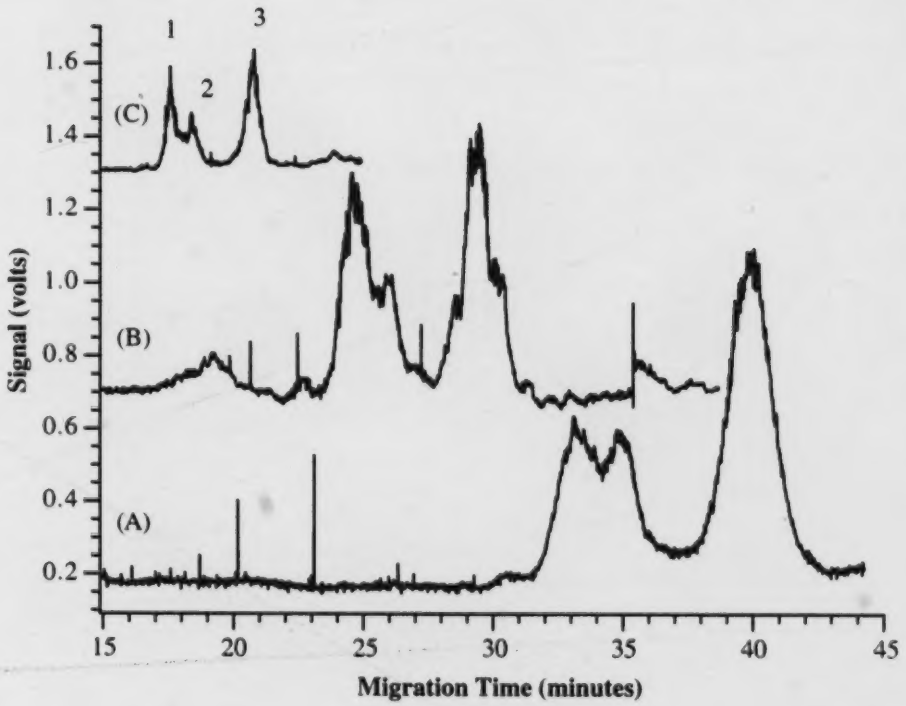

Figure 4.5 Standardization curves at various electric field strengths using 1% HEC in a LPA Grignard coated capillary.

Conditions and samples as in Figure 4.4.

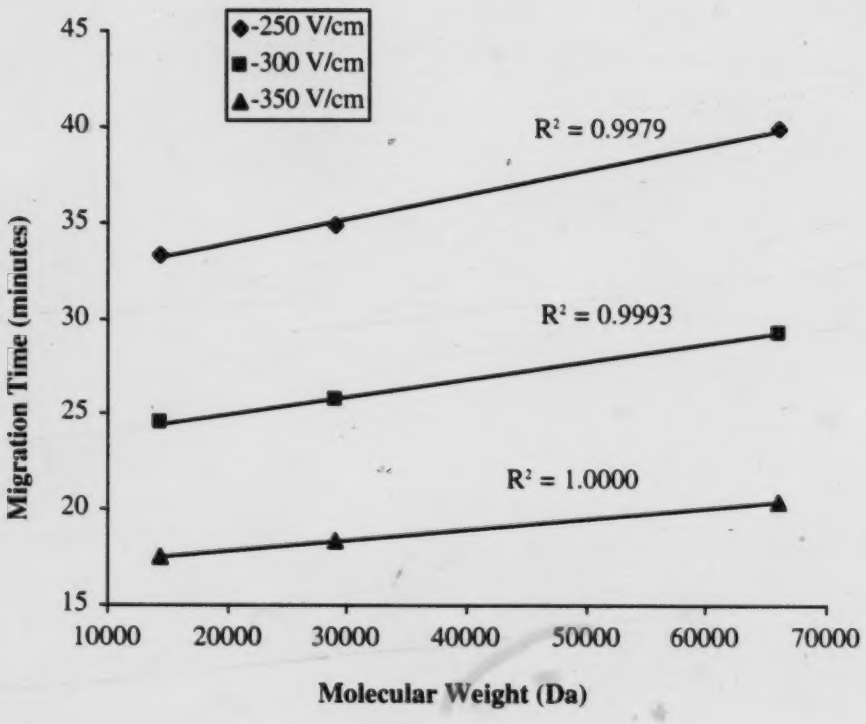

Figure 4.6 Comparison of separations at different electric field strengths using 1% HEC and a polyAAP Grignard coated capillary.

See Section 4.2.2. for sample preparation details. Field strengths (V/cm) are: (A) -300, (B) -350, and (C) -400. Samples are labeled as: (1) 5×10^{-6} M lysozyme, (2) 5×10^{-6} M glyceraldehyde-3-phosphate dehydrogenase, (3) 1×10^{-6} M BSA, and (4) 5×10^{-6} M phosphorylase b. CE conditions: capillary: polyAAP Grignard coated, 35 cm × 140 µm O.D. × 50 µm I.D., running and sheath flow buffers: 10 mM TrisHCl, 5 mM SDS, pH 8.0, sample injection: 5 s, -425 V/cm, excitation: 488 nm, emission filter : 630DF30.

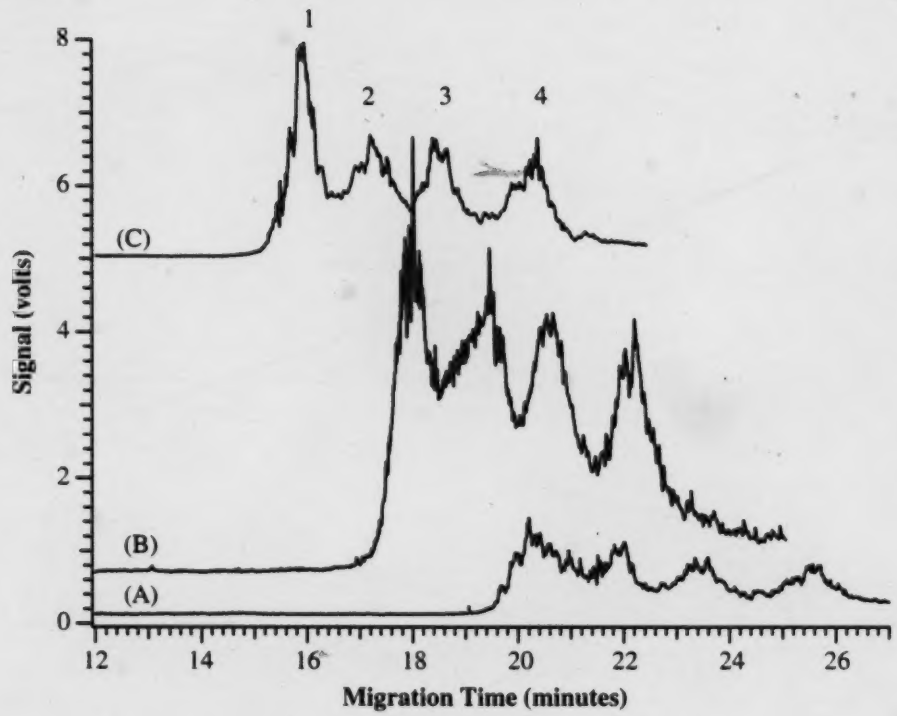

Both Figures 4.6 and 4.7 show how the separation window changes very little with respect to changes in separation electric field strength. Both of the separations performed at -300 V/cm and -350 V/cm produce separation windows of about 7 minutes in width while the run at -400 V/cm has a separation window of about 6 minutes. These are not great changes when compared to those obtained with different electric field strengths using a LPA Grignard coated capillary.

Figure 4.7 shows the standardization curves of migration time versus molecular weight of the protein standards and how the standardization curves change with changes in separation electric field strength. The R^2 values of each of the standardization curves indicates good linearity irregardless of field strength. For the separation at -300V/cm, R^2 is 0.9972, for -350 V/cm, R^2 is 0.9913, and for -400 V/cm, R^2 is 0.9966. There is no dependence of standardization curve linearity on the electric field strength used to perform the separation.

It would be very challenging for this combination of a 1% HEC sieving matrix and polyAAP Grignard coated capillary to separate a complex mixture of proteins. Peaks are from 1-2 minutes wide in each of the electropherograms. Furthermore, all of the peaks overlap to a great extent, even though their molecular weights differ by 20 to 30 kDa.

4.3.6 Effect of electric field on separation using a polyAAP Grignard coated capillary with HEC as a sieving matrix and running buffer

Figure 4.8 demonstrates how changing the electric field affects the separation of four protein standards in a polyAAP Grignard coated capillary utilizing 1% HEC as the sieving matrix and running buffer. Using an electric field of -150 V/cm, at least 22 minutes are required for the separation to be accomplished, however using an electric field of -400 V/cm, the separation is achieved in less than 9 minutes. It is not known whether or not the HEC in the running buffer is responsible for these extremely short separation times as not enough studies were performed with HEC in the running buffer to draw such a conclusion. Changing the separation field from -150 V/cm to -400 V/cm, the migration times of all of the proteins is just more than halved. The separation window is also decreased by 50% as the electric field is changed from -150 V/cm to -400 V/cm. Using a separation field strength of -150 V/cm, the separation window is about 6 minutes wide, while when the separation is carried out under an electric field of -400 V/cm, the separation window is only 3 minutes wide. At most, the

Figure 4.7 Standardization curves at various electric field strengths using a 1% HEC sieving matrix in a polyAAP Grignard coated capillary.

Conditions and samples as in Figure 4.6.

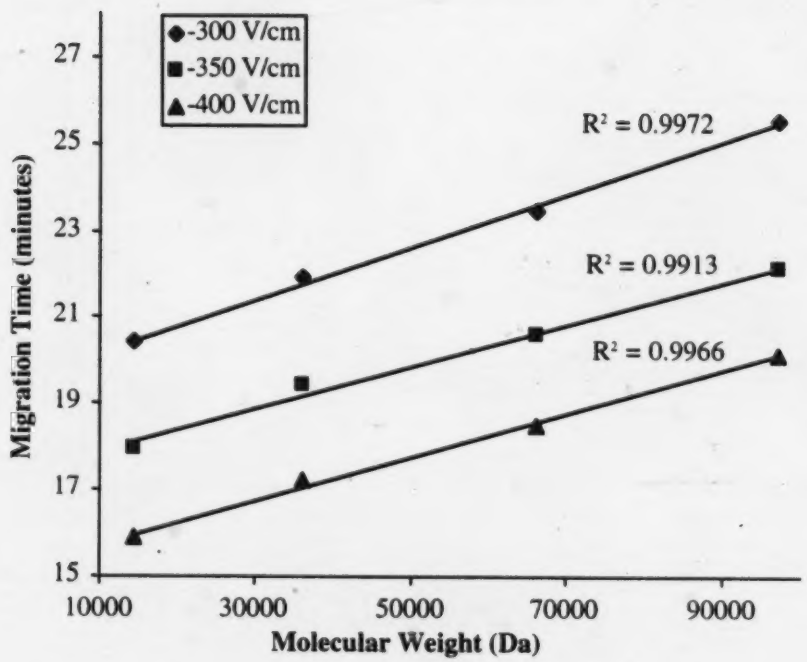

Figure 4.8 Comparison of separations at different electric field strengths using 1% HEC as a sieving matrix and running buffer with a polyAAP Grignard coated capillary.

See Section 4.2.2. for sample preparation details. Field strengths (V/cm) are: (A) -150, (B) -200, and (C) -250, (D) -300, (E) -350, and (F) -400. Samples are labeled as: (1) 5×10^{-6} M lysozyme, (2) 5×10^{-6} M glyceraldehyde-3-phosphate dehydrogenase, (3) 8×10^{-7} M BSA (4) 5×10^{-6} M phosphorylase b. CE conditions: capillary: polyAAP Grignard coated, 35.5 cm × 140 µm O.D. × 50 µm I.D., sheath flow buffer: 10 mM TrisHCl, 5 mM SDS, pH 8.0, running buffer: 1% HEC in 10 mM TrisHCl, 5 mM SDS, pH 8.0, sample injection: 5 s, -425 V/cm, excitation: 488 nm, emission filter : 630DF30.

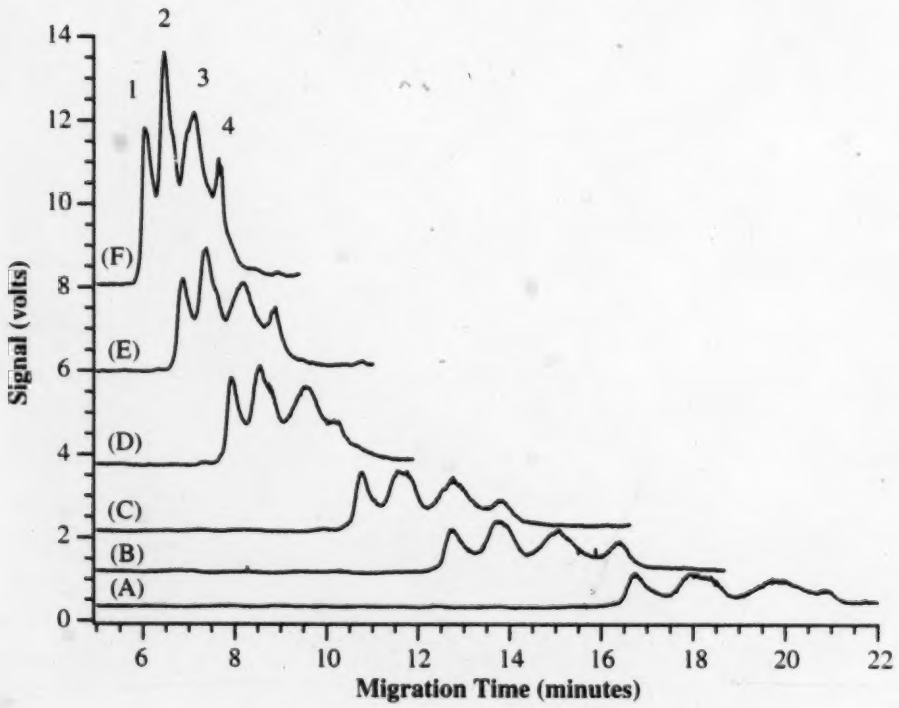

resolution between any two peaks is between 0.5 and 0.7, which is considered resolved.

Figure 4.9 displays the standardization curves of migration time versus molecular weight of the protein standards as the electric field strength of the separation is changed. As with using a polyAAP Grignard coated capillary without HEC in the running buffer, it can be seen that the R^2 values, and thus the linearity, of the standardization curves cannot be correlated to changes in electric field. All of the R^2 values are very high, regardless of the field strength used for the separation.

As with the cases of using a LPA Grignard coated capillary and a polyAAP Grignard coated capillary without HEC in the running buffer, again the overall separation of these four protein standards is not very suitable. It would be very challenging to separate a complex sample mixture given that the protein peaks here once again overlap even though there is 20 to 30 kDa difference in molecular weight.

4.3.7 Plots of time versus inverse electric field strength for different capillary coatings

Jorgenson and Lukacs explained that the time required for a solute to migrate the length of the capillary is inversely proportional to electric field strength of the separation (39):

$$t = \frac{L}{\mu E} \qquad (4.1)$$

where t is the migration time of the sample in seconds, L is the distance traveled to the detector in metres, μ is the electrophoretic mobility of the sample in units of m^2/Vs, and E is the electric field strength in V/m. From Equation 4.1, it is seen that a plot of migration time versus the inverse of electric field strength will result in a y-intercept of zero and a slope equal to effective capillary length divided by the electrophoretic mobility of the sample.

Figures 4.10-4.12 demonstrate the linearity of the relationship between migration time and the inverse of electric field strength for different sets of separation conditions all employing a HEC sieving matrix. Figure 4.10 displays the linear plots of migration time versus inverse electric field for a series of standard proteins separated by a 1% HEC sieving matrix inside a LPA Grignard coated capillary. Figure 4.11 shows the linear plots of migration time versus inverse electric field for a series of standard proteins separated by a 1% HEC sieving matrix inside a polyAAP Grignard coated capillary. Figure 4.12 demonstrates the linearity of plots of migration time versus inverse electric field for a series of standard proteins separated by a 1% HEC sieving

Figure 4.9 Calibration curves at various electric field strengths using a 1% HEC sieving matrix and 1% HEC in the running buffer with a polyAAP Grignard coated capillary.

Conditions and samples as in Figure 4.8.

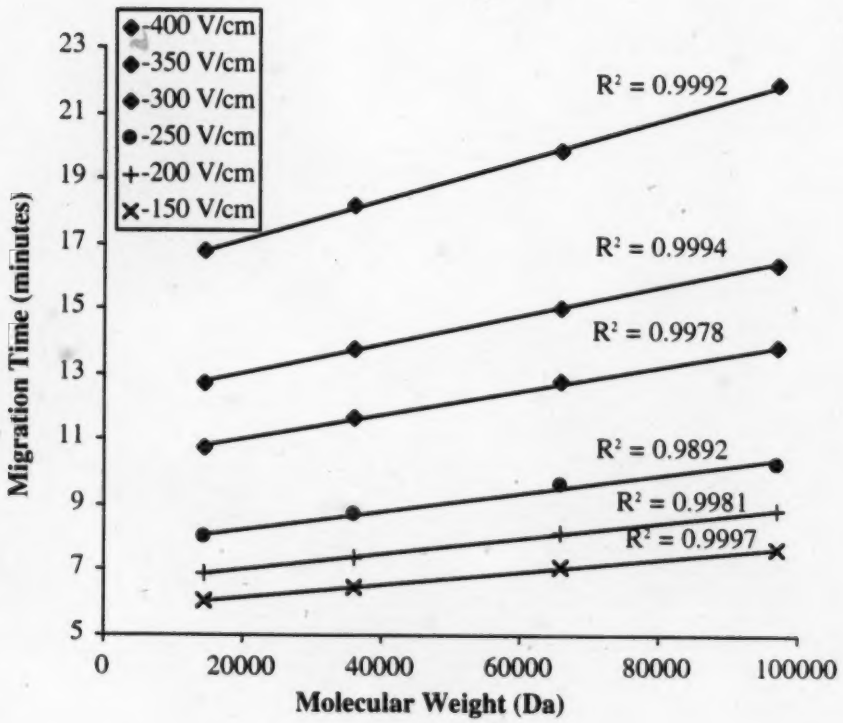

Figure 4.10 Migration time versus inverse of electric field strength using a 1% HEC sieving matrix and a LPA Grignard coated capillary.

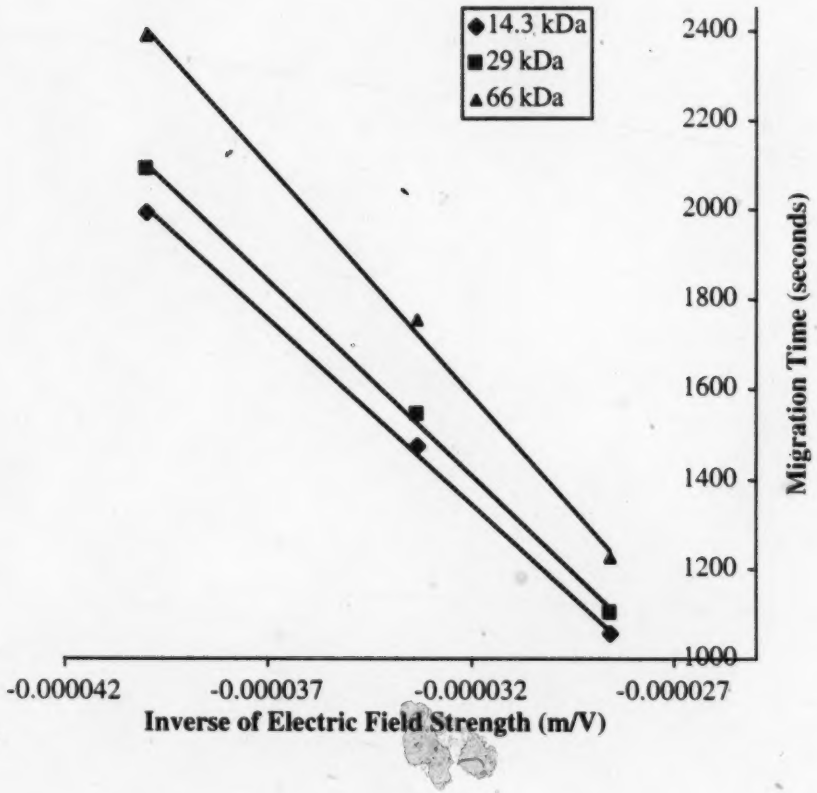

Figure 4.11 Migration time versus inverse of electric field strength using a 1% HEC sieving matrix in a polyAAP Grignard coated capillary.

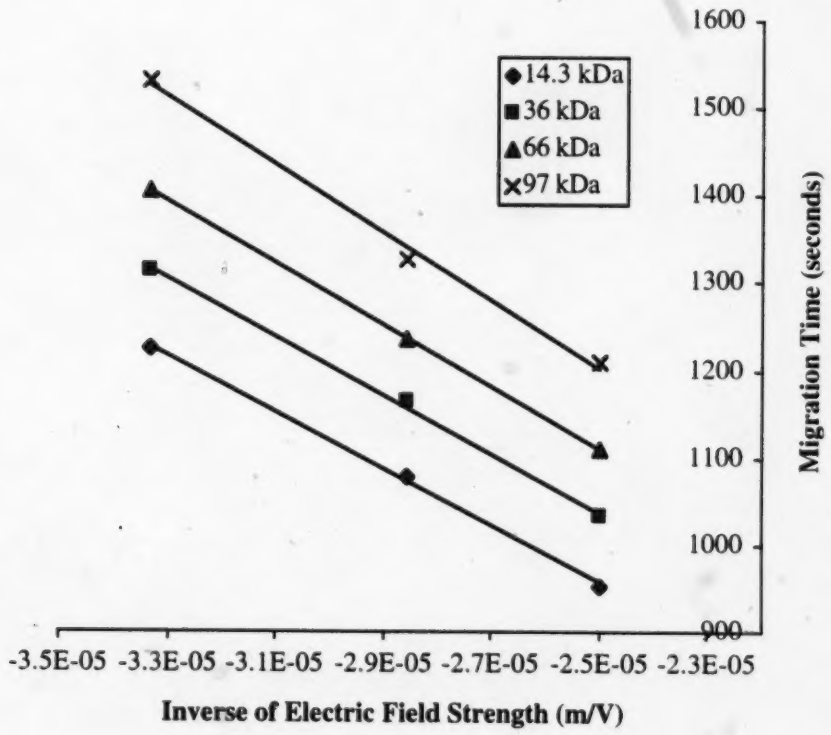

matrix with 1% HEC inside the running buffer utilizing a polyAAP Grignard coated capillary. Table 4.1 shows the correlation coefficients obtained from these plots. All of the correlation coefficients indicate good linearity in the relationship between migration time and inverse of the electric field strength. Table 4.2 shows the line equations obtained for each of the plots. This table illustrates that the y-intercepts of the plots are clearly not zero. However a trend is deduced whereby the plots generated with data from the LPA Grignard coated capillary deviate the most from zero in terms of y-intercept. The next largest deviation from a zero y-intercept are the data from the polyAAP Grignard coated capillary without HEC in the running buffer. Lastly, the closest y-intercepts to zero result from the plots of data obtained from standards run in a polyAAP Grignard coated capillary with a 1% HEC sieving matrix and HEC in the running buffer. The fact that the y-intercepts do not equal zero suggests that there exists residual electro-osmotic flow in the capillaries which expels the HEC sieving matrix and the rest of the capillary's contents from the capillary. Secondly, the LPA Grignard coated capillary has the highest residual electro-osmotic flow as it deviates the most from theory. The best adherence to theory is the case of the polyAAP Grignard coated capillary with HEC in the running buffer. This may be a result of closely matching transference numbers between the capillary's contents and the running buffer, thus the decrease in expulsion of the capillary's contents from the capillary (40-42).

4.3.8 Same-day migration time variability

As mentioned in Section 4.3.2 migration times were highly irreproducible even within the same day. Figure 4.13 shows the same-day migration time differences for three standard proteins using a LPA Grignard coated capillary with 1% HEC as a sieving matrix. As can be seen for lysozyme, the migration time is anywhere from 15 minutes to almost 23 minutes. For BSA, the fastest migration time is about 17 minutes, while the longest is about 25 minutes. There is also a large variation for phosphorylase b which has migration times between 18 and 28 minutes.

Table 4.3 displays the average calculated migration times and standard deviations for each of the standard proteins. An overall goal is to be able to utilize this HEC sieving matrix as a separation tool to estimate molecular weights of unknown proteins. SDS-PAGE techniques can estimate the molecular weight of a protein within an accuracy of 10% which is considered acceptable. For all of the proteins on the standardization curve, the relative standard deviations of migration times are 17-18%.

Figure 4.12 Migration time versus inverse of electric field strength using a 1% HEC sieving matrix and 1% HEC in the running buffer with a polyAAP Grignard coated capillary.

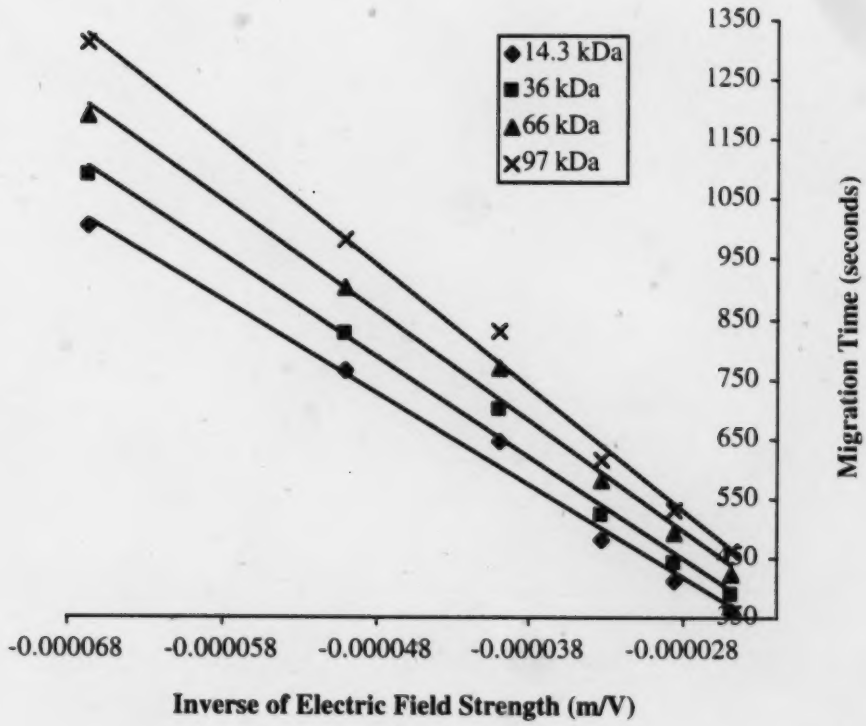

Table 4.1 Correlation coefficients obtained from plots of migration time versus the inverse of the electric field strength for standard proteins separated under different conditions.

	Correlation Coefficient		
	Grignard coated capillary and running buffer utilized		
Standard Molecular Weight (kDa)	LPA capillary with no HEC in running buffer	AAP capillary with no HEC in running buffer	AAP capillary with 1% HEC in running buffer
14.3	0.9990	0.9987	0.9912
29	0.9987	not done	not done
36	not done	0.9978	0.9910
66	0.9979	0.9999	0.9916
97	not done	0.9953	0.9932

Table 4.2 Line equations obtained from plots of migration time versus the inverse of the electric field strength for standard proteins separated under different conditions.

	Line Equation		
	Grignard coated capillary and running buffer utilized		
Standard Molecular Weight (kDa)	LPA capillary with no HEC in running buffer	AAP capillary with no HEC in running buffer	AAP capillary with 1% HEC in running buffer
14.3	-8.2e7x-1.3e3	-3.3e7x-1.4e2	-1.6e7x-22
29	-8.6e7x-1.4e3	not done	not done
36	not done	-3.4e7x-2.0e2	-1.7e7x-31
66	1.0e8x-1.7e3	-3.6e7x-2.2e2	-1.9e7x-25
97	not done	-3.9e7x-2.2e2	-3.1e7x-49

Figure 4.13 Same-day variation in migration times using a 1% HEC sieving matrix with a LPA Grignard coated capillary.

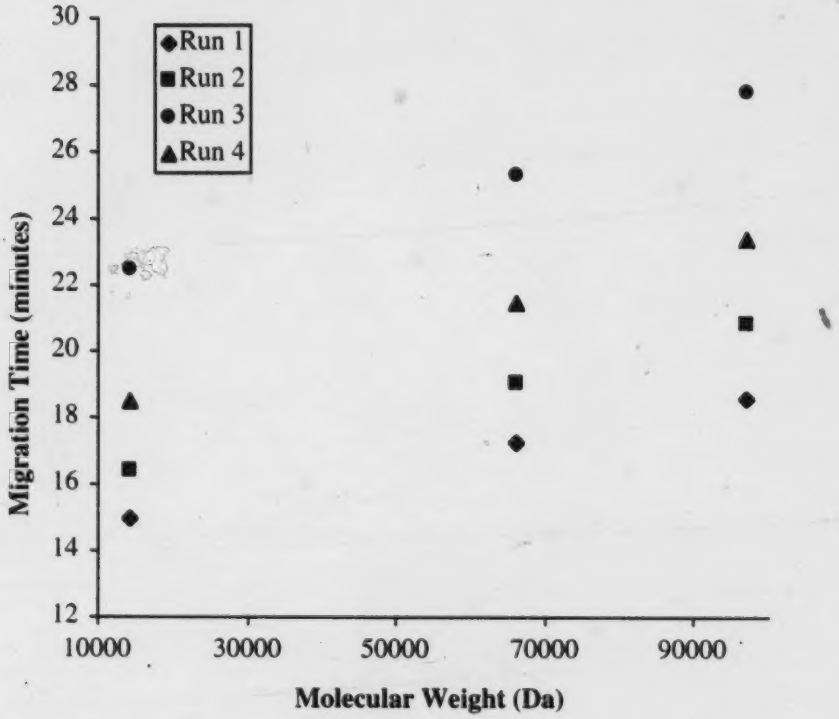

Table 4.3 Average migration times of 3 protein standards run on the same day using a 1% HEC sieving matrix with a LPA Grignard coated capillary and an electric field of -400 V/cm.

Protein	Average Migration Time (minutes) (n=4)
Lysozyme	18.1±3.3
BSA	20.8±3.5
Phosphorylase b	22.6±4.0

The migration time irreproducibility of this method presented is a factor which could alter hugely the molecular weight estimates of unknown proteins.

Figure 4.14 shows the same-day differences in migration times of four standard proteins separated in a polyAAP Grignard coated capillary utilizing a 1% HEC sieving matrix. It must be noted that it is purely coincidental that the migration times were shorter for each successive run; this trend did not always occur. For lysozyme, the migration times range from 5 minutes to 8.3 minutes. For glyceraldehyde-3-phosphate dehydrogenase, the migration times range from a low of 6 minutes to a high of 9 minutes. Migration times for BSA are also within a 3 minute window, ranging from 6.7 minutes to 9.6 minutes. Phosphorylase b has a migration time window spanning 7.7 minutes to 10.4 minutes. These four standard proteins all migrate within approximately 3 minute windows, however this is still a large variation in migration times of samples run on the same day.

Table 4.4 displays the average migration times and standard deviations for each of the four protein standards run using a polyAAP Grignard coated capillary with a 1% HEC sieving matrix. Here the relative standard deviations associated with each average migration time are 16-21%. This is a huge difference in migration time. If unknown protein molecular weights are determined using this separation procedure, large errors would be made.

An obvious solution to this migration time problem is to use an internal standard. However the search for a suitable internal standard for this system failed. Samples were spiked with fluorescein which should migrate out of the capillary much ahead of sample components (in this case the protein standards were lysozyme, glyceraldehyde-3-phosphate dehydrogenase, phosphorylase b). However, it was discovered that fluorescein not only co-migrated with the last two proteins, fluorescein was still faintly observed exiting the capillary after the separation. This discovery affirms the belief that sample components adhere to the capillary wall during these separations. As suggested in Section 4.3.7 through the observation of a residual electro-osmotic flow, perhaps there are some portions of the capillary wall which are not fully coated, and thus may interact with the sample components. Further studies must be performed to find an appropriate internal standard. It has been suggested that migration time reproducibility can be aided by careful temperature control of experiments which may be another solution to the migration time irreproducibility problem (18, 43).

Figure 4.14 Same-day variation in migration times using a 1% HEC sieving matrix with a polyAAP Grignard coated capillary.

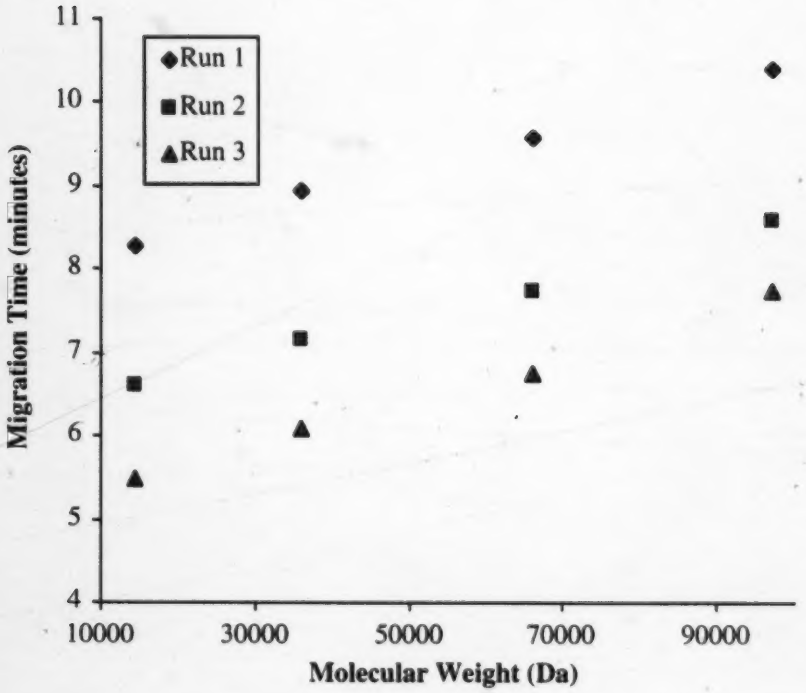

Table 4.4 Average migration times of 3 protein standards run on the same day using a 1% HEC sieving matrix with polyAAP Grignard coated capillary and an electric field of -400 V/cm.

Protein	Average Migration Time (minutes) (n=3)
Lysozyme	6.8±1.4
Glyceraldehyde-3-phosphate dehydrogenase	7.4±1.4
BSA	8.0±1.4
Phosphorylase b	8.9±1.4

4.3.9 Day-to-day migration time variability

Figure 4.15 shows the migration time variability from day-to-day using a 1% HEC sieving matrix in the same LPA Grignard coated capillary for three protein standards. For each protein, the migration time variability is within an approximately 6-7 minute window. For lysozyme, the migration time is as low as 12.9 minutes and as high as 18.5 minutes. BSA has migration times which range from 15 minutes to 21.5 minutes depending on the day the separation is performed. Lastly, phosphorylase b has migration times from 16 to 23.4 minutes.

Table 4.5 displays the migration time averages and their standard deviations for each of the three standard proteins separated on different days utilizing the same capillary. The relative standard deviations for these protein standards are 16-18%. Once again this is a huge variation in migration time which requires correction. Again the ideal solution to this migration time irreproducibility is to find a suitable internal standard for this system. Further work on this should entail the application of an internal standard to the separations as well as temperature control of the system.

4.3.10 Capillary failure

It is to be noted that when capillaries failed to perform any longer, this was judged by the inability to perform suitable separations rather than failure to support current. Experiments showed that coating was still present inside the capillary, so it is believed that proteins adhering to the capillary wall were the cause of capillary failure. As mentioned in Section 4.3.8, fluorescein was observed to be adhering to the walls when attempts were made to use it as an internal standard for separations. Furthermore, lysozyme (theoretical pI 9.32) and glyceraldehyde-3-phosphate dehydrogenase (theoretical pI 8.52) are very basic proteins (44) which, it is believed, may adhere to any residual silanol groups present in the capillary (even after coating). Perhaps commercial capillary coatings are more robust than the Grignard coatings employed for these separations and should be tested with this 1% HEC sieving matrix.

The polyAAP Grignard coated capillaries performed well anywhere from 2-4 days, which corresponds to 13-48 experiments. As with the LPA Grignard coated capillaries, capillary failure was signaled by poorer than usual separation, rather than an inability to support current. Experiments again showed that coating still remained inside of the capillary, so it is believed that even this robust polyAAP coating method leaves residual silanol groups to which proteins bind during separations.

Figure 4.15 Day-to-day variation in migration times using a 1% HEC sieving matrix with a LPA Grignard coated capillary.

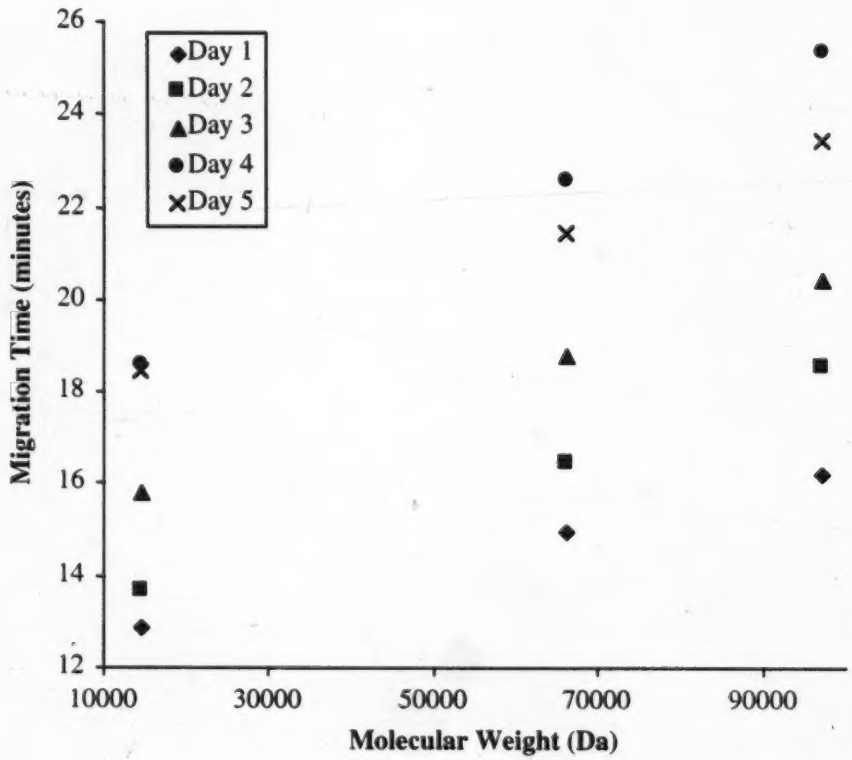

Table 4.5 Average migration times of 3 protein standards run on the different days using a 1% HEC sieving matrix in the same LPA Grignard coated capillary using an electric field of -400 V/cm.

Protein	Average Migration Time (minutes) (n=5)
Lysozyme	15.9±2.6
BSA	18.8±3.2
Phosphorylase b	20.8±3.7

4.3.11 Protein concentration limits

Satisfactory separations were not achieved with lower concentrations of proteins than those presented, i.e. around 10^{-6} M. Comparable concentration detection limits for SDS CGE LIF have been noted by two other groups (43, 45). Gump *et. al.* describe detecting 5×10^{-7} M of a mixture of myoglobin, α-chymotrypsinogen A, and conalbumin (45). Harvey *et. al.* detected protein concentrations of approximately 10^{-6} M of carbonic anhydrase and ovalbumin, and $5\text{-}7 \times 10^{-7}$ M of BSA and conalbumin (43). However, compared to other reports, the detection limits presented in this chapter are high. Wise *et. al.* were able to detect 3.8×10^{-10} M of BSA (9) while Craig *et. al.* were able to detect a mixture of 1.8×10^{-8} M trypsinogen, ovalbumin, and conalbumin (14).

It has been suggested that post-denaturation labeling, like that used here, leads to higher detection limits as the heavy coating of SDS around the protein electrostatically repulses and sterically hinders the labeling reagents (14). It is believed that the detection limits presented here are not due to the labeling reagent used as in all aforementioned cases the dyes are amine-reactive. Instead it is thought that higher detection limits demonstrated here are due to a combination of the sieving abilities of HEC and proteins adhering to the capillary wall. Specifically, as mentioned in Section 4.3.10, the basic proteins of lysozyme and glyceraldehyde-3-phosphate dehydrogenase may adhere to any residual silanol groups on the capillary wall.

Furthermore, sensitivity was greatly affected by large peak widths, as was also noted by Craig *et. al.* (14). In most separations, the protein peaks were at least 1 minute wide, with BSA producing a wider peak than the other proteins. The phenomenon of a wide BSA peak, also noted by Wise *et. al.* (9), is due to the number of derivatizable groups present in BSA. The occurrence of broad peaks is due to multiple labeling of each protein as dye reacts with its free amine groups (14, 46, 47) in the presence of SDS which causes the heterogeneously labeled peaks to collapse into one broad peak (45).

4.4 Conclusion

This chapter demonstrates the use of HEC as a sieving matrix in SDS CGE with LIF detection. Different protein standards were fluorescently labeled, separated by molecular weight in a 1% HEC sieving matrix, and detected with LIF utilizing either LPA or polyAAP Grignard coated capillaries. Running buffer with or without HEC produced the same results. Linear standardization curves of migration time versus

molecular weight were constructed from separations performed using electric fields which varied from -150V/cm to -400V/cm. Migration time reproducibility problems were encountered- both same-day and day to day. Further work needs to be done to find an appropriate internal standard for this system to correct for this migration time-reproducibility problem. It is deduced that HEC is limited as a sieving matrix due to the narrow separation window it produces as well as its resolving capabilities.

4.5 References

(1) Weber, K.; Osborn, M. *Journal of Biological Chemistry* **1969,** *244*, 4406-4412.

(2) Hjertén, S. *Journal of Chromatography* **1983,** *270*, 1-6.

(3) Cohen, A. S.; Karger, B. L. *Journal of Chromatography* **1987,** *397*, 409-417.

(4) Tsuji, K. *Journal of Chromatography* **1991,** *550*, 823-830.

(5) Manabe, T. *Electrophoresis* **1995,** *16*, 1468-1473.

(6) Wu, D.; Regnier, F. E. *Journal of Chromatography* **1992,** *608*, 349-356.

(7) Widhalm, A.; Schwer, C.; Blaas, D.; Kenndler, E. *Journal of Chromatography* **1991,** *549*, 446-451.

(8) Ganzler, K.; Greve, K. S.; Cohen, A. S.; Karger, B. L.; Guttman, A.; Cooke, N. C. *Analytical Chemistry* **1992,** *64*, 2665-2671.

(9) Wise, E. T.; Singh, N.; Hogan, B. L. *Journal of Chromatography A* **1996,** *746*, 109-121.

(10) Guttman, A.; Horvath, J.; Cooke, N. *Analytical Chemistry* **1993,** *65*, 199-203.

(11) Karim, M. R.; Janson, J.-C.; Takagi, T. *Electrophoresis* **1994,** *15*, 1531-1534.

(12) Takagi, T.; Karim, M. R. *Electrophoresis* **1995,** *16*, 1463-1467.

(13) Zhang, Y.; Lee, H. K.; Li, S. F. Y. *Journal of Chromatography A* **1996,** *744*, 249-257.

(14) Craig, D. B.; Polakowski, R. M.; Arriaga, E.; Wong, J. C. Y.; Ahmadzadeh, H.; Stathakis, C.; Dovichi, N. J. *Electrophoresis* **1998,** *19*, 2175-2178.

(15) Benedek, K.; Thiede, S. *Journal of Chromatography A* **1994,** *676*, 209-217.

(16) Nakatani, M.; Shibukawa, A.; Nakagawa, T. *Electrophoresis* **1996,** *17*, 1584-1586.

(17) Guttman, A.; Nolan, J. A.; Cooke, N. *Journal of Chromatography* **1993,** *632*, 171-175.

(18) Shieh, P. C. H.; Hoang, D.; Guttman, A.; Cooke, N. *Journal of Chromatography A* **1994,** *676*, 219-226.

(19) Pollard, N. J.; Wrigley, C. W.; Bekes, F.; Aumatell, A.; MacRitchie, F. *Electrophoresis* **1996,** *17*, 221-223.

(20) Klyushnichenko, V.; Kula, M.-R. *Electrophoresis* **1997,** *18*, 2019-2023.

(21) Kundu, S.; Fenters, C.; Lopez, M.; Varma, A.; Brackett, J.; Kuemmerle, S.; Hunt, J. C. *Journal of Capillary Electrophoresis* **1997,** *4*, 7-13.

(22) Schmerr, M. J.; Jenny, A.; Cutlip, R. C. *Journal of Chromatography B* **1997,** *697*, 223-229.

(23) Werner, W. E.; Demorest, D. M.; Stevens, J.; Wiktorowicz, J. E. *Analytical Biochemistry* **1993,** *212*.

(24) Grossman, P. D.; Soane, D. S. *Journal of Chromatography* **1991,** *559*, 257-266.

(25) Grossman, P. D.; Soane, D. S. *Biopolymers* **1991,** *31*, 1221-1228.

(26) McCord, B. R.; Jung, J. M.; Holleran, E. A. *Journal of Liquid Chromatography* **1993,** *16*, 1963-1981.

(27) Barron, A. E.; Soane, D. S.; Blanch, H. W. *Journal of Chromatography A* **1993,** *652*, 3-16.

(28) Zhu, H.; Clark, S. M.; Benson, S. C.; Rye, H. S.; Glazer, A. N.; Mathies, R. A. *Analytical Chemistry* **1994,** *66*, 1941-1948.

(29) Butler, J. M.; McCord, B. R.; Jung, J. M.; Allen, R. O. *Biotechniques* **1994,** *17*, 4-7.

(30) Butler, J. M.; McCord, B.; Jung, J.; Wilson, M.; Budowle, B.; Allen, R. *Journal of Chromatography B* **1994,** *658*, 271-280.

(31) Barron, A. E.; Sunada, W. M.; Blanch, H. W. *Electrophoresis* **1996,** *17*, 744-757.

(32) Oda, R. P.; Wick, M.; Reuckert, L. M.; Lust, J.; Landers, J. P. *Electrophoresis* **1996,** *17*, 1491-1498.

(33) Minarik, M.; Gas, B.; Kenndler, E. *Electrophoresis* **1997,** *18*, 98-103.

(34) Oda, R. P.; Prasad, R.; Stout, R. L.; Coffin, D.; Patton, W. P.; Kraft, D. L.; O'Brien, J. F.; Landers, J. P. *Electrophoresis* **1997,** *18*, 1819-1826.

(35) Bossi, A.; Righetti, P. G. *Electrophoresis* **1997,** *18*, 2012-2018.

(36) Capelli, L.; Stoyanov, A. V.; Wajcman, H.; Righetti, P. G. *Journal of Chromatography A* **1997,** *791*, 313-322.

(37) Righetti, P. G.; Olivieri, E.; Viotti, A. *Electrophoresis* **1998,** *19*, 1738-1741.

(38) Capelli, L.; Forlani, F.; Perini, F.; Guerrieri, N.; Cerletti, P.; Righetti, P. G. *Electrophoresis* **1998,** *19*, 311-318.

(39) Jorgenson, J. W.; Lukacs, K. D. *Analytical Chemistry* **1981,** *53*, 1298-1302.

(40) Swerdlow, H.; Dew-Jager, K. E.; Brady, K.; Grey, R.; Dovichi, N. J.; Gesteland, R. *Electrophoresis* **1992,** *13*.

(41) Figeys, D.; Renborg, A.; Dovichi, N. J. *Electrophoresis* **1994,** *15*, 1512-1517.

(42) Figeys, D.; Dovichi, N. J. *Journal of Chromatography A* **1996,** *744*, 333-339.

(43) Harvey, M. D.; Bandilla, D.; Banks, P. R. *Electrophoresis* **1998,** *19*, 2169-2174.

(44) http:www.expasy.ch/cgi-bin/pi_tool.

(45) Gump, E. L.; Monnig, C. A. *Journal of Chromatography A* **1995,** *715*, 167-177.

(46) Zhao, J. Y.; Waldron, K. C.; Miller, J.; Zhang, J.; Harke, H.; Dovichi, N. J. *Journal of Chromatography* **1992,** *608*, 239-242.

(47) Craig, D. B.; Dovichi, N. J. *Analytical Chemistry* **1998,** *70*, 2493-2494.

Chapter 5
Linear Polyacrylamide as a Sieving Matrix for Sodium Dodecyl Sulfate Capillary Gel Electrophoresis with Laser-Induced Fluorescence Detection of Human Colorectal Cancer Proteins

5.1 Introduction

Polyacrylamide (PA), both cross-linked and non-cross-linked, has been utilized for the sodium dodecyl sulfate capillary gel electrophoretic (SDS CGE) molecular weight based separations of proteins. Initially, Hjertén made use of a glass capillary column filled with polyacrylamide to separate membrane proteins (1). In 1987, the first report of capillary SDS gel electrophoresis was that of Cohen *et. al.* who manufactured cross-linked PA to separate myoglobin fragments and a mixture of standard proteins (2). In another paper that same year, Cohen *et. al.* reported the employment of cross-linked PA as a SDS CGE sieving matrix for the separation of genetically engineered human growth hormone and its byproduct of manufacture (3). However this separation was accomplished under nondenaturing conditions (3). A number of other research groups have since reported the utilization of cross-linked PA for SDS CGE separations. Tsuji reported the SDS CGE separation of molecular weight reference standards using cross-linked PA as a sieving matrix from which standardization curves were generated and applied to the molecular weight determination of recombinant biotechnology-derived proteins (4). Manabe also reported the use of cross-linked PA for SDS CGE separations of molecular weight standards in very short capillaries (5). However the utilization of cross-linked PA in capillaries is limited by problems caused by polymerization inside the capillary, for example, void formation due to gel shrinkage inside the column (6).

As with the early evolution of CGE DNA sequencing, researchers have progressed to employing linear PA (LPA) as a sieving matrix for effective SDS CGE protein separations. The first report of LPA as sieving matrix for SDS CGE protein separations was that of Widhalm *et. al.* in which a series of four standard proteins was separated (7). Other research groups have also reported the use of LPA as a sieving matrix to separate recombinant human growth hormone from its dimer (8), myoglobin fragments (6), fluorescently-labeled molecular weight standards (9), and fluorescently-labeled molecular weight markers and a purified enzyme from *Escherichia coli* (10). The aforementioned separations have all been performed utilizing noncommercial LPA. A number of other research groups have also employed and reported on the employment of a commercial replaceable LPA sieving matrix which has since gone off the market (11-14).

This chapter describes the use of LPA as a sieving matrix for the SDS CGE separation with laser-induced fluorescence (LIF) detection of both standard proteins

and fractionated human colorectal cancer (HT29) cells. All reports thus far of PA SDS CGE protein size-based separations have utilized UV detection except two which have employed LIF detection (9, 10). Percentages of LPA ranging from 6-9% were tested for ability to sieve protein standards by size based on constructed Ferguson plots. Linear standardization curves were constructed of migration time versus protein standard molecular weight. Given that only a few reports of complex sample separation utilizing a LPA SDS CGE method exist in the literature, this technique was then applied to the separation of HT29 water-soluble proteins and four fractions of HT29 cells obtained by differential detergent fractionation.

5.2 Experimental

5.2.1 Materials and reagents

Fused-silica capillary (50 µm I.D., 140 µm O.D.) was purchased from PolyMicro Technologies (Phoenix, AZ). Ethanol was obtained from Commercial Alcohols (Winnipeg, Canada). The following chemicals were from Sigma (St. Louis, MO): γ-methacryloxypropyltrimethoxysilane (silane), tris[hydroxymethyl]aminomethane (Trizma base), 2-[*N*-cyclohexylamino]ethane-sulfonic acid (CHES), piperazine-*N,N'*-bis(2-ethanesulfonic acid) (PIPES), phenylmethylsulfonyl fluoride (PMSF), t-octylphenoxypolyethoxyethanol (Triton X-100), polyoxyethylenesorbitan monopalmitate (Tween-40), and deoxycholic acid (DOC). Acrylamide, Dulbecco's Modified Eagle Medium, fetal bovine serum, gentamycin, and trypsin-EDTA were purchased from GibcoBRL (Grand Island, NY). Bio-Rad (Hercules, CA) supplied the following items: ammonium persulfate (APS), *N,N,N',N'*- tetramethylethylenediamine (TEMED), 10X TGS buffer, and the Silver Stain Plus Kit. The sodium dodecyl sulfate (SDS) was from Caledon (Georgetown, Canada). From Pharmacia (Quebec, Canada) the following was purchased: 2% (w/v) methylene bisacrylamide, 40% (w/v) acrylamide IEF, and the Pharmacia Low Molecular Weight Calibration Kit. The digitonin was obtained from Fluka (Oakville, Canada). The FMC Bioproducts Prosieve® Protein Markers were purchased from Mandel Scientific (Guelph, Canada). The supplier of sucrose, magnesium chloride hexahydrate ($MgCl_2 \cdot 6H_2O$), ethylenediaminetetra-acetic acid sodium salt (EDTA), potassium chloride (KCl), sodium chloride (NaCl), and di-sodium tetraborate (borate) was BDH (Vancouver, Canada). From Fisher (Fair Lawn, NJ) the following was acquired: sodium phosphate, dibasic (Na_2HPO_4), sodium phosphate, monobasic

($NaH_2PO_4 \cdot H_2O$), potassium phosphate, monobasic (KH_2PO_4), and T_{25} flasks. β-mercaptoethanol, sodium cyanide (NaCN), and bromophenol blue were all from Aldrich (Milwaukee, WI). Glycerol was purchased from ACP (Montreal, Canada). Concentrated hydrochloric acid was acquired from Anachemia (Montreal, Canada). The 3-(2-furoyl)quinoline-2-carboxyaldehyde (FQ) was obtained from Molecular Probes (Eugene, OR).

5.2.2 Cell culture

The HT29 cell line was cultured in T_{25} flasks in a 37°C incubator with a 5% CO_2 atmosphere. The cells were grown to 80% confluence in Dulbecco's Modified Eagle Medium, supplemented with 10% fetal bovine serum in 40 μg/mL gentamycin.

5.2.3 Cell extract preparation and fractionation

The water-soluble proteins of HT29 cells were prepared as described by Zhang *et. al.* (15). Approximately 10^6 cells were washed three times with phosphate-buffered saline (PBS). The cells were then resuspended in approximately 100 μL of distilled deionized water. The suspension was sonicated for 20 minutes at 4°C followed by a spin for 10 minutes at 2000*g*. The supernatant was removed and stored at -20°C.

The cells were separated into 4 fractions utilizing a differential detergent fractionation method (16). Figure 5.1 is a basic depiction of the fractionation method. Table 5.1 describes the components in each of the extraction buffers. 1.4×10^6 HT29 cells were suspended in cold PBS, pelleted out and divided up between two centrifuge tubes. 500 μL of ice-cold digitonin extraction buffer was added to each tube, the tubes were vortexed, mixed on ice for 15 minutes, vortexed again, and spun at 480*g* for 3 minutes. The supernatants (cytosolic proteins) were removed and stored at -70°C. The pellets were resuspended in 250 μL of ice-cold Triton X-100 extraction buffer with shaking on ice for 30 minutes. The mixtures were vortexed briefly and spun for 10 minutes at 5000*g*. The supernatants (membrane/organelle fraction) were removed and stored at -70°C. The pellets were resuspended in 180 μL ice-cold Tween/DOC extraction buffer with shaking for 15 minutes. The mixtures were vortexed briefly and spun for 10 minutes at 6780*g*. The supernatants (nuclear fraction) were removed and stored at -70°C. The pellets were resuspended in 150 μL ice-cold PBS with shaking for 15 minutes. The solutions were centrifuged for 10 minutes at 12000*g*. Both tubes of this cytoskeletal/nuclear matrix fraction were suspended in 150 μL nondenaturing cytoskeleton solubilization buffer, combined, and stored at –70°C.

Figure 5.1 Differential detergent fractionation method utilized to fractionate HT29 cells.

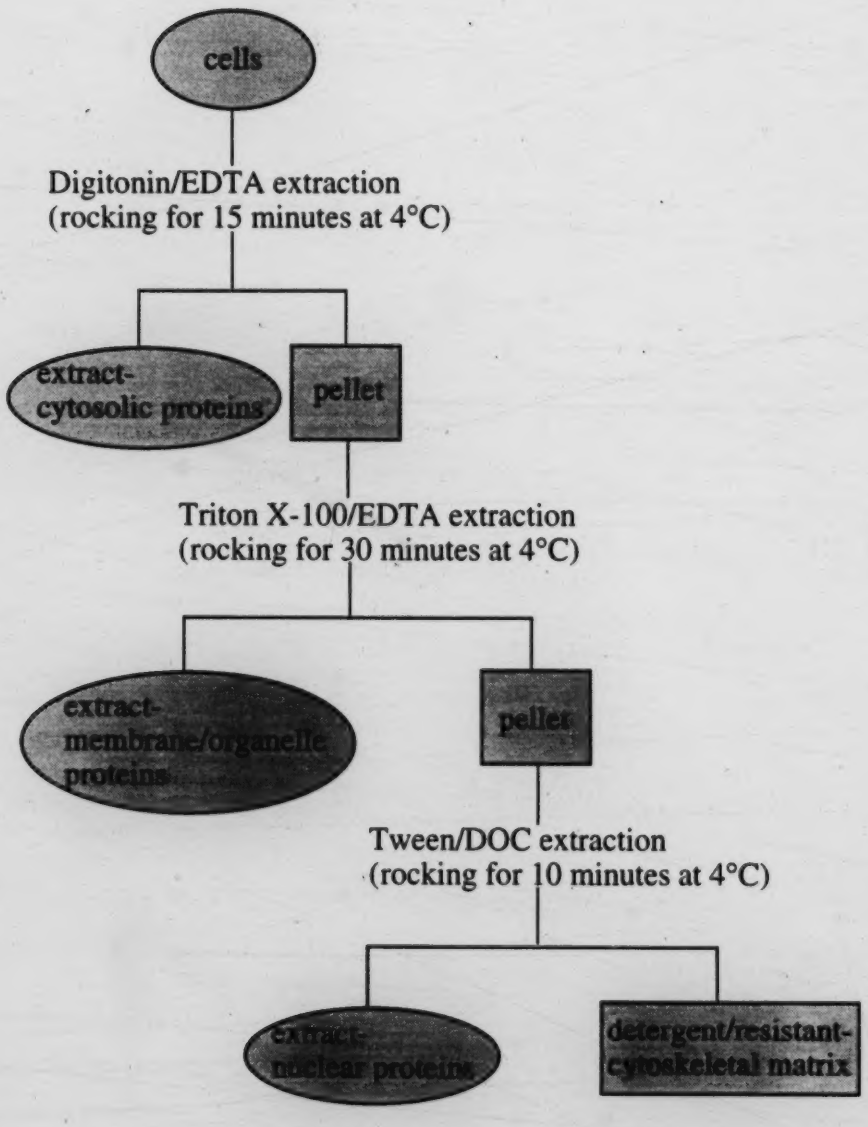

Table 5.1 Differential detergent fractionation extraction buffers and their compositions.

Extraction Buffer	Composition
Digitonin	10 mM PIPES, pH 6.8, 0.015% (w/v) digitonin, 300 mM sucrose, 100 mM NaCl, 3 mM $MgCl_2$, 5 mM EDTA, 1mM PMSF
Triton X-100	10 mM PIPES, pH 7.4, 0.5% (v/v) Triton X-100, 300 mM sucrose, 100 mM NaCl, 3 mM $MgCl_2$, 5 mM EDTA, 1 mM PMSF
Tween-40/deoxycholate	10 mM PIPES, pH 7.4, 1% (v/v) Tween-40, 0.5% (v/v) deoxycholate, 1 mM $MgCl_2$, 1 mM PMSF
Cytoskeletal solubilization (nondenaturing)	5% (w/v) SDS, 10 mM sodium phosphate, pH 7.4

5.2.4 SDS-PAGE sample preparation

For SDS-PAGE, 10 µL of each cell fraction was diluted 1:1 with SDS reducing buffer (0.0625 M TrisHCl, pH 6.8, 2.3% (w/v) SDS, 5% (v/v) β-mercaptoethanol, 10% (w/v) glycerol, 0.00125% (w/v) bromophenol blue). The sample was denatured at 95°C for at least 5 minutes and then pulsed in the centrifuge to spin down any accumulated condensation. The entire 20 µL was then loaded into the sample well on the gel. Standards utilized were 1 µL of FMC Bioproducts Prosieve® Protein Markers which were diluted in 9 µL of SDS reducing buffer. The standards were also denatured and spun before loading the entire 10 µL on to the gel.

5.2.5 FQ labeling of standard proteins

A vial of Pharmacia Low Molecular Weight Electrophoresis Calibration standards was reconstituted in 100 µL of reducing buffer (10 mM borate, 5 mM SDS, 1.5 mM NaCN, and 1% (w/v) β-mercaptoethanol, pH 9.3). From this, a 10 µL aliquot was denatured at 95°C for 5 minutes. This denatured aliquot was then added to a vial containing 100 nmol dry FQ and reacted at 65°C for 15 minutes. 1 µL of the labeled standards was then diluted with 4-14 µL of 0.1 M TrisCHES, 0.1% (w/v) SDS buffer.

5.2.6 FQ labeling of HT29 samples

Cell fractions were fluorescently labeled with FQ as follows: 5 µL of cell fraction and 5 µL of reducing buffer (10 mM borate, 5 mM SDS, 1.5 mM NaCN, and 1% (w/v) β-mercaptoethanol, pH 9.3) were added to a vial of 100 nmol dry FQ and reacted at 65°C for 5 minutes. 10 µL of 0.1 M TrisCHES, 0.1% SDS was added to slow the reaction. 20 µL of 5% (w/v) SDS was also added to the vial. The mixture was then denatured at 95°C for 5 minutes. Lastly the mixture was diluted with 40 µL of 0.1 M TrisCHES, 0.1% SDS.

5.2.7 SDS-PAGE

The Bio-Rad Mini-PROTEAN system was employed for SDS-PAGE separations. Mini-gels (7 cm × 10 cm) 1 mm thick consisted of a 12% polyacrylamide (12% T, 2.7% C) separating gel and a 4% polyacrylamide (4% T, 2.7% C) stacking gel. The electrophoresis buffer consisted of 25 mM Tris, 192 mM glycine, and 0.1% (w/v) SDS, pH 8.3. Samples were loaded and run at 200 V. The gels were visualized using the Bio-Rad Silver Stain Plus Kit.

5.2.8 Capillary preparation

The capillaries were coated with a solution of 980 µL ethanol and 20 µL γ-methacryloxypropyltrimethoxysilane. The capillaries were purged (using the water aspirator) with the silane solution for 45 minutes, followed by air for at least 15 minutes. During the silanization, the acrylamide solution was prepared using a slightly modified version of that of Wise *et. al.* (9). 0.9 g acrylamide was dissolved in 10 mL of 0.1 M TrisCHES (pH 8.8). The solution was 0.22 µm filtered, degassed, and covered with a blanket of argon. To this solution, 200 µL 10% (w/v) fresh APS, 4 µL TEMED, and 100 µL 10% (w/v) SDS were added, and the solution was stirred. The capillaries were filled with the polymerizing acrylamide solution using a water aspirator for 10 minutes. The solution was polymerized *in situ* for at least two hours or overnight with both ends of the capillary immersed in polymer solution.

5.2.9 Capillary electrophoresis instrument

See Section 2.2.5 for details of the single-capillary instrument with sheath-flow cuvette and LIF detector that was employed. A blue argon ion laser (3.5 mW, $\lambda = 488$ nm) (Uniphase, San Jose, CA) was used for sample excitation. Fluorescence was filtered through a 630DF30 bandpass filter (Omega Optical, Brattleboro, VT) and was then detected with an R1477 photomultiplier tube (Hamamatsu, Middlesex, NJ).

5.2.10 SDS CGE protein separations

The SDS CGE-LIF separation was performed with a running buffer of 0.1 M TrisCHES, 0.1% (w/v) SDS, pH 8.8, and sheath flow buffer of 0.1 M TrisCHES, pH 8.8. Electrokinetic injection for 20-30 seconds at -250V/cm was utilized and the subsequent separations were carried out at -250V/cm.

5.3 Results and Discussion

5.3.1 SDS CGE of standard proteins using different percentages of LPA sieving matrices

Figure 5.2 shows a comparison of molecular weight based separations of standard proteins employing different percentages of a LPA (i.e. 6%-9%) sieving matrix. It must be noted that migration times can be compared only between the 7-9% LPA sieving matrices as these were performed in a capillary 35 cm in length. The 6% LPA sieving matrix was polymerized inside a capillary which was 43 cm in length. The

Figure 5.2 The molecular weight-based separation of standard proteins utilizing different percentages of a LPA sieving matrix.

See Section 5.2.5 for sample preparation details and Section 5.2.8 for details of capillary preparation. LPA sieving matrices are: (A) 9%, (B) 8%, (C) 7%, and (D) 6%. Samples are labeled as: (1) α-lactalbumin (14.4 kDa), (2) soybean trypsin inhibitor (20.1 kDa), (3) carbonic anhydrase (30 kDa), (4) ovalbumin (43 kDa), (5) bovine serum albumin (67 kDa), and (6) phosphorylase b (94 kDa). CE conditions: silane coated capillary, 35 or 43 cm × 140 µm O.D. × 50 µm I.D., running buffer: 0.1 M TrisCHES, 0.1% (w/v) SDS, pH 8.8, sheath flow buffer: 0.1 M TrisCHES, pH 8.8, sample injection: 20-30 s, -250 V/cm, running voltage: -250 V/cm, excitation: 488 nm, emission filter: 630DF30.

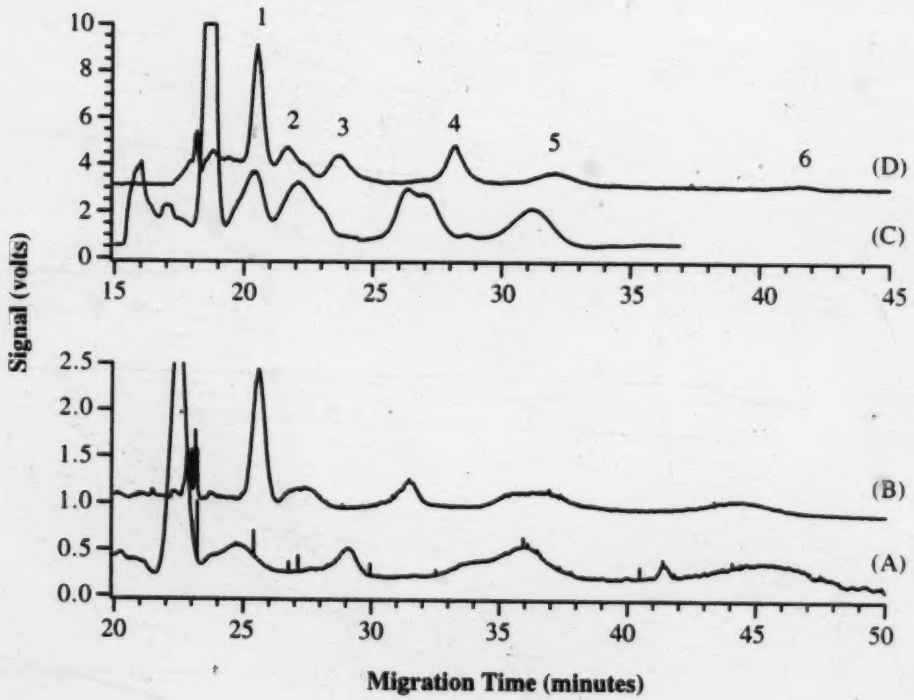

migration order of the proteins has been determined to be: α-lactalbumin (14.4 kDa), soybean trypsin inhibitor (20.1 kDa), carbonic anhydrase (30 kDa), ovalbumin (43 kDa), bovine serum albumin (67 kDa), and phosphorylase b (94 kDa). The 6% and 7% LPA sieving matrices produce peaks which are narrower than the 8% and 9% LPA sieving matrices. This is due to the fact that these proteins spend less time in the capillary and thus there is less diffusion of the zones as they migrate through the capillary.

In general the separations of molecular weight standards ranging from 14.4-94 kDa were achieved in less than one hour. Furthermore, the separation windows varied depending on which percentage of LPA was used. Since some of the experiments were stopped before all six proteins migrated out of the capillary, separation windows are defined here as the time for the first five proteins to migrate out of the capillary. A 6% LPA sieving matrix produced a separation window of 14 minutes. The 7% LPA sieving matrix resulted in an 18-minute separation window. The 8% LPA sieving matrix had a separation window of 27 minutes, while use of a 9% LPA sieving matrix resulted in a separation window of 29 minutes.

5.3.2 Ferguson plot analysis of LPA sieving matrices

Ferguson plots are constructed by plotting log mobility versus the polymer concentration for a given sieving matrix. Following Smithies (17), Ferguson demonstrated experimentally that a linear plot of log mobility of a protein versus agarose gel concentration has a slope which is proportional to molecular size (18). The relationship between log mobility and polymer sieving matrix concentration is written as follows:

$$\log(\mu) = \log(\mu_o) - K_r T \qquad (5.1)$$

where μ is the mobility of the protein in m^2/Vs, μ_o is the free solution mobility of the protein (i.e. the protein's mobility without the employment of a sieving matrix) in m^2/Vs, K_r is the retardation coefficient, and T is the sieving matrix concentration (12, 19, 20). The retardation coefficient is directly proportional to the protein's radius as follows:

$$K_r = \pi l'(r + R)^2 \times 10^{-16} \qquad (5.2)$$

where l' is the matrix fibre length in cm/g, r is the radius of the fibre in nm, and R is the protein's radius in nm (12).

If the y-intercepts for proteins plotted on a Ferguson plot are identical, this indicates that the free mobilities of the proteins are identical. This in turn means that the

proteins have identical mass-to-charge ratios (12). This identical mass-to-charge ratio is a result of the common binding ratio of SDS to all proteins mentioned earlier in Section 4.1.

The Ferguson plots of the 5 protein standards are shown in Figure 5.3. The linearity of these plots demonstrates that the LPA sieving matrix indeed separates the proteins by molecular weight (20). It is seen that the slopes of the two lowest molecular weight standards intersect at a location which corresponds to approximately 6.3% LPA on the x-axis. This intersection of lines indicates that the employment of a LPA concentration less than 6.3% will result in similar migration orders of the two smallest protein standards. Therefore LPA concentrations above 6.3% must be utilized to ensure the correct migration of proteins based on molecular weight.

Table 5.2 lists the retardation coefficients for the five protein standards. As Equation 5.1 shows, these retardation coefficients are the slope values from the Ferguson plots. As Equation 5.2 shows, the retardation coefficient is proportional to the protein's radius. As would be expected, a trend is observed whereby the retardation coefficients increase as the molecular weights of the proteins increase. The 14.4 kDa protein has the smallest K_r, thus indicating it possesses the smallest radius, and the 67 kDa protein has the largest K_r, thus indicating that it has the largest radius of the five proteins.

Table 5.3 shows the y-intercept values for the Ferguson plots. As Equation 5.1 shows, the y-intercept value is indicative of the free solution mobility of a protein. From Table 5.3, it is evident that the free solution mobilities of the proteins are nearly identical which indicates that the proteins have nearly identical mass-to-charge ratios. As previously mentioned, this identical mass-to-charge ratio is a result of the binding of SDS to denatured proteins in a ratio of 1.4 g to 1 g (21). Since these proteins have identical mass-to-charge ratios, the only way they are separated is by size. This evidence further demonstrates that the LPA is effective in sieving the proteins according to size.

5.3.3 Standardization curve construction

For the 6-9% LPA sieving matrices, it was found that linear standardization curves were obtainable by plotting migration time versus molecular weight. Figure 5.4 demonstrates one such standardization curve for the size-based separation of proteins achieved utilizing a 9% LPA sieving matrix. Table 5.4 demonstrates the linearity of standardization curves obtained utilizing different percentages of LPA sieving matrix.

Figure 5.3 Ferguson plot for 6-9% LPA sieving matrices.

Note that the 94 kDa protein data are not included as only two points were available. Slopes are as follows: 14.4 kDa: -0.018±0.022, 20.1 kDa: -0.030±0.025, 30 kDa: -0.042±0.033, 43 kDa: -0.045±0.031, 67 kDa: -0.061±0.040.

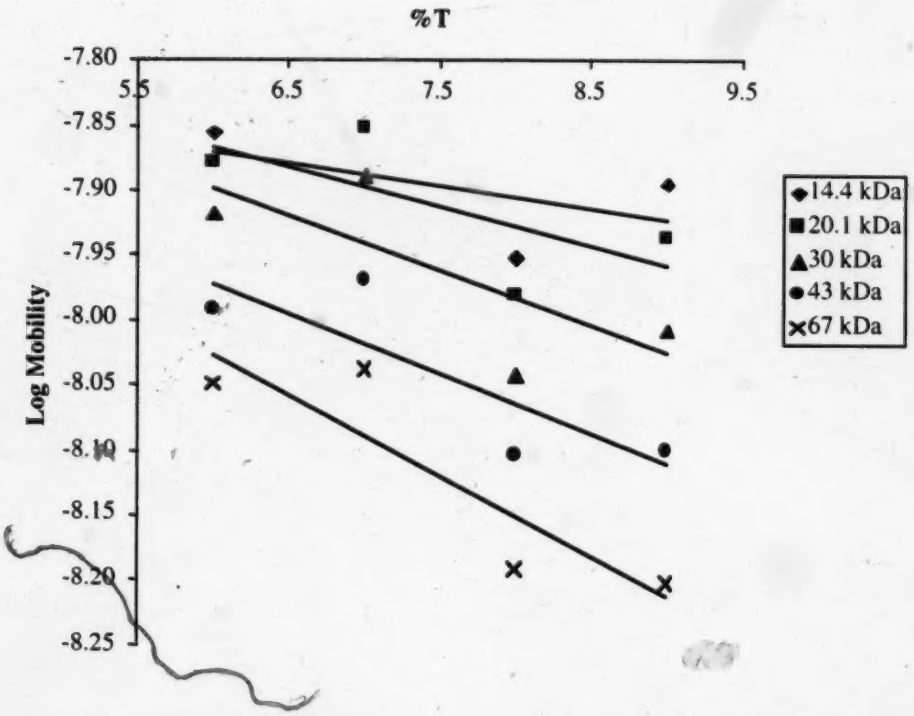

Table 5.2 Retardation coefficients of the 5 protein standards derived from a Ferguson plot.

Protein Molecular Weight (kDa)	K_r
14.4	-0.018
20.1	-0.030
30	-0.042
43	-0.045
67	-0.061

Table 5.3 Ferguson plot y-intercept values for the 5 protein standards utilizing LPA concentrations of 6-9%.

Note that the standard deviation for these values is ±0.04.

Protein Molecular Weight (kDa)	Y-Intercept Value
14.4	-7.76
20.1	-7.68
30	-7.65
43	-7.70
67	-7.66

Figure 5.4 Standardization curve of migration time versus molecular weight utilizing a 9% LPA sieving matrix.

See Section 5.2.5 for sample preparation details and Section 5.2.8 for details of capillary preparation. CE conditions: sample: mixture of α-lactalbumin, soybean trypsin inhibitor, carbonic anhydrase, ovalbumin, bovine serum albumin, and phosphorylase b, capillary: 9% LPA in a silane coated capillary, 35 cm × 140 µm O.D. × 50 µm I.D., running buffer: 0.1 M TrisCHES, 0.1% (w/v) SDS, pH 8.8, sheath flow buffer: 0.1 M TrisCHES, pH 8.8, sample injection: 25 s, -250 V/cm, running voltage: -250 V/cm, excitation: 488 nm, emission filter: 630DF30.

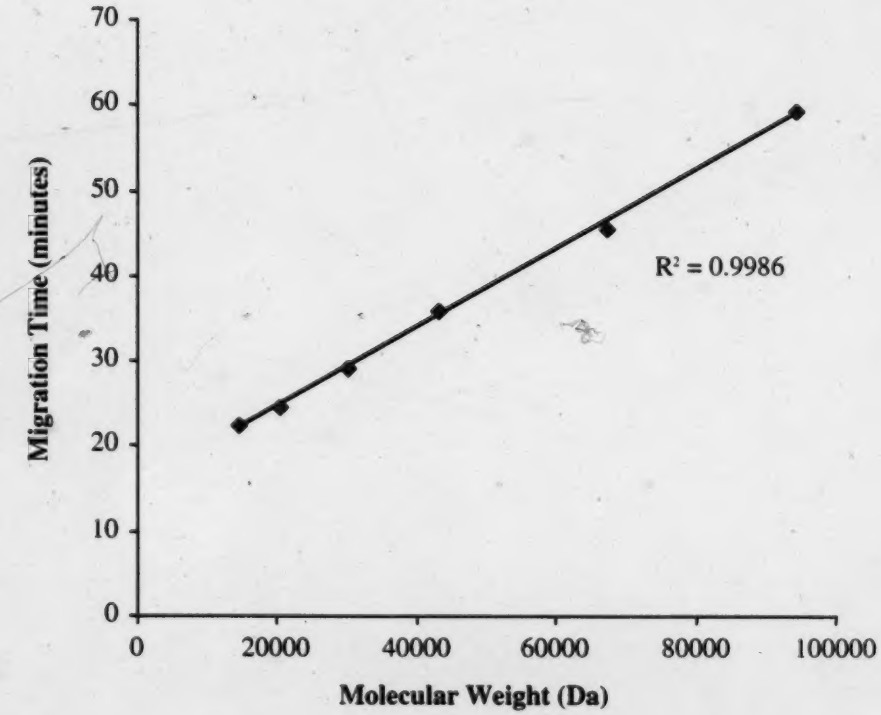

Table 5.4 Comparison of standardization curve linearity for different percentages of LPA sieving matrices.

% LPA	R^2
6	0.9857
7	0.9825
8	0.9985
9	0.9986

As can be seen in the table, the 6% and 7% sieving matrices have slightly lower correlation coefficients of 0.9857 and 0.9825 respectively when compared to those of the 8% and 9% sieving matrices of 0.9985 and 0.9986 respectively. As mentioned in Section 5.3.2, the Ferguson plots demonstrate that the migration times of lower molecular weight proteins sieved by the 6% matrix may not always correspond correctly to the proper molecular weight. The slightly poorer correlation coefficients of the standardization curves of 6% LPA sieving matrix may also indicate the potential ill effects on migration order.

5.3.4 Application of LPA sieving matrices to the separation of water soluble HT29 cell extract proteins

Figure 5.5 shows the application of a 9% LPA sieving matrix to the separation of water-soluble proteins from HT29 cell extract. Portion (A) of the figure displays the entire electropherogram for this sample. Qualitatively, the resolving power of this sieving matrix for such a complex sample is not very good. It can be seen that there is a large peak off-scale signal at the very beginning of the run. This suggests that there are many low molecular weight proteins in this sample that are not resolved. Portion (B) of the figure is a zoomed-in view of a section of the electropherogram. As is noted in the figure caption, the data are filtered every 5 points. Any spurious peaks due to bubbles or small particles are removed by such a median filter. Portion (B) thus shows that there are many proteins seen in the separation, however these are not baseline resolved and thus appear as one large mass. The zoomed-in view shows that some of these proteins are discernable upon closer examination and are not merely artifacts as such peaks are removed by a median filter.

5.3.5 Application of LPA sieving matrices to the separation of fractionated HT29 cell extract proteins

It is shown in Section 5.3.4 that there is little hope of a 9% LPA sieving matrix resolving a complicated sample such as the water-soluble proteins from a whole cell HT29 extract. It was believed that simplifying the samples before separation would be beneficial. As explained in Section 5.2.3 the proteins were fractionated into 4 parts utilizing differential detergent fractionation. Figures 5.6-5.9 show both the slab gel electrophoresis and the SDS CGE separation utilizing a 9% LPA sieving matrix results of these 4 protein fractions.

Figure 5.5 SDS CGE separation of HT29 water-soluble proteins employing a 9% LPA sieving matrix.

See Sections 5.2.3 and 5.2.6 for water-soluble protein preparation and labeling and see Section 5.2.8 for capillary preparation details. Note that the data are median filtered every 5 points. The electropherograms are labeled as follows: (A) the entire run, and (B) a zoom in of a the run between 21 and 39 minutes. CE conditions: capillary: 9% LPA in a silane coated capillary, 35 cm × 140 µm O.D. × 50 µm I.D., running buffer: 0.1 M TrisCHES, 0.1% (w/v) SDS, pH 8.8, sheath flow buffer: 0.1 M TrisCHES, pH 8.8, sample injection: 25 s, -250 V/cm, running voltage: -250 V/cm, excitation: 488 nm, emission filter: 630DF30.

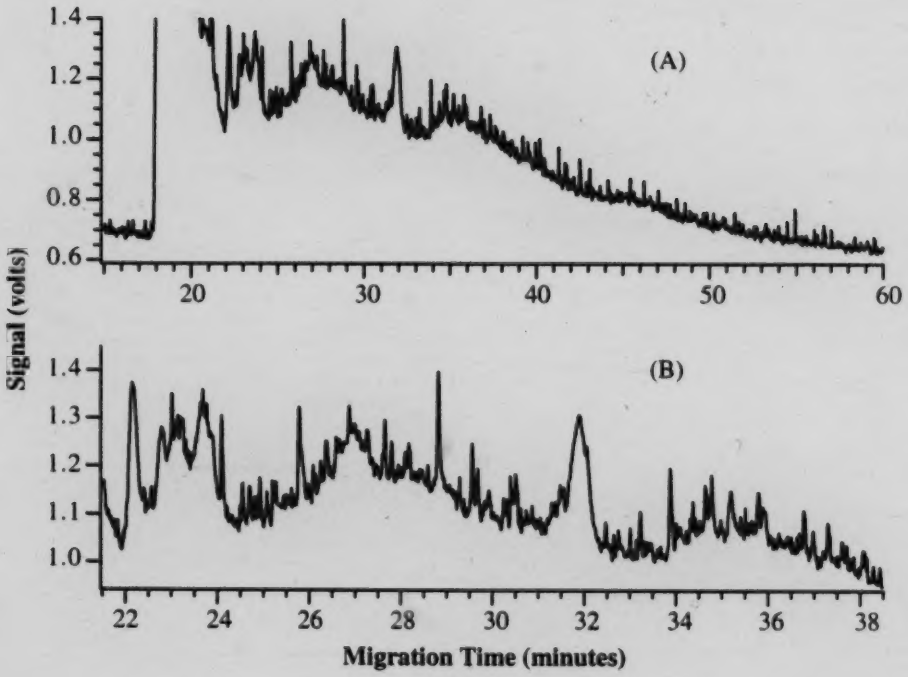

Figure 5.6 shows a comparison of slab gel electrophoresis and SDS CGE utilizing a 9% LPA sieving matrix to separate the components of the membrane/organelle fraction of HT29 cells. The labels of 25 kDa and 150 kDa on the slab gel are used as a guide to determine approximate molecular weights of the visualized bands. As can be seen upon examination of the slab gel results, there are between 20 and 30 bands discernable on the gel. This fraction represents approximately half of the total proteins in a cell (16). Obviously the visualized bands are representative of only the highly abundant membrane/organelle proteins within the cells. Upon comparison of these slab gel results with the SDS CGE results, a drastic decrease in resolving power of the latter technique stands out. A few low molecular weight proteins are distinguishable, though most likely these are co-migrations of many proteins. There is a large peak which begins at about 22 minutes and continues to migrate out of the capillary until approximately 35 minutes. This is obviously a large number of proteins which are not resolved. Furthermore, as was discussed in Section 5.3.1, the larger molecular weight proteins spend more time in the capillary and thus are subject to more diffusion, rendering these proteins not easily discernable from one another. As was seen with the standard separations in Section 5.3.1, the higher molecular weight proteins in general had a lower signal due to this diffusion and were sometimes barely detected at all.

Figure 5.7 shows a comparison of slab gel electrophoresis and SDS CGE utilizing a 9% LPA sieving matrix to separate the components of the cytosolic fraction of HT29 cells. The molecular weights of 25 kDa and 150 kDa labeling the slab gel are used as a rough guide to approximate the molecular weights of the visualized proteins. Many proteins are seen on this gel, and this fraction represents approximately 35% of the total proteins in a cell (16). Again the SDS CGE results utilizing a 9% LPA sieving matrix show some resolution of low molecular weight proteins, but few distinguishable higher molecular weight proteins. There is again a large plateau at the beginning of migration of sample out of the capillary which suggests the presence of many low molecular weight proteins. However the slab gel results indicate that there are also many medium to high molecular weight proteins, but these are not seen well with the CGE results. This again is probably a result of diffusion of the proteins occurring in the capillary during separation.

Figure 5.8 displays a comparison of slab gel electrophoresis and SDS CGE utilizing a 9% LPA sieving matrix to separate the components of the cytoskeletal fraction of HT29 cells. The labels indicating molecular weights of 25 kDa and 150 kDa

Figure 5.6 Comparison of SDS-PAGE gel and SDS CGE separations of the HT29 membrane/organelle fraction.

CE conditions: see Sections 5.2.3 and 5.2.6 for protein preparation and labeling, see Section 5.2.8 for capillary preparation details, capillary: 9% LPA in a silane coated capillary, 35 cm × 140 µm O.D. × 50 µm I.D., running buffer: 0.1 M TrisCHES, 0.1% (w/v) SDS, pH 8.8, sheath flow buffer: 0.1 M TrisCHES, pH 8.8, sample injection: 25 s, -250 V/cm, running voltage: -250 V/cm, excitation: 488 nm, emission filter: 630DF30. Slab gel conditions: see Section 5.2.4 for sample preparation details, 4% stacking gel/12% separating gel, 1 mm thick, run at 200 V, silver stained.

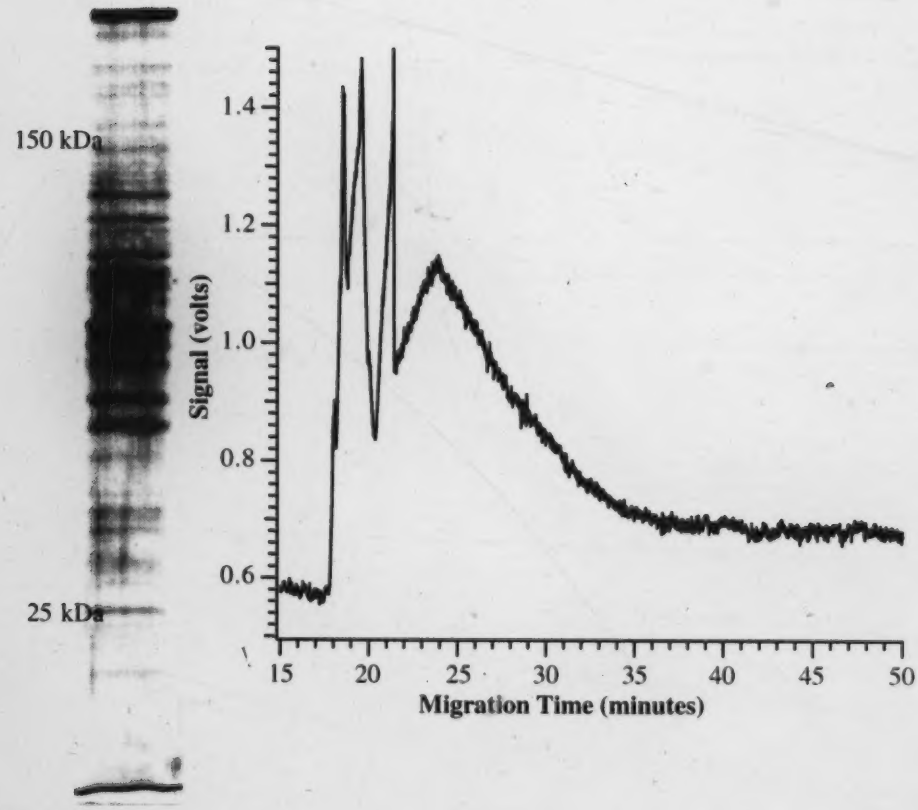

Figure 5.7 Comparison of SDS-PAGE gel and SDS CGE separations of the HT29 cytosolic fraction.

CE conditions: see Sections 5.2.3 and 5.2.6 for protein preparation and labeling, see Section 5.2.8 for capillary preparation details, capillary: 9% LPA in a silane coated capillary, 35 cm × 140 µm O.D. × 50 µm I.D., running buffer: 0.1 M TrisCHES, 0.1% (w/v) SDS, pH 8.8, sheath flow buffer: 0.1 M TrisCHES, pH 8.8, sample injection: 25 s, -250 V/cm, running voltage: -250 V/cm, excitation: 488 nm, emission filter: 630DF30. Slab gel conditions: see Section 5.2.4 for sample preparation details, 4% stacking gel/12% separating gel, 1 mm thick, run at 200 V, silver stained.

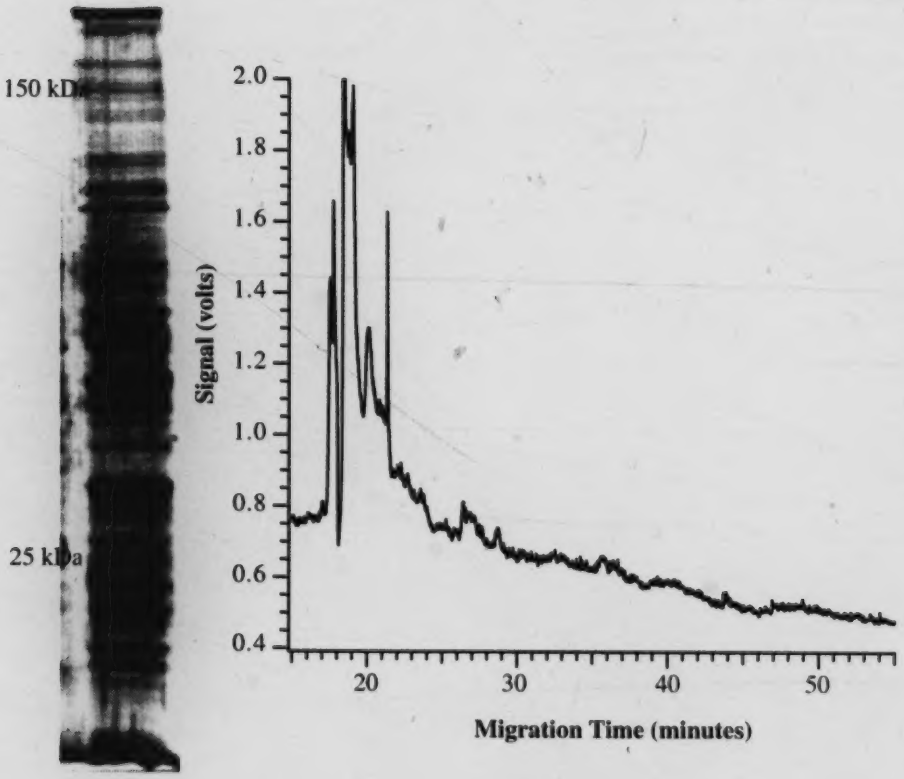

Figure 5.8 Comparison of SDS-PAGE gel and SDS CGE separations of the HT29 cytoskeletal fraction.

CE conditions: see Sections 5.2.3 and 5.2.6 for protein preparation and labeling, see Section 5.2.8 for capillary preparation details, capillary: 9% LPA in a silane coated capillary, 40 cm × 140 µm O.D. × 50 µm I.D., running buffer: 0.1 M TrisCHES, 0.1% (w/v) SDS, pH 8.8, sheath flow buffer: 0.1 M TrisCHES, pH 8.8, sample injection: 25 s, -250 V/cm, running voltage: -250 V/cm, excitation: 488 nm, emission filter: 630DF30. Slab gel conditions: see Section 5.2.4 for sample preparation details, 4% stacking gel/12% separating gel, 1 mm thick, run at 200 V, silver stained.

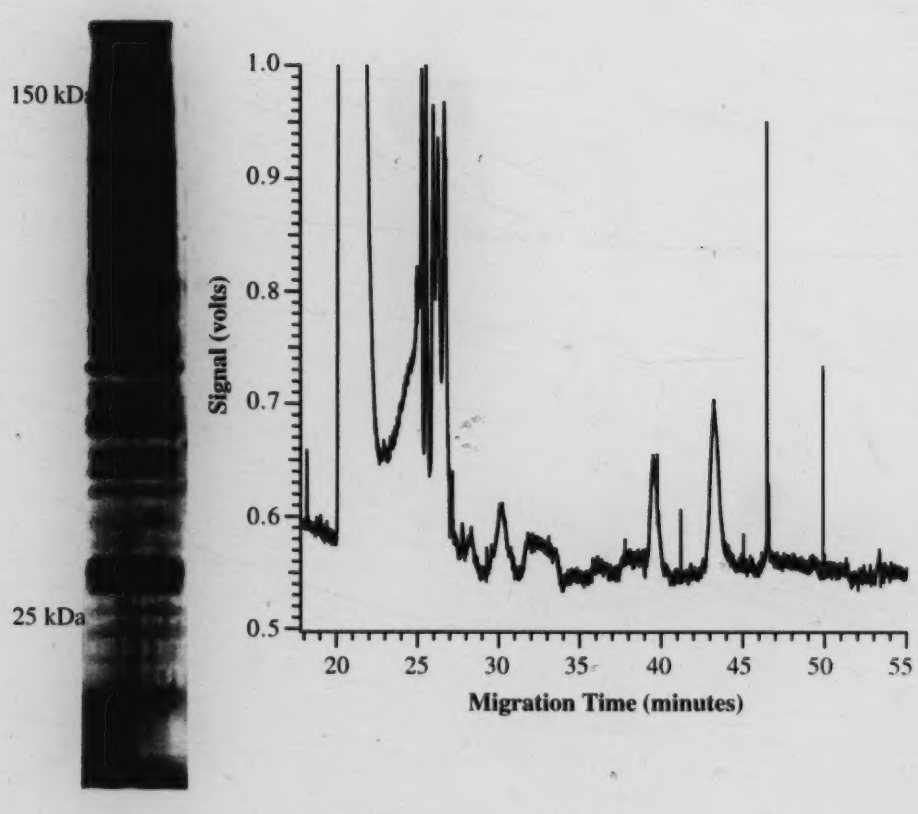

on the slab gel aid to approximate the molecular weights of the visualized proteins. The proteins seen on this gel represent approximately 10% of the total proteins in a cell (16). The SDS CGE results of this fraction appear to be the most successful of the SDS CGE separations with this sieving matrix. Here again there are many low to medium molecular weight proteins which appear either as a large co-migrating peak or as discrete peaks. There are also some large proteins seen in the vicinity of the 90-100 kDa region (approximated utilizing the protein standard separations). The baseline of this separation is quite nice and stable throughout the run. Perhaps it is due to the nature of the proteins in this particular fraction to which the success of the separation may be attributed.

Figure 5.9 exhibits a comparison of slab gel electrophoresis and SDS CGE employing a 9% LPA sieving matrix to separate the components of the nuclear fraction of HT29 cells. Again the labels which indicate molecular weights of 25 kDa and 150 kDa on the slab gel help in approximating the molecular weights of the visualized proteins. The proteins seen on this gel represent approximately 5% of the total proteins in a cell (16). The quality of the SDS CGE separation of this fraction was very poor. The electropherogram shows one large peak at 20 minutes. This is followed by a plateau which plummets sharply to baseline. There is evidence of some high molecular weight proteins as seen by the large plateau which forms between 30 and 35 minutes. It must be noted that subsequent experiments with labeling of nuclear fractions showed that one of the nuclear extraction buffer components (PIPES, a tertiary amine) was highly reactive with the FQ which was used to fluorescently label the nuclear proteins. Part of the signal contributing to the large peak which begins at 20 minutes into the run most likely is from the FQ-labeled PIPES component of the buffer.

5.4 Conclusion

This chapter demonstrates the use of LPA sieving matrices with SDS CGE for separations of both standard proteins and HT29 cell extract proteins based on molecular weight. A series of standard proteins was successfully separated using ranges of LPA between 6% and 9%. Ferguson plot analysis demonstrated that these separations were indeed based on molecular weight and that the optimum LPA concentrations for separating low molecular weight proteins by size were the 7-9% sieving matrices. Linear standardization curves of molecular weight versus migration time were constructed from the data for each percentage of sieving matrix employed. The separation technique employing 9% LPA as a sieving matrix was then applied to the

Figure 5.9 Comparison of SDS-PAGE gel and SDS CGE separations of the HT29 nuclear fraction.

CE conditions: see Sections 5.2.3 and 5.2.6 for protein preparation and labeling, see Section 5.2.8 for capillary preparation details, capillary: 9% LPA in a silane coated capillary, 40 cm × 140 µm O.D. × 50 µm I.D., running buffer: 0.1 M TrisCHES, 0.1% (w/v) SDS, pH 8.8, sheath flow buffer: 0.1 M TrisCHES, pH 8.8, sample injection: 25 s, -250 V/cm, running voltage: -250 V/cm, excitation: 488 nm, emission filter: 630DF30. Slab gel conditions: see Section 5.2.4 for sample preparation details, 4% stacking gel/12% separating gel, 1 mm thick, run at 200 V, silver stained.

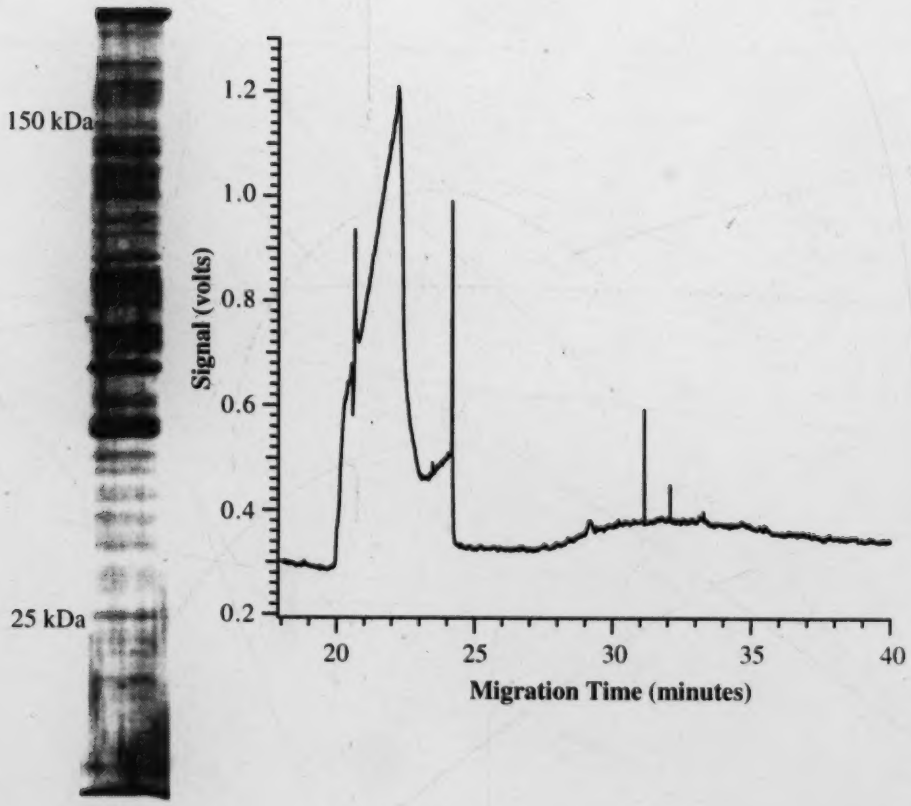

analysis of water-soluble proteins from HT29 cell extracts. This sample proved too complicated for the resolving power of LPA, so the HT29 cells were fractionated into four parts (membrane/organelle, cytosolic, cytoskeletal, and nuclear proteins) by differential detergent fractionation, and then each fraction was separated utilizing a 9% LPA sieving matrix. The qualitative resolution of the proteins of each fraction was quite poor, showing some success with separating mostly low and medium molecular weight proteins. The high molecular weight proteins likely underwent too much diffusion during the separation and migrated out of the capillary as elongated zones. As stated by Kenndler *et. al.*, "A broader application of this method [SDS CGE size-based separations] to real samples ... seems to be an area requiring work in the future" (22).

5.5 References

(1) Hjertén, S. *Journal of Chromatography* **1983,** *270*, 1-6.

(2) Cohen, A. S.; Karger, B. L. *Journal of Chromatography* **1987,** *397*, 409-417.

(3) Cohen, A. S.; Paulus, A.; Karger, B. L. *Chromatographia* **1987,** *24*, 15-24.

(4) Tsuji, K. *Journal of Chromatography* **1991,** *550*, 823-830.

(5) Manabe, T. *Electrophoresis* **1995,** *16*, 1468-1473.

(6) Wu, D.; Regnier, F. E. *Journal of Chromatography* **1992,** *608*, 349-356.

(7) Widhalm, A.; Schwer, C.; Blaas, D.; Kenndler, E. *Journal of Chromatography* **1991,** *549*, 446-451.

(8) Ganzler, K.; Greve, K. S.; Cohen, A. S.; Karger, B. L.; Guttman, A.; Cooke, N. C. *Analytical Chemistry* **1992,** *64*, 2665-2671.

(9) Wise, E. T.; Singh, N.; Hogan, B. L. *Journal of Chromatography A* **1996,** *746*, 109-121.

(10) Harvey, M. D.; Bandilla, D.; Banks, P. R. *Electrophoresis* **1998,** *19*, 2169-2174.

(11) Werner, W. E.; Demorest, D. M.; Stevens, J.; Wiktorowicz, J. E. *Analytical Biochemistry* **1993,** *212*.

(12) Werner, W. E.; Demorest, D. M.; Wiktorowicz, J. E. *Electrophoresis* **1993,** *14*, 759-763.

(13) Werner, W. E.; Wiktorowicz, J. E.; Kasarda, D. D. *Cereal Chemistry* **1994,** *71*, 397-402.

(14) Weegels, P. L.; Hamer, R. J.; Schofield, J. D. *Journal of Cereal Science* **1995,** *22*, 211-224.

(15) Zhang, Z.; Krylov, S.; Arriaga, E. A.; Polakowski, R.; Dovichi, N. J. *Analytical Chemistry* **2000,** *72*, 318-322.

(16) Ramsby, M. L.; Makowski, G. S. In *2-D Proteome Analysis Protocols*; Link, A. J., Ed.; Humana Press, Inc.: Totowa, 1999, pp 53-85.

(17) Smithies, O. *Archives of Biochemistry and Biophysics, Supplement* **1962,** *1*, 125-131.

(18) Ferguson, K. A. *Metabolism* **1964,** *13*, 985-1002.

(19) Tietz, D. *Advances in Electrophoresis* **1989,** *2*, 112-169.

(20) Simo-Alfonso, E.; Conti, M.; Gelfi, C.; Righetti, P. G. *Journal of Chromatography A* **1995,** *689*, 85-96.

(21) Weber, K.; Osborn, M. *Journal of Biological Chemistry* **1969,** *244*, 4406-4412.

(22) Kenndler, E.; Poppe, H. *Journal of Capillary Electrophoresis* **1994,** *1*, 144-157.

Chapter 6
Dextran as a Sieving Matrix for Sodium Dodecyl Sulfate Capillary Gel Electrophoresis of Proteins with Laser-Induced Fluorescence Detection

6.1 Introduction

Few reports of dextran as a sieving matrix for SDS CGE separations of proteins exist. Among other things, dextran has been employed for different CE separations as a capillary coating agent to help reduce electro-osmotic flow (1, 2), in the CE separation of rat liver microsome components (3), in micellar electrokinetic chromatography to aid in the enantiomeric separations of basic drugs (4, 5), and as a sieving matrix to separate small oligonucleotides (6). Dextran is a desirable SDS CGE separating matrix for a number of reasons. One such reason is that most research groups employ UV detection with SDS CGE separations and dextran, unlike cross-linked and linear polyacrylamide, is not UV absorbant (7, 8). Furthermore, dextran solutions are of relatively low viscosity and can be replaced between each capillary use, removing the possibility of cross-contamination from run to run. The utilization of replaceable sieving matrices is also desirable as on-column polymerization presents problems such as difficulty in controlling the reaction, bubble formation, and volume changes which may be associated with the polymerization reaction (8-11).

The first report of dextran as a sieving matrix for use in SDS CGE separations was in 1992 by Ganzler *et. al.* (7). The authors utilized dextran of 3 different molecular weights (i.e. 72 000 Da , 500 000 Da, and 2 000 000 Da) to demonstrate the size-based separations of proteins standards and rat plasma samples (7). Following the introduction of dextran as sieving matrix for SDS CGE separations, a number of its properties have since been studied. Guttman *et. al.* described how temperature effects separations involving branched dextran (12). The authors discovered that migration time decreased and peak efficiency increased with increases in temperature (12). Further research has also been performed to see how dextran molecular weight effects protein separations (10, 13). It was found that both higher molecular weight dextrans as well as mixtures of different molecular weight dextrans produce the best resolution of standard proteins (10). Lausch *et. al.* utilized dextran in rapid SDS CGE separations with electric fields up to 740 V/cm to separate both standard proteins and the heavy and light chains of human immunoglobulin G (8). Dextran has also been successfully employed as a sieving matrix to separate myoglobin molecular mass markers (11). All reports of dextran as a sieving matrix for SDS CGE proteins separations involve employment of UV detectors except that of Craig *et. al.* who utilized LIF detection for the separation of protein standards (14).

This chapter demonstrates the utilization of dextran as a sieving matrix for SDS CGE separations of both standard proteins and real, complex samples. Protein standards are separated by a range of percentages of dextran. These separations are proven to be size-based by the construction of Ferguson plots. Linear standardization curves are also constructed for these protein standard separations of logarithm of migration time versus logarithm of molecular weight. The effects of different buffers utilized to dissolve the dextran and as sheath flow and running buffers are also examined. Reproducibility is presented for both same-day separations and day-to-day separations. Lastly, this dextran sieving matrix is applied to both the separations of water-soluble proteins of A549 (human lung cancer) cells and the nuclear proteins of A549 cells.

6.2 Experimental

6.2.1 Materials and reagents

Fused-silica capillary (50 μm I.D., 140 μm O.D.) was purchased from PolyMicro Technologies (Phoenix, AZ). Sigma (St. Louis, MO) was the supplier of the following: dextran (average molecular weight 2 M Da), tris[hydroxymethyl]aminomethane (Trizma base), 2-[*N*-cyclohexylamino]ethane-sulfonic acid (CHES), piperazine-*N,N'*-bis(2-ethanesulfonic acid) (PIPES), phenylmethylsulfonyl fluoride (PMSF), t-octylphenoxypolyethoxyethanol (Triton X-100), polyoxyethylenesorbitan monopalmitate (Tween-40), and deoxycholic acid (DOC). Ammonium persulfate (APS) and *N,N,N',N'*- tetramethylethylenediamine (TEMED) were acquired from Bio-Rad (Hercules, CA). The sodium dodecyl sulfate (SDS) and sodium hydroxide (NaOH) were from Caledon (Georgetown, Canada). Digitonin was obtained from Fluka (Oakville, Canada). BDH (Vancouver, Canada) was the supplier of sucrose, magnesium chloride hexahydrate ($MgCl_2 \cdot 6H_2O$), ethylenediaminetetra-acetic acid sodium salt (EDTA), potassium chloride (KCl), sodium chloride (NaCl), and di-sodium tetraborate (borate). Acrylamide, Dulbecco's Modified Eagle Medium, fetal bovine serum, penicillin, streptomycin, and trypsin-EDTA were purchased from GibcoBRL (Grand Island, NY). The 3-(2-furoyl)quinoline-2-carboxyaldehyde (FQ) and potassium cyanide (KCN) were obtained from Molecular Probes (Eugene, OR). Anachemia (Montreal, Canada) provided the concentrated hydrochloric acid. Pharmacia (Quebec, Canada) was the supplier of the Pharmacia Low Molecular Weight Calibration Kit. From Fisher (Fair Lawn, NJ) the

following was acquired: sodium phosphate, dibasic (Na_2HPO_4), sodium phosphate, monobasic ($NaH_2PO_4 \cdot H_2O$), potassium phosphate, monobasic (KH_2PO_4), methanol, and T_{25} flasks. Glycerol was purchased from ACP (Montreal, Canada). From Aldrich (Milwaukee, WI) β-mercaptoethanol, vinylmagnesium bromide, tetrahydrofuran (THF), and bromophenol blue were obtained. Thionyl chloride was purchased from Acros Organics (Geel, Belgium). Millipore (Bedford, MA) supplied the Microcon YM-10 centrifugal device filters.

6.2.2 Cell culture

The A549 (human lung cancer) cell line was cultured in T_{25} flasks in an incubator at 37°C in a 5% CO_2 atmosphere. The cells were grown to 80% confluence in Dulbecco's Modified Eagle Medium/F12, supplemented with 10% fetal bovine serum and 50 mg/mL penicillin/streptomycin.

6.2.3 Cell extract preparation and fractionation

The water-soluble proteins of A549 cells were prepared as described by Zhang *et. al.* (15). Approximately 3-5 × 10^6 cells were washed three times with phosphate-buffered saline (PBS). The cells were then resuspended in approximately 100 µL of water. The suspension was sonicated for 80 minutes at 4°C, followed by a spin for 10 minutes at 2000*g*. The supernatant was removed and stored at -20°C.

As described in Section 5.2.3, the cells were fractionated into 4 fractions utilizing a differential detergent fractionation method (16). However in this chapter, only the nuclear fraction was of interest, so the cells were only fractionated into 3 fractions, after which the remnants of the cells were discarded. Furthermore, also differing from Section 5.2.3, the monolayer cell proteins were extracted by adding extraction buffers directly to the T_{25} flasks and removing the subsequent extraction solutions from the flask at the end of an incubation period. Two T_{25} flasks were worked up at once and the resulting extracts were combined. To a T_{25} flask containing approximately 1.7 × 10^6 A549 cells, 1 mL of ice-cold digitonin extraction buffer was added. The flask was rocked on ice for 15 minutes, at which time the extraction solution was removed from the flask. The extraction solution contained cytosolic proteins, was aliquoted, and stored at -70°C. Next 1 mL of ice-cold Triton X-100 extraction buffer was added to the flask. The flask was rocked for 30 minutes on ice. The extraction liquid, which contained the membrane/organelle proteins, was removed from the flask, aliquoted, and stored at -70°C. To the T_{25} flask, 500 µL of ice-cold

Tween/DOC extraction buffer was added. The flask was rocked on ice for 15 minutes. The extraction liquid, which contained the nuclear proteins, was removed from the flask, aliquoted, and stored at -70°C. The T_{25} flasks still contained some cellular residue, so they were filled with 10% (v/v) bleach for at least an hour and then disposed of in the biohazard waste.

6.2.4 A549 nuclear protein concentration

200 µL of A549 nuclear proteins were placed on the filter unit of a Microcon YM-10 (i.e. a 10 kDa molecular weight cut-off filter). The column was then spun at 14 000*g* for 13 minutes. After this time, the filter portion was removed from the tube and inverted into a new tube. The retentate was spun out of the filter portion for 3 minutes at 1 000*g*. The filter was then vortexed briefly with 180 µL of 5 mM TrisHCl, 0.1% SDS, inverted into the tube containing the retentate, and spun for 3 minutes at 1 000*g*. The solution in the tube was then transferred to the filter of a new Microcon YM-10. The column was spun for 14 minutes at 14 000*g*. The filter portion was inverted into a new tube and the retentate was spun out for 3 minutes at 1 000*g*. The filter portion was then vortexed with 10 µL of 5 mM TrisHCl, 0.1% SDS, inverted, and spun into the column again for 3 minutes at 1 000*g*. The resulting nuclear proteins were concentrated from a 200 µL solution to one of 34 µL. Henceforth this solution will be referred to as the concentrated nuclear protein solution.

6.2.5 FQ labeling of standard proteins

A vial of lyophilized Pharmacia Low Molecular Weight Electrophoresis Calibration standards was reconstituted in 100 µL of reducing buffer (25 mM TrisHCl, 2.3% (w/v) SDS, and 5% (v/v) β-mercaptoethanol, pH 8). From this stock a 9 µL aliquot was denatured for 5 minutes at 95°C. This sample was then added to 100 nmol dry FQ and 1 µL of 25 mM KCN (in 10 mM borate), mixed, and reacted at 65°C for 15 minutes. 1 µL of these labeled standards was diluted in the buffer appropriate for the experiment.

6.2.6 FQ labeling of A549 protein samples

A 5 µL aliquot of A549 nuclear proteins or concentrated nuclear proteins was mixed with 4 µL of reducing buffer (25 mM TrisHCl, 2.3% (w/v) SDS, and 5% (v/v) β-mercaptoethanol, pH 8). This solution was reduced for 5 minutes at 95°C. Next the

solution was added to 100 nmol dry FQ and 1 μL of 25 mM KCN (in 10 mM borate), mixed, and reacted at 65°C for 15 minutes. The labeled proteins were diluted 10-75 times with the appropriate buffer for each experiment.

6.2.7 Capillary preparation

See Section 3.2.8 for complete capillary preparation details of polyacryloylaminopropyl (polyAAP) Grignard coated capillaries. LPA Grignard coated capillaries were prepared in the same manner as polyAAP coated capillaries. However a polymerizing 3% (w/v) acrylamide mixture was flushed through the capillary on the last day of coating instead of a polymerizing AAP mixture.

6.2.8 Dextran sieving matrix preparation

A dextran stock solution was prepared containing 20% (w/v) dextran (2 000 000 Da) in water. The solution was stirred overnight at room temperature to ensure complete dissolution of all of the dextran. Stock solutions were diluted accordingly with the appropriate buffer for the experiment. SDS was also added to the sieving matrix solution to achieve a final concentration of 0.1% (w/v).

6.2.9 CE instrument

See Section 2.2.5 for details of the single-capillary instrument with sheath-flow cuvette and LIF detector used. A blue argon ion laser (3.5 mW, λ = 488 nm) (Uniphase, San Jose, CA) was used for sample excitation. Fluorescence was filtered through a 630DF30 bandpass filter (Omega Optical, Brattleboro, VT) and was detected with an R1477 photomultiplier tube (Hamamatsu, Middlesex, NJ).

6.2.10 SDS CGE separations

Before each experiment, the capillary was filled with dextran sieving matrix by syringe. The SDS CGE-LIF separations were performed with varying running and sheath flow buffers. These buffers will be specified for each experiment. It is noted, though, that the running buffer for each experiment was identical to the dextran solution which was used to fill the capillary prior to each separation. Capillaries were pre-run for 5-10 minutes before injections were performed. Electrokinetic injection was utilized at various parameters and will be specified in figure captions. The separations were performed at different electric fields again to be specified for each experiment.

6.3 Results and Discussion

6.3.1 SDS CGE of standard proteins utilizing different percentages of dextran sieving matrices

Figure 6.1 demonstrates the use of 6%, 8%, 10%, and 12% dextran sieving matrices to separate standard proteins by molecular weight. These dextran sieving matrices were made in 50 mM TrisCHES, 0.1% SDS buffer (henceforth termed "high ionic strength buffer"), which was also utilized as the sheath flow buffer. It has been determined that the order of migration of the six standard proteins is: α-lactalbumin (14.4 kDa), soybean trypsin inhibitor (20.1 kDa), carbonic anhydrase (30 kDa), ovalbumin (43 kDa), bovine serum albumin (67 kDa), and phosphorylase b (94 kDa). Qualitatively, the resolution between the standards appears to be quite satisfactory. It is noted though that the last two migrating protein standards have very low signals and are very wide peaks. This can be attributed to the reasons previously discussed in Section 5.3.1. The larger proteins spend more time in the capillary and are thus subject to greater diffusion of zones. This results in the protein peaks appearing as short, elongated zones. In some of the electropherograms, degradation products of proteins maybe seen as more than one peak appears for one standard (8). The cause of this degradation is not known. In the case of the 10% dextran sieving matrix, it is seen that for soybean trypsin inhibitor there are two peaks, for ovalbumin there are 2 peaks, and for bovine serum albumin, there appears to be one major peak flanked by two smaller peaks. In this case, the sample was prepared on the same day the experiment was carried out. For the other cases, the sample was prepared two days prior to the experiments' performances. In the latter case, it is more understandable that degradation occurred, but in the former case, the degradation of sample is a mystery. The separation using the 6% dextran matrix is accomplished in about 15 minutes with a separation window of about 6 minutes. The 8% dextran matrix separates the protein standards in a total time of 18 minutes with a separation window of 8 minutes. The total separation time and separation window for the 10% dextran sieving matrix are 23 minutes and 11 minutes respectively. The 12% dextran sieving matrix has a total separation time of 33 minutes with a separation window roughly 18 minutes in length.

Figure 6.2 displays the use of 10%, 12%, and 14% dextran sieving matrices to separate the 6 protein standards by molecular weight. These dextran sieving matrices were constituted in 5 mM TrisHCl, 0.1% SDS buffer (henceforth referred to as "low ionic strength buffer"). The same buffer was utilized as the running buffer. This figure

Figure 6.1 Separation of standard proteins utilizing different percentages of dextran with a high ionic strength buffer.

See Section 6.2.5 for sample preparation details and Section 6.2.7 for capillary preparation. Dextran sieving matrices are: (A) 12%, (B) 10%, (C) 8%, and (D) 6%. Samples are labeled as: (1) α-lactalbumin (14.4 kDa), (2) soybean trypsin inhibitor (20.1 kDa), (3) carbonic anhydrase (30 kDa), (4) ovalbumin (43 kDa), (5) bovine serum albumin (67 kDa), and (6) phosphorylase b (94 kDa). CE conditions: 3% LPA Grignard coated capillary, 29 cm × 140 µm O.D. × 50 µm I.D., sheath flow buffer: 50 mM TrisCHES, 0.1% (w/v) SDS, pH 8.8, running buffer: dextran in 50 mM TrisCHES, 0.1% (w/v) SDS, pH 8.8, prerun: 10 minutes, -350 V/cm, sample: standards diluted 50×, sample injection: (A) 8 s, -400 V/cm, (B-D) 5 s, -400 V/cm, running voltage: -350 V/cm, excitation: 488 nm, emission filter: 630DF30.

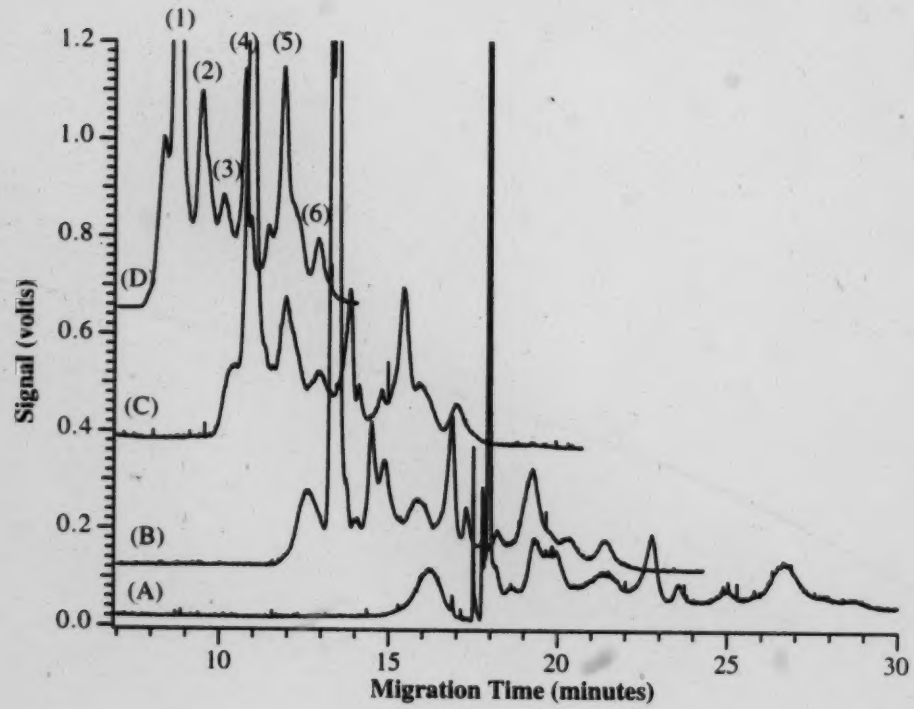

Figure 6.2 Separation of standard proteins utilizing different percentages of dextran with a low ionic strength buffer.

See Section 6.2.5 for sample preparation details and Section 6.2.7 for capillary preparation. Data are median filtered every 5 points. Dextran sieving matrices are: (A) 14%, (B) 12%, and (C) 10%. Samples are labeled as: (1) α-lactalbumin (14.4 kDa), (2) soybean trypsin inhibitor (20.1 kDa), (3) carbonic anhydrase (30 kDa), (4) ovalbumin (43 kDa), (5) bovine serum albumin (67 kDa), and (6) phosphorylase b (94 kDa). CE conditions: 3% LPA Grignard coated capillary, 29 cm × 140 µm O.D. × 50 µm I.D., sheath flow buffer: 5 mM TrisHCl, 0.1% (w/v) SDS, pH 8.8, running buffer: dextran in 5 mM TrisHCl, 0.1% (w/v) SDS, pH 8.8, prerun: 2.5-4 minutes, -350 V/cm, followed by 2.5-4 minutes, -400 V/cm, sample: standards diluted 50×, sample injection: 5 s, -400 V/cm, running voltage: -400 V/cm, excitation: 488 nm, emission filter: 630DF30.

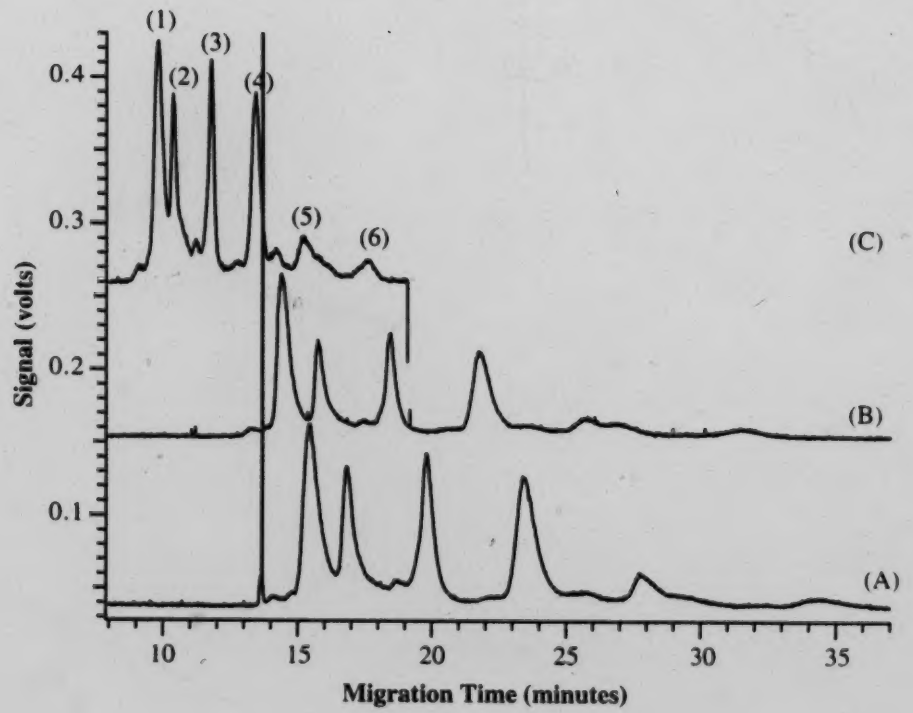

demonstrates the employment of a much lower ionic strength buffer when compared to Figure 6.1. Qualitatively Figure 6.2 shows better resolution between protein standards than the separations in Figure 6.1. However there is some slight peak tailing with the use of 12% and 14% dextran. Again a marked decrease in signal is observed for the largest of the two protein standards. Utilizing a lower ionic strength buffer, the 10% dextran sieving matrix requires 19 minutes for the separation to be achieved and has a separation window of 10 minutes. Employment of the 12% dextran sieving matrix accomplishes separation in 34 minutes with a 21-minute wide separation window. The 14% sieving matrix requires 37 minutes to complete the separation with a separation window of 23 minutes.

Comparing Figures 6.1 and 6.2 shows that the lower ionic strength buffer produces sharper peaks which appear more completely resolved from one another. Examining overall separation times of identical percentage dextran matrices shows few differences. The separation window comparison yields similar results as well. In Section 6.3.2, some discussion will take place on the quantitative effects these buffer ionic strengths yield on separations. Furthermore, qualitative effects of different buffers on the separations of standard proteins will be discussed in Section 6.3.4.

6.3.2 Ferguson plot analysis of dextran sieving matrices with high and low ionic strength buffers

The background information on Ferguson plots was discussed in Section 5.3.2. Briefly, the linearity of the plot of log mobility of a protein versus sieving matrix concentration is an indication that the separation is size-based. Figure 6.3 is the Ferguson plot constructed from separation data of 6%, 8%, 10%, and 12% dextran sieving matrices which were constituted in 50 mM TrisCHES, 0.1% SDS buffer. The linearity of these plots indicates that the dextran sieving matrices employed are sieving by size (17). None of the slopes intersect at any point on the graph which indicates that the migration order of the proteins for these given dextran percentages is correctly predicted by molecular weight.

The Ferguson plot constructed from separation data of 10%, 12%, and 14% dextran sieving matrices which were constituted in low ionic strength buffer of 5 mM TrisHCl, 0.1% SDS is shown in Figure 6.4. As can be seen, the plots are again linear which indicates that the dextran matrix is indeed sieving the proteins according to size. The trendlines of the plots do not intersect on the graph which shows that the migration order of the proteins will be predicted by molecular weight.

Figure 6.3 Ferguson plot for 8-12% dextran sieving matrices with a high ionic strength buffer.

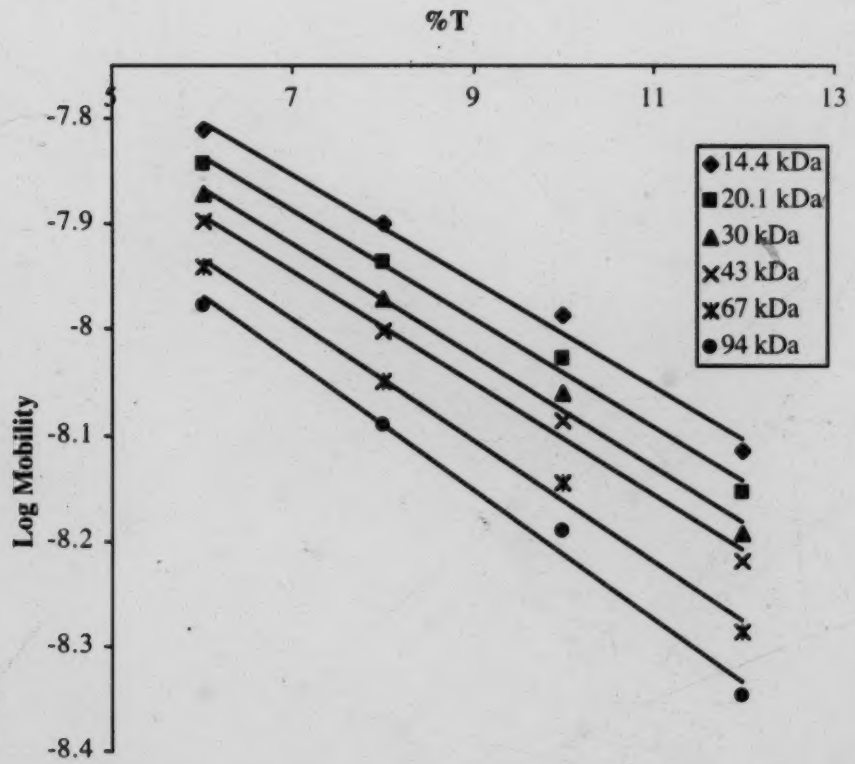

Figure 6.4 Ferguson plot for 10-14% dextran sieving matrices with a low ionic strength buffer.

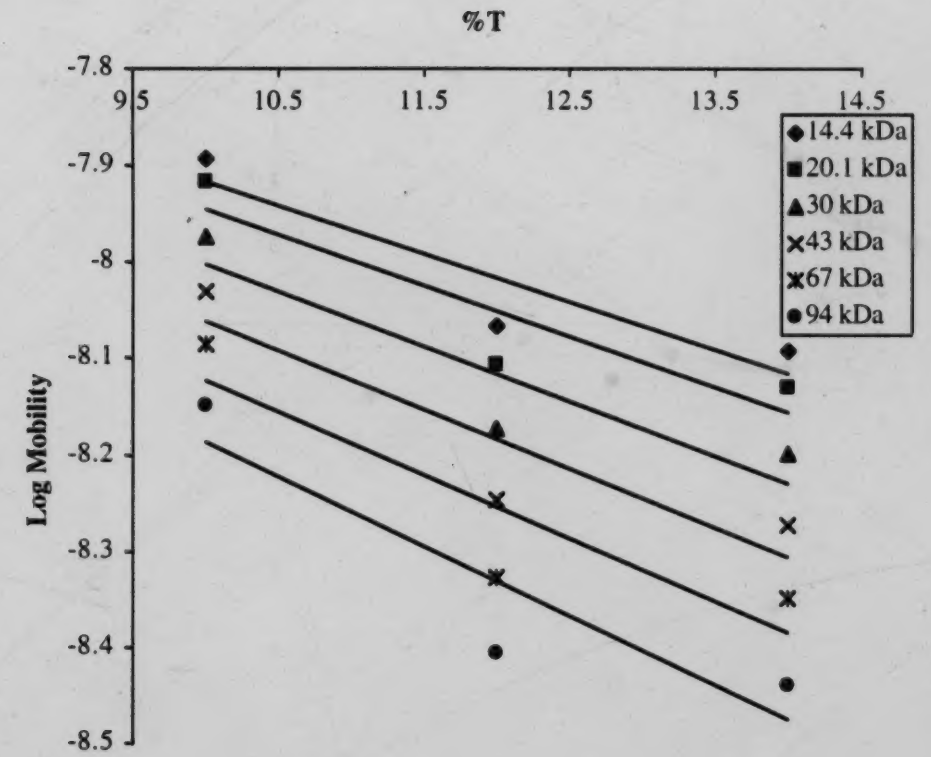

As explained in Section 5.3.2 by Equation 5.1, the retardation coefficient of a protein is equivalent to the slope of a Ferguson plot. Furthermore, Equation 5.2 demonstrates the proportionality between the retardation coefficient and the protein's radius. Table 6.1 displays the 6 standard proteins' retardation coefficients derived from Ferguson plots of dextran sieving matrices dissolved in a high ionic strength buffer. The expected trend is that as the standards' molecular weight increases, so does the retardation coefficient accordingly. In general this trend is seen in the table except for the two middle standards of carbonic anhydrase (30 kDa) and ovalbumin (43 kDa). This indicates that in this particular buffer solution (50 mM TrisCHES, 0.1% SDS) these two proteins have similar sized radii. This finding suggests either that carbonic anhydrase's structure uncoils to have a larger radius or that ovalbumin becomes more compact and acquires a smaller radius upon exposure to this high ionic strength buffer. The other proteins are either less effected by this change or all effected identically so that the overall trend remains unchanged. This evidence indicates how the tertiary structure of the protein can change according to the environment to which it is exposed.

Table 6.2 shows the retardation coefficients of the 6 protein standards derived from Ferguson plots of dextran sieving matrices dissolved in a low ionic strength buffer. As is expected, the table shows that as molecular weight increases, so does the radius of the protein. Unlike utilization of a high ionic strength buffer, a low ionic strength buffer does not effect the conformations of the proteins or at least not enough to see a change in its properties.

As Equation 5.1 demonstrates in Section 5.3.2, if the Ferguson plot y-intercept values of the proteins are identical, this attests that the free mobilities of the proteins are identical. If the free mobilities of the proteins are identical, it is deduced that the mass-to-charge ratios of the proteins are also identical (as is the case when proteins are complexed with enough SDS) (18). Table 6.3 displays the Ferguson plot y-intercept values for separations in a high ionic strength buffer. Essentially the y-intercept values of the protein standards are identical and it can thus be said that they have identical mass-to-charge ratios. This being the case, the dextran sieving matrices are in fact separating the proteins by size otherwise the proteins would co-migrate.

The Ferguson plot y-intercept values obtained for separations of protein standards in a low ionic strength buffer are presented in Table 6.4. As can be seen by the values, the free mobilities of the proteins are essentially indistinguishable. Again this shows that the proteins share the same mass-to-charge ratios and thus are separated

Table 6.1 Retardation coefficients of 6 protein standards obtained using a high ionic strength buffer.

Protein Molecular Weight (kDa)	K_r
14.4	-0.050
20.1	-0.051
30	-0.052
43	-0.052
67	-0.057
94	-0.061

Table 6.2 Retardation coefficients of 6 protein standards obtained using a low ionic strength buffer.

Protein Molecular Weight (kDa)	K_r
14.4	-0.050
20.1	-0.053
30	-0.057
43	-0.061
67	-0.066
94	-0.072

Table 6.3 Ferguson plot y-intercept values for 6 protein standards employing a high ionic strength buffer.

Note that the standard deviation of these values is ±0.04.

Protein Molecular Weight (kDa)	Y-Intercept Value
14.4	-7.50
20.1	-7.53
30	-7.55
43	-7.58
67	-7.60
94	-7.61

Table 6.4 Ferguson plot y-intercept values for 6 protein standards employing a low ionic strength buffer.

Note that the standard deviation of these values is ±0.02.

Protein Molecular Weight (kDa)	Y-Intercept Value
14.4	-7.42
20.1	-7.42
30	-7.43
43	-7.45
67	-7.47
94	-7.46

by size with the dextran sieving matrices. If this separation were not so, the proteins would co-migrate.

6.3.3 Standardization curve construction

Different research groups have reported the construction of different types of standardization curves for dextran sieving matrices employed with SDS CGE separations of proteins. Many have reported the construction of linear curves of logarithm of molecular weight versus migration time (8, 11, 19) whereas others have reported linear curves obtained from logarithm of molecular weight versus logarithm of migration time (14). From the buffer systems utilized in these experiments, the most linear plots were obtained from logarithm of migration time versus logarithm of molecular weight. Figure 6.5 demonstrates the linear standardization curve obtained by plotting logarithm of migration time versus logarithm of molecular weight for a separation employing a 6% dextran sieving matrix and a high ionic strength buffer. The same curves were constructed for the low ionic strength buffer dextran sieving matrices.

Tables 6.5 and 6.6 show the linearity of the standardization curves by comparing the correlation coefficient values for different percentages of dextran sieving matrices for both the high and low ionic strength buffers. First examining Table 6.5, it is obvious that the lower concentrations (6% and 8%) of dextran produce more linear standardization curves with correlation coefficients of 0.9949 and 0.9960 respectively. Separations with the higher concentrations (10% and 12%) of dextran produce lower standardization curve coefficients of 0.9897 and 0.9769 respectively. Table 6.6 shows that separations obtained with all of the different concentrations of dextran sieving matrices in low ionic strength buffer produced similar correlation coefficients. The correlation coefficient of the standardization curve for the 10% dextran sieving matrix was 0.9910, for the 12% dextran sieving matrix it was 0.9927, and for the 14% dextran sieving matrix, the value was 0.9905. Again, as in Section 6.3.2, it is seen that the higher ionic strength buffer system effects the overall separation of proteins or the proteins themselves in varying ways. However, it is reaffirmed that the low ionic strength buffer system either does not effect the overall separation, or it effects the proteins each in a consistent way so that no overall effect is observed.

6.3.4 Qualitative effects of different buffer systems on the SDS CGE separations

Figures 6.6 to 6.10 display the SDS CGE separations of the 6 protein standards

Figure 6.5 Standardization curve of log of migration time versus log of molecular weight constructed from a separation utilizing a 6% dextran sieving matrix.

See Section 6.2.5 for sample preparation details and Section 6.2.7 for capillary preparation. CE conditions: 3% LPA Grignard coated capillary, 29 cm × 140 µm O.D. × 50 µm I.D., sheath flow buffer: 50 mM TrisCHES, 0.1% (w/v) SDS, pH 8.8, running buffer: 6% dextran in 50 mM TrisCHES, 0.1% (w/v) SDS, pH 8.8, prerun: 10 minutes, -350 V/cm, sample: standards diluted 50×, sample injection: 5 s, -400 V/cm, running voltage: -350 V/cm, excitation: 488 nm, emission filter: 630DF30.

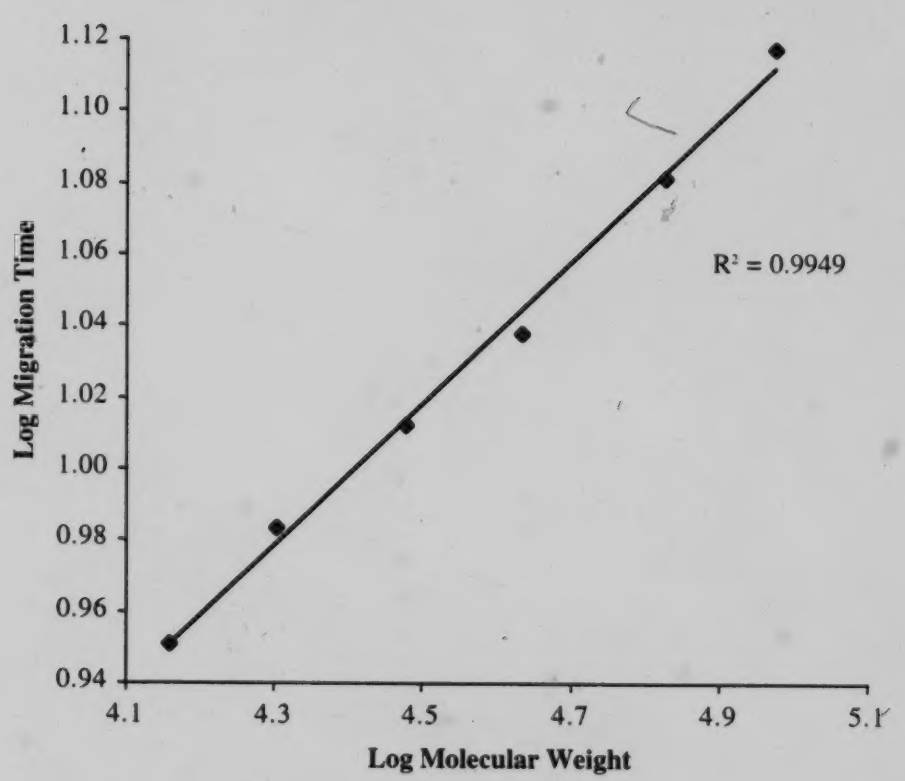

Table 6.5 Comparison of standardization curve linearity for different percentages of dextran sieving matrices in high ionic strength buffer.

% Dextran	R^2
6	0.9949
8	0.9960
10	0.9897
12	0.9769

Table 6.6 Comparison of standardization curve linearity for different percentages of dextran sieving matrices in low ionic strength buffer.

% Dextran	R^2
10	0.9910
12	0.9927
14	0.9905

accomplished with 10% dextran sieving matrices all dissolved in different buffers. Figure 6.6 shows the separation of protein standards utilizing a 10% dextran sieving matrix which is constituted in 50 mM TrisCHES, 0.1% SDS, pH 8.8. The sheath flow buffer is also of 50 mM TrisCHES, 0.1% SDS, pH 8.8, and the running buffer contains 10% dextran in buffer. As can be seen, the resolution between peaks is not baseline and the peak-widths are between 0.5-1 minute. It is also noted that some of the proteins appear as more than one peak, indicating the presence of degradation products as discussed in Section 6.3.1. The separation window for these protein standards is about 9 minutes and the total separation time is about 23 minutes.

Figure 6.7 shows the separation of protein standards with the employment of a 10% dextran sieving matrix which is dissolved in 50 mM TrisHCl, 0.1% SDS, pH 8.8. The sheath flow buffer is made of 50 mM TrisHCl, 0.1% SDS, pH 8.8, and the running buffer contains 10% dextran dissolved in this buffer. The peaks here are again not baseline resolved and the peaks are about 1-2 minutes wide, sometimes 3 minutes wide. It can be seen here that the soybean trypsin inhibitor peak and the bovine serum albumin peak also show signs of degradation products as there is one major peak for each of these as well as some smaller ones flanking the large one. This separation was only performed at -200 V/cm due to the high current which was generated utilizing higher electric fields. To decrease the risk of bubbles forming with high current, the electric field was decreased. For this reason the separation window is about 14 minutes wide, and the total time for the separation to be achieved is about 33 minutes.

The separation of protein standards with a 10% dextran sieving matrix constituted in 10 mM TrisHCl, 0.1% SDS, pH 8.8, is seen in Figure 6.8. The sheath flow buffer is made of 10 mM TrisHCl, 0.1% SDS, pH 8.8, and the running buffer contains 10% dextran dissolved in this buffer. This separation qualitatively appears much nicer than those in Figures 6.6 and 6.7. The peaks are nearly baseline separated in all cases except for the smallest two standards. The peaks are still quite wide though at 1-2 minutes. Furthermore there appears to be some tailing of the peaks which is especially pronounced for the larger molecular weight standards. This may be a result of these standards adhering to the capillary walls during the separation. There is no evidence of product degradation in this electropherogram as each protein standard appears as it should as one peak. The separation window for these standards is about 12 minutes and the time for the separation to be complete is 23 minutes.

Figure 6.9 demonstrates the separation of protein standards with a 10% dextran sieving matrix which is dissolved in a buffer of 7.5 mM TrisHCl, 0.1% SDS, pH 8.8.

Figure 6.6 Separation of standard proteins utilizing a 10% dextran sieving matrix and 50 mM TrisCHES, 0.1% SDS buffer system.

See Section 6.2.5 for sample preparation details and Section 6.2.7 for capillary preparation. Samples are labeled as: (1) α-lactalbumin (14.4 kDa), (2) soybean trypsin inhibitor (20.1 kDa), (3) carbonic anhydrase (30 kDa), (4) ovalbumin (43 kDa), (5) bovine serum albumin (67 kDa), and (6) phosphorylase b (94 kDa). CE conditions: 3% LPA Grignard coated capillary, 29 cm × 140 µm O.D. × 50 µm I.D., sheath flow buffer: 50 mM TrisCHES, 0.1% (w/v) SDS, pH 8.8, running buffer: 10% dextran in 50 mM TrisCHES, 0.1% (w/v) SDS, pH 8.8, prerun: 10 minutes, -350 V/cm, sample: standards diluted 50×, sample injection: 5 s, -400 V/cm, running voltage: -350 V/cm, excitation: 488 nm, emission filter: 630DF30.

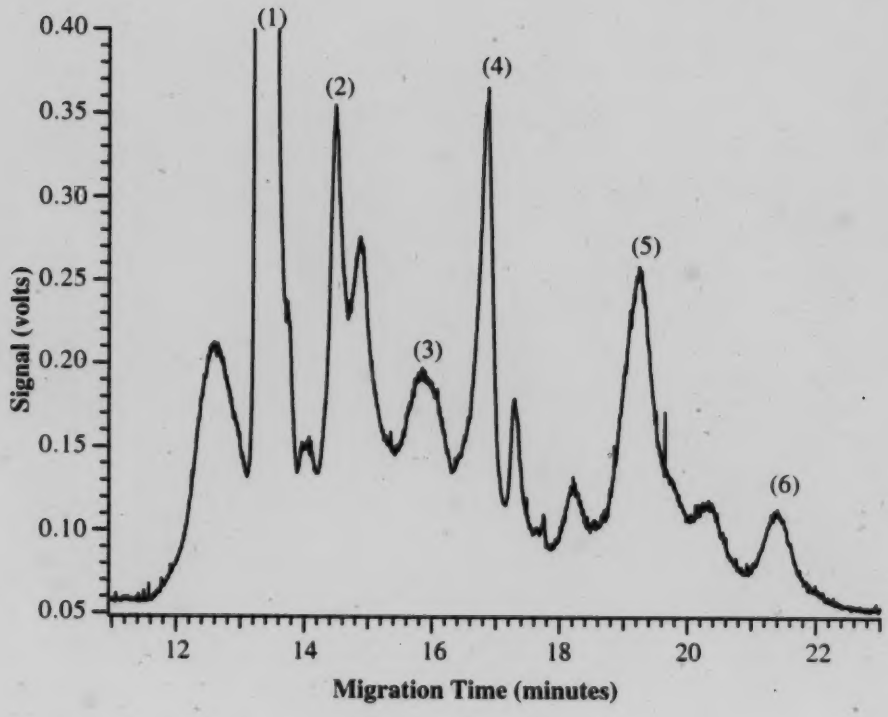

Figure 6.7 Separation of standard proteins utilizing a 10% dextran sieving matrix and 50 mM TrisHCl, 0.1% SDS buffer system.

See Section 6.2.5 for sample preparation details and Section 6.2.7 for capillary preparation. Data are median filtered every 5 points. Samples are labeled as: (1) α-lactalbumin (14.4 kDa), (2) soybean trypsin inhibitor (20.1 kDa), (3) carbonic anhydrase (30 kDa), (4) ovalbumin (43 kDa), (5) bovine serum albumin (67 kDa), and (6) phosphorylase b (94 kDa). CE conditions: 3% LPA Grignard coated capillary, 30 cm × 140 µm O.D. × 50 µm I.D., sheath flow buffer: 50 mM TrisHCl, 0.1% (w/v) SDS, pH 8.8, running buffer: 10% dextran in 50 mM TrisHCl, 0.1% (w/v) SDS, pH 8.8, prerun: 5 minutes, -200 V/cm, sample: standards diluted 50×, sample injection: 5 s, -300 V/cm, running voltage: -200 V/cm, excitation: 488 nm, emission filter: 630DF30.

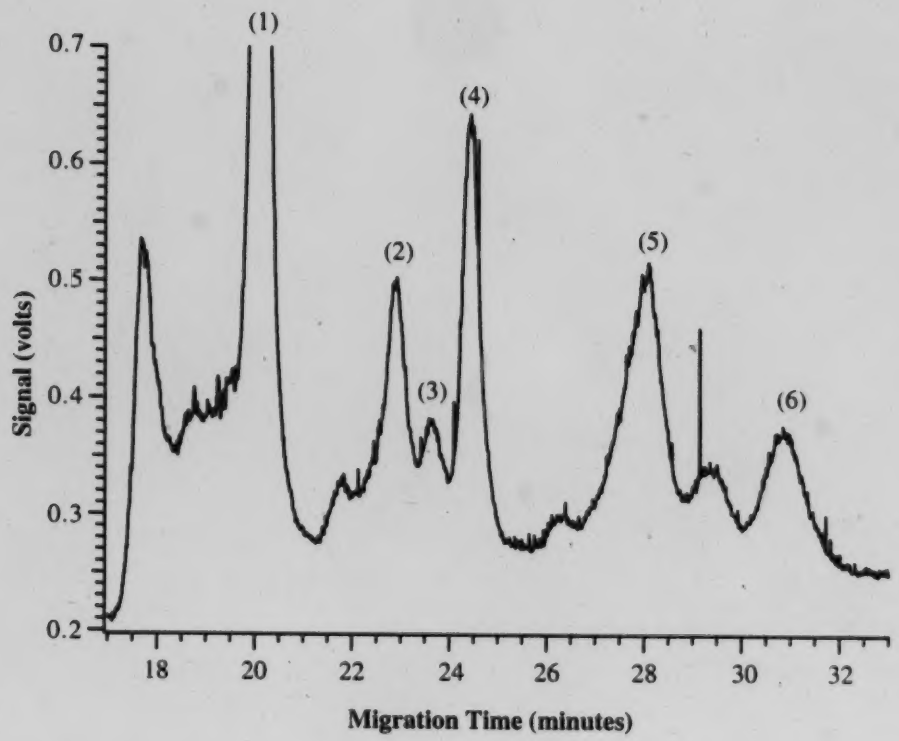

Figure 6.8 Separation of standard proteins utilizing a 10% dextran sieving matrix and 10 mM TrisHCl, 0.1% SDS buffer system.

See Section 6.2.5 for sample preparation details and Section 6.2.7 for capillary preparation. Samples are labeled as: (1) α-lactalbumin (14.4 kDa), (2) soybean trypsin inhibitor (20.1 kDa), (3) carbonic anhydrase (30 kDa), (4) ovalbumin (43 kDa), (5) bovine serum albumin (67 kDa), and (6) phosphorylase b (94 kDa). CE conditions: 3% LPA Grignard coated capillary, 30 cm × 140 μm O.D. × 50 μm I.D., sheath flow buffer: 10 mM TrisHCl, 0.1% (w/v) SDS, pH 8.8, running buffer: 10% dextran in 10 mM TrisHCl, 0.1% (w/v) SDS, pH 8.8, prerun: 10 minutes, -350 V/cm, sample: standards diluted 50×, sample injection: 8 s, -400 V/cm, running voltage: -400 V/cm, excitation: 488 nm, emission filter: 630DF30.

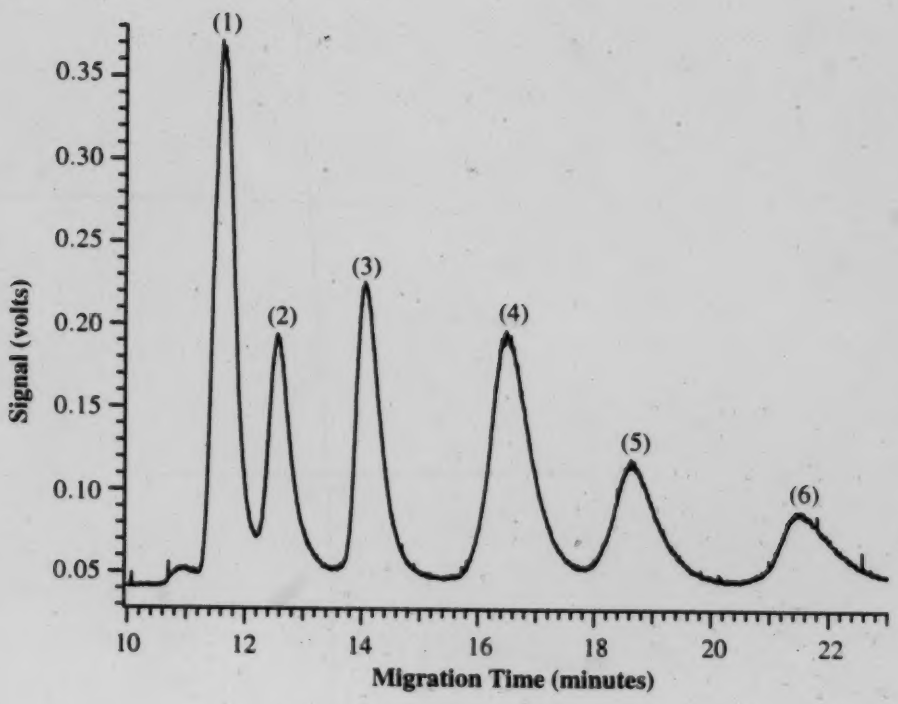

Figure 6.9 Separation of standard proteins utilizing a 10% dextran sieving matrix and 7.5 mM TrisHCl, 0.1% SDS buffer system.

See Section 6.2.5 for sample preparation details and Section 6.2.7 for capillary preparation. Data are median filtered every 5 points. Samples are labeled as: (1) α-lactalbumin (14.4 kDa), (2) soybean trypsin inhibitor (20.1 kDa), (3) carbonic anhydrase (30 kDa), (4) ovalbumin (43 kDa), (5) bovine serum albumin (67 kDa), and (6) phosphorylase b (94 kDa). CE conditions: 3% LPA Grignard coated capillary, 30 cm × 140 µm O.D. × 50 µm I.D., sheath flow buffer: 7.5 mM TrisHCl, 0.1% (w/v) SDS, pH 8.8, running buffer: 10% dextran in 7.5 mM TrisHCl, 0.1% (w/v) SDS, pH 8.8, prerun: 8 minutes, -350 V/cm, 3 minutes, -400 V/cm, sample: standards diluted 50×, sample injection: 5 s, -350 V/cm, running voltage: -350 V/cm, excitation: 488 nm, emission filter: 630DF30.

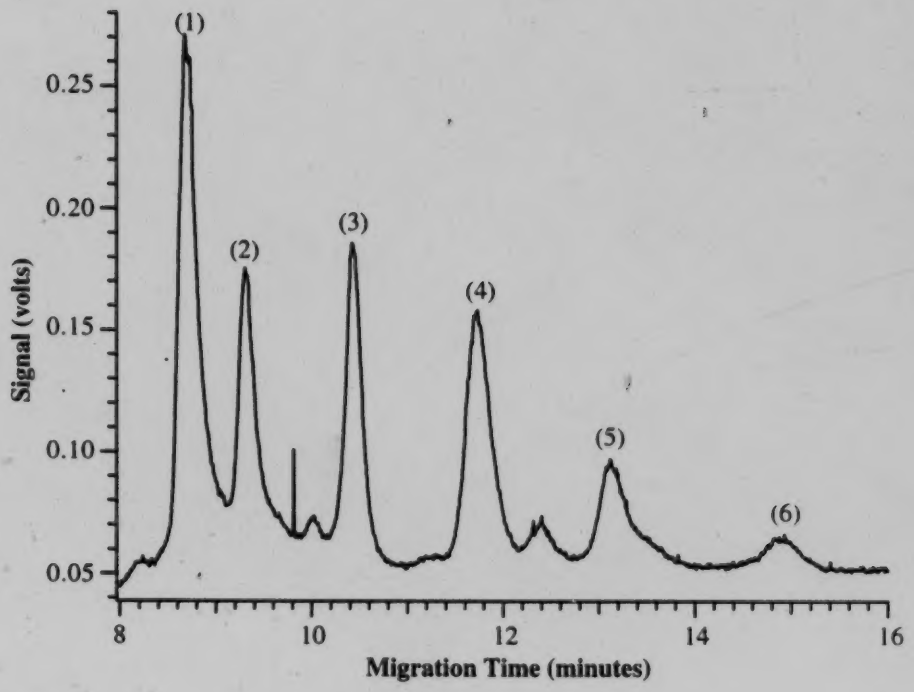

The sheath flow buffer is 7.5 mM TrisHCl, 0.1% SDS, pH 8.8, and the running buffer contains 10% dextran dissolved in this buffer. This separation, like the one in Figure 6.8, appears much nicer than those with the higher ionic strength buffers in Figures 6.6. and 6.7. There is nearly baseline resolution between all of the protein standards, the exception again being with the smallest protein standards. The peaks are much less than one minute wide and appear to be only slightly tailed. This tailing is again much more noticeable with the larger molecular weight standards. This tailing and the fact that the last two standards have such low signals may be attributed to these two protein standards adhering to the capillary wall. However the low signal may also be due to diffusion that these proteins experience as they travel through the capillary. The separation window produced is about 8 minutes wide and the total separation time is rapid at just under 16 minutes.

The separation of protein standards accomplished utilizing a 10% dextran sieving matrix in a buffer of 5 mM TrisHCl, 0.1% SDS, pH 8.8, is seen in Figure 6.10. The sheath flow buffer is 5 mM TrisHCl, 0.1% SDS, pH 8.8, and the running buffer contains 10% dextran dissolved in this buffer. The proteins again are nearly baseline resolved except for the smallest two protein standards. The first three protein peaks are slightly less than one minute wide while the largest three proteins have peak-widths of at least one minute. The two largest proteins, bovine serum albumin and phosphorylase b, produce very low signal and are slightly tailed. Again these two proteins may be adhering to the capillary wall or simply experiencing more diffusion than the other proteins during the separation. The separation window for this system is about 9 minutes wide while the total separation time is about 19 minutes.

These experiments with different buffer compositions indicate that the separations are more successful with lower ionic strength buffers. Utilizing a lower ionic strength buffer allows larger electric fields to be applied for separation. This results in a decrease in separation time and thus resolution is usually better as the proteins experience less diffusion inside the capillary. Furthermore there is evidence of fewer protein degradation products when lower ionic strength buffers are employed. This indicates that lower ionic strength buffers effect the protein conformation less than higher ionic strength buffers.

6.3.5 Migration time for replicate runs

A plot of same-day migration time differences for replicate runs with a 10% dextran sieving matrix in 5 mM TrisHCl, 0.1% SDS, pH 8.8 is shown in Figure 6.11.

Figure 6.10 Separation of standard proteins utilizing a 10% dextran sieving matrix and 5 mM TrisHCl, 0.1% SDS buffer system.

See Section 6.2.5 for sample preparation details and Section 6.2.7 for capillary preparation. Data are median filtered every 5 points. Samples are labeled as: (1) α-lactalbumin (14.4 kDa), (2) soybean trypsin inhibitor (20.1 kDa), (3) carbonic anhydrase (30 kDa), (4) ovalbumin (43 kDa), (5) bovine serum albumin (67 kDa), and (6) phosphorylase b (94 kDa). CE conditions: 3% LPA Grignard coated capillary, 30 cm × 140 µm O.D. × 50 µm I.D., sheath flow buffer: 5 mM TrisHCl, 0.1% (w/v) SDS, pH 8.8, running buffer: 10% dextran in 5 mM TrisHCl, 0.1% (w/v) SDS, pH 8.8, prerun: 4 minutes, -350 V/cm, 4 minutes, -400 V/cm, sample: standards diluted 50×, sample injection: 5 s, -400 V/cm, running voltage: -400 V/cm, excitation: 488 nm, emission filter: 630DF30.

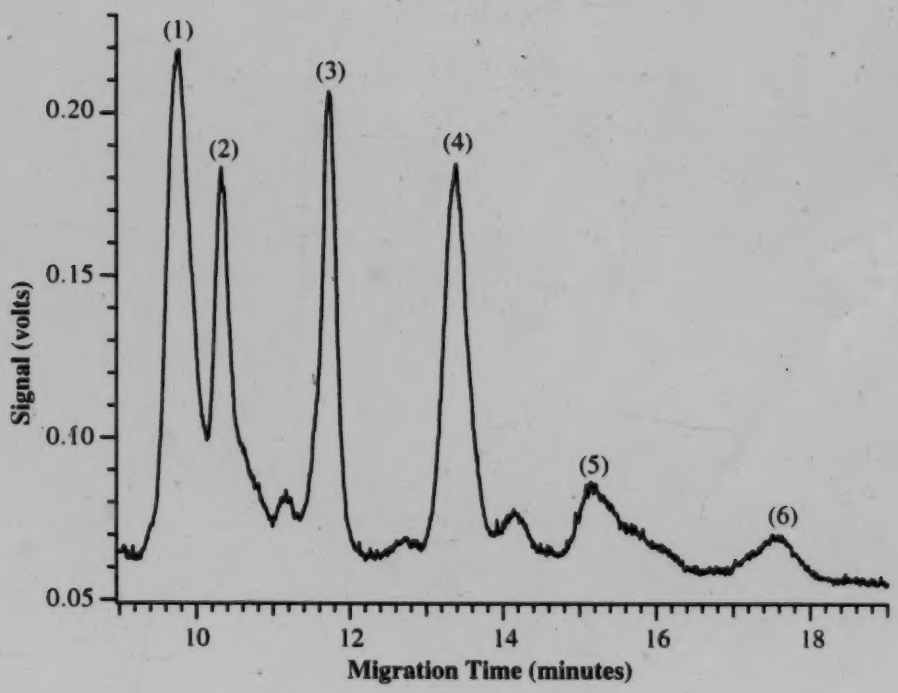

Figure 6.11 Migration time of replicate runs utilizing a 10% dextran sieving matrix with a 5 mM TrisHCl, 0.1% SDS, pH 8.8, buffer.

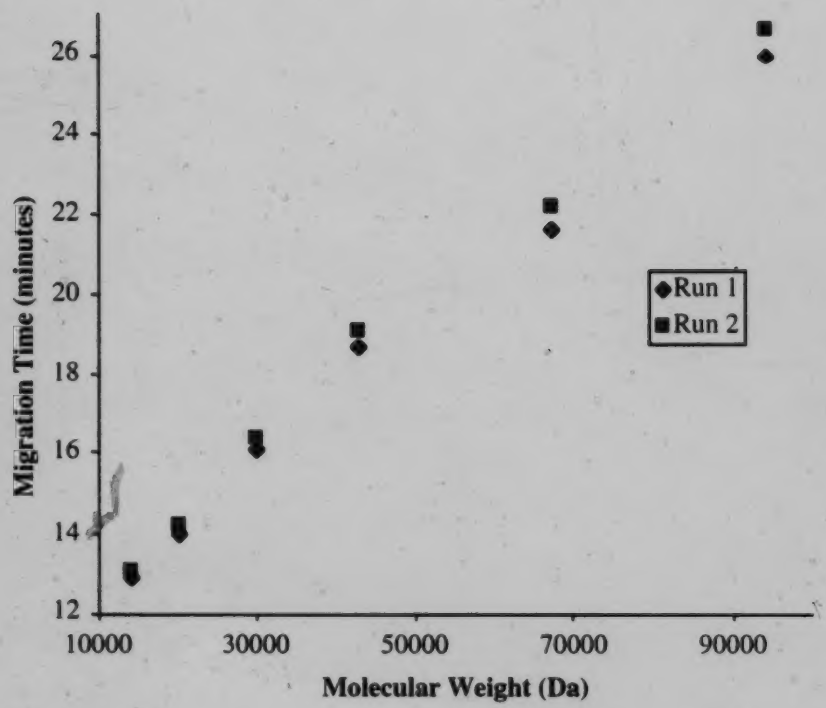

The differences between two runs on the same day for any given protein standard are seldom more than 0.5 minutes. The use of internal standards would alleviate these migration time variations. Table 6.7 shows the same-day average migration times for each of the standard proteins and their corresponding standard deviations. The table shows that as the molecular weight of the standard increases, so does the standard deviation in migration time. The standard deviations are equal to between 1.5-2% of the average migration times for any given protein standard. These values are considered reasonable. If this technique was utilized to estimate the molecular weight of an unknown protein, it is acceptable for the weight to be within 10% of the actual weight. The table indicates that the separation conditions detailed in the table will give acceptable molecular weight estimates of unknown proteins.

Figure 6.12 shows a graph of same-day migration time variation for replicate runs with a 12% dextran sieving matrix in 5 mM TrisHCl, 0.1% SDS, pH 8.8. There is slightly more variation in migration times of replicate runs for this 12% sieving matrix than with the 10% matrix. Here the migration times differ for any protein standard between 2.5-6 minutes. Table 6.8 displays the average migration times and their standard deviations for each of the 6 protein standards. Again as with the 10% sieving matrix, as the molecular weight of the protein increases, so does the standard deviation of its migration time. It is seen that the standard deviations are substantially larger with this sieving matrix than with the 10% sieving matrix. The standard deviations here correspond to between 8% and 11% of the average migration times. Again these values are considered acceptable when estimating the molecular weight of an unknown protein.

The plot of same-day migration time variation for replicate runs with a 14% dextran sieving matrix in 5 mM TrisHCl, 0.1% SDS, pH 8.8, is shown in Figure 6.13. As is noted, the analysis is only performed for 5 of the 6 protein standards as the phosphorylase b data were difficult to analyze. Here the protein standard migration times vary from run-to-run anywhere between 1-4 minutes. The larger differences are again seen with the later-migrating proteins. Table 6.9 shows the average migration times of 5 standard proteins and their corresponding standard deviations. As with the other two sieving matrices, there is an increasing trend in standard deviations with increasing molecular weight. The standard deviations correspond to between 4% and 10% of the migration time values. This shows that this sieving matrix would be suitable to employ to estimate the molecular weight of an unknown protein as it would predict its molecular weight within the acceptable 10% value.

Table 6.7 Average migration times for the 6 protein standards run on the same day utilizing a 10% dextran sieving matrix with a 5 mM TrisHCl, 0.1% SDS, pH 8.8, buffer and an electric field of -400 V/cm.

Protein	Average Migration Time (minutes) (n=2)
α-lactalbumin	13.0±0.2
soybean trypsin inhibitor	14.1±0.2
carbonic anhydrase	16.2±0.2
ovalbumin	18.9±0.3
bovine serum albumin	21.9±0.4
phosphorylase b	26.3±0.5

Figure 6.12 Migration time of replicate runs utilizing a 12% dextran sieving matrix with a 5 mM TrisHCl, 0.1% SDS, pH 8.8, buffer.

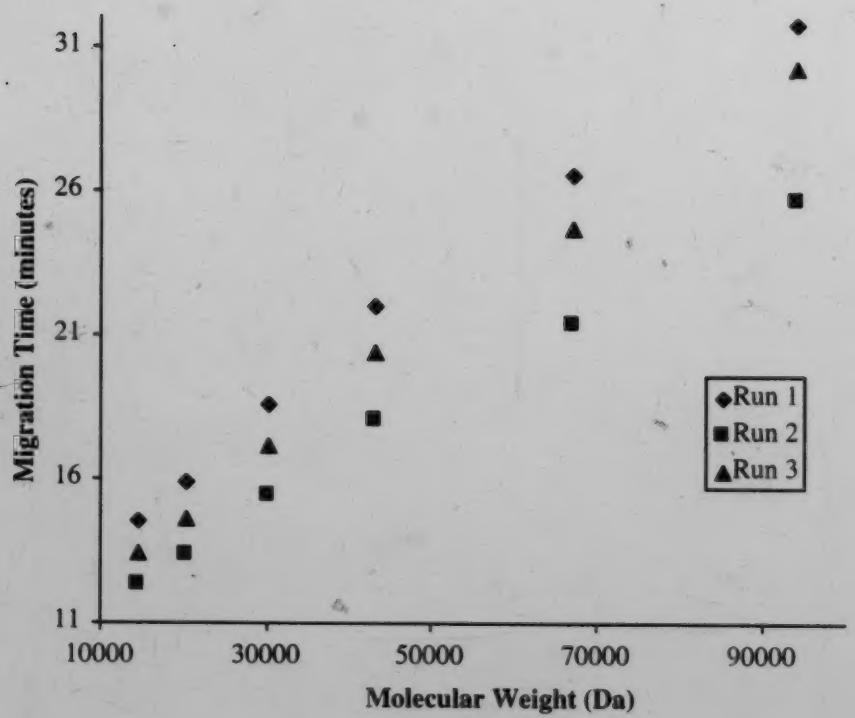

Table 6.8 Average migration times for the 6 protein standards run on the same day utilizing a 12% dextran sieving matrix with a 5 mM TrisHCl, 0.1% SDS, pH 8.8, buffer and an electric field of -400 V/cm.

Protein	Average Migration Time (minutes) (n=3)
α-lactalbumin	13.5±1.1
soybean trypsin inhibitor	14.6±1.3
carbonic anhydrase	17.1±1.6
ovalbumin	20.2±2.0
bovine serum albumin	24.2±2.6
phosphorylase b	29.2±3.2

Figure 6.13 Migration time of replicate runs utilizing a 14% dextran sieving matrix with a 5 mM TrisHCl, 0.1% SDS, pH 8.8, buffer.

Note that data for the phosphorylase b were exluded as these peaks were difficult to analyze.

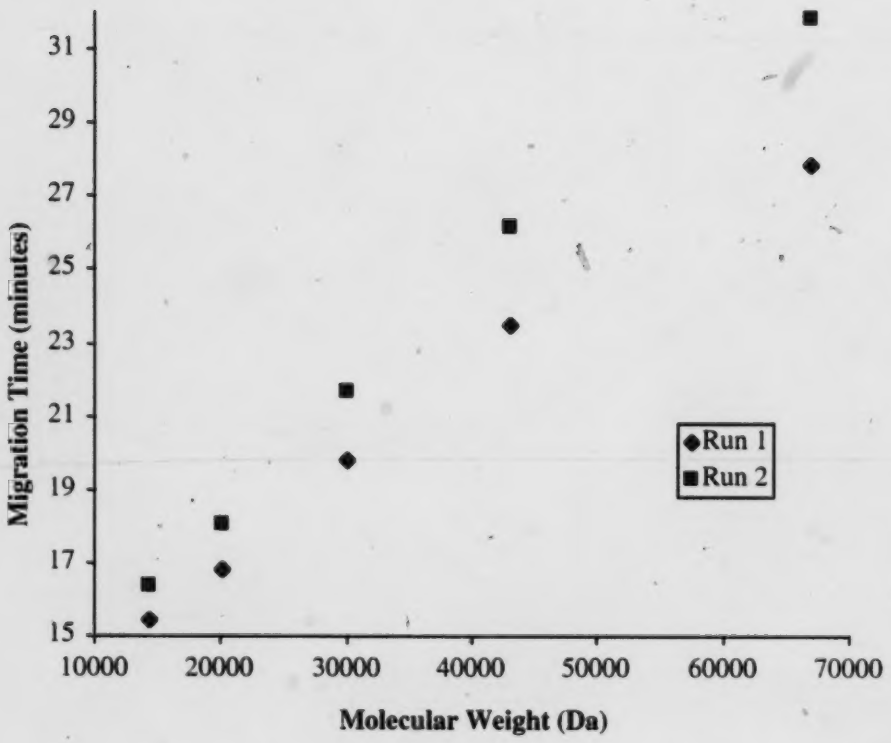

Table 6.9 Average migration times for the 5 protein standards run on the same day utilizing a 14% dextran sieving matrix with a 5 mM TrisHCl, 0.1% SDS, pH 8.8, buffer and an electric field of -400 V/cm.

Note that data for the phosphorylase b were exluded as these peaks were difficult to analyze.

Protein	Average Migration Time (minutes) (n=2)
α-lactalbumin	15.9±0.7
soybean trypsin inhibitor	17.5±0.9
carbonic anhydrase	20.7±1.3
ovalbumin	24.8±1.9
bovine serum albumin	29.8±2.8

6.3.6 Day-to-day migration time variability

A plot of variation in migration times of the 6 protein standards separated employing a 10% dextran sieving matrix in 5 mM TrisHCl, 0.1% SDS, pH 8.8, is shown in Figure 6.14. Day-to-day the fluctuation in migration time for any given standard is between 4 and 10 minutes. Again the largest deviations in migration times are observed with the largest protein standards. Table 6.10 shows the average migration times of the 6 standard proteins and their respective standard deviations. As with the trend seen with the same-day migration time variability study in Section 6.3.5, it is noted that the standard deviations increase with increasing molecular weight. The standard deviations in migration time represent between 13% and 17% of the overall migration time. This variability indicates that if this 10% dextran sieving matrix were to be utilized to predict molecular weights of unknown proteins, a suitable internal standard would have to be found for the system.

6.3.7 Application of a dextran sieving matrix to the SDS CGE separation of water-soluble A549 cell extract proteins

Figure 6.15 displays the electropherogram of a SDS CGE separation of water-soluble A549 proteins employing a 12% dextran sieving matrix. Qualitatively it is noted that the resolving power of this dextran sieving matrix is not very acceptable for such a complex mixture of proteins. However there is some degree of separation for the initial few peaks. After about 20 minutes into the run the migration of sample out of the capillary appears as only a plateau with no peak differentiation whatsoever. This sieving matrix shows some promise for the resolution of complex sample mixtures, however it was thought to be more productive to apply this dextran sieving matrix to the separation of a simpler sample.

6.3.8 Application of a dextran sieving matrix to the SDS CGE separation of A549 nuclear proteins

Figure 6.16 demonstrates the SDS CGE separation of A549 nuclear proteins utilizing a 10% dextran sieving matrix. Portion A of the figure shows the overall separation, portion B is a close-up of the huge plateau which occurs beginning at about 20 minutes, and portion C is a zoom-in of the smaller peaks which appear after the plateau seen in portion B. Samples for this separation were microconcentrated as discussed in Section 6.2.4 with a two-fold purpose: the first purpose was to

Figure 6.14 Day-to-day variation in migration times employing a 10% dextran sieving matrix with a 5 mM TrisHCl, 0.1% SDS, pH 8.8, buffer.

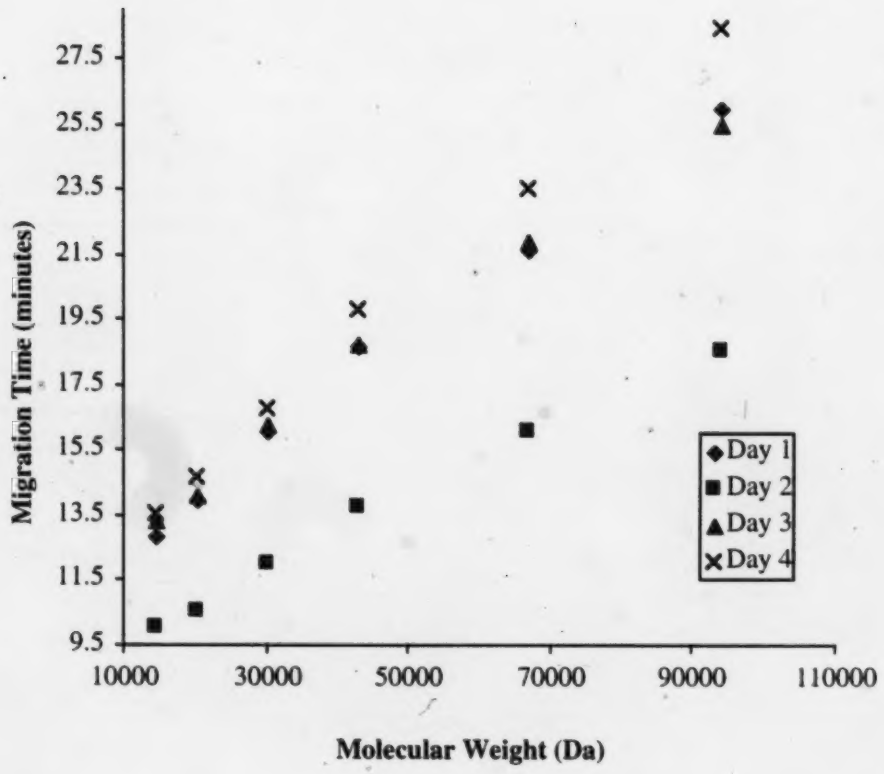

Table 6.10 Average migration times for the 6 protein standards run on different days utilizing a 10% dextran sieving matrix with a 5 mM TrisHCl, 0.1% SDS, pH 8.8, buffer and an electric field of -400 V/cm.

Protein	Average Migration Time (minutes) (n=4)
α-lactalbumin	12.5±1.6
soybean trypsin inhibitor	13.3±1.9
carbonic anhydrase	15.3±2.2
ovalbumin	17.8±2.7
bovine serum albumin	20.8±3.3
phophorylase b	24.6±4.2

Figure 6.15 SDS CGE separation of A549 water-soluble proteins employing a 12% dextran sieving matrix.

See Sections 6.2.3 and 6.2.6 for sample preparation details and Section 6.2.7 for capillary preparation. Data are median filtered every 5 points. CE conditions: 3% LPA Grignard coated capillary, 30 cm × 140 µm O.D. × 50 µm I.D., sheath flow buffer: 10 mM TrisHCl, 0.1% (w/v) SDS, pH 8.8, running buffer: 12% dextran in 10 mM TrisHCl, 0.1% (w/v) SDS, pH 8.8, prerun: 8 minutes, -350 V/cm, 2 minutes, -400 V/cm, sample injection: 8 s, -400 V/cm, running voltage: -400 V/cm, excitation: 488 nm, emission filter: 630DF30.

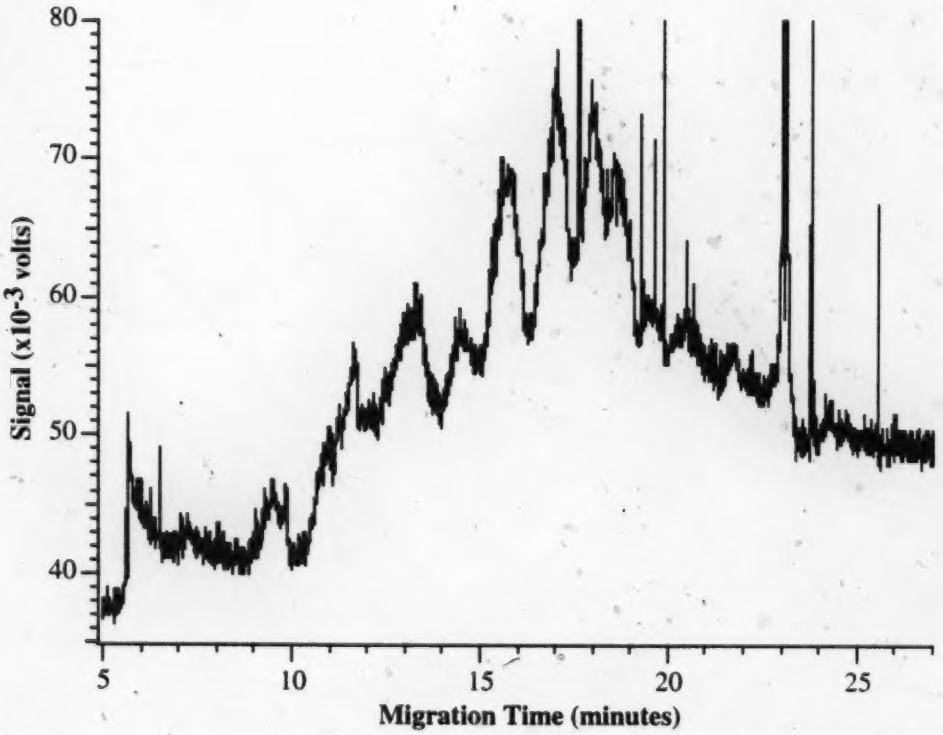

Figure 6.16 SDS CGE separation of A549 nuclear proteins employing a 10% dextran sieving matrix.

See Sections 6.2.3, 6.2.4, and 6.2.6 for sample preparation details and Section 6.2.7 for capillary preparation. Portions are: (A) overall separation, (B) close-up of plateau, and (C) close-up of 23-33 minutes. CE conditions: 3% LPA Grignard coated capillary, 30 cm × 140 µm O.D. × 50 µm I.D., sheath flow buffer: 50 mM TrisHCl, 0.1% (w/v) SDS, pH 8.8, running buffer: 10% dextran in 50 mM TrisHCl, 0.1% (w/v) SDS, pH 8.8, prerun: 5 minutes, -200 V/cm, sample injection: 10 s, -300 V/cm, running voltage: -200 V/cm, excitation: 488 nm, emission filter: 630DF30.

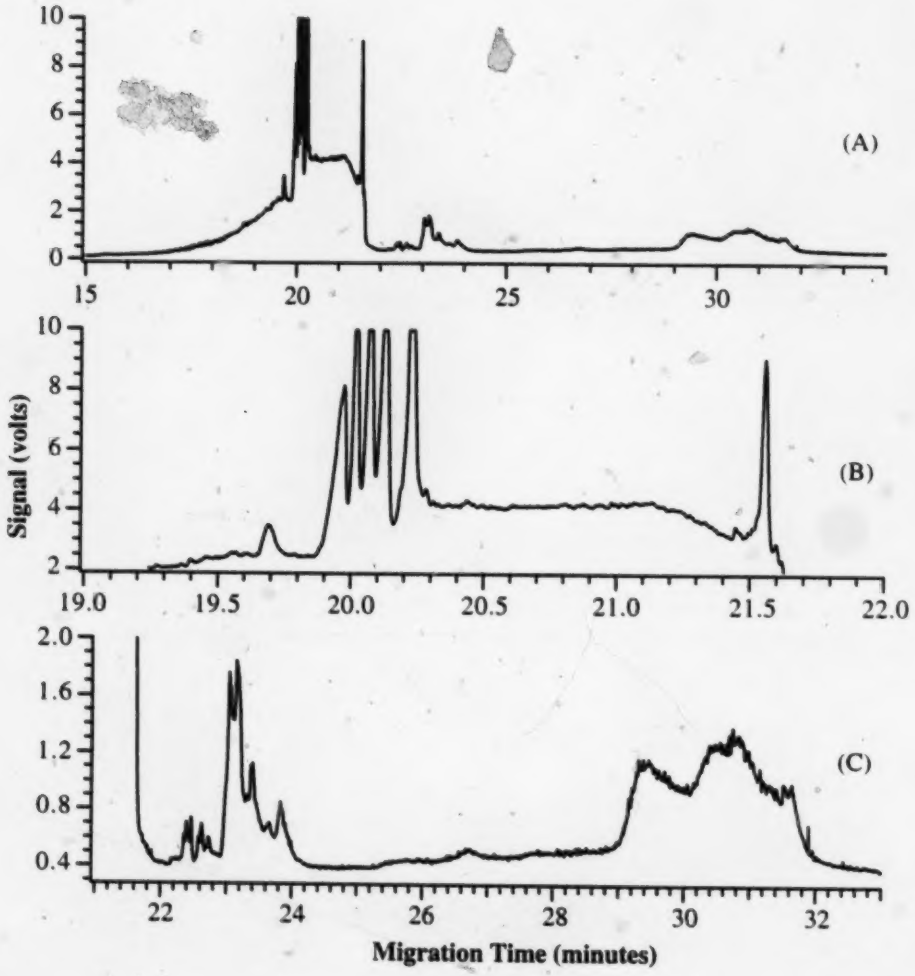

concentrate the protein samples for labeling and detection, and the second reason was to filter out the small nuclear extraction buffer component which was also labeled with FQ (as discussed in Section 5.3.5). As can be seen, there are a number of small molecular weight components in the sample which co-migrate through the capillary. Portion B shows that there are some resolved components in this low molecular weight region, however they are only resolved to the plateau, not to the baseline. Portion C displays a small cluster of medium molecular weight components and some high molecular weight proteins which appear as a large unresolved mass. This 10% dextran sieving matrix shows some promise for the separations of A549 nuclear proteins.

A 1 in 30 dilution of the nuclear protein sample from Figure 6.16 was SDS CGE separated with a 10% dextran sieving matrix and is seen in Figure 6.17. Portion A is an overview of the entire separation and portion B is a close-up of the smaller peaks seen in the separation. Again there are a large number of small molecular sample components which co-migrate and remain unresolved by the 10% dextran sieving matrix. However there are also a large number of small to medium molecular weight proteins which are resolved, albeit not to baseline. There are also some high molecular weight components which appear as wide peaks. The nuclear protein samples were diluted in a 0.1% SDS-containing buffer as it was unclear as to whether or not there was enough SDS in the original buffer to properly complex all of the protein components in the sample. If all of the proteins were not complexed with SDS, they would not have an overall negative charge, and thus would not necessarily migrate to the detector at the cathode end of the instrument. Figure 6.17 shows that this dextran sieving matrix has the potential to separate slightly more complicated samples than standard proteins. However, future work is needed to increase the resolving power of this dextran sieving matrix.

6.4 Conclusion

This chapter illustrates the employment of dextran as a sieving matrix for SDS CGE size-based separations of both standard proteins and complex protein mixtures. Standard proteins were separated by a range of different dextran sieving matrices. These separations were proven to be based on size through the construction of Ferguson plots. Standardization curves for standard proteins demonstrated linear dependence of logarithm of migration time on logarithm of molecular weight. The effects of different buffer compositions on the separations were examined briefly. Migration time variability both on a same-day and day-to-day basis was examined.

Figure 6.17 SDS CGE separation of A549 nuclear proteins employing a 10% dextran sieving matrix.

This sample is a 1 in 30 dilution of the sample seen in Figure 6.16. See Sections 6.2.3, 6.2.4, and 6.2.6 for sample preparation details and Section 6.2.7 for capillary preparation. Data are median filtered every 5 points. Portions are labeled as: (A) entire separation, and (B) close-up of 17-28 minutes. CE conditions: 3% LPA Grignard coated capillary, 30 cm × 140 µm O.D. × 50 µm I.D., sheath flow buffer: 50 mM TrisHCl, 0.1% (w/v) SDS, pH 8.8, running buffer: 10% dextran in 50 mM TrisHCl, 0.1% (w/v) SDS, pH 8.8, prerun: 5 minutes, -200 V/cm, sample injection: 10 s, -300 V/cm, running voltage: -200 V/cm, excitation: 488 nm, emission filter: 630DF30.

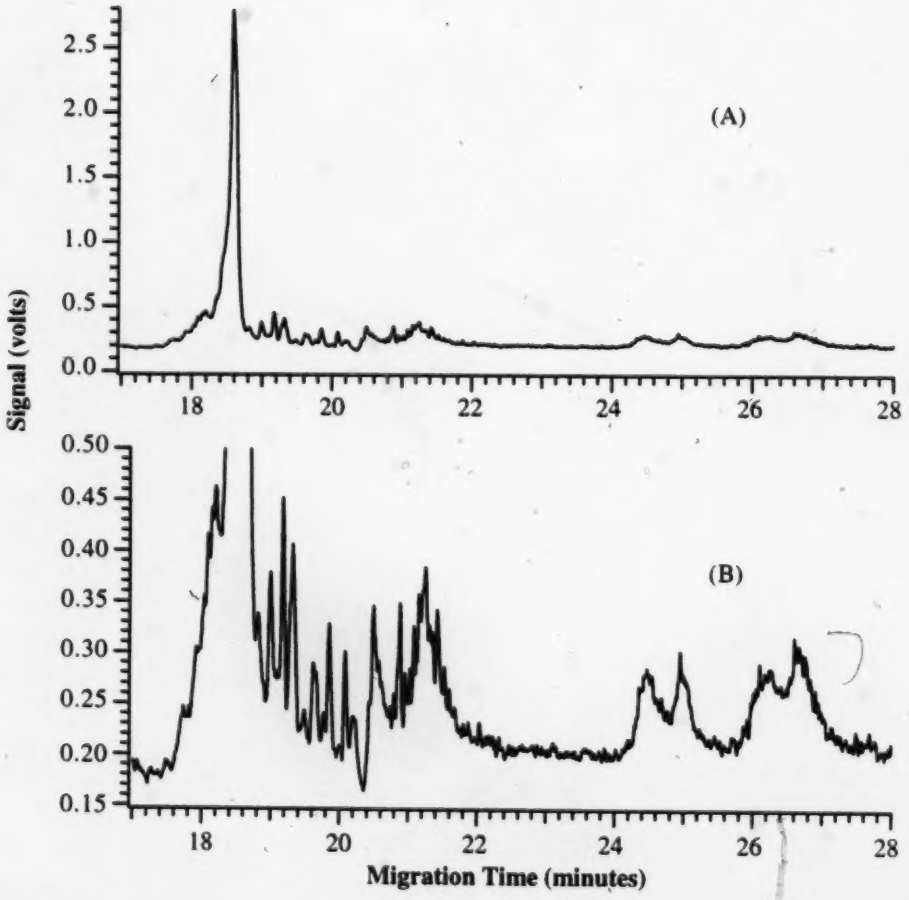

Utilizing a suitable internal standard for this dextran separation system would be the optimum solution to migration time variation. SDS CGE size-based separations of both water-soluble proteins of A549 cells and A549 nuclear proteins prove to be promising although future work is necessary to optimize separation conditions.

6.5 References

(1) Hjertén, S.; Kubo, K. *Electrophoresis* **1993,** *14*, 390-395.

(2) Mechref, Y.; El Rassi, Z. *Electrophoresis* **1995,** *16*, 617-624.

(3) Radko, S. P.; Sokoloff, A. V.; Garner, M. M.; Chrambach, A. *Electrophoresis* **1995,** *16*, 981-982.

(4) Nishi, H.; Terabe, S. *Journal of Chromatographic Science* **1995,** *33*, 698-703.

(5) Nishi, H. *Journal of Chromatography A* **1996,** *735*, 345-351.

(6) Barmé, I.; Bruin, G. J. M.; Paulus, A.; Ehrat, M. *Electrophoresis* **1998,** *19*, 1445-1451.

(7) Ganzler, K.; Greve, K. S.; Cohen, A. S.; Karger, B. L.; Guttman, A.; Cooke, N. C. *Analytical Chemistry* **1992,** *64*, 2665-2671.

(8) Lausch, R.; Scheper, T.; Reif, O.-W.; Schlösser, J.; Fleischer, J.; Freitag, R. *Journal of Chromatography A* **1993,** *654*, 190-195.

(9) Wu, D.; Regnier, F. E. *Journal of Chromatography* **1992,** *608*, 349-356.

(10) Karim, M. R.; Janson, J.-C.; Takagi, T. *Electrophoresis* **1994,** *15*, 1531-1534.

(11) Zhang, Y.; Lee, H. K.; Li, S. F. Y. *Journal of Chromatography A* **1996,** *744*, 249-257.

(12) Guttman, A.; Horvath, J.; Cooke, N. *Analytical Chemistry* **1993,** *65*, 199-203.

(13) Takagi, T.; Karim, M. R. *Electrophoresis* **1995,** *16*, 1463-1467.

(14) Craig, D. B.; Polakowski, R. M.; Arriaga, E.; Wong, J. C. Y.; Ahmadzadeh, H.; Stathakis, C.; Dovichi, N. J. *Electrophoresis* **1998,** *19*, 2175-2178.

(15) Zhang, Z.; Krylov, S.; Arriaga, E. A.; Polakowski, R.; Dovichi, N. J. *Analytical Chemistry* **2000,** *72*, 318-322.

(16) Ramsby, M. L.; Makowski, G. S. In *2-D Proteome Analysis Protocols*; Link, A. J., Ed.; Humana Press, Inc.: Totowa, 1999, pp 53-85.

(17) Simo-Alfonso, E.; Conti, M.; Gelfi, C.; Righetti, P. G. *Journal of Chromatography A* **1995,** *689*, 85-96.

(18) Werner, W. E.; Demorest, D. M.; Wiktorowicz, J. E. *Electrophoresis* **1993,** *14*, 759-763.

(19) Reif, O.-W.; Freitag, R. *Journal of Chromatography A* **1994,** *680*, 383-394.

Chapter 7
Observation and Identification of Irradiation-Induced Nuclear Protein Changes From Human Lung Cancer Cells

7.1 Introduction

One approach to proteomics is differential display to complement genomics (1). The rationale behind such an approach is to observe phenotypic differences between treatments, for example the differences between cancerous tissue versus normal tissue (2). This subtractive method carries out further analysis on proteins whose levels are altered between control and experimental conditions (3). This methodology allows for quick identification of differences between the two samples and for a focus on discovering the nature of these differences (2). It is worth noting that a change in modification of a protein or a protein's absence is just as telling as the appearance of an altogether new protein (2). When a small number of gels are being analyzed, simply comparing the gel patterns for differences by eye is sufficient (4); however as the number of proteins and gels being studied increases, it is necessary to utilize specialized software for comparative analysis (4). A number of computer programs have been developed for this purpose (5-11).

In 2-D electrophoresis, sample fractionation is a useful tool to study both the composition and properties of purified cellular components (12). Knowing the original cellular location of a protein aids in narrowing the range of functions of a protein and thus helps in later identification (13). Furthermore, fractionation enables the visualization of more of a cell's proteins by partitioning a complex cell lysate into smaller compartments for individual analysis (14). The 2-D gels of the cell's fractions can then be pieced back together to gain a more global view of protein expression within the cell. Low abundance proteins in a 2-D gel of a cell lysate are surely to be lost. For proteins, there is no comparable amplification method to that of PCR for DNA amplification. Instead, amplification of proteins must be achieved by an enrichment process (2, 13). One such enrichment process is subcellular fractionation in which proteins are differentially extracted on the basis of different properties (2), for example solubility (15, 16), organelle location (17), or physical characteristics (18).

Differential display proteomics is a strategy which can be utilized to discover how cells are affected by radiation treatment in cancer patients. Ionizing radiation with γ-rays is widely utilized in cancer treatment. Radiation therapy results in damage to both healthy and diseased cells, however the healthy cells are capable of repairing faster and more completely than the diseased cells. Cells are composed mainly of water. When photons of a γ-ray interact with water molecules in cells, the water molecules may be ionized. This ionization results in the formation of short-lived ion radicals which

quickly decay into free radicals. These highly reactive free radicals are capable of diffusing short distances in order to reach critical targets in the cell. Usually it is a hydroxyl radical which produces damage to the cell's DNA. This damage results in the induction of a series of genes involved in the DNA repair process (19). The dose of radiation given is a large factor in how the cells respond and what changes occur in the cell after irradiation (20).

Irradiation leads to many different effects manifested by the cell. The main effect of irradiation on the cells is with regards to their reproductive capabilities rather than their functionality capabilities (21, 22). The presence of mitotic cells and cell division is delayed by radiation and is dependent on cell type, dose, and physiological conditions of the cells (21). Upon irradiation, some cells undergo sufficient modifications to prove fatal (22), however after the division delay the survivors will continue to divide indefinitely (21). The normal growth process of cells is also affected by irradiation. Although some cells are fatally damaged by radiation, they may still be capable of producing large amounts of DNA, RNA, protein, and other cell components for a period of time (21).

This chapter illustrates the results of dose-response studies of human lung cancer (A549) cell nuclear proteins. Cells were subjected to γ-irradiation in doses of 2, 5, or 10 Gray from a ^{60}Co γ-source and incubated from 0 to 24 hours. Nuclear proteins were extracted using differential detergent fractionation, quantitated, and then separated using both SDS-PAGE and 2-D gel electrophoresis. Differential display techniques were utilized and showed two visible differences irregardless of irradiation level: a high molecular weight protein repressed by irradiation and a low molecular weight protein induced by irradiation. These two protein bands were removed from the gels, subjected to tryptic digestion, the extracted peptides were analyzed by MALDI TOF MS, and the resulting information was used for protein identification via an internet database (SwissProt). From the low molecular protein of interest, potential identification information resulted. When further analyzed by tandem MS, the protein's identity was confirmed utilizing a the Mascot internet database.

7.2 Experimental

7.2.1 Materials and reagents

GibcoBRL (Grand Island, NY) provided the Dulbecco's Modified Eagle Medium, fetal bovine serum, penicillin, streptomycin, and tryspin-EDTA.

Tris[hydroxymethyl]aminomethane (Trizma base), piperazine-*N,N'*-bis(2-ethanesulfonic acid) (PIPES), phenylmethylsulfonyl fluoride (PMSF), t-octylphenoxypolyethoxyethanol (Triton X-100), polyoxyethylenesorbitan monopalmitate (Tween-40), mineral oil, deoxycholic acid (DOC), trypsin, α-cyano-4-hydroxycinnamic acid (4-HCCA), and formaldehyde (37%) were all obtained from Sigma (St. Louis, MO). Sucrose, sodium chloride (NaCl), magnesium chloride hexahydrate ($MgCl_2 \cdot 6H_2O$), ethylenediaminetetra-acetic acid sodium salt (EDTA), potassium chloride (KCl), and acetonitrile were purchased from BDH (Vancouver, Canada). Fluka (Oakville, Canada) supplied the digitonin. The ammonium bicarbonate was purchased from Mallinckrodt (Paris, KY). From Fisher (Fair Lawn, NJ) the following was purchased: sodium phosphate, dibasic (Na_2HPO_4), sodium phosphate, monobasic ($NaH_2PO_4 \cdot H_2O$), potassium phosphate, monobasic (KH_2PO_4), and T_{25} flasks. Caledon (Georgetown, Canada) provided the sodium dodecyl sulfate (SDS) and methanol. From Aldrich (Milwaukee, WI) the following was obtained: β-mercaptoethanol, bromophenol blue, and iodoacetamide. Bio-Rad (Hercules, CA) supplied the ammonium persulfate (APS), *N,N,N',N'*- tetramethylethylenediamine (TEMED), 10X TGS buffer, and the Silver Stain Plus Kit. The glacial acetic acid, concentrated hydrochloric acid (HCl), calcium chloride, and sodium thiosulfate pentahydrate ($Na_2S_2O_3 \cdot 5H_2O$) were from Anachemia (Montreal, Canada). The FMC Bioproducts Prosieve® Protein Markers were purchased from Mandel Scientific (Guelph, Canada). Glycerol and silver nitrate ($AgNO_3$) were acquired from ACP (Montreal, Canada). From ICN Biomedicals (Aurora, OH) dithiothreitol (DTT) and urea were purchased. Millipore (Bedford, MA) supplied the Microcon YM-10 centrifugal device filters. From Pharmacia (Quebec, Canada) the following was obtained: 2% (w/v) methylene bisacrylamide, 40% (w/v) acrylamide IEF, IPG Buffer (pH 3-10 L), and Immobiline™ DryStrip, pH 3-10, 7 cm strips. The Coomassie® Protein Plus Assay and the bovine gamma globulin were from Pierce (Rockford, IL).

7.2.2 Cell culture

The A549 (human lung cancer) cell line was cultured in T_{25} flasks in an incubator at 37°C in a 5% CO_2 atmosphere. The cells were grown to 80% confluence in Dulbecco's Modified Eagle Medium/F12, supplemented with 10% fetal bovine serum and 50 mg/mL penicillin/streptomycin.

7.2.3 γ-Irradiation of cells

Two T_{25} flasks were irradiated and worked up simultaneously. The flasks were removed from the incubator and the media was removed from the cells. The cells were rinsed of media with two portions of 5 mL cold PBS (phosphate-buffered saline). The flasks were irradiated with a γ-^{60}Co source (Atomic Energy, Canada) with doses of either 2 Gy, 5 Gy, or 10 Gy. To each of the flasks, 10 mL of media was added and the flasks were placed back into the incubator until extraction procedures were carried out. There were two controls for the irradiation experiments. One control flask was treated the same as the others except this flask was not irradiated and is referred to as "control." The irradiation control was irradiated, however immediately following irradiation, instead of media being placed back into the flasks and the flasks put back into the incubator, the first extraction buffer was put on the cells and fractionation was initiated. This control is referred to as "T_0" because the cells were not allowed any time to recover following irradiation. The rest of the cells were incubated and allowed to recover for time intervals between 2-24 hours.

7.2.4 Cell fractionation

The cell fractionation method is described in Section 6.2.3.

7.2.5 Protein quantitation

The protein content of the nuclear extracts was quantitated utilizing the Coomassie® Plus Protein Assay kit. All tubes were siliconized (Fisher, Fair Lawn, NJ) so as to minimize protein loss. The blank consisted of 0.5 M NaCl. Standards of bovine gamma globulin diluted with 0.5 M NaCl were of the following concentrations: 30 µg/mL, 25 µg/mL, 20 µg/mL, 15 µg/mL, and 10 µg/mL. Serial dilutions of nuclear extracts in 0.5 M NaCl were made of 1 in 100, 1 in 200, and 1 in 300. 150 µL of each sample was pipetted into the well of a 96-well microtitre plate (Costar, Acton, MA). The blank and the calibration standards were each put into two wells. Then 150 µL of Coomassie® Plus Protein Assay Reagent was added to each well and mixed several times with a pipet. The reaction was allowed 5-10 minutes to complete. The well absorbances at 590 nm were read in a Thermomax microplate reader (Molecular Devices, Sunnyvale, CA).

7.2.6 SDS-PAGE sample preparation

Utilizing the protein quantitation results from Section 7.2.5, 12 µg or 18 µg for mini-gels and 30 µg for large gels of each sample was prepared to load into each lane. The samples were diluted at least 1:1 with SDS reducing buffer (0.0625 M TrisHCl, pH 6.8, 2.3% (w/v) SDS, 5% (v/v) β-mercaptoethanol, 10% (w/v) glycerol, 0.00125% (w/v) bromophenol blue). The sample was denatured at 95°C for at least 5 minutes and pulsed in the centrifuge to spin down condensation. The entire sample was loaded onto the gel lane. Standards employed were 1 µL of FMC Bioproducts Prosieve® Protein Markers diluted in 9 µL of SDS reducing buffer. The standards were denatured and spun before loading the entire 10 µL onto the gel.

7.2.7 Two-dimensional (2-D) electrophoresis sample preparation

400 µg (~180 µL) of protein was placed in a 600 µL Eppendorf tube and spun for 20 minutes at 13 200 rpm. The supernatant was transferred to the top portion of a Microcon YM-10 centrifugation filter. The device was spun at 12 200 rpm for 11 minutes. The filter was then removed from the device and the retentate spun out of the filter into a new tube at 3 200 rpm for 30 seconds. Deionized distilled water (~160 µL) was added to the Microcon filter and the filter was briefly vortexed. The filter was then inverted again and spun into the liquid in the bottom tube. The liquid was then transferred to a new filter unit and spun for 11 minutes at 12 200 rpm. The filter was again inverted into a new tube and the retentate was spun into the tube for 30 seconds at 3 200 rpm. To the filter, ~90 µL rehydration buffer (8M urea, 2% (w/v) Triton X-100, 0.5% (v/v) IPG Buffer, 0.28% (w/v) DTT, trace bromophenol blue) was added, vortexed lightly, and spun into the sample tube at 3 200 rpm for 30 seconds. The final sample volume was 125 µL.

7.2.8 SDS-PAGE

The Bio-Rad Mini-PROTEAN and the Gibco BRL Vertical Gel Electrophoresis systems were employed for SDS-PAGE separations. Both mini-gels (1 mm × 7 cm × 10 cm) and large gels (1.5 mm × 19 cm × 20 cm) consisted of a 12% polyacrylamide (12% T, 2.7% C) separating gel and a 4% polyacrylamide (4% T, 2.7% C) stacking gel. The electrophoresis buffer consisted of 25 mM Tris, 192 mM glycine, and 0.1% (w/v) SDS, pH 8.3. Samples were loaded and run at 200 V. The gels were visualized

with silver stain using the Bio-Rad Silver Stain Plus Kit or by an alternative noncommercial method (23).

7.2.9 2-D electrophoresis

The 7 cm Immobiline™ DryStrips (pH 3-10 linear gradient) and corresponding strip holders were utilized for the first dimension of IEF. The sample from Section 7.2.7 was applied evenly to the bottom of the strip holder. The Immobiline™ DryStrip's plastic backing was removed and the strip was applied gel-side towards the sample, taking care not to introduce bubbles into the sample. The strip was then covered with about 400 µL of mineral oil to prevent sample dehyration, and the strip holder cover was placed on top of the strip holder. The strip was then rehydrated overnight (between 12-17 hours) at 20°C on the IPGphor unit (Pharmacia, Quebec, Canada). The following morning, electrode wicks (inhouse-made from filter paper) were added to the strip holder. The small pieces of filter paper were dampened with water and then blotted of excess water on another piece of filter paper. The wicks were then applied over top of each electrode of the strip holder. Caution was used to prevent the introduction of any bubbles into the sample solution. If required, more mineral oil was added to the strip holder to prevent sample dehydration during isoelectric focusing (IEF).

Table 7.1 shows the IEF program utilized for the protein samples. After completion of the IEF dimension, each strip was equilibrated in two different solutions to ensure complete denaturation of the proteins before the second dimension. Each strip was placed in a 15 mL Fisher tube which contained 3 mL of DTT-containing equilibration solution (50 mM TrisHCl, pH 8.8, 6 M urea, 30% (v/v) glycerol, 2% (w/v) SDS, 1% (w/v) DTT, and trace bromophenol blue). The Fisher tube was rocked for 15 minutes. The IEF strip was then removed from the Fisher tube and rinsed gently with deionized distilled water. The IEF strip was then placed in a 15 mL Fisher tube containing 3 mL of iodoacetamide-containing SDS equilibration solution (same composition as the DTT-containing equilibration solution, except it contained 2.5% (w/v) iodoacetamide instead of DTT). The tube was rocked again for 15 minutes. The IEF strip was removed from the Fisher tube, rinsed gently with water, and then placed on top of an SDS-PAGE gel. Molecular weight size standards were loaded to the gel and electrophoresis was at 200 V. The Bio-Rad Silver Stain Plus Kit was utilized to visualize the gels.

Table 7.1 IEF program utilized for 2-D electrophoresis of A549 nuclear extracts.

Note that the current is limited to 50-75 μA per strip. The protocol is also programmed based on the attainment of volthours.

Step	Volts	Volthours	Gradient
1	500	250	step and hold
2	1000	500	step and hold
3	8000	8000	step and hold

7.2.10 Protein digestion

Protein spots were excised from either 1-D or 2-D gels utilizing a glass cover slip. The gel pieces were stored in 600 µL siliconized tubes (Rose Scientific, Edmonton, Canada). The in-gel digestion was a slightly modified version of those described by Shevchenko *et. al.* (24) and Wilm *et. al.* (24). To the gel pieces, 40 µL of acetonitrile was added. The samples were dehydrated by agitation for 20 minutes on a vortex (Fisher Vortex Genie 2, Fisher, Fair Lawn, NJ). If necessary, the samples were spun down and the acetonitrile was removed. The dehydrated gel pieces were transferred to new tubes and vacuum centrifuged to complete dryness. Next 10 mM DTT in 100 mM NH_4HCO_3 was added to cover the gel pieces. The pieces were rehydrated with vortexing for a couple of minutes. If necessary, the samples were spun down and then incubated at 56°C for one hour. The tubes were removed from the incubator, spun down, and cooled to room temperature. The excess DTT-solution was removed and discarded. To each tube, 55 mM iodoacetamide in 100 mM NH_4HCO_3 was added to cover the gel pieces. The samples were vortexed briefly and spun down if necessary. The tubes were stored in the dark for 45 minutes. After this time period, the excess iodoacetamide-solution was removed from each tube and replaced with about 50 µL of 100 mM NH_4HCO_3. The gel pieces were vortexed for 10 minutes, spun down, and the liquid removed. The gel pieces were then dehydrated with acetonitrile for 10 minutes on the vortex. The samples were then spun down and the liquid removed. Then the NH_4HCO_3-washing and acetonitrile-dehydrating steps were repeated. The dehyrated gel pieces were then transferred to new siliconized vials and vacuum dried.

The tryptic digest was performed as follows. To the dehydrated gel pieces, buffer containing 50 mM NH_4HCO_3, 5 mM $CaCl_2$, and 12.5 ng/mL trypsin was added. The gel pieces were vortexed until rehydrated, and then placed on ice for 45 minutes. This time allowed for the trypsin to move into the gel pieces. After 45 minutes, the excess liquid around the gel pieces was removed and discarded. The solution was replaced with 50 mM NH_4HCO_3. The samples were then placed in an incubator at 37°C overnight to digest. The following day the peptide extracts were removed from the sample tubes. The samples were removed from the incubator and the excess liquid was removed and saved. The remaining peptides were extracted with one change of 20 mM NH_4HCO_3 in 50% acetonitrile, two changes of 1% trifluoroacetic acid in 50% acetonitrile, and one change of 1% trifluoroacetic acid in 75% acetonitrile. Between changes the gel pieces were vortexed for 20 minutes. All extracts were combined and dried down to about 5-10 µL in a vacuum centrifuge.

Some extracts were also cleaned with a ZipTip™ (Millipore, Bedford, MA) protocol before analyzed by mass spectrometry (MS). After concentrating the extracts in a vacuum centrifuge, about 5 µL of 0.1% TFA was added and mixed. The 10 µL ZipTip™ was utilized according to the manufacturer's instructions with minor variations. The peptides were bound to the $ZipTip_{C18}$ with 40 aspirations of sample. Similarly, the peptides were eluted from the $ZipTip_{C18}$ with 40 aspirations of 50% acetonitrile in water. To this concentrated extract solution, a small amount of the matrix was added and mixed.

7.2.11 MALDI-TOF MS and database search

The matrix employed for the MS analysis was 4-HCCA. The MALDI-TOF instrument utilized was the PerSeptive Biosystems Voyager Elite (Framingham, MA). The tandem MS analysis was performed at MDS Ocata (Toronto, Canada) on a MALDI Qstar (MDS Sciex, Toronto, Canada). The database employed for protein identification from peptide fingerprint mapping was SwissProt (25) via Protein Prospector's MS-Fit tool (26). The database employed for protein identification from MS/MS fragmentation results was Mascot (27).

7.3 Results and Discussion

7.3.1 Irradiation-induced changes in A549 nuclear protein expression detected by SDS-PAGE

Figure 7.1 shows the changes induced in A549 nuclear protein expression as a result of irradiation with a dose of 5 Gy. There are five samples shown in total. Section 7.2.3 explains the sample's labels. Briefly, the control cells were not irradiated. The recovery times from irradiation before the nuclear proteins were extracted from the cells were 0 (termed irradiation control), 2, 4, and 24 hours. The figure clearly demonstrates that γ-irradiation of the A549 nuclear proteins is responsible for two distinct changes in the SDS-PAGE protein profile. Irradiation represses a high molecular protein which is highly visible in the control lane of the gel and then decreases with longer recovery times. Twenty-four hours after irradiation the protein is barely visible. The second major change in protein profile is a low molecular weight protein which is induced upon exposure to irradiation. This protein band is faint in the control lane and grows increasingly dark as the recover time increases.

Figure 7.1 SDS-PAGE of A549 nuclear fractions irradiated with 5 Gy.

See Section 7.2.6 for sample preparation details. Samples are labeled as: control- not irradiated, T_0- irradiation control, T_2, T_4, & T_{24}- subscript numbers refer to recovery time (in hours) allowed. Labels: (A)- irradiation repressed high molecular weight protein, (B)- irradiation induced low molecular weight protein. Separation details: gel: 12% separating gel, 4% stacking gel, sample: 12 µg/lane, electrophoresis voltage: 200 V, stain: silver stain.

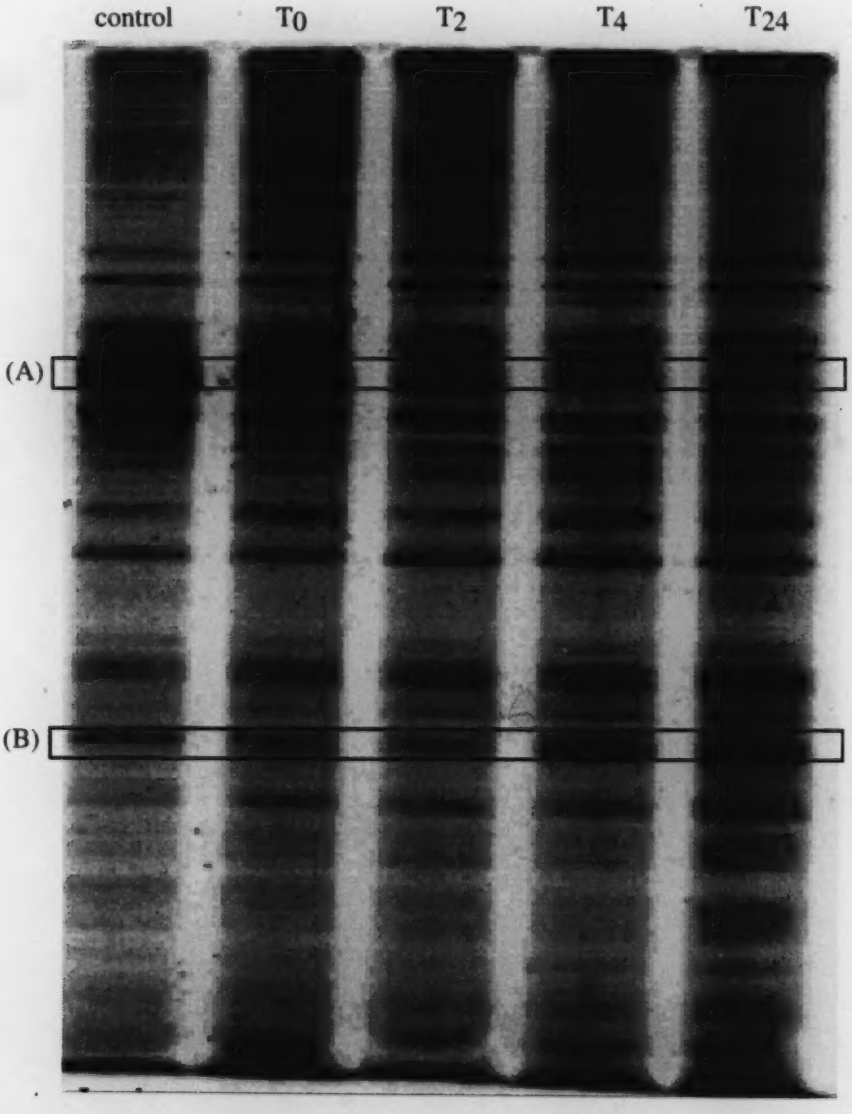

Figure 7.2 shows the changes induced in protein expression of A549 nuclear proteins as a result of exposure of the cells to an irradiation dose of 10 Gy. This dose of irradiation is considered a lethal dose. Figure 7.2 shows the protein profiles of cells which were allowed to recover for 0, 4, and 24 hours after irradiation before the nuclear proteins were extracted. The figure displays a similar trend in protein expression as a result of irradiation as the 5 Gy dose cells did.

Figure 7.3 displays the nuclear protein expression changes which are induced by the administration of a nonlethal dose of irradiation, 2 Gy. This dose is of similar value to ones which humans receive when being treated by irradiation therapy. The largest differences are seen between the control and 24-hour recovery samples which are shown in Figure 7.3. Again, as in both Figure 7.1 and 7.2, there is an irradiation-repressed protein of high molecular weight, and an irradiation-induced low molecular weight protein.

The results of Figures 7.1, 7.2, and 7.3 all show that regardless of irradiation dose, the same two conclusions are drawn. First, irradiation induces the expression of a low molecular weight protein. Second, irradiation represses the expression of a high molecular weight protein. Utilizing molecular weight markers on gels, the approximate molecular weights of the proteins are estimated to be about 30 kDa and 65 kDa. It is not known for certain whether or not these single bands are representative of a single protein or many and likewise whether or not the protein is post-translationally modified or not. More about the properties of these proteins needed to be studied, so the next step was to carry out 2-D electrophoresis on these nuclear extracts.

7.3.2 Irradiation-induced changes in A549 nuclear protein expression detected by 2-D electrophoresis

Figure 7.4 is a picture of a 2-D electrophoresis gel run of the A549 nuclear protein control sample for the 5 Gy dose batch. The high molecular weight protein which is repressed by irradiation is denoted by the arrow. The position of the protein on this gel indicates that it is quite acidic with a pI in the range of about 3.5-4.5. Furthermore, this protein appears as a smear on the gel instead of a spot. This indicates that the protein band seen on the SDS-PAGE gel is most likely a protein which is post-translationally modified in some manner. This may make protein identification through mass spectrometric methods difficult.

Figure 7.2 SDS-PAGE of A549 nuclear fractions irradiated with 10 Gy.

See Section 7.2.6 for sample preparation details. Samples are labeled as: T_0- irradiation control, T_4 & T_{24}- subscript numbers refer to recovery time (in hours) allowed. Labels: (A)- irradiation repressed high molecular weight protein, (B)- irradiation induced low molecular weight protein. Separation details: gel: 12% separating gel, 4% stacking gel, sample: 12 µg/lane, electrophoresis voltage: 200 V, stain: silver stain.

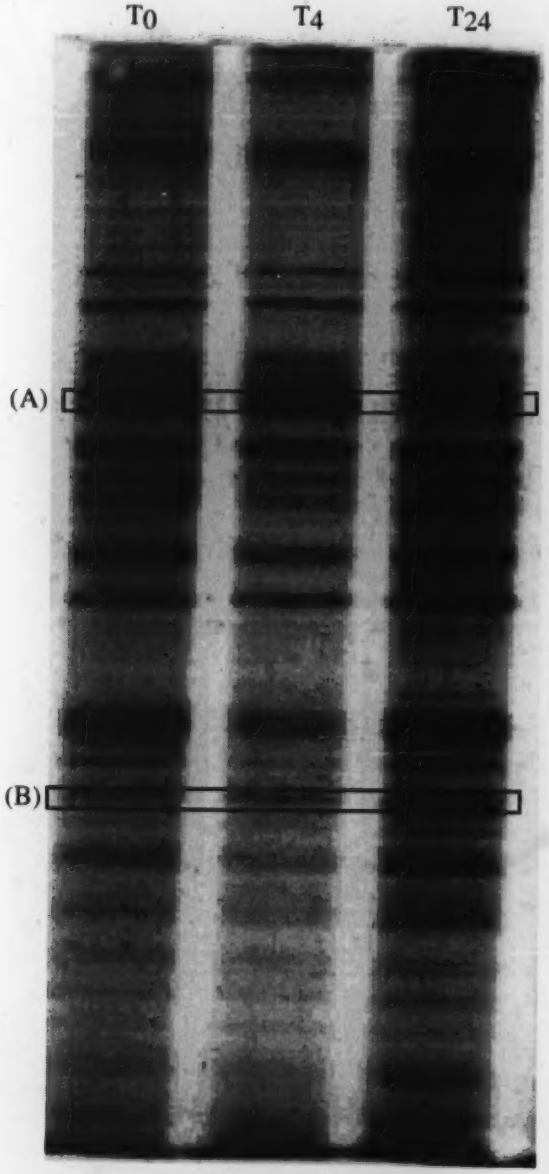

Figure 7.3 SDS-PAGE of A549 nuclear fractions irradiated with 2 Gy.

See Section 7.2.6 for sample preparation details. Samples are labeled as: T_0- irradiation control, & T_{24}- 24 hours for recovery allowed. Labels: (A)- irradiation repressed high molecular weight protein, (B)- irradiation induced low molecular weight protein. Separation details: gel: 12% separating gel, 4% stacking gel, sample: 12 µg/lane, electrophoresis voltage: 200 V, stain: silver stain.

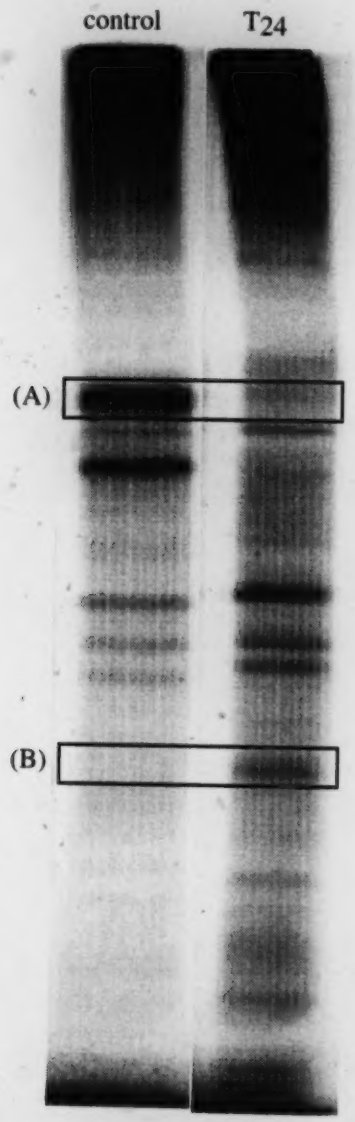

Figure 7.4 2-D electrophoresis gel of A549 nuclear fraction control sample.

See Section 7.2.7 for sample preparation details. The arrow denotes the location of the high molecular weight protein which is expression repressed upon exposure to irradiation. Separation details: IEF: Immobiline™ DryStrip pH 3-10 linear gradient, 7 cm long, see Section 7.2.9 for IEF program utilized, SDS-PAGE: gel: 12% separating gel, 4% stacking gel, electrophoresis voltage: 200 V, stain: silver stain.

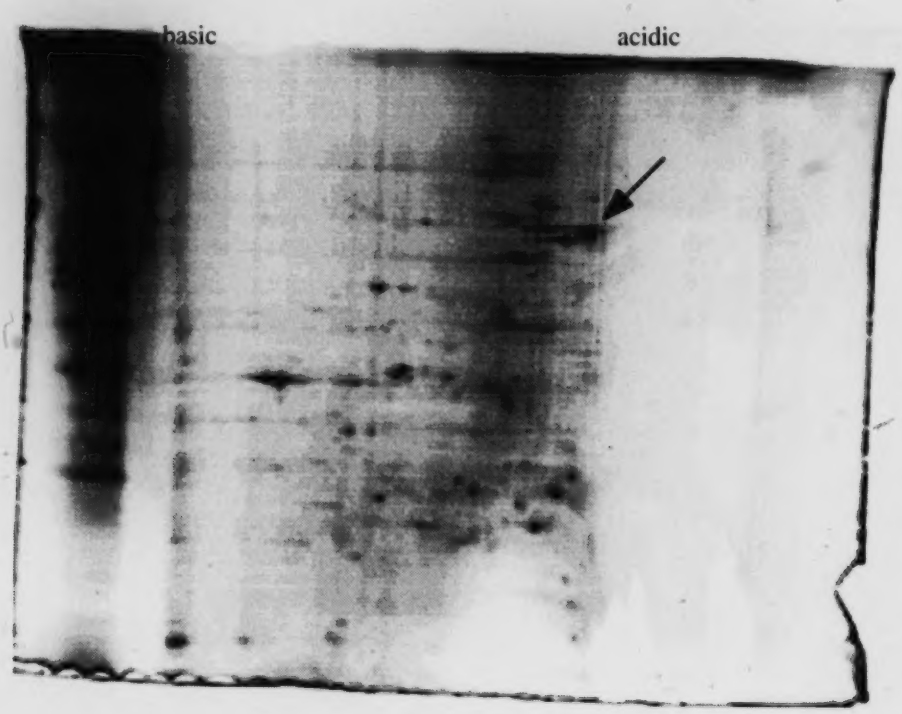

Figure 7.5 is a photograph of a 2-D electrophoresis gel run of the A549 nuclear protein sample which was allowed to recover for 24 hours from a dose of 5 Gy before its work up. Since the most pronounced changes are seen between the sample extremes of control and 24-hour recovery, only these two gels are displayed here. The arrow denotes the location of the high molecular weight protein which is irradiation repressed. When comparing this gel to that of Figure 7.4, the disappearance of this protein is very pronounced. Again the location of the protein confirms an acidic pI.

It is to be noted that the low molecular weight protein of interest could not be identified by examining the gels by eye. As a result, the pI of this protein was not determined.

7.3.3 Problems and solutions encountered while attempting to identify nuclear proteins utilizing MALDI-TOF MS

Many problems were encountered with the identification of the two nuclear proteins of interest. This section will deal with these problems and possible solutions.

The largest problem encountered was lack of peptide peaks in the MS spectra. Autolysis peaks were seen from trypsin which thus indicated that the enzyme was active and not the problem. Unidentifiable peaks were seen in both sample and blank spectra, however all of these peaks matched up indicating that no peaks due to only sample were present.

As a gel's polyacrylamide percentage increases, the pore size of the gel decreases. The protocol utilized a 12% separating gel. It is possible that such a gel has pores small enough to make diffusion of the peptides out of the gel and into the extract solution very difficult. If the pores are very small, only a few peptides may diffuse into the extract solution and may not be detected by the MS. One suggestion was to utilize lower percentage polyacrylamide gels for the separation of the nuclear proteins (28). Polyacrylamide gels of 7.5% and 10% were poured and run. The larger pore size did not have any effect on the extract analysis by MS.

One factor which was changed in attempts to recover peptides from the in-gel digestion was the stain which was utilized. It was believed that perhaps the silver stain was binding the protein too tightly in the gel and the protein was somehow not digested or the peptides were not able to leave the gel. One suggestion to this problem is to employ a reverse stain such as a zinc stain (29), which does not bind to the protein in the gel, but rather binds to the gel which does not contain protein. The utilization of such a stain did not change the MS results. It has also been suggested that different

Figure 7.5 2-D electrophoresis of A549 nuclear fraction 24 hour recovery sample irradiated with 5 Gy.

See Section 7.2.7 for sample preparation details. The arrow denotes the location of the high molecular weight protein which is expression repressed upon exposure to irradiation. Separation details: IEF: Immobiline™ DryStrip pH 3-10 linear gradient, 7 cm long, see Section 7.2.9 for IEF program utilized, SDS-PAGE: gel: 12% separating gel, 4% stacking gel, electrophoresis voltage: 200 V, stain: silver stain.

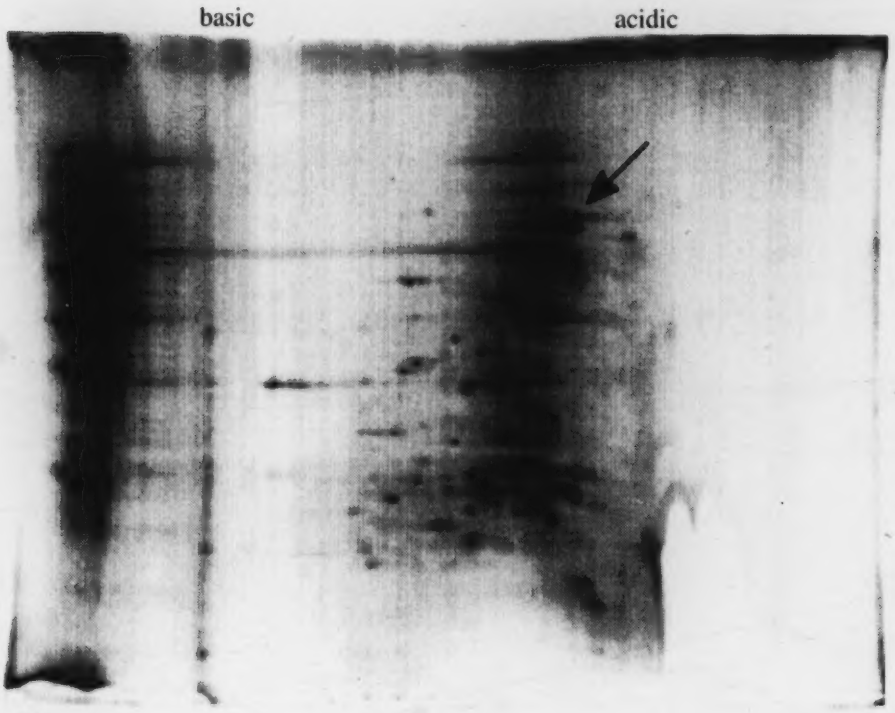

silver stains are more or less compatible with MS analysis (28). One such more compatible silver stain (23) was also employed to no avail. Some believe that destained gel pieces enhance peptide mass signal in MS (30). A destain method (30) was employed with the gel pieces of these nuclear proteins but did not yield beneficial results. The samples were also run on gels which were Coomassie stained, and very few proteins were detected utilizing this method. This evidence suggested that not enough protein was loaded onto the gel for the MS to detect it.

It was believed that chromatographic fractionation of the sample would help to both concentrate the sample and clean up the sample. The chromatographic fractionation method utilized was similar to that employed by Rout *et. al.* with yeast nuclear proteins (30). Four milligrams of total nuclear protein were loaded onto a column and 2 mL fractions were collected. Every fourth fraction was microconcentrated and quantitated before it was run on an SDS-PAGE gel. From the results of the SDS-PAGE gel, it was determined which fractions contained the proteins of interest. The fractions of interest were then microconcentrated, quantitated, and run on an SDS-PAGE gel. The two proteins of interest were excised from these gels and subjected to in-gel digestion after destaining. This lengthy and tedious procedure failed to produce any beneficial results.

The last solutions to the lack of peptide signal in the MS were the utilization of a clean hood for all preparations and the pooling together of gel pieces before digestion (32). It was believed that the spurious peaks present in both sample and blank MS spectra were due to human contamination, i.e. keratins from the skin and hair being digested along with the protein of interest. If there is enough of this type of contamination, it can basically swamp out any signal that would be due to peptides of interest. The pooling together or many gel pieces was done in attempts to increase the amount of peptide within the extract for analysis.

7.3.4 Failure to identify the high molecular weight protein of interest

No tentative identification of the high molecular weight protein of interest can be made. The sample mass spectra matched those of the blank. No unique peaks were seen upon comparison of the spectra. One reason for this may be due to the fact that this protein is highly acidic in nature. This means that digestion with trypsin will yield a few large peptides which may not be seen by the MS. Another possibility is that the protein is highly hydrophobic and is not easily removed from the gel matrix once it is in it. It is believed that lack of protein was not a problem as a large amount of protein was

loaded onto the gel and then gel spots were pooled together in large quantities to combat this problem.

7.3.5 Identification of the low molecular weight protein of interest

The mass spectrum of the low molecular weight protein and that of the blank for the low molecular weight region were identical except for the portion shown in Figure 7.6. Figure 7.6 shows the mass to charge ratio (m/z) region from 1800 to about 2600. There are two starred peaks which are unique to this spectrum. The starred peak at m/z 1991.2 was not identified. However the starred peak at m/z 1951.9 is particularly interesting. Since this peak was one of the only unique peptides for this protein, tandem MS analysis of this peptide to obtain its sequence information was necessary to identify this protein. The protein digest and a blank were sent to MDS Ocata where this analysis was carried out on a MALDI Qstar. From a theoretical digest performed in the database, the peak at m/z 1951.9 corresponds to the amino acid sequence of VFEVSLADLQNDEVAFR (33). MS/MS analysis of this peptide confirmed that this is the actual sequence. This peak's m/z value and other relevant information were entered into the database and matched a ribosomal protein S3a (accession number P49241). This protein has a molecular weight of 29 814 Da (34) which corresponds well with the SDS-PAGE findings. Furthermore, this protein has a very basic pI of 9.75 (35) which would explain why it was not spotted on the 2-D gels of the nuclear extracts. The Immobiline™ DryStrips which were employed were pH 3-10 and the wick electrodes occupy part of this pH gradient. So in actuality, the pH range of the gel may be slightly less than pH 3-10. If the protein is in the gel, it is most likely on the very basic edge. Others have demonstrated that partial sequence information from one specific peptide can be enough for unambiguous protein identification (36, 37).

It is believed that this cytosolic protein was extracted with the nuclear proteins due to the many RNA molecules which interact with this subunit. This ribosomal protein is involved in cell protein assembly. Most likely this protein is up-regulated following irradiation to increase the production of certain proteins within the cell. The proteins which are manufactured in increasing numbers after irradiation are most likely DNA-repair associated proteins, such as DNA-repair enzymes.

7.4 Conclusion

This chapter presents the results of dose-response studies of human lung cancer (A549) cell nuclear proteins. Cells were subjected to ^{60}Co γ-irradiation of different

Figure 7.6 Unique portion of the mass spectrum of the low molecular weight protein.

The starred peaks are unknown peaks. The peaks marked with "T" are known trypsin autolysis peaks.

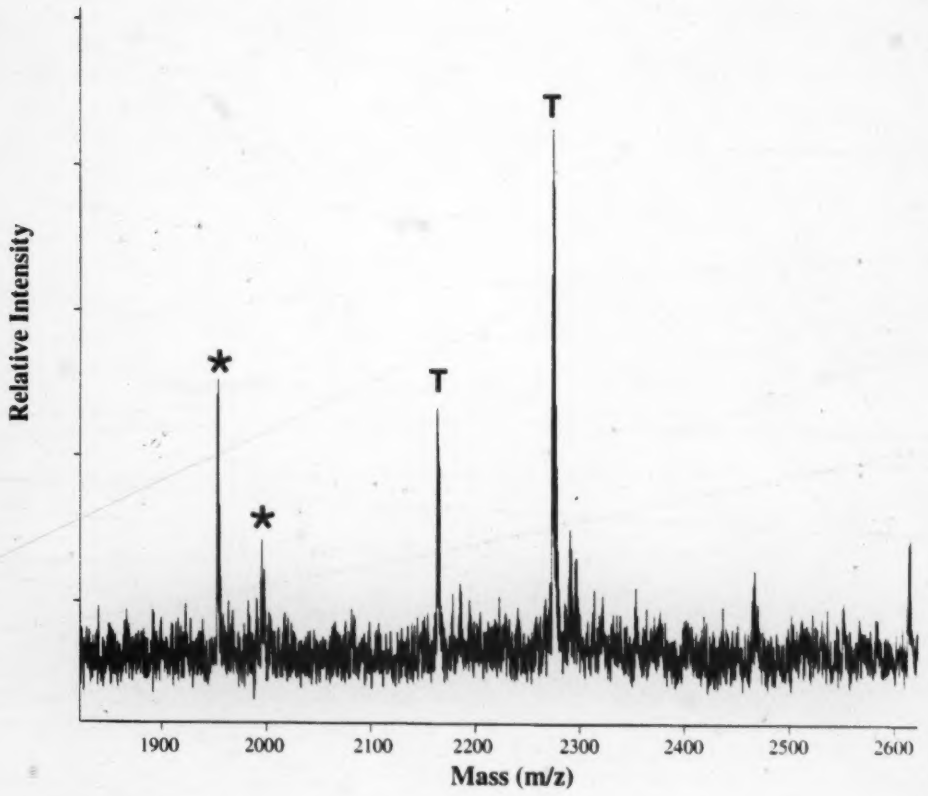

doses (2, 5, or 10 Gray) and incubated to allow for recovery from 0 to 24 hours. Following recovery, nuclear proteins were extracted by differential detergent fractionation, quantitated, and then separated using both SDS-PAGE and 2-D gel electrophoresis. Differential display techniques were employed and showed two differences between samples irregardless of irradiation level: a high molecular weight protein repressed by irradiation and a low molecular weight protein induced by irradiation. These two protein bands of interest were then subjected to a peptide mapping approach to protein identification. The two protein bands were excised from the gels, subjected to tryptic digestion, the extracted peptides were analyzed by MALDI TOF MS, and the resulting information was used for protein identification via the SwissProt internet database. However one peptide of the low molecular weight protein was subjected to tandem MS analysis which provided confirmation that this protein is the 40S ribosomal protein S3a.

7.5 References

(1) Szallasi, Z. *Nature Biotechnology* **1998,** *16*, 1292-1293.

(2) Williams, K. *Electrophoresis* **1999,** *20*, 678-688.

(3) Quadroni, M.; James, P. *Electrophoresis* **1999,** *20*, 664-677.

(4) Cash, P. *Journal of Chromatography A* **1995,** *698*, 203-224.

(5) Anderson, N. L.; Taylor, J.; Scandora, A. E.; Coulter, B. P.; Anderson, N. G. *Clinical Chemistry* **1981,** *27*, 1807-1820.

(6) Olson, A. D.; Miller, M. J. *Analytical Biochemistry* **1988,** *169*, 49-70.

(7) Pun, T.; Hochstrasser, D. F.; Appel, R. D.; Funk, M.; Villars-Augsburger, V.; Pellegrini, C. *Applied and Theoretical Electrophoresis* **1988,** *1*, 3-9.

(8) Garrels, J. I. *Journal of Biological Chemistry* **1989,** *264*, 5269-5282.

(9) Appel, R. D.; Vargas, J. R.; Palagi, P. M.; Walther, D.; Hochstrasser, D. F. *Electrophoresis* **1997,** *18*, 2735-2748.

(10) Sinha, P.; Hutter, G.; Kottgen, E.; Dietel, M.; Schadendorf, D.; Lage, H. *Journal of Biochemical and Biophysical Methods* **1998,** *37*, 105-116.

(11) Oh, J. M. C.; Hanash, S. M.; Teichroew, D. *Electrophoresis* **1999,** *20*, 766-774.

(12) Pasquali, C.; Fialka, I.; Huber, L. A. *Journal of Chromatography B* **1999,** *722*, 89-102.

(13) Yates III, J. R. *Journal of Mass Spectrometry* **1998,** *33*, 1-19.

(14) James, P. *Biochemical and Biophysical Research Communications* **1997,** *132*, 1-6.

(15) Molloy, M. P.; Herbert, B. R.; Walsh, B. J.; Tyler, M. I.; Sanchez, J.-C.; Hochstrasser, D. F.; Williams, K. L.; Gooley, A. A. *Electrophoresis* **1998,** *19*, 837-844.

(16) Ramsby, M. L.; Makowski, G. S. In *2-D Proteome Analysis Protocols*; Link, A. J., Ed.; Humana Press, Inc.: Totowa, 1999, pp 53-85.

(17) Anderson, N. G. *Methods in Biochemical Analysis* **1967,** *15*, 271-310.

(18) Herbert, B. R. *Electrophoresis* **1999,** *20*, 660-663.

(19) Kim, C. Y.; Giaccia, A. J.; Strulovici, B.; Brown, J. M. *British Journal of Cancer* **1992,** *66*, 844-849.

(20) Hall, E. J. *Radiobiology for the Radiologist*, 4 ed.; J.B. Lippincott Company: Philadelphia, 1994.

(21) Elkind, M. M.; Whitmore, G. F. *The Radiobiology of Cultured Mammalian Cells*; Gordon and Breach: New York, 1967.

(22) Andrews, R. J. *The Radiobiology of Human Cancer Radiotherapy*, 2nd ed.; University Park Press: Baltimore, 1978.

(23) http://depts.washington.edu/~reudilab/methods/AGstain.html

(24) Shevchenko, A.; Wilm, M.; Vorm, O.; Mann, M. *Analytical Chemistry* **1996,** *68*, 850-858.

(25) http://www.expasy.ch/sprot/

(26) http://prospector.ucsf.edu/ucsfhtml3.2/msfit.htm

(27) http://www.matrixscience.com/cgi/index.pl?page=../home.html

(28) Aebersold, R., personal communication.

(29) Fernandez-Patron, C.; Castellanos-Serra, L.; Hardy, E.; Estevez, E.; Mehl, E.; Frank, R. W. *Electrophoresis* **1998,** *19*, 2398-2406.

(30) Gharahdaghi, F.; Weinberg, C. R.; Meagher, D. A.; Imai, B. S.; Mische, S. M. *Electrophoresis* **1999,** *20*, 601-605.

(31) Rout, M. P.; Aitchison, J. D.; Suprapto, A.; Hjertaas, K.; Zhao, Y.; Chait, B. T. *Journal of Cell Biology* **2000,** *148*, 635-651.

(32) Li, L., personal communication.

(33) http://expasy.cbr.nrc.ca/cgi-bin/peptide-mass.pl.

(34) http://expasy.cbr.nrc.ca/cgi-bin/sprot-search-ac?p49241.

(35) http://www.expasy.ch/cgi-bin/pi_tool1?P49241@noft@.

(36) Perkins, D. N.; Pappin, D. J. C.; Creasy, D. M.; Cottrell, J. S. *Electrophoresis* **1999,** *20*, 3551-3567.

(37) Wilkins, M. R.; Gasteiger, E.; Tonella, L.; Ou, K.; Tyler, M.; Sanchez, J.-C.; Gooley, A. A.; Walsh, B. J.; Bairoch, A.; Appel, R. D.; Williams, K. L.; Hochstrasser, D. F. *Journal of Molecular Biology* **1998,** *278*, 599-608.

Chapter 8
Conclusions and Future Work

8.1 Thesis summary and future directions

The separation techniques presented in this thesis represent the evolution of separation science from the genomic era to that of proteomics. The main focus of this thesis has been protein separations which sprung out of DNA sequencing by capillary gel electrophoresis (CGE) with laser-induced fluorescence (LIF) detection. Future work will be in the area of protein separation and identification.

The earliest work chronicled in this thesis was the development and employment of a replaceable sieving matrix for CGE DNA sequencing with LIF detection. A nonviscous polydimethylacrylamide (PDMA) sieving matrix was developed which is capable of being replaced after each use in an uncoated capillary. Such a sieving matrix is important for the use of high throughput DNA sequencing and is closely related to the POP6® DNA sequencing polymer marketed by PE Biosystems. The POP6® polymer has been utilized along with a multicapillary instrument by Celera Genomics to sequence the entire human genome as well as over one billion bases of the mouse genome (1, 2). Future studies should be conducted on the effects of lifetime of the sieving matrix on the overall separations as were conducted on linear polyacrylamide (LPA) by Figeys *et. al.* (3). Furthermore, the preliminary studies of electric field strength effects on separations from Section 2.3.4 should be further examined.

Capillary isoelectric focusing (CIEF) with LIF detection is a very powerful tool which combines the concentrating power of IEF with the superior detection limits of LIF to create an ultra-sensitive technique. Thus the technique exudes the potential be incredibly useful with biological applications, for example to detect low copy number proteins. However one of the main drawbacks of the utilization of this technique is that fluorescently derivatizing proteins can result in changes in isoelectric points (pIs) due to a change in the protein's charge (4) or in the three dimensional structure of the protein (4, 5) upon reaction with a dye. Evidence for both of these occurrences upon fluorescent derivatization of green fluorescent protein is demonstrated in Chapter 3. Future work should be done to discover fluorescent labeling methods which do not change the native protein in terms of conformation or charge and thus do not change its pI.

Sodium dodecyl sulfate (SDS) capillary gel electrophoresis (CGE) is still a very young technique which requires much development to make it accessible to applications involving complex samples. While original matrices such as cross-linked

polyacrylamide (PA) and LPA are often utilized, it is rarely for the purpose of separating complex mixtures such as cell extracts. This thesis presents the attempted utilization of different sieving matrices to separate complex cell extract samples. Hydroxyethylcellulose (HEC) was employed as a sieving matrix for SDS CGE separations of protein standards only. It is clear that more work needs to be done with HEC sieving matrices in order for HEC to become a high resolution separation matrix. Work should be done on the buffer systems employed with HEC as an SDS CGE sieving matrix. As has been successfully done with LPA for CGE DNA sequencing separations (6), it is possible that improved SDS CGE protein separations may result from the formulation of an HEC sieving matrix involving a mixture of different molecular weights. Furthermore, for HEC to be utilized routinely as an acceptable sieving matrix for SDS CGE protein separations, an answer to its inherent migration time irreproducibility problems must be found. One such solution is the discovery of an appropriate internal standard for the system. Another solution may be the careful thermostat of separation temperature (7, 8).

In the development of a new separation, it is often wisest to first separate standards to prove the method. After successfully completing such a test, the next step is to apply the separation technique to complex samples. In Chapter 5, a method was presented utilizing a LPA sieving matrix to separate a mixture of cell extract proteins from human colorectal (HT29) cells. However the sample was too complex for such a system, so a differential detergent fractionation method (9) was employed to simplify the cell extract into specified cellular components. The LPA sieving matrix showed some promise for separating fractions of HT29 cells, however more work needs to be done to improve the separations. Perhaps as with the LPA CGE DNA sequencing sieving matrices (6) previously mentioned it would be beneficial to utilize a LPA SDS CGE sieving matrix composed of different molecular weights of LPA. Furthermore different buffer systems should be tested with this LPA sieving matrix. Different LPA polymerization conditions can also be investigated to find the ideal set of polymerization conditions. Temperature control of the separation may also be an issue which should be examined (7, 8).

Also included in the search for a suitable SDS CGE sieving matrix was the utilization of dextran to separate complex protein mixtures. Dextran promises much potential in the way of separating complex samples as it demonstrates very reliable protein standard separations. Furthermore, when applied as a sieving matrix for the separation of human lung cancer (A549) cell nuclear extracts, many proteins were

resolved. However future work needs to be focussed on the reproducibility of complex protein patterns seen from run-to-run. Further attention also needs to be drawn to the ability of dextran to resolve well the separation of complex samples.

Chapter 7 details the undertaking to identify two human lung cancer cell nuclear proteins of interest which change when irradiated with different doses of a ^{60}Co γ-ray source. The chapter chronicles the powerful potential of peptide mass fingerprinting as well as many of the difficulties of proteomics which may be encountered along the path to protein identification. No useful identity information could be obtained for one of the proteins whereas information which pointed to the identity of the second protein was obtained. Tandem MS was performed on the promising sample and the protein was identified.

This thesis examines a shift from the genomic paradigm to that of the proteomics era in separation science. Many capillary electrophoresis-based separations techniques are presented which aim to separate real, complex samples. The techniques are first developed utilizing standards and if they succeed are employed to separate complex sample mixtures. One of the focuses of separation science in the new millennium will be proteomics-based research. Reliable, rugged techniques must be developed to deal with the overwhelming tasks presented by this proteomics research.

8.2 References

(1) http://www.pe-corp.com/press/prccorp040600.html.

(2) http://www.pe-corp.com/press/prccorp060100.html.

(3) Figeys, D.; Dovichi, N. J. *Journal of Chromatography A* **1995,** *717*, 105-111.

(4) Shimura, K.; Kasai, K.-i. *Electrophoresis* **1995,** *16*, 1479-1484.

(5) Williamson, A. R.; Salamam, M. R.; Kreth, H. W. *Annals of the New York Academy of Science* **1973,** *209*, 210-224.

(6) Salas-Solano, O.; Carrilho, E.; Kotler, L.; Miller, A. W.; Goetzinger, W.; Sosic, Z.; Karger, B. L. *Analytical Chemistry* **1998,** *70*, 3996-4003.

(7) Shieh, P. C. H.; Hoang, D.; Guttman, A.; Cooke, N. *Journal of Chromatography A* **1994,** *676*, 219-226.

(8) Harvey, M. D.; Bandilla, D.; Banks, P. R. *Electrophoresis* **1998,** *19*, 2169-2174.

(9) Ramsby, M. L.; Makowski, G. S. In *2-D Proteome Analysis Protocols*; Link. A. J., Ed.; Humana Press, Inc.: Totowa, 1999, pp 53-85.